Photosynthetic and Fermentative Bacteria Reveal New Pathways for Biological Mercury Reduction

Daniel Grégoire

A thesis submitted in partial fulfillment of the requirements for the

Doctorate in Philosophy degree in Biology

Department of Biology

Faculty of Science

University of Ottawa

Abstract

Mercury (Hg) is a global pollutant and potent neurotoxin that bioaccumulates in aquatic and terrestrial food webs as monomethylmercury (MeHg). Anaerobic microbes are largely responsible for MeHg production, which depends on the bioavailability of inorganic Hg substrates to methylators. Hg redox cycling pathways such as Hg reduction play a key role in determining Hg's availability in the environment. Although abiotic photochemical Hg reduction typically dominates in oxic surface environments, Hg reduction pathways mediated by photosynthetic and anaerobic microbes are thought to play an important role in anoxic habitats where light is limited and MeHg production occurs. Currently, the physiological mechanisms driving phototrophic and anaerobic Hg reduction remain poorly understood. The main objective of my thesis is to provide mechanistic details on novel anaerobic and phototrophic Hg reduction pathways. I used a combination of physiological, biochemical and trace Hg analytical techniques to study Hg reduction pathways in a variety of anaerobic and photosynthetic bacteria. I demonstrated that Hg redox cycling was directly coupled to anoxygenic photosynthesis in aquatic purple non-sulphur bacteria that reduced Hg^{II} when cells incurred a redox imbalance. I discovered that terrestrial fermentative bacteria reduced Hg through pathways that relied on the generation of reduced redox cofactors. I also showed that sulphur assimilation controlled Hg reduction in an anoxygenic phototroph isolated from a rice paddy. In addition, I developed methods to explore cryptic anaerobic Hg redox cycling pathways using Hg stable isotope fractionation. At its core, my thesis underscores the intimate relationship between cell redox state and microbial Hg reduction and suggests a wide diversity of microbes can participate in anaerobic Hg redox cycling.

Résumé

Le mercure (Hg) est un polluant global et une neurotoxine puissante qui se bioaccumule dans les réseaux trophiques sous forme de monométhylmercure (MeHg). Les microorganismes anaérobiques sont en grande partie responsables de la production du MeHg qui dépend notamment de la biodisponibilité du Hg inorganique aux méthylateurs. Les réactions d'oxydoréduction, telles que la réduction du Hg inorganique divalent en Hg élémentaire, modèrent la biodisponibilité du Hg. Bien que la réduction photochimique du Hg domine dans les environnements de surface oxiques, la réduction biologique du Hg par les microorganismes anaérobiques joue un rôle important dans les habitats anoxiques où le MeHg est produit. Ces mécanismes biologiques sont actuellement mal compris et l'objectif principal de ma thèse, en utilisant une combinaison d'approches physiologiques et biochimiques, était de mieux comprendre le rôle des microorganismes phototrophiques et anaerobiques sur le cycle redox du Hg. J'ai montré que la réduction du Hg est liée à l'équilibre redox intracellulaire chez des bactéries pourpres non-sulfureuses. J'ai aussi découvert que la réduction du Hg dépend de la génération d'équivalents réducteurs pendant la fermentation et que l'assimilation du soufre peut contrôler la réduction du Hg chez les bactéries phototrophes. En outre, j'ai mis au point de nouvelles méthodologies pour explorer le cycle redox du Hg, basées sur le fractionnement des isotopes stables. Mes travaux de thèse montrent qu'il existe une relation intime entre l'état redox intracellulaire et la réduction du Hg dans l'environnement et que de nombreux microorganismes peuvent participer à l'oxydoréduction du Hg dans les environnements anoxiques.

Acknowledgments

I would first like to thank my thesis supervisor, Dr. Alexandre Poulain. Alexandre, you have been the best supervisor a student could ask for. I appreciate how you always made time to discuss my research with me and how much you helped me become a more independent researcher over the last six years. You never hesitated to let me explore new horizons and I appreciate the emphasis you placed on work-life balance. I admire your drive, ambition, and perseverance, and I hope to emulate these qualities in my career.

Secondly, I would like to thank my committee members Dr. Frances Pick, Dr. Charles Darveau, Dr. Alex Wong and Dr. Carl Mitchell. Frances, you have shaped my research career for ten years and I always keep you in mind when thinking of the broader environmental applications of my research. Charles, your expertise in the realm of physiology has helped me tackle some of the more challenging questions surrounding microbial metabolism in my thesis. Alex, your insights into the evolutionary dynamics of microbes have helped me think of how my work fits into a larger evolutionary context. Carl, your comments as my external evaluator provided a welcomed perspective that helped me finalize a stronger version of my original thesis.

I would also like to extend my gratitude to my lab mates and research collaborators. Some special thanks go to Emmanuel Yumvihoze. Emmanuel, I can't say how much I appreciate your patience and support, almost all the results that in are my thesis were obtained because of the training you provided me. Additional thanks go to Philip Pelletier. Phil, I greatly appreciate the time you took to train me on molecular biology techniques despite such methods not being the focus of my research. To my colleagues in Wisconsin, Sarah Janssen and Michael Tate, I thank you for teaching me

about the fascinating world of isotope chemistry. Finally, some thanks go to members of the Poulain lab. Mija, Martin, Ben, Galen, Graham, Aaron and Matti, thank you for listening to my research talks and taking time to discuss science with me. These discussions led to ideas that I included in my thesis and I am forever grateful.

I've also had the pleasure of training some wonderful students. Danielle Prapavessis, Sruthee Govindaraj, and Noémie Lavoie, you were all a joy to work with and I can only hope you learned as much from me as I did from you. A special thank you goes to Noémie, you worked extremely hard during our time together and I am proud of the research scientists you have become. I am thrilled that you will be continuing to explore how photosynthetic microbes can alter the fate of metals in the environment.

To my family and friends, I cannot thank you enough for the support you have shown throughout my academic career. I know that my workload has often kept me from family and social gatherings, however you never stopped supporting me even when I was absent. A special thank you goes to the Grégoire family who are the best support network I could ask for when it comes to encouraging my scientific and entrepreneurial endeavours.

My final thanks are to my wife, Sarah Grégoire. While you often joke that you should get an honorary PhD given how much you have helped me throughout my graduate studies I can honestly say I wouldn't have been able to complete my thesis without you. I thank you for your endless patience, unwavering support and the sacrifices you made to help me get through my PhD. You have been with me since my first day in graduate school and although this chapter of our lives has proved challenging, I am eternally in your debt for being there with me through it all.

Dedication

In memory of Steven Grégoire

Thank you for teaching me the importance of hard work and perseverance

Table of contents

List of figures

List of tables

Abbreviations

[x]	Concentration of compound x
AMR	Anaerobic mercury reducer
APS	Adenosine- 5'-phosphosulphate
ATP	Adenosine triphosphate
BMAA	Minimal exposure medium
C1	One carbon compound
Cys/Cyst	Cysteine
DMSO	Dimethylsulphoxide
DOC	Dissolved organic carbon
DOM	Dissolved organic matter
DMRB	Dissimilatory metal reducing bacteria
DSMZ	German Collection of Microorganisms and Cell Cultures
e-	Electron
EPA	Environmental Protection Agency
FAD+	Flavin adenine dinucleotide (oxidized)
FADH	Flavin adenine dinucleotide (reduced)
FbFP	Flavin based fluorescent protein
Fd ox	Ferredoxin (oxidized)
Fd red	Ferredoxin (reduced)
FEM	Purple non-sulphur bacteria defined medium
FNR	Ferredoxin-$NAD(P)^+$ oxidoreductase
FR	Fumarate reduction
GNSB	Green non-sulphur bacteria
GSB	Green sulphur bacteria
GSMM	Minimal medium for *Geobacter sulfurreducens* PCA
HAH	Hydroxylamine hydrochloride
HPLC-DAD	High performance liquid chromatography with diode array detector
Hg	Mercury
HgS	Cinnabar/mercury sulphide
hv	Light
IRB	Iron reducing bacteria
LB	Lysogeny broth
LH	Light-harvesting
LOM	Labile organic matter
LPS	Lipopolysaccharide
MC-ICP-MS	Multicollector-inductively coupled plasma mass spectrophotometer
MDF	Mass dependent fractionation
MeHg/MMHg	Monomethylmercury
Met	Methionine
MIF	Mass independent fractionation
MOPS	3-(N-morpholino)-propanesulphonic acid

MR	Mercuric reductase
NAD+	Nicotinamide adenine dinucleotide (oxidized)
NADH	Nicotinamide adenine dinucleotide (reduced)
NADP+	Nicotinamide adenine dinucleotide phosphate (oxidized)
NADPH	Nicotinamide adenine dinucleotide phosphate (reduced)
NIST	National Institute of Standards and Technology
NOM	Natural organic matter
NTZ	Nitazoxanide
O.D. 600	Optical density at 600 nm
OD	Oxidative demethylation
OL	Organomercury lyase
PAPS	3'- phospho – adenosine 5' – phosphosulphate
PAR	Photosynthetically active radiation
PCR	Polymerase chain reaction
PDH	Pyruvate dehydrogenase
PFL	Pyruvate formate lyase
PFOR	Pyruvate ferredoxin oxidoreductase
PHB	Polyhydroxybutyrate
PNSB	Purple non-sulphur bacteria
PSB	Purple sulphur bacteria
PS-RC	Photosynthetic reaction centre
PSI	Photosystem I
PSII	Photosystem II
PTFE	Polytetrafluoroethylene (Teflon)
PYE	Pyruvate yeast growth medium
PYEΔSO_4^{-2}	Pyruvate yeast growth medium without sulphate salts
PYX	Rich growth medium for fermentative bacteria
Q	Quinone
RD	Reductive demethylation
SH	Thiol group/bond
SR	Sulphate reduction
SRB	Sulphate reducing bacteria
TEA	Terminal electron acceptor
TCA	Tricarboxylic acid cycle
THg	Total mercury
UNEP	United Nations Environmental Programme
UQ	Ubiquinone
YE	Yeast extract
YP	Yeast peptone medium

Chapter 1: General introduction

1.1 BACKGROUND INFORMATION ON MERCURY

Mercury (Hg) is a global pollutant and potent neurotoxin that is primarily emitted in its elemental and volatile form Hg^0 [1]. Hg^0 can originate from natural sources including volcanoes, forest fires and hydrothermal vents and anthropogenic sources such as small-scale artisanal gold mining, metal refining, and coal combustion [1]. As a gas, Hg^0 can travel in the atmosphere for six months up to a year before being oxidized to Hg^{II}, which enters aquatic and terrestrial ecosystems through wet (e.g. precipitation) and dry (e.g. dust transport) [2] deposition pathways. From that point, Hg can be re-emitted to the atmosphere as Hg^0, buried in sediments in its mineral form (HgS) or converted to its organic form monomethylmercury (MeHg) through a number of abiotic and biotic pathways [3].

Although all chemical forms of Hg are toxic, MeHg is the most concerning from a human health perspective. MeHg is produced by anaerobic bacteria that do not require oxygen to generate energy [4-7] and thrive in habitats such as aquatic sediments and flooded soils [8]. The MeHg produced in these habitats can easily cross cell membranes and bioaccumulates in the tissues of organisms at concentrations several orders of magnitude higher than ambient levels of Hg [9]. Hg bioaccumulation is more pronounced in organisms that occupy higher trophic levels, which contributes to why humans become exposed to Hg through the consumption of predatory fish [9]. Recently, the consumption of contaminated rice has also emerged as a route of Hg exposure because the flooded conditions in rice paddies are conducive to MeHg production [10].

Once inside of the cell, Hg's toxicity is attributable to its high affinity for thiol-containing amino acids [11], which can lead to protein denaturation and the disruption of essential cellular functions [12-16]. Foetuses and young infants are particularly vulnerable to Hg toxicity and typically become exposed to Hg through their mother's diet during development [16]. Chronic Hg exposure can lead to physical birth defects and permanent neurological damage in humans and remains an ongoing issue for people that live in areas impacted by Hg pollution [16, 17].

Hg's high toxicity and pervasiveness in the environment have made it the number one global priority contaminant. Recently, there has been a global effort initiated by the United Nations Environmental Programme (UNEP) to curb the impacts of Hg pollution through the Minamata Convention [18]. As of January 2019, 101 countries including Canada have ratified this legally binding document that regulates the emission, usage, transport and disposal of Hg. The most recent UNEP report has identified the need to better understand the processes that affect Hg deposition, methylation and uptake by organisms in the food web and how these processes will respond to global environmental change [19]. The goal in addressing these knowledge gaps through scientific research is to develop novel strategies that limit the impacts of Hg accumulation in aquatic and terrestrial ecosystems. For my PhD research, I explore how novel Hg transformation pathways tied to microbial metabolism can control Hg's mobility and toxicity in the environment.

1.2 MERCURY REDOX CYCLING

Hg redox cycling ultimately determines the inorganic Hg substrate available to Hg methylators. Although Hg^0 oxidation supplies the dissolved Hg^{II} required to produce MeHg, the same Hg^{II} can be rapidly re-reduced and re-emitted to the atmosphere from surface environments as volatile Hg^0 [2]. Hg reduction is typically dominated by abiotic photochemical reactions in aquatic and terrestrial surface environments where light is present [20-28] but can also occur via microbe-mediated pathways that are ubiquitous in the environment. For my thesis, I am primarily interested in the role that microbes play in controlling Hg speciation through Hg reduction pathways in anoxic habitats. In the following section, I will summarize what is currently known about microbial Hg reduction pathways and highlight outstanding knowledge gaps. Additional information on microbial Hg cycling can be found in the published literature reviews that comprise **Chapter 2** [29] and **Chapter 3** [30] of this thesis.

1.3 MICROBIAL MERCURY REDUCTION

The majority of research on microbial Hg reduction published to date has focused on the role of aerobic chemotrophic microbes that rely on the oxidation of inorganic and organic matter and the use of oxygen as a terminal electron acceptor to generate energy [29]. The best-studied microbial Hg reduction pathways are Hg detoxification strategies that employ a dedicated mercuric reductase (MerA) encoded by the *mer* operon [31, 32]. *Mer*-mediated Hg reduction has large energy demands in terms of the reducing power [e.g. reduced redox cofactors such as NAD(P)H] required to reduce Hg^{II} to Hg^0, which can evade the cell [31], and typically arise when the selective pressure exerted by Hg toxicity is

high. Such selective pressure is more pronounced in dark oxic environments where abiotic photoreduction is limited [33, 34]. This selective pressure has resulted in *mer*-based strategies being coupled to aerobic chemotrophic lifestyles and largely absent in anaerobes and phototrophs [29, 30, 33]. There is a growing body of evidence that suggests anaerobes and phototrophs can participate in Hg reduction through non *mer*-mediated pathways whose contributions to environmental Hg cycling remain overlooked.

1.4 ANAEROBIC AND PHOTOTROPHIC MERCURY REDUCTION

Prior to beginning my thesis research, most of work published on anaerobic Hg reduction used chemotrophic dissimilatory metal reducing bacteria (DMRB) as model organisms. These studies showed that DMRB could reduce Hg^{II} directly through iron-dependent pathways that use electron transport machinery central to anaerobic respiration [35-38]. DMRB can also reduce Hg^{II} indirectly via the intracellular and extracellular production of the iron mineral magnetite (i.e. green rust) [39, 40] or through the generation of free radicals in molecules of natural organic matter [41]. Although the obligate anaerobe *Geobacter bemidjiensis* Bem was recently shown to support a *mer*-like pathway for Hg^{II} reduction [42] there is currently no evidence of a complete *mer* operon in an obligate anaerobe [30]. Whether other types of anaerobic metabolism such as fermentation can support Hg^{II} reduction remained unexplored prior to my PhD research.

In comparison with chemotrophic Hg transformation pathways, the role of phototrophs remains understudied [29, 30]. Most of the work published to date has addressed the role of primary producers such as algae as the entry point for Hg in the food web [29]. Despite this trend, several studies have emerged over the last fifty years demonstrating that oxygenic phototrophs, which produce oxygen as a by-product of photosynthesis, can directly alter the chemical speciation of Hg. Indeed, organisms including algae [43-45], cyanobacteria [46], diatoms [47, 48] and in one study a flagellated protist *Euglena gracilis* [49] have all shown they can participate in Hg^{II} reduction through pathways that are poorly characterized at present.

At the laboratory scale, the first reports of phototrophic Hg^{II} reduction suggested that green algae exposed to high levels of Hg (e.g. mM) could enzymatically reduce Hg^{II} through detoxification strategies linked to photosynthesis [43, 50]. Since then, additional studies have provided support for a link between Hg^{II} detoxification, Hg^0 production and photosynthesis [51-54]. At the environmental scale, there is evidence that suggests phytoplankton blooms are tied to increased Hg^0 evasion [55, 56]. Whether this Hg^0 evasion is directly linked to photosynthetic activity or the indirect catalysis of abiotic photoreduction through the excretion of photoreactive compounds [48, 53, 57] remains unclear.

Although phototrophs rely on the same solar radiation that contributes to abiotic photochemical Hg^{II} reduction and Hg^0 evasion, phytoplankton blooms often occur at depths in thermally stratified aquatic systems where irradiance is attenuated [58]. A number of studies have observed peaks in Hg^0 that occur alongside phytoplankton blooms at depths where abiotic photoreduction alone cannot explain the Hg redox cycling observed

[25, 58-61]. Despite the number of laboratory and environmental studies providing the observational basis for the role of phototrophs in Hg redox cycling, mechanistic details for the direct coupling of photosynthesis to Hg^{II} reduction have been elusive.

To date, the studies that address phototrophic Hg reduction have largely ignored the diversity of phototrophic metabolisms that can potentially participate in Hg redox cycling. All the studies published prior to beginning my thesis research used oxygenic phototrophs as model organisms and the role of anoxygenic phototrophs, which do not produce oxygen during photosynthesis, had been completely ignored. Furthermore, previous work focused on the role of primary producers (e.g. autotrophs) that use light energy to convert inorganic carbon into biomass. Many phototrophs exhibit a mixotrophic lifestyle that relies on the acquisition of multiple carbon sources (inorganic and organic) and light to generate energy [62]. Mixotrophs are widely distributed in the environment and thrive in habitats such as the deep waters of thermally stratified lakes where peaks in Hg redox cycling have been observed [62]. Although it has been suggested that mixotrophic phytoplankton communities can participate in Hg redox cycling in environments where visible light is attenuated [58], whether there exists metabolic coupling points between Hg^{II} reduction, photosynthesis and carbon metabolism has yet to be demonstrated.

1.5 RATIONALE FOR THESIS

The overarching objective of my thesis is to provide mechanistic details for novel anaerobic and phototrophic Hg reduction pathways. The role that anaerobes play in Hg redox cycling is important to address because they occupy a similar ecological niche as

Hg methylators. As such, anaerobes are poised to control Hg bioavailability to Hg methylators through Hg redox cycling in anoxic habitats. My thesis focuses substantially on the role that anoxygenic phototrophs play in Hg cycling. The role of phototrophs in Hg cycling is important to address given the changes that are predicted to occur in phototrophic communities in the wake of global environmental change. Increased global temperatures, prolonged ice-free seasons and more pronounced thermal stratification in aquatic ecosystems will likely contribute to more frequent phytoplankton blooms and the eutrophication of aquatic ecosystems [63]. These changes in phototrophic community dynamics stand to have far reaching impacts on Hg cycling that must be accounted for when predicting Hg's fate in the environment under scenarios of continued anthropogenic Hg emissions.

1.6 THESIS OBJECTIVES

I have organized my thesis into two major sections. The first is comprised of literature reviews on microbial Hg transformations that compare the role of chemotrophs and phototrophs in the global Hg cycle (**Chapters 2** and **3**). These reviews were published four years apart and offer a historical perspective on how the field of research has changed over the course of my PhD research. The second section is comprised of experimental data chapters. In these chapters, I detail novel mechanisms for Hg reduction in a variety of anaerobic and phototrophic bacteria (**Chapters 4, 5, 6** and **7**). All chapters were written as standalone manuscripts and formatted for the journals in which they have been published or will be submitted to. I conclude my thesis by providing a synthesis of

my research contributions and recommendations for future research directions to pursue in the field of Hg biogeochemistry (**Chapter 8**).

The objective in **Chapters 2** and **3** was to provide a unifying framework for the scientific literature that exists on anaerobic and phototrophic Hg cycling pathways. **Chapter 2** was published at the beginning of my thesis and serves as a general summary of microbial Hg cycling that synthesizes research from the last fifty years [29]. **Chapter 3** was published at the end of my thesis and provides a more in depth view of the research published in the last five years [30]. To the best of my knowledge, these are the first reviews to critically analyze the literature on anaerobic and phototrophic Hg cycling.

The objective in **Chapter 4** was to provide mechanistic details for Hg reduction pathways supported during anoxygenic photosynthesis. In this study, I chose to work with anoxygenic phototrophic purple non-sulphur bacteria (PNSB) as model organisms because of their metabolic versatility. PNSB can grow chemotrophically (in the dark), photoautotrophically (using light for energy and inorganic carbon for biosynthesis), but they prefer growing photoheterotrophically (using light for energy and organic carbon for biosynthesis) [64, 65]. When growing photoheterotrophically, PNSB generate more reducing power than is required for biosynthesis [64, 65], which can lead to a redox imbalance that inhibits growth. PNSB maintain redox homeostasis by reducing exogenous electron sinks such as CO_2 and dimethylsulphoxide (DMSO) [64, 65]. Based on this metabolic restriction, I tested the hypothesis that Hg^{II} could act as an electron sink during photoheterotrophic growth, which would lead to Hg^0 production.

The objective in **Chapter 5** was to test whether the Hg^{II} reduction pathways observed in PNSB were present in other ecologically and phylogenetically distinct families of anoxygenic phototrophs. In this study, I chose to work with *Heliobacterium modesticaldum* Ice1, a thermophilic representative from the family Heliobacteria. Heliobacteria are a metabolically versatile family of terrestrial spore-forming obligate anaerobes that can grow photoheterotrophically and chemotrophically via fermentation [66, 67]. The decision to work with Heliobacteria was motivated by the fact that many Heliobacteria isolates originate from environments such as rice paddies [66, 68, 69] where Hg accumulation is becoming a food safety issue [70, 71]. Although *H. modesticaldum* was isolated from volcanic soils, it was selected as a model because its carbon metabolism is well-characterized [72] and it is the only Heliobacteria strain with a sequenced genome [73].

The objective in **Chapter 6** was to build on the previously established connections between cellular redox metabolism by identifying metabolic coupling points between sulphur assimilation pathways and phototrophic Hg reduction. I chose to focus on sulphur because it can act as a ligand that controls Hg's bioavailability in anoxic habitats and it is an essential nutrient that drives Hg methylation by sulphate reducing bacteria (SRB)[74]. The role of sulphur in microbial Hg reduction is poorly understood, however. In this study I chose to work with a microbial strain that was more environmentally relevant with respect to Hg cycling in rice paddies. To that gain, I examined phototrophic Hg^{II} reduction in *Heliobacillus mobilis* Romero/Guest 6, a mesophilic Heliobacteria originally isolated from a rice paddy in Thailand. This strain can grow on a variety of oxidized and reduced sulphur sources [75]. Thanks to this metabolic versatility, I was able to test the hypothesis that oxidized sulphur sources

would require more reducing power to assimilate into biomass vs more reduced sulphur sources thereby decreasing the reducing power available for photosynthetic Hg^{II} reduction.

The main objective in **Chapter 7** was to explore new methods that could be used to provide mechanistic details for anaerobic Hg redox cycling pathways. This study was primarily motivated by the recent use of Hg stable isotope fractionation as biogeochemical proxies for abiotic and biotic Hg transformation pathways [76, 77]. All biotic and abiotic Hg transformations studied to date display a mass dependent signature following Hg transformation (e.g. product pool is enriched with lighter isotopes) [76]. Some abiotic photochemical pathways also show a strong mass independent signature (e.g. enrichment of isotopes beyond what is predicted based on mass dependent models) that can be distinguished in environmental samples [76, 78]. Hg stable isotope fractionation has been used to study the mechanisms supporting several microbial Hg transformations including Hg methylation [79-81], MeHg demethylation [82] and Hg reduction [45, 83, 84]. My goal in this chapter was to develop a method to compare stable isotope fractionation during anoxygenic photosynthetic and fermentative Hg reduction in *H. modesticaldum*.

1.7 REFERENCES

1. Obrist, D.; Kirk, J. L.; Zhang, L.; Sunderland, E. M.; Jiskra, M.; Selin, N. E., A review of global environmental mercury processes in response to human and natural perturbations: Changes of emissions, climate, and land use. *Ambio* **2018,** *47*, (2), 116-140.

2. Selin, N. E.; Jacob, D. J.; Park, R. J.; Yantosca, R. M.; Strode, S.; Jaegle, L.; Jaffe, D., Chemical cycling and deposition of atmospheric mercury: Global constraints from observations. *Journal of Geophysical Research-Atmospheres* **2007,** *112*, (D2).

3. Selin, N. E., Global biogeochemical cycling of mercury: A review. In 2009; Vol. 34, pp 43-63.

4. Choi, S. C.; Chase Jr, T.; Bartha, R., Metabolic pathways leading to mercury methylation in *Desulfovibrio desulfuricans* LS. *Applied and Environmental Microbiology* **1994,** *60*, (11), 4072-4077.

5. Choi, S. C.; Chase Jr, T.; Bartha, R., Enzymatic catalysis of mercury methylation by *Desulfovibrio desulfuricans* LS. *Applied and Environmental Microbiology* **1994,** *60*, (4), 1342-1346.

6. Fleming, E. J.; Mack, E. E.; Green, P. G.; Nelson, D. C., Mercury methylation from unexpected sources: Molybdate-inhibited freshwater sediments and an iron-reducing bacterium. *Applied and Environmental Microbiology* **2006,** *72*, (1), 457-464.

7. Han, S.; Narasingarao, P.; Obraztsova, A.; Gieskes, J.; Hartmann, A. C.; Tebo, B. M.; Allen, E. E.; Deheyn, D. D., Mercury speciation in marine sediments under sulfate-limited conditions. *Environmental Science and Technology* **2010,** *44*, (10), 3752-3757.

8. Gilmour, C. C.; Podar, M.; Bullock, A. L.; Graham, A. M.; Brown, S.; Somenahally, A. C.; Johs, A.; Hurt, R.; Bailey, K. L.; Elias, D., Mercury methylation by novel microorganisms from new environments. *Environmental Science & Technology* **2013**.

9. Sunderland, E. M., Mercury exposure from domestic and imported estuarine and marine fish in the U.S. seafood market. *Environmental Health Perspectives* **2007,** *115*, (2), 235-242.

10. Zhang, H.; Feng, X.; Larssen, T.; Qiu, G.; Vogt, R. D., In inland China, rice, rather than fish, is the major pathway for methylmercury exposure. *Environmental Health Perspectives* **2010,** *118*, 1183-1188.

11. Rooney, J. P. K., The role of thiols, dithiols, nutritional factors and interacting ligands in the toxicology of mercury. *Toxicology* **2007,** *234*, (3), 145-156.

12. Matson, R. S.; Mustoe, G. E.; Chang, S. B., Mercury inhibition on lipid biosynthesis in freshwater algae. *Environmental Science & Technology* **1972,** *6*, (2), 158-160.

13. Singh, R.; Srivastava, P. K.; Singh, V. P.; Dubey, G.; Prasad, S. M., Light intensity determines the extent of mercury toxicity in the cyanobacterium *Nostoc muscorum*. *Acta Physiologiae Plantarum* **2012,** *34*, (3), 1119-1131.

14. Murthy, S.; Mohanty, P., Mercury ions inhibit photosynthetic electron transport at multiple sites in the cyanobacterium *Synechococcus* 6301. *Journal of biosciences* **1993,** *18*, (3), 355-360.

15. Sarafian, T.; Verity, M. A., Oxidative mechanisms underlying methyl mercury neurotoxicity. *International Journal of Developmental Neuroscience* **1991,** *9*, (2), 147-153.

16. Mergler, D.; Anderson, H. A.; Chan, L. H. M.; Mahaffey, K. R.; Murray, M.; Sakamoto, M.; Stern, A. H., Methylmercury exposure and health effects in humans: A worldwide concern. *Ambio* **2007,** *36*, (1), 3-11.

17. Harada, M., Minamata disease: Methylmercury poisoning in Japan caused by environmental pollution. *Critical Reviews in Toxicology* **1995,** *25*, 1-24.

18. Program, U. N. E. The Minamata Convention. http://www.mercuryconvention.org/

19. UNEP, Global mercury assessment 2013 sources, emissions, releases and environmental transport. United Nations Environment Programme. **2013**.

20. Gustin, M. S.; Biester, H.; Kim, C. S., Investigation of the light-enhanced emission of mercury from naturally enriched substrates. *Atmospheric Environment* **2002,** *36*, (20), 3241-3254.

21. Amyot, M.; Lean, D.; Mierle, G., Photochemical formation of volatile mercury in high Arctic lakes. *Environmental Toxicology and Chemistry* **1997,** *16*, (10), 2054-2063.

22. Whalin, L.; Kim, E. H.; Mason, R., Factors influencing the oxidation, reduction, methylation and demethylation of mercury species in coastal waters. *Marine Chemistry* **2007,** *107*, (3), 278-294.

23. Poulain, A. J.; Amyot, M.; Findlay, D.; Findlay, S.; Telor, S.; Barkay, T.; Hintelmann, H.; Amyot, M.; Findlay, D., Biological and photochemical production of dissolved gaseous mercury in a boreal lake. *Limnology* **2011,** *49*, 2265-2275.

24. Carpi, A.; Lindberg, S. E., Sunlight-mediated emission of elemental mercury from soil amended with municipal sewage sludge. *Environmental Science and Technology* **1997,** *31*, (7), 2085-2091.

25. Vandal, G. M.; Fitzgerald, W. F.; Rolfhus, K. R.; Lamborg, C. H., Modeling the elemental mercury cycle in Pallette Lake, Wisconsin, USA. *Water, air, and soil pollution* **1995,** *80*, (1-4), 529-538.

26. Zhang, H.; Lindberg, S. E., Sunlight and iron(III)-induced photochemical production of dissolved gaseous mercury in freshwater. *Environmental Science and Technology* **2001,** *35*, (5), 928-935.

27. Zhang, H., Photochemical redox reactions of mercury. In *Recent Developments in Mercury Science*, Atwood, D. A., Ed. 2006; Vol. 120, pp 37-79.

28. O'Driscoll, N. J.; Lean, D. R. S.; Loseto, L. L.; Carignan, R.; Siciliano, S. D., Effect of dissolved organic carbon on the photoproduction of dissolved gaseous mercury in lakes: Potential impacts of forestry. *Environmental science & technology* **2004,** *38*, (9), 2664-2672.

29. Grégoire, D. S.; Poulain, A. J., A little bit of light goes a long way: The role of phototrophs on mercury cycling. *Metallomics* **2014,** *6*, (3), 396-407.

30. Grégoire, D. S.; Poulain, A. J., Shining light on recent advances in microbial mercury cycling. *FACETS* **2018,** *3*, (1), 858-879.

31. Barkay, T.; Miller, S. M.; Summers, A. O., Bacterial mercury resistance from atoms to ecosystems. *FEMS microbiology reviews* **2003,** *27*, (2-3), 355-384.

32. Barkay, T.; Wagner-Dobler, I., Microbial transformations of mercury: Potentials, challenges, and achievements in controlling mercury toxicity in the environment. In

Advances in Applied Microbiology, Vol 57, Laskin, A. I.; Bennett, J. W.; Gadd, G. M., Eds. 2005; Vol. 57, pp 1-52.

33. Barkay, T.; Kritee, K.; Boyd, E.; Geesey, G., A thermophilic bacterial origin and subsequent constraints by redox, light and salinity on the evolution of the microbial mercuric reductase. *Environmental Microbiology* **2010,** *12*, (11), 2904-2917.

34. Schaefer, J. K.; Letowski, J.; Barkay, T., *mer*-mediated resistance and volatilization of Hg(II) under anaerobic conditions. *Geomicrobiology Journal* **2002,** *19*, (1), 87-102.

35. Sugio, T.; Fujii, M.; Takeuchi, F.; Negishi, A.; Maeda, T.; Kamimura, K., Volatilization of mercury by an iron oxidation enzyme system in a highly mercury-resistant *Acidithiobacillus ferrooxidans* strain MON-1. *Bioscience, Biotechnology and Biochemistry* **2003,** *67*, (7), 1537-1544.

36. Wiatrowski, H. A.; Ward, P. M.; Barkay, T., Novel reduction of mercury(II) by mercury-sensitive dissimilatory metal reducing bacteria. *Environmental Science and Technology* **2006,** *40*, (21), 6690-6696.

37. Qian, C.; Johs, A.; Chen, H.; Mann, B. F.; Lu, X.; Abraham, P. E.; Hettich, R. L.; Gu, B., Global proteome response to deletion of genes related to mercury methylation and dissimilatory metal reduction reveals changes in respiratory metabolism in *Geobacter sulfurreducens* PCA. *Journal of Proteome Research* **2016,** *15*, (10), 3540-3549.

38. Lin, H.; Morrell-Falvey, J. L.; Rao, B.; Liang, L.; Gu, B., Coupled mercury-cell sorption, reduction, and oxidation on methylmercury production by *Geobacter sulfurreducens* PCA. *Environmental Science and Technology* **2014,** *48*, (20), 11969-11976.

39. Wiatrowski, H. A.; Das, S.; Kukkadapu, R.; Ilton, E. S.; Barkay, T.; Yee, N., Reduction of Hg(II) to Hg(0) by magnetite. *Environmental Science and Technology* **2009,** *43*, (14), 5307-5313.

40. Liu, S.; Wiatrowski, H. A., Reduction of Hg(II) to Hg(0) by biogenic magnetite from two magnetotactic bacteria. *Geomicrobiology Journal* **2018,** *35*, (3), 198-208.

41. Lee, S.; Kim, D. H.; Kim, K. W., The enhancement and inhibition of mercury reduction by natural organic matter in the presence of *Shewanella oneidensis* MR-1. *Chemosphere* **2018,** *194*, 515-522.

42. Lu, X.; Liu, Y.; Johs, A.; Zhao, L.; Wang, T.; Yang, Z.; Lin, H.; Elias, D. A.; Pierce, E. M.; Liang, L.; Barkay, T.; Gu, B., Anaerobic mercury methylation and demethylation by *Geobacter bemidjiensis* Bem. *Environmental Science and Technology* **2016,** *50*, (8), 4366-4373.

43. Ben-Bassat, D.; Shelef, G.; Gruner, N.; Shuval, H. I., Growth of *Chlamydomonas* in a medium containing mercury. *Nature* **1972,** *240*, (5375), 43-44.

44. Kelly, D. J. A.; Budd, K.; Lefebvre, D. D., Biotransformation of mercury in pH-stat cultures of eukaryotic freshwater algae. *Archives of Microbiology* **2007,** *187*, (1), 45-53.

45. Kritee, K.; Motta, L. C.; Blum, J. D.; Tsui, M. T.-K.; Reinfelder, J. R., Photomicrobial visible light-induced magnetic mass independent fractionation of mercury in a marine microalga. *ACS Earth and Space Chemistry* **2017**.

46. Lefebvre, D. D.; Kelly, D.; Budd, K., Biotransformation of Hg(II) by cyanobacteria. *Applied and Environmental Microbiology* **2007,** *73*, (1), 243-249.

47. Pickhardt, P. C.; Fisher, N. S., Accumulation of inorganic and methylmercury by freshwater phytoplankton in two contrasting water bodies. *Environmental Science and Technology* **2007,** *41*, (1), 125-131.

48. Lanzillotta, E.; Ceccarini, C.; Ferrara, R.; Dini, F.; Frontini, F. P.; Banchetti, R., Importance of the biogenic organic matter in photo-formation of dissolved gaseous mercury in a culture of the marine diatom *Chaetoceros* sp. *Science of the Total Environment* **2004,** *318*, (1-3), 211-221.

49. Devars, S.; Avilés, C.; Cervantes, C.; Moreno-Sánchez, R., Mercury uptake and removal by *Euglena gracilis*. *Archives of Microbiology* **2000,** *174*, (3), 175-180.

50. Ben-Bassat, D.; Mayer, A. M., Volatilization of mercury by algae. *Physiologia Plantarum* **1975,** *33*, (2), 128-132.

51. Deng, L.; Wu, F.; Deng, N.; Zuo, Y., Photoreduction of mercury(II) in the presence of algae, *Anabaena cylindrical*. *Journal of Photochemistry and Photobiology B: Biology* **2008,** *91*, (2-3), 117-124.

52. Deng, L.; Deng, N.; Mou, L.; Zhu, F., Photo-induced transformations of Hg(II) species in the presence of *Nitzschia hantzschiana*, ferric ion, and humic acid. *Journal of Environmental Sciences* **2010,** *22*, (1), 76-83.

53. Deng, L.; Fu, D.; Deng, N., Photo-induced transformations of Hg(II) species in the presence of algae, *Chlorella vulgaris*. *Journal of Hazardous Materials* **2009,** *164*, (2-3), 798-805.

54. Morelli, E.; Ferrara, R.; Bellini, B.; Dini, F.; Di Giuseppe, G.; Fantozzi, L., Changes in the non-protein thiol pool and production of dissolved gaseous mercury in the

marine diatom *Thalassiosira weissflogii* under mercury exposure. *Science of the Total Environment* **2009,** *408,* (2), 286-293.

55. Baeyens, W.; Leermakers, M., Elemental mercury concentrations and formation rates in the Scheldt estuary and the North Sea. *Marine Chemistry* **1998,** *60,* (3–4), 257-266.

56. Rolfhus, K. R.; Fitzgerald, W. F., Mechanisms and temporal variability of dissolved gaseous mercury production in coastal seawater. *Marine Chemistry* **2004,** *90,* (1–4), 125-136.

57. Ben-Bassat, D.; Mayer, A. M., Reduction of mercury chloride by *Chlorella*: Evidence for a reducing factor. *Physiologia Plantarum* **1977,** *40,* (3), 157-162.

58. Poulain, A. J.; Amyot, M.; Findlay, D.; Telor, S.; Barkay, T.; Hintelmann, H., Biological and photochemical production of dissolved gaseous mercury in a boreal lake. *Limnology and Oceanography* **2004,** *49,* (6), 2265-2275.

59. Amyot, M.; Gill, G. A.; Morel, F. M. M., Production and loss of dissolved gaseous mercury in coastal seawater. *Environmental Science and Technology* **1997,** *31,* (12), 3606-3611.

60. Mason, R. P.; Morel, F. M. M.; Hemond, H. F., The role of microorganisms in elemental mercury formation in natural waters. *Water, air, and soil pollution* **1995,** *80,* (1-4), 775-787.

61. Peretyazhko, T.; Charlet, L.; Muresan, B.; Kazimirov, V.; Cossa, D., Formation of dissolved gaseous mercury in a tropical lake (Petit-Saut reservoir, French Guiana). *Science of the Total Environment* **2006,** *364,* (1-3), 260-271.

62. Raven, J. A., Contributions of anoxygenic and oxygenic phototrophy and chemolithotrophy to carbon and oxygen fluxes in aquatic environments. *Aquatic Microbial Ecology* **2009,** *56*, (2-3), 177-192.

63. Krabbenhoft, D. P.; Sunderland, E. M., Global change and mercury. *Science* **2013,** *341*, (6153), 1457-1458.

64. McKinlay, J. B.; Harwood, C. S., Carbon dioxide fixation as a central redox cofactor recycling mechanism in bacteria. *Proceedings of the National Academy of Sciences of the United States of America* **2010,** *107*, (26), 11669-11675.

65. Richardson, D. J.; King, G. F.; Kelly, D. J.; McEwan, A. G.; Ferguson, S. J.; Jackson, J. B., The role of auxiliary oxidants in maintaining redox balance during phototrophic growth of *Rhodobacter capsulatus* on propionate or butyrate. *Archives of Microbiology* **1988,** *150*, (2), 131-137.

66. Asao, M.; Madigan, M. T., Taxonomy, phylogeny, and ecology of the Heliobacteria. *Photosynthesis Research* **2010,** *104*, (2-3), 103-111.

67. Tang, K. H.; Yue, H.; Blankenship, R. E., Energy metabolism of *Heliobacterium modesticaldum* during phototrophic and chemotrophic growth. *Bmc Microbiology* **2010,** *10*.

68. Stevenson, A. K.; Kimble, L. K.; Woese, C. R.; Madigan, M. T., Characterization of new phototrophic Heliobacteria and their habitats. *Photosynthesis Research* **1997,** *53*, (1), 1-12.

69. Ormerod, J. G.; Kimble, L. K.; Nesbakken, T.; Torgersen, Y. A.; Woese, C. R.; Madigan, M. T., Endospore-forming Heliobacteria from rice field soils. *Archives of Microbiology* **1996,** *165*, 226-234.

70. Zhang, H.; Feng, X. B.; Larssen, T.; Qiu, G. L.; Vogt, R. D., In inland China, rice, rather than fish, is the major pathway for methylmercury exposure. *Environmental Health Perspectives* **2010,** *118*, (9), 1183-1188.

71. Rothenberg, S. E.; Windham-Myers, L.; Creswell, J. E., Rice methylmercury exposure and mitigation: A comprehensive review. *Environmental Research* **2014,** *133*, 407-423.

72. Tang, K. H.; Feng, X. Y.; Zhuang, W. Q.; Alvarez-Cohen, L.; Blankenship, R. E.; Tang, Y. J., Carbon flow of Heliobacteria is related more to Clostridia than to the green sulfur bacteria. *Journal of Biological Chemistry* **2010,** *285*, (45), 35104-35112.

73. Sattley, W. M.; Swingley, W. D., Properties and Evolutionary Implications of the Heliobacterial Genome. In *Genome Evolution of Photosynthetic Bacteria*, Beatty, J. T., Ed. 2013; Vol. 66, pp 67-97.

74. Jeremiason, J. D.; Engstrom, D. R.; Swain, E. B.; Nater, E. A.; Johnson, B. M.; Almendinger, J. E.; Monson, B. A.; Kolka, R. K., Sulfate addition increases methylmercury production in an experimental wetland. *Environmental Science and Technology* **2006,** *40*, 3800-3806.

75. Beer-Romero, P.; Gest, H., *Heliobacillus mobilis*, a peritrichously flagellated anoxyphototroph containing bacteriochlorophyll g. *FEMS Microbiology Letters* **1987,** *41*, 109-114.

76. Blum, J. D.; Sherman, L. S.; Johnson, M. W., Mercury isotopes in Earth and environmental sciences. *Annual Review of Earth and Planetary Sciences* **2014,** *42*, (1), 249-269.

77. Kritee, K.; Blum, J. D.; Reinfelder, J. R.; Barkay, T., Microbial stable isotope fractionation of mercury: A synthesis of present understanding and future directions. *Chemical Geology* **2013,** *336*, 13-25.

78. Bergquist, B. A.; Blum, J. D., Mass-dependent and -independent fractionation of Hg isotopes by photoreduction in aquatic systems. *Science* **2007,** *318*, (5849), 417-420.

79. Janssen, S. E.; Schaefer, J. K.; Barkay, T.; Reinfelder, J. R., Fractionation of mercury stable isotopes during microbial methylmercury production by iron- and sulfate-reducing bacteria. *Environmental Science & Technology* **2016,** *50*, (15), 8077-8083.

80. Rodríguez-González, P.; Epov, V. N.; Bridou, R.; Tessier, E.; Guyoneaud, R.; Monperrus, M.; Amouroux, D., Species-specific stable isotope fractionation of mercury during Hg(II) methylation by an anaerobic bacteria (*Desulfobulbus propionicus*) under dark conditions. *Environmental Science & Technology* **2009,** *43*, (24), 9183-9188.

81. Perrot, V.; Bridou, R.; Pedrero, Z.; Guyoneaud, R.; Monperrus, M.; Amouroux, D., Identical Hg isotope mass dependent fractionation signature during methylation by sulfate-reducing bacteria in sulfate and sulfate-free environment. *Environmental Science & Technology* **2015,** *49*, (3), 1365-1373.

82. Kritee, K.; Barkay, T.; Blum, J. D., Mass dependent stable isotope fractionation of mercury during mer mediated microbial degradation of monomethylmercury. *Geochimica et Cosmochimica Acta* **2009,** *73*, (5), 1285-1296.

83. Kritee, K.; Blum, J. D.; Barkay, T., Mercury stable isotope fractionation during reduction of Hg(II) by different microbial pathways. *Environmental Science & Technology* **2008,** *42*, (24), 9171-9177.

84. Kritee, K.; Blum, J. D.; Johnson, M. W.; Bergquist, B. A.; Barkay, T., Mercury stable isotope fractionation during reduction of Hg(II) to Hg(0) by mercury resistant microorganisms. *Environmental Science and Technology* **2007,** *41*, (6), 1889-1895.

Chapter 2: A little bit of light goes a long way: the role of phototrophs on mercury cycling

Daniel S. Grégoire [a] & Alexandre J. Poulain [a]

a - Biology Department, University of Ottawa, 30 Marie Curie, Ottawa, ON, K1N 6N5, Canada.

This literature review was originally published as: **Grégoire, D. S.**; Poulain, A. J., A little bit of light goes a long way: The role of phototrophs on mercury cycling. *Metallomics* **2014,** *6*, (3), 396-407.

Direct link:

https://pubs.rsc.org/en/Content/ArticleLanding/2014/MT/c3mt00312d#!divAbstract

2.1 ABSTRACT

Among toxic metals, mercury (Hg) is a global priority contaminant due to the biomagnification of the most toxic form methylmercury (MeHg) in food webs, even in remote regions, such as the high Arctic. The importance of Hg as a chemical of major concern to human health was underscored by the recent adoption of the Minamata Convention on Mercury, a legally binding treaty that requires government agencies be equipped to monitor processes affecting global mercury transport and cycling. For several decades now, field and laboratory experiments have shown that phototrophs can directly interact with Hg and affect its speciation and fate. While an important body of work on the role of chemotrophic microbes on Hg cycling has been undertaken, the role of phototrophs is too often overlooked. Strikingly, what is known about phototroph-Hg interactions pertains mostly to oxygenic phototrophs with relatively little being known about anoxygenic phototrophs. Ongoing environmental change will no doubt affect the physical and chemical properties of aquatic ecosystems, which in turn will alter all phototrophic community dynamics. How these changes will affect the Hg cycle represents an important knowledge gap. After synthesizing what is currently known about chemotrophic Hg transformations, we describe the current state of knowledge on what is known about how phototrophs (bacteria and algae) affect Hg cycling (i.e., alteration of Hg redox state, Hg scavenging, potential for methylation) as well as describe the cellular and molecular targets of Hg toxicity in phototrophs. We discuss these interactions in an evolutionary context and provide recommendations for future research directions.

2.2 INTRODUCTION

Mercury (Hg) is a global pollutant and a potent neurotoxin [1] and as such, a serious health concern to humans [2] and wildlife [3]. Anthropogenic sources of Hg pollution include metal production, gold mining, chlor-alkali plants, waste incineration and fossil fuel combustion [4] while natural sources include volcanic activity and forest fires [5]. Hg is emitted primarily as volatile elemental Hg (Hg^0), which can travel long distances through the atmosphere for up to a year before settling in terrestrial or aquatic ecosystems [5]. Hg is deposited within ecosystems chiefly through wet and dry depositions in its oxidized form, Hg^{II} [6]. From that point, Hg can potentially be subject to methylation, thereby entering aquatic food webs, reduction to Hg^0 and potentially be re-emitted to the atmosphere, or sequestration in sediments [7].

The Hg biogeochemical cycle involves several abiotic and biotic pathways. Biological pathways are of particular interest because they can act as a route for Hg bioaccumulation; they also have a direct impact on its fate by altering Hg speciation. Microbes that respond strongly to environmental variables such as temperature [8-11], pH [12] and salinity [13, 14], also influence Hg biogeochemical cycling. Given that global environmental changes have resulted in considerable fluctuation of these variables in aquatic ecosystems [15-17], the effects these changes will have on microbial activity and their role in the biogeochemical cycle of Hg stand to change as well.

Microorganisms inhabiting soil and aquatic environments capable of affecting Hg speciation include chemotrophic and phototrophic microorganisms, deriving their energy from the oxidation of inorganic or organic matter or harvesting light energy, respectively. An important body of work on the role of chemotrophic microbes on Hg cycling has been

undertaken and reviewed elsewhere [18-22]. The role of phototrophs, however, is too often overlooked, even though they are key ecological players in aquatic ecosystems. Indeed, most phototrophic microorganisms are also primary producers within ecosystems; as such, their activity directly reflects their immediate physical and chemical environment, rapidly changing due to ongoing environmental changes [23]. Over the last few years, there have been many key advances in the field of mercury microbiology; after synthesizing of what is known of Hg transformation by chemotrophs, we critically evaluate the current state of knowledge on how phototrophs (algae and bacteria carrying out oxygenic and anoxygenic photosynthesis) affect Hg cycling and offer suggestions for research directions aiming at filling knowledge gaps in our understanding of the interplay between Hg cycling and photosynthesis.

2.3 CHEMOTROPHIC MERCURY TRANSFORMATIONS

2.3.1 Mercury methylation

Several groups of bacteria, typically anaerobes, including sulphate reducing bacteria (SRB)[24, 25], iron reducing bacteria (IRB) [26], methanogens [27] and members of the Firmicutes phylum have recently been linked to Hg methylation in a broad array of environments including aquatic systems, rice paddies and animal guts [28]. Methylation in marine environments has also been associated with oxic pelagic microbial communities [29, 30]. Methylation is thought to be an intracellular process limited by the uptake of inorganic Hg species [31-34]. Methylation was initially thought to be related to the activity of acetyl-CoA [24] and a corrinoid type protein involved in the methyl group transfer [25] and recent work has identified two genes, *hgcA* and *hgcB*, which support the involvement of a

corrinoid type protein and a ferredoxin in methylation [35]. The recent discovery of these genes has provided a genetic marker to assess the diversity of potential methylators that is now known to span several families including the Proteobacteria, Firmicutes and Euryarchaoaeta [28, 35, 36].

2.3.2 Mercury demethylation

Bacteria exhibiting broad-spectrum resistance to MeHg and Hg^{II} have shown a dedicated detoxification pathway by way of reductive demethylation (RD) [18]. The resistance to MeHg is attributed to the presence of the organomercurylyase enzyme (OL) encoded by the *merB* gene as part of the *mer* operon [19]. OL is a cytosolic enzyme that removes methyl groups by splitting the C-Hg bond [37]. This pathway is dependent on intracellular Hg concentrations and the toxicity of the Hg species present, which is why it is typically observed in more heavily impacted environments [18, 38]. Such environments include both terrestrial and aquatic ecosystems in proximity to industrial inputs of Hg, mining operations and fuel combustion from which pollution can also be transported via streams and rivers [39]. Several environmental conditions affect how microorganisms demethylate Hg. Within the water column and sediments of these systems, redox conditions influence RD, which typically occurs at the oxic/anoxic transition zone where concentrations of MeHg are higher [20, 40-43]. An additional pathway for demethylation exists in the environment involving SRB which degrade $(MeHg)_2S$ to CH_4 and MeHg [44] although it is non-dependent on the OL enzyme.

Oxidative demethylation (OD) of MeHg is a non-specific pathway that occurs as part of a cometabolic process involving simple carbon sources (i.e. C1 compounds) [21]. OD resembles monomethylamine degradation by methanogens [18] and acetate oxidation by SRB [45] although precise mechanistic details are currently lacking. The pathway is characterized by the production of Hg^{II} and CO_2 although CO_2 can also arise due to the anaerobic oxidation of CH_4 following RD [37]. OD is not induced by Hg and instead depends on the general metabolic capabilities of the bacteria and the availability of MeHg as seen in several different types environments [41, 46, 47]. While it has been observed under aerobic [40] and anaerobic conditions [45], several studies suggest that this pathway is more prevalent in anaerobic environments [45, 48, 49] where methanogens [46] and SRB [49] are known to thrive. These microbes that contribute to OD are also dependent on environmental concentrations and competition for electron donors such as H_2 and carbon sources such as acetate; indeed, SRB-driven OD tends to outcompete methanogens in marine waters although both contribute to varying degrees in freshwater [45, 50, 51].

2.3.3 Mercury reduction

Hg^{II} reduction is responsible for Hg evasion from terrestrial [52-54] and aquatic ecosystems [55-58], as Hg^0 is volatile [59, 60]. Abiotically, photochemical reactions are the predominant pathway of Hg reduction in terrestrial and aquatic ecosystems where light is present [52, 55-58, 61-65] but Hg reduction can also occur in the dark due to chemical reactions with green rust [53], mixed phase Fe^{II}/Fe^{III} [66] and reactive groups on humic substances in both oxic [67] and anoxic conditions [68, 69]. Hg reduction also occurs via biological pathways involving microorganisms and is ubiquitous in the environment. It is prevalent in environments

where light alone cannot provide the energy required to abiotically reduce Hg^{II} to Hg^{0} or where higher concentrations of Hg are present or environmental conditions enhance its toxicity thereby exerting a selective pressure for dedicated resistance strategies to arise [70, 71].

Bacteria can be involved in Hg reduction via activity of the mercuric reductase (MR) enzyme. MR is a cytosolic protein coded by the *merA* gene observed in gram-negative bacteria, gram-positive bacteria and archaea [19]. Hg reduction via MR is a two-step process dependent on the intracellular concentration of Hg^{II} [72]. Hg species in the environment are taken up by the cell via a series of scavenging and transport proteins (e.g., MerP and MerT, respectively) followed by diffusion into the cytoplasm where NAD(P)H and FADH dependent Hg reduction by the MR (MerA) occurs [73]. The dependence of this pathway on reducing equivalents carries an important energy cost and is fully induced only when Hg is highly toxic. Conditions that increase Hg's toxicity are found in the presence of oxygen favouring the presence of oxidized Hg species and the generation of reactive oxygen species [72]. Aerobic conditions also possibly decrease the abundance of binding sites for Hg (e.g., thiol groups) on the exterior of the cell membrane favouring its transport to the cytoplasm [72].

Non *mer*-mediated enzymatic pathways also exist. For instance, it has been observed in Hg resistant strains of the autotrophic acidophile *Acidithiobacillus ferooxidans*, which reduced Hg^{II} to Hg^{0} in media amended with high concentrations of Fe^{II} despite the absence of the *merA* gene [74]. The bacterium's ability to reduce Hg was attributed to the activity of cytochrome c oxidase enzymes involved in Fe oxidation [74]. In anaerobic conditions, the dissimilatory metal reducing bacterium *Shewanella oneidensis* MR-1 was

able to reduce Hg^{II} via an Fe^{II} dependent pathway, although this was not ubiquitous across metal reducing bacteria likely due to physiological differences in the respiratory chain [75]. Additional work involving the Fe redox cycle has showed that mixed Fe^{II}/Fe^{III} magnetite produced by bacteria can indirectly contribute to Hg^{II} reduction as well [66].

2.3.4 Mercury oxidation

One of the least studied and understood processes of the Hg geochemical cycle is Hg^0 oxidation. The potential for bacterial Hg^0 oxidation was first proposed when researchers observed that chemotrophic bacteria incubated in the presence of Hg^0 as the sole source of Hg suffered growth inhibition despite the non-toxic nature of Hg^0 [76]. Although these studies provided no mechanistic details, formation of Hg^{II} was suspected as the source of growth inhibition [76]. A potential pathway involving the catalase enzyme has been explored as a means for biological oxidation of Hg [77-79]. Very recently, alternate pathways for Hg oxidation have been explored under anoxic conditions. The obligate anaerobe SRB, *Desulfovibrio desulfuricans*, was able to oxidize Hg^0 to Hg^{II} [80]. Similar work has also shown that different SRB and IRB species were able to oxidize Hg^0 under anoxic conditions with some capable of methylating Hg^0 [81]. In these cases, Hg^0 oxidation is predicted to occur extracellularly, via low molecular weight thiols bearing stable –SH groups located on the cell membrane [80].

2.4 PHOTOTROPHIC MICROBIAL MERCURY TRANSFORMATIONS

For several decades now, field and laboratory experiments have shown that phototrophs such as algae, cyanobacteria, diatoms and in one study, a flagellated protist *Euglena gracilis*, can directly interact with Hg and affect its speciation [11, 82-86]. Most of the work performed with phototrophs, which does not focus on Hg bioaccumulation, pertains to Hg^{II} reduction leading to the formation of Hg^0. Hg^{II} reduction to Hg^0 in biological systems is often thought of as a detoxification mechanism as it leads to the formation of a less toxic, readily evaded species, Hg^0. When tentatively applied to phototrophs, this perception is somehow challenged by the fact that phototrophs are dependent on the same light energy that is otherwise involved in photochemical reduction of Hg^{II} to Hg^0. Due to ecological constraints, however, phototrophic blooms often occur at depths where incident light energy, although harvested by phototrophic microbes for growth purposes, cannot catalyze photochemical Hg reduction [58]. On the other hand, with light energy available for growth in oxic environments where Hg tends to be more toxic, conditions may have been conducive to develop alternative strategies to the demanding *mer* operon.

The case of phototrophs provides an interesting evolutionary perspective from which to discuss how metabolically diverse microorganisms can affect Hg speciation. With this evolutionary perspective in mind, the focus of this section is to provide a unified framework for the key findings supporting the role of phototrophs in Hg transformations. This section of the review is organized around **Fig 2.1**, which highlights proposed and tested pathways for phototrophic Hg cycling.

2.4.1 Mercury uptake by phototroph cells

Phototrophs are ubiquitous in aquatic ecosystems where, as primary producers, they support higher trophic level consumers and are the entry point for Hg in the food web [87]. So far it is thought that inorganic Hg enters phototrophic cells predominantly in the form of neutrally charged Hg complexes by passive diffusion through biological membranes [88, 89]. Active uptake is also thought to play a role, as Hg can be taken up by transport mechanisms used for other vital cations, which are powered by photosynthesis-derived energy [90-92].

Most phototrophs possess a cell wall in addition to the cytoplasmic membrane, between the intracellular environment and aqueous solution of which composition varies. Cell walls in oxygenic phototrophs include the cellulose wall in algae [93], peptidoglycan layer in cyanobacteria [94], and silica frustule in diatoms. As a barrier, the cell wall exerts distinct effects on the accidental uptake of inorganic and organic Hg species. A common aspect of these cell walls is a high polysaccharide content rich in phosphate moieties, carboxylates [95] and thiol groups that favour Hg binding to the outside of the cell [96]. The high degree of irreversible Hg binding to the exterior of the cell is ultimately what reduces the accumulation of inorganic Hg species in the cell cytoplasm [97, 98] as compared to organic Hg species that tend to bioaccumulate in larger quantities [99]. As such, organic Hg complexes tend to bioaccumulate in phototroph cells as they diffuse more freely through lipophilic membranes [88] (see **Fig 2.1, (1)**). Organic Hg species can also be actively transported into the cell cytoplasm, although the pathways remain unknown [100, 101]. Photosynthesis influences this transport by supplying the energy and molecules necessary for the production of metabolites that act as transport agents, namely peptides

rich in cysteine residues and thiols, which increase the efficiency of organo-Hg complex transport [100, 102, 103].

Anoxygenic phototrophs, including purple sulphur bacteria (PSB), green sulphur bacteria (GSB) and purple non-sulphur bacteria (PNSB) exhibit a gram-negative type cell wall structure characterized by the presence of a lipopolysaccharide (LPS) layer [104-106]. Green non-sulphur bacteria (GNSB) and Heliobacteria cell walls are devoid of an LPS layer but still exhibit a peptidoglycan layer [104, 105, 107]. Strikingly, and despite their diversity and the metal requirement for the photosynthetic apparatus [98, 108], very few studies addressed metal interaction with cell membranes or uptake in anoxygenic phototrophs [109-111]; to date no studies have focused on Hg uptake by anoxygenic phototrophs.

2.4.2 Mercury sequestration by phototroph cells

Once in the cytoplasm, Hg^{II} reacts with sulphydryl rich ligands including protein and non-protein thiol moieties [112]. Non-protein thiol moieties can be found in abundance in peptides such as phytochelatins [113, 114] and glutathione (the precursor to phytochelatin synthesis [115]) in algae and metallothioneins in cyanobacteria [116]. These peptides act as Hg chelating agents, representing a non-redox detoxification pathway for phototrophs by diverting Hg from binding to essential proteins [116-118] (see **Fig 2.1, (2)**). The role of these chelating peptides as a resistance strategy is further supported by the ability of phototrophs to respond to increased concentrations of not only Hg [119], but also other heavy metals such as Cu, Cd and Zn, by increasing the synthesis of phytochelatins [117, 120].

It was also proposed that phototrophic organisms might catalyze the formation of insoluble Hg species as a detoxification mechanism [121]. This pathway involves the formation of cinnabar (HgS) and the more soluble meta-cinnabar (β-HgS) [122]. The production of β-HgS via the intracellular thiol ligand pool (see **Fig 2.1, (2)**) has actually been observed in different Phyla of phototrophs including cyanobacteria [11] and algae [84, 121]. HgS formation was shown to occur simultaneously with Hg^0 evolution, providing support for the role of phototrophs in Hg^0 production and indicating the potential for multiple resistance strategies [11]. This is not the only example of phototrophs controlling the solubility of elements with previously reported cases of silicate, carbonate and Fe biomineralization [123]. Given that the ability to catalyze HgS formation spans the two domains of life harbouring phototrophs, perhaps these strategies are more widespread than currently perceived.

2.4.3 Mercury toxicity towards photosynthetic machinery

Once the Hg scavenging capacity of the cell has been exceeded, Hg will target essential components of the photosynthetic apparatus. Much of the work performed to date toward characterizing the effects of Hg on photosynthesis has focused on the oxygenic photosynthetic machinery of algae [101, 124-130], cyanobacteria [91, 131, 132] and diatoms [101, 128, 133]. In oxygenic phototrophs, the affinity of Hg^{II} for structural bonds in proteins and ability to accept electrons are the main modes of action in which it affects photosynthetic machinery [112, 127, 128]. Inhibition of pigment synthesis and pigment degradation, likely via core-cation substitution with Hg^{II} and binding to key functional carboxylate groups in chlorophyll, are common effects associated with Hg exposure [91, 129, 134]. Hg interacts with

PSII by increasing the number inactive reaction centers, thus preventing efficient transfer of light energy, [126, 135] and disrupts the operation of the oxygen evolving complex [134, 135] by replacing the Mn^{II} cofactor with Hg^{II} [91, 125]. Organic and inorganic Hg complexes can inhibit several aspects of electron transport by affecting proteins synthesizing electron carrier components or directly interacting with them via redox reactions (e.g., with the quinone pools [126, 127], cytochrome b_6f [132, 136], Fe-S clusters in PSI [131] and disrupt electron transfer between PSII and PSI [125, 133] through direct interaction with plastocyanin [136]). Thus far, there have been no tests as to whether the aforementioned interactions are linked to changes in Hg speciation, although we can speculate that they may alter its redox state, as further discussed herein.

Metal toxicity under anaerobic conditions is poorly understood and remained until very recently mostly unexplored; indeed, transition metals are mostly toxic by interacting with oxygen and mechanisms of toxicity under anoxic conditions have historically been overlooked. It only recently became the focus of research with studies investigating Fe, Cu [137, 138], Co, Ni [110] and Hg [90, 139] toxicity towards anoxygenic phototrophs, particularly PNSB. In PNSB, Hg damages light harvesting (LH) complex and reaction center structural integrities [90, 140], it also impedes cyclical electron transport by reacting with cytochrome c_2 and quinone pools [90]. We still don't know how PNSB handle Hg stress but one study suggests that *R. sphaeroides* can reduce Hg^{II} during lag phase [139], as previously observed for chemotrophs [19]. While Hg^{II} reduction is a likely pathway for detoxification, no mechanistic details on Hg resistance were provided. Note, that the *mer* operon is absent in PNSB, as such they may use a novel reductase similar to what was recently observed in a cyanobacterium [141].

2.4.4 Phototrophic mercury reduction

The potential for phototrophic organisms to directly contribute to Hg cycling through enzymatic production of Hg^0 was first proposed when green algae exposed to high concentrations of Hg^{II} [82] (e.g. mM range) produced Hg^0 as a suspected detoxification mechanism linked to their photosynthetic activity [142] (see **Fig 2.1, (3-5)**). This work was followed by the isolation of metabolites referred to as reductive compounds that seemed to alleviate the toxicity of Hg [143]. Since then, there have been similar observations in different phototrophic organisms exposed to lower concentrations (e.g. nM range), supporting the involvement of photosynthesis in Hg detoxification [144-146]. The involvement of photosynthesis in Hg^0 production is also supported by laboratory observations where actively growing phototrophic cells produced more Hg^0 than heat killed cells [82, 147] and light exposed diatoms produced Hg^0 at a decreasing rate once light was removed [119].

In surface waters, through the excretion of photoreactive organic compounds, algae can affect Hg redox cycling (see **Fig 2.1, (5)**) [83, 143, 145]. Often, phytoplankton blooms in ocean surface waters are associated with increased Hg^0 evasion [148-150]; however, in these cases, it is unclear whether phototrophs are directly involved in Hg^0 production by coupling Hg^{II} reduction to their photosynthetic machinery or indirectly responsible for Hg^0 production via the release of photoreactive compounds. At depth, field studies suggest that maximum activity in redox cycling seems correlated to algal and bacterial metalimnetic blooms [56, 58, 62, 151]. These blooms occur during the summer, the fall and under ice cover, in freshwater and marine environment both at depths and light levels that challenge the role of abiotic photochemical reactions and seem correlated

to the carbon acquisition strategy of the dominant phototrophic population [58, 152, 153], supporting a link between photosynthesis and Hg redox cycling. Regardless of the mechanisms involved, whether or not anoxygenic phototrophs contribute to Hg reduction remains to be tested.

Interestingly, the *mer* operon has yet to be widely observed in anaerobic and phototrophic microorganisms [72, 154]. Under anaerobic conditions, Hg toxicity is lowered due to reducing conditions favouring the formation of inorganic sulphides, a strong Hg scavenger that can eventually lead to Hg precipitation, and the short lifespan of reactive oxygen species [155]. For phototrophs, the dependence on light energy and its abundance in their preferred habitat where photochemical pathways likely dominate Hg reduction would alleviate toxicity as Hg is transformed into less toxic and readily volatile Hg^0. Interestingly, phototrophs have the ability to reduce Hg through mostly unspecified pathways [62]. Until very recently, and to the best of our knowledge, a sole study investigated the activity of MerA-like enzyme in a phototroph, the cyanobacterium *Synechocystis*, with the enzyme operating in the reduction of Hg and U [141]).

Except in the case of a *Synechocystis* strain, which used a glutaredoxin-mediated pathway [141], the mechanistic details of direct phototrophic reduction of Hg^{II} remain unknown, and older studies need to be carefully interpreted in light of the importance of photoreduction, even if only visible radiations were used. Further characterization of genetic determinants encoding photosynthesis driven Hg reduction is an important topic to pursue as it may lead to optimizing phototroph-mediated reduction processes, often used in bioremediation. As a starting point, there exist several redox-reactive sites within the electron transport chain where Hg^{II} could be reduced, such as the quinone pools,

cytochromes (e.g. cytochrome b_6f in oxygenic phototrophs [136] and c_2 in anoxygenic phototrophs [90]), Fe-S clusters [131] and plastocyanin [136], which Hg is already known to react with.

2.4.5 Phototrophic methylation of mercury

While phototrophic blooms have been associated with increases in Hg^0 production they also contribute indirectly to MeHg production by creating environments conducive to methylation. Indeed, phytoplankton die-offs associated with eutrophication create anoxic conditions deep in the water column that stimulate the activity of methylators such as SRB [156]. Algal mats can also act as a colonization surface and source of nutrients for epiphytic methylating bacteria [157]; this is supported by positive correlations between phototrophic productivity and methylation rates in stream algal blooms [158]. Finally, phototrophs can indirectly affect the availability of Hg as a substrate for the bacterial methylating community through the biogenic production of iodomethane (ICH_3) that solubilizes mineral HgS and possibly increases its availability to epiphytic methylators [157] (see **Fig 2.1, (6)**).

Cases of direct phototrophic methylation have been observed [159, 160] although they are few in number, and mechanistic details have yet to be elucidated. Thus far, direct MeHg production in phototrophs has shown to be a laboratory phenomenon producing very low and variable concentration across species [159, 160] (see **Fig 2.1, (7)**). Given the poor understanding of direct methylation of Hg by phototrophs and the important implications it may have on bioaccumulation dynamics, clarification of what environmental variables affect its occurrence is important to develop to properly assess its influence in nature.

2.4.6 Phototrophic oxidation of mercury

Thus far, no studies have addressed the potential of phototrophic organisms to oxidize Hg^0 and we can only speculate based on what is known of the redox chemistry of photosynthesis. Redox potential of PSII has been estimated at ranging from +1.1 to 1.2 V, depending on which species and pigments are present [161, 162], which would allow for electrons to flow from Hg^0 to PSII, ($0.7V < E^0(Hg^0/Hg^{2+}) < 0.85V$, depending on the environmental conditions[163]). The redox potential of PSI, the only photosystem of anoxygenic phototrophs ($0.3\ V < E_{PSI} < 0.5V$) [161, 162, 164, 165], is too low to catalyze Hg^0 oxidation in a one step, two-electron transfer. However, PSI could catalyze a one electron transfer reaction between Hg^0 and Hg^I (present as Hg_2^{2+} with $E^0(Hg^0/Hg_2^{2+}) = 0.4V$ [163]). Note that Hg redox potential will change with the nature of the ligands present in solution, and whether Hg^0 oxidation can be catalyzed by one of the photosystems remains to be tested. That being said, newly produced Hg^{II} would bind to essential proteins of the photosynthetic apparatus (as shown in previous sections of this review) thereby greatly impairing cell metabolism. It is therefore unlikely that cells evolved the ability to use Hg^0 as an electron donor without a whole suite of chaperone proteins to alleviate Hg^{II} or Hg^I toxicity. Finally, Hg^0 oxidation by phototrophs may not occur intracellularly but be catalyzed by membrane bound thiols similar to what has been observed for chemotrophs [80, 81].

2.5 CONCLUDING REMARKS

The case of phototrophic Hg transformations is perplexing mainly in terms of the mechanistic details of their ability to alter Hg speciation. As previously mentioned, their optimal habitat in surface waters is both conducive to high concentration of toxic Hg species but also a prime environment for photoreduction to alleviate this stress. When we consider pathways such as those involving the *mer* operon likely evolved in thermophilic environments where high levels of Hg were present [154], the dominant selective pressure seems intuitive. The case with phototrophs is more complex given their dependence on light, which bears the question: Are light driven phototrophic Hg transformations a detox mechanism?

Phototrophs have developed several strategies for resisting Hg including chelating peptides [113] and so far mostly uncharacterized enzymatic pathways catalyzing redox Hg transformations [82, 139, 141, 143]. At the cellular scale, numerous questions remain to be asked as to the mechanisms of Hg interactions with phototrophs both in terms of what affects Hg uptake and how Hg interacts with the photosynthetic machinery.

At the ecosystem level, phototrophs are poised to play an important role in the toxicity and mobility of Hg, particularly within the context of climate change [166]. Their role is complex; for instance, an increase in primary productivity can affect Hg^{II} reduction, potentially leading to its evasion [167], phytoplankton blooms can contribute to MeHg biodilution within food webs [147, 168] but such blooms, to the extreme, can also lead to eutrophication, setting the stage for conditions conducive to Hg methylation. Given that there is continued input of anthropogenic Hg to terrestrial and aquatic ecosystems [169], and that environmental variables such as temperatures, pH, and nutrient concentrations

are slated to change significantly [166], understanding the timing and extent of phototrophs' responses to these changes and what this means for Hg cycling will become increasingly important, particularly within the context of remediation where their potential to directly affect Hg transformation remains untapped.

2.6 ACKNOWLEDGMENTS

We would like to thank Kelsey Huus and the Poulain lab members for constructive comments on earlier version of this manuscript. We would like to thank Tamar Barkay for many stimulating discussions on how phototroph may have evolved in the presence of Hg. We would like to thank the Natural Sciences and Engineering Research Council of Canada for supporting Hg biogeochemistry research conducted in the Poulain laboratory.

2.7 REFERENCES

1. Clarkson, T. W., The toxicology of mercury. *Critical Reviews in Clinical Laboratory Sciences* **1997,** *34*, (4), 369-403.

2. Sarafian, T.; Verity, M. A., Oxidative mechanisms underlying methyl mercury neurotoxicity. *International Journal of Developmental Neuroscience* **1991,** *9*, (2), 147-153.

3. Lawson, N. M.; Mason, R. P., Accumulation of mercury in estuarine food chains. *Biogeochemistry* **1998,** *40*, (2-3), 235-247.

4. Galbreath, K. C.; Zygarlicke, C. J., Mercury speciation in coal combustion and gasification flue gases. *Environmental Science and Technology* **1996,** *30*, (8), 2421-2426.

5. Selin, N. E.; Jacob, D. J.; Park, R. J.; Yantosca, R. M.; Strode, S.; Jaegle, L.; Jaffe, D., Chemical cycling and deposition of atmospheric mercury: Global constraints from observations. *Journal of Geophysical Research-Atmospheres* **2007,** *112*, (D2).

6. Fitzgerald, W. F.; Engstrom, D. R.; Mason, R. P.; Nater, E. A., The case for atmospheric mercury contamination in remote areas. *Environmental Science and Technology* **1998,** *32*, (1), 1-7.

7. Selin, N. E., Global biogeochemical cycling of mercury: A review. In 2009; Vol. 34, pp 43-63.

8. Bell, C.; McIntyre, N.; Cox, S.; Tissue, D.; Zak, J., Soil microbial responses to temporal variations of moisture and temperature in a Chihuahuan Desert Grassland. *Microbial Ecology* **2008,** *56*, (1), 153-167.

9. Zogg, G. P.; Zak, D. R.; Ringelberg, D. B.; MacDonald, N. W.; Pregitzer, K. S.; White, D. C., Compositional and functional shifts in microbial communities due to soil warming. *Soil Science Society of America Journal* **1997,** *61*, (2), 475-481.

10. Barkay, T.; Kroer, N.; Poulain, A. J., Some like it cold: Microbial transformations of mercury in polar regions. *Polar Research* **2011,** *30*, (SUPPL.1).

11. Lefebvre, D. D.; Kelly, D.; Budd, K., Biotransformation of Hg(II) by cyanobacteria. *Applied and Environmental Microbiology* **2007,** *73*, (1), 243-249.

12. Meron, D.; Atias, E.; Kruh, L. I.; Elifantz, H.; Minz, D.; Fine, M.; Banin, E., The impact of reduced pH on the microbial community of the coral *Acropora eurystoma*. *Isme Journal* **2011,** *5*, (1), 51-60.

13. Witt, V.; Wild, C.; Anthony, K. R. N.; Diaz-Pulido, G.; Uthicke, S., Effects of ocean acidification on microbial community composition of, and oxygen fluxes through, biofilms from the Great Barrier Reef. *Environmental Microbiology* **2011,** *13*, (11), 2976-2989.

14. Compeau, G.; Bartha, R., Methylation and demethylation of mercury under controlled redox, pH and salinity conditions. *Applied and Environmental Microbiology* **1984,** *48*, (6), 1203-1207.

15. Parmesan, C., Ecological and evolutionary responses to recent climate change. In *Annual Review of Ecology Evolution and Systematics*, 2006; Vol. 37, pp 637-669.

16. Schindler, D. W.; Curtis, P. J.; Parker, B. R.; Stainton, M. P., Consequences of climate warming and lake acidification for UV-B penetration in North American boreal lakes. *Nature* **1996,** *379*, (6567), 705-708.

17. Macdonald, R. W.; Harner, T.; Fyfe, J., Recent climate change in the Arctic and its impact on contaminant pathways and interpretation of temporal trend data. *Science of the Total Environment* **2005,** *342*, (1-3), 5-86.

18. Barkay, T.; Wagner-Dobler, I., Microbial transformations of mercury: Potentials, challenges, and achievements in controlling mercury toxicity in the environment. In *Advances in Applied Microbiology, Vol 57*, Laskin, A. I.; Bennett, J. W.; Gadd, G. M., Eds. 2005; Vol. 57, pp 1-52.

19. Barkay, T.; Miller, S. M.; Summers, A. O., Bacterial mercury resistance from atoms to ecosystems. *FEMS microbiology reviews* **2003,** *27*, (2-3), 355-384.

20. Fitzgerald, W. F.; Lamborg, C. H.; Hammerschmidt, C. R., Marine biogeochemical cycling of mercury. *Chemical Reviews* **2007,** *107*, (2), 641-662.

21. Hsu-Kim, H.; Kucharzyk, K. H.; Zhang, T.; Deshusses, M. A., Mechanisms regulating mercury bioavailability for methylating microorganisms in the aquatic environment: A critical review. *Environmental Science and Technology* **2013,** *47*, (6), 2441-2456.

22. Baldi, F., Microbial transformation of mercury species and their importance in the biogeochemical cycle of mercury. *Metal ions in biological systems* **1997,** *34*, 213-258.

23. Smol, J. P.; Wolfe, A. P.; Birks, H. J. B.; Douglas, M. S. V.; Jones, V. J.; Korhola, A.; Pienitz, R.; Rühland, K.; Sorvari, S.; Antoniades, D.; Brooks, S. J.; Fallu, M.-A.; Hughes, M.; Keatley, B. E.; Laing, T. E.; Michelutti, N.; Nazarova, L.; Nyman, M.; Paterson, A. M.; Perren, B.; Quinlan, R.; Rautio, M.; Saulnier-Talbot, É.; Siitonen, S.; Solovieva, N.; Weckström, J., Climate-driven regime shifts in the biological communities of arctic lakes. *Proceedings of the National Academy of Sciences of the United States of America* **2005,** *102*, (12), 4397-4402.

24. Choi, S. C.; Chase Jr, T.; Bartha, R., Metabolic pathways leading to mercury methylation in *Desulfovibrio desulfuricans* LS. *Applied and Environmental Microbiology* **1994,** *60*, (11), 4072-4077.

25. Choi, S. C.; Chase Jr, T.; Bartha, R., Enzymatic catalysis of mercury methylation by *Desulfovibrio desulfuricans* LS. *Applied and Environmental Microbiology* **1994,** *60*, (4), 1342-1346.

26. Fleming, E. J.; Mack, E. E.; Green, P. G.; Nelson, D. C., Mercury methylation from unexpected sources: Molybdate-inhibited freshwater sediments and an iron-reducing bacterium. *Applied and Environmental Microbiology* **2006,** *72*, (1), 457-464.

27. Han, S.; Narasingarao, P.; Obraztsova, A.; Gieskes, J.; Hartmann, A. C.; Tebo, B. M.; Allen, E. E.; Deheyn, D. D., Mercury speciation in marine sediments under sulfate-limited conditions. *Environmental Science and Technology* **2010,** *44*, (10), 3752-3757.

28. Gilmour, C. C.; Podar, M.; Bullock, A. L.; Graham, A. M.; Brown, S.; Somenahally, A. C.; Johs, A.; Hurt, R.; Bailey, K. L.; Elias, D., Mercury methylation by novel microorganisms from new environments. *Environmental Science & Technology* **2013**.

29. Monperrus, M.; Tessier, E.; Amouroux, D.; Leynaert, A.; Huonnic, P.; Donard, O. F. X., Mercury methylation, demethylation and reduction rates in coastal and marine surface waters of the Mediterranean Sea. *Marine Chemistry* **2007,** *107*, (1), 49-63.

30. Lehnherr, I.; St. Louis, V. L.; Hintelmann, H.; Kirk, J. L., Methylation of inorganic mercury in polar marine waters. *Nature Geoscience* **2011,** *4*, 298.

31. Drott, A.; Lambertsson, L.; Björn, E.; Skyllberg, U., Importance of dissolved neutral mercury sulfides for methylmercury production in contaminated sediments. *Environmental Science and Technology* **2007,** *41*, (7), 2270-2276.

32. Liu, J.; Valsaraj, K. T.; Delaune, R. D., Inhibition of mercury methylation by iron sulfides in an anoxic sediment. *Environmental Engineering Science* **2009,** *26*, (4), 833-840.

33. Hammerschmidt, C. R.; Fitzgerald, W. F., Methylmercury cycling in sediments on the continental shelf of southern New England. *Geochimica et Cosmochimica Acta* **2006,** *70*, (4), 918-930.

34. Hammerschmidt, C. R.; Fitzgerald, W. F., Geochemical controls on the production and distribution of methylmercury in near-shore marine sediments. *Environmental Science and Technology* **2004,** *38*, (5), 1487-1495.

35. Parks, J. M.; Johs, A.; Podar, M.; Bridou, R.; Hurt Jr, R. A.; Smith, S. D.; Tomanicek, S. J.; Qian, Y.; Brown, S. D.; Brandt, C. C.; Palumbo, A. V.; Smith, J. C.; Wall, J. D.; Elias, D. A.; Liang, L., The genetic basis for bacterial mercury methylation. *Science* **2013,** *339*, (6125), 1332-1335.

36. Schaefer, J. K.; Kronberg, R. M.; Morel, F. M. M.; Skyllberg, U., Detection of a key Hg methylation gene, *hgcA*, in wetland soils. *Environmental Microbiology Reports* **2014,** *6*, (5), 441-447.

37. Marvin-Dipasquale, M.; Agee, J.; McGowan, C.; Oremland, R. S.; Thomas, M.; Krabbenhoft, D.; Gilmour, C. C., Methyl-mercury degradation pathways: A comparison among three mercury impacted ecosystems. *Environmental Science and Technology* **2000,** *34*, (23), 4908-4916.

38. Mason, R. P.; Lawrence, A. L., Concentration, distribution, and bioavailability of mercury and methylmercury in sediments of Baltimore Harbor and Chesapeake Bay, Maryland, USA. *Environmental Toxicology and Chemistry* **1999,** *18*, (11), 2438-2447.

39. Hollweg, T. A.; Gilmour, C. C.; Mason, R. P., Methylmercury production in sediments of Chesapeake Bay and the mid-Atlantic continental margin. *Marine Chemistry* **2009,** *114*, (3-4), 86-101.

40. Baldi, F.; Gallo, M.; Marchetto, D.; Fani, R.; Maida, I.; Horvat, M.; Fajon, V.; Zizek, S.; Hines, M., Seasonal mercury transformation and surficial sediment detoxification by bacteria of Marano and Grado lagoons. *Estuarine, Coastal and Shelf Science* **2012,** *113*, 105-115.

41. Hines, M. E.; Faganeli, J.; Adatto, I.; Horvat, M., Microbial mercury transformations in marine, estuarine and freshwater sediment downstream of the Idrija Mercury Mine, Slovenia. *Applied Geochemistry* **2006,** *21*, (11), 1924-1939.

42. Hines, M. E.; Poitras, E. N.; Covelli, S.; Faganeli, J.; Emili, A.; Žižek, S.; Horvat, M., Mercury methylation and demethylation in Hg-contaminated lagoon sediments

(Marano and Grado Lagoon, Italy). *Estuarine, Coastal and Shelf Science* **2012,** *113*, 85-95.

43. Langer, C. S.; Fitzgerald, W. F.; Visscher, P. T.; Vandal, G. M., Biogeochemical cycling of methylmercury at Barn Island Salt Marsh, Stonington, CT, USA. *Wetlands Ecology and Management* **2001,** *9*, (4), 295-310.

44. Baldi, F.; Pepi, M.; Filippelli, M., Methylmercury resistance in *Desulfovibrio desulfuricans* strains in relation to methylmercury degradation. *Applied and Environmental Microbiology* **1993,** *59*, (8), 2479-2485.

45. Oremland, R. S.; Culbertson, C. W.; Winfrey, M. R., Methylmercury decomposition in sediments and bacterial cultures: Involvement of methanogens and sulfate reducers in oxidative demethylation. *Applied and Environmental Microbiology* **1991,** *57*, (1), 130-137.

46. Hamelin, S.; Amyot, M.; Barkay, T.; Wang, Y.; Planas, D., Methanogens: Principal methylators of mercury in lake periphyton. *Environmental Science and Technology* **2011,** *45*, (18), 7693-7700.

47. Achá, D.; Hintelmann, H.; Yee, J., Importance of sulfate reducing bacteria in mercury methylation and demethylation in periphyton from Bolivian Amazon region. *Chemosphere* **2011,** *82*, (6), 911-916.

48. Marvin-DiPasquale, M. C.; Oremland, R. S., Bacterial methylmercury degradation in Florida Everglades peat sediment. *Environmental Science & Technology* **1998,** *32*, (17), 2556-2563.

49. Bridou, R.; Monperrus, M.; Gonzalez, P. R.; Guyoneaud, R.; Amouroux, D., Simultaneous determination of mercury methylation and demethylation capacities of

various sulfate-reducing bacteria using species-specific isotopic tracers. *Environmental Toxicology and Chemistry* **2011,** *30*, (2), 337-344.

50. Schaefer, J. K.; Yagi, J.; Reinfelder, J. R.; Cardona, T.; Ellickson, K. M.; Tel-Or, S.; Barkay, T., Role of the bacterial organomercury lyase (MerB) in controlling methylmercury accumulation in mercury-contaminated natural waters. *Environmental Science and Technology* **2004,** *38*, (16), 4304-4311.

51. Isa, Z.; Grusenmeyer, S.; Verstraete, W., Sulfate reduction relative to methane production in high-rate anaerobic digestion: Microbiological aspects. *Applied and Environmental Microbiology* **1986,** *51*, (3), 580-587.

52. Gustin, M. S.; Biester, H.; Kim, C. S., Investigation of the light-enhanced emission of mercury from naturally enriched substrates. *Atmospheric Environment* **2002,** *36*, (20), 3241-3254.

53. O'Loughlin, E. J.; Kelly, S. D.; Kemner, K. M.; Csencsits, R.; Cook, R. E., Reduction of Ag(I), Au(III), Cu(II), and Hg(II) by Fe(II)/Fe(III) hydroxysulfate green rust. *Chemosphere* **2003,** *53*, (5), 437-446.

54. Graydon, J. A.; St. Louis, V. L.; Lindberg, S. E.; Hintelmann, H.; Krabbenhoft, D. P., Investigation of mercury exchange between forest canopy vegetation and the atmosphere using a new dynamic chamber. *Environmental Science & Technology* **2006,** *40*, (15), 4680-4688.

55. Nriagu, J. O., Mechanistic steps in the photoreduction of mercury in natural waters. *Science of the Total Environment* **1994,** *154*, (1), 1-8.

56. Amyot, M.; Mierle, G.; Lean, D.; McQueen, D. J., Effect of solar radiation on the formation of dissolved gaseous mercury in temperate lakes. *Geochimica et Cosmochimica Acta* **1997,** *61*, (5), 975-987.

57. Whalin, L.; Kim, E. H.; Mason, R., Factors influencing the oxidation, reduction, methylation and demethylation of mercury species in coastal waters. *Marine Chemistry* **2007,** *107*, (3), 278-294.

58. Poulain, A. J.; Amyot, M.; Findlay, D.; Telor, S.; Barkay, T.; Hintelmann, H., Biological and photochemical production of dissolved gaseous mercury in a boreal lake. *Limnology and Oceanography* **2004,** *49*, (6), 2265-2275.

59. Amyot, M.; Gill, G. A.; Morel, F. M. M., Production and loss of dissolved gaseous mercury in coastal seawater. *Environmental Science and Technology* **1997,** *31*, (12), 3606-3611.

60. Fitzgerald, W. F.; Mason, R. P.; Vandal, G. M., Atmospheric cycling and air-water exchange of mercury over mid-continental lacustrine regions. *Water, air, and soil pollution* **1991,** *56*, (SPEC. VOL.), 745-767.

61. Carpi, A.; Lindberg, S. E., Sunlight-mediated emission of elemental mercury from soil amended with municipal sewage sludge. *Environmental Science and Technology* **1997,** *31*, (7), 2085-2091.

62. Vandal, G. M.; Fitzgerald, W. F.; Rolfhus, K. R.; Lamborg, C. H., Modeling the elemental mercury cycle in Pallette Lake, Wisconsin, USA. *Water, air, and soil pollution* **1995,** *80*, (1-4), 529-538.

63. Zhang, H.; Lindberg, S. E., Sunlight and iron(III)-induced photochemical production of dissolved gaseous mercury in freshwater. *Environmental Science and Technology* **2001,** *35*, (5), 928-935.

64. O'Driscoll, N. J.; Lean, D. R. S.; Loseto, L. L.; Carignan, R.; Siciliano, S. D., Effect of dissolved organic carbon on the photoproduction of dissolved gaseous mercury in lakes: Potential impacts of forestry. *Environmental science & technology* **2004,** *38*, (9), 2664-2672.

65. Zhang, H., Photochemical redox reactions of mercury. In 2006; Vol. 120, pp 37-79.

66. Wiatrowski, H. A.; Das, S.; Kukkadapu, R.; Ilton, E. S.; Barkay, T.; Yee, N., Reduction of Hg(II) to Hg(0) by magnetite. *Environmental Science and Technology* **2009,** *43*, (14), 5307-5313.

67. Allard, B.; Arsenie, I., Abiotic reduction of mercury by humic substances in aquatic system - An important process for the mercury cycle. *Water, air, and soil pollution* **1991,** *56*, (SPEC. VOL.), 457-464.

68. Gu, B.; Bian, Y.; Miller, C. L.; Dong, W.; Jiang, X.; Liang, L., Mercury reduction and complexation by natural organic matter in anoxic environments. *Proceedings of the National Academy of Sciences of the United States of America* **2011,** *108*, (4), 1479-1483.

69. Zhang, H., Photochemical redox reactions of mercury. In *Recent Developments in Mercury Science*, Atwood, D. A., Ed. 2006; Vol. 120, pp 37-79.

70. Poulain, A. J.; Ní Chadhain, S. M.; Ariya, P. A.; Amyot, M.; Garcia, E.; Campbell, P. G. C.; Zylstra, G. J.; Barkay, T., Potential for mercury reduction by

microbes in the high Arctic. *Applied and Environmental Microbiology* **2007,** *73*, (7), 2230-2238.

71. Freedman, Z.; Zhu, C.; Barkay, T., Mercury resistance and mercuric reductase activities and expression among chemotrophic thermophilic aquificae. *Applied and Environmental Microbiology* **2012,** *78*, (18), 6568-6575.

72. Schaefer, J. K.; Letowski, J.; Barkay, T., *mer*-mediated resistance and volatilization of Hg(II) under anaerobic conditions. *Geomicrobiology Journal* **2002,** *19*, (1), 87-102.

73. Daughney, C. J.; Siciliano, S. D.; Rencz, A. N.; Lean, D.; Fortin, D., Hg(II) adsorption by bacteria: A surface complexation model and its application to shallow acidic lakes and wetlands in Kejimkujik National Park, Nova Scotia, Canada. *Environmental science & technology* **2002,** *36*, (7), 1546-1553.

74. Sugio, T.; Fujii, M.; Takeuchi, F.; Negishi, A.; Maeda, T.; Kamimura, K., Volatilization of mercury by an iron oxidation enzyme system in a highly mercury-resistant *Acidithiobacillus ferrooxidans* strain MON-1. *Bioscience, Biotechnology and Biochemistry* **2003,** *67*, (7), 1537-1544.

75. Wiatrowski, H. A.; Ward, P. M.; Barkay, T., Novel reduction of mercury(II) by mercury-sensitive dissimilatory metal reducing bacteria. *Environmental Science and Technology* **2006,** *40*, (21), 6690-6696.

76. Holm, H. W.; Cox, M. F., Transformation of elemental mercury by bacteria. *Journal of Applied Microbiology* **1975,** *29*, (4), 491-494.

77. Magos, L.; Halbach, S.; Clarkson, T. W., Role of catalase in the oxidation of mercury vapor. *Biochemical Pharmacology* **1978,** *27*, (9), 1373-1377.

78. Smith, T.; Pitts, K.; McGarvey, J. A.; Summers, A. O., Bacterial oxidation of mercury metal vapor, Hg(0). *Applied and Environmental Microbiology* **1998,** *64*, (4), 1328-1332.

79. Siciliano, S. D.; Lean, D. R. S., Methyltransferase: An enzyme assay for microbial methylmercury formation in acidic soils and sediments. *Environmental Toxicology and Chemistry* **2002,** *21*, (6), 1184-1190.

80. Colombo, M. J.; Ha, J.; Reinfelder, J. R.; Barkay, T.; Yee, N., Anaerobic oxidation of Hg(0) and methylmercury formation by *Desulfovibrio desulfuricans* ND132. *Geochimica et Cosmochimica Acta* **2013,** *112*, 166-177.

81. Hu, H.; Lin, H.; Zheng, W.; Tomanicek, S. J.; Johs, A.; Feng, X.; Elias, D. A.; Liang, L.; Gu, B., Oxidation and methylation of dissolved elemental mercury by anaerobic bacteria. *Nature Geoscience* **2013,** *6*, 751-754.

82. Ben-Bassat, D.; Shelef, G.; Gruner, N.; Shuval, H. I., Growth of *Chlamydomonas* in a medium containing mercury. *Nature* **1972,** *240*, (5375), 43-44.

83. Lanzillotta, E.; Ceccarini, C.; Ferrara, R.; Dini, F.; Frontini, F. P.; Banchetti, R., Importance of the biogenic organic matter in photo-formation of dissolved gaseous mercury in a culture of the marine diatom *Chaetoceros* sp. *Science of the Total Environment* **2004,** *318*, (1-3), 211-221.

84. Kelly, D. J. A.; Budd, K.; Lefebvre, D. D., Biotransformation of mercury in pH-stat cultures of eukaryotic freshwater algae. *Archives of Microbiology* **2007,** *187*, (1), 45-53.

85. Pickhardt, P. C.; Fisher, N. S., Accumulation of inorganic and methylmercury by freshwater phytoplankton in two contrasting water bodies. *Environmental Science and Technology* **2007,** *41*, (1), 125-131.

86. Devars, S.; Avilés, C.; Cervantes, C.; Moreno-Sánchez, R., Mercury uptake and removal by *Euglena gracilis*. *Archives of Microbiology* **2000,** *174*, (3), 175-180.

87. Chasar, L. C.; Scudder, B. C.; Stewart, A. R.; Bell, A. H.; Aiken, G. R., Mercury cycling in stream ecosystems. 3. Trophic dynamics and methylmercury bioaccumulation. *Environmental Science and Technology* **2009,** *43*, (8), 2733-2739.

88. Mason, R. P.; Reinfelder, J. R.; Morel, F. M. M., Uptake, toxicity, and trophic transfer of mercury in a coastal diatom. *Environmental Science and Technology* **1996,** *30*, (6), 1835-1845.

89. Le Faucheur, S.; Tremblay, Y.; Fortin, C.; Campbell, P. G. C., Acidification increases mercury uptake by a freshwater alga, *Chlamydomonas reinhardtii*. *Environmental Chemistry* **2011,** *8*, (6), 612-622.

90. Asztalos, E.; Sipka, G.; Kis, M.; Trotta, M.; Maróti, P., The reaction center is the sensitive target of the mercury(II) ion in intact cells of photosynthetic bacteria. *Photosynthesis Research* **2012,** *112*, (2), 129-140.

91. Singh, R.; Srivastava, P. K.; Singh, V. P.; Dubey, G.; Prasad, S. M., Light intensity determines the extent of mercury toxicity in the cyanobacterium *Nostoc muscorum*. *Acta Physiologiae Plantarum* **2012,** *34*, (3), 1119-1131.

92. Muñoz, R.; Guieysse, B., Algal–bacterial processes for the treatment of hazardous contaminants: A review. *Water Research* **2006,** *40*, (15), 2799-2815.

93. Heumann, H. G., Effects of heavy metals on growth and ultrastructure of *Chara vulgaris*. *Protoplasma* **1987,** *136*, (1), 37-48.

94. Cain, A.; Vannela, R.; Woo, L. K., Cyanobacteria as a biosorbent for mercuric ion. *Bioresource technology* **2008,** *99*, (14), 6578-6586.

95. Rakhshaee, R.; Giahi, M.; Pourahmad, A., Studying effect of cell wall's carboxyl-carboxylate ratio change of *Lemna minor* to remove heavy metals from aqueous solution. *Journal of Hazardous Materials* **2009,** *163*, (1), 165-173.

96. Schiewer, S.; Wong, M. H., Ionic strength effects in biosorption of metals by marine algae. *Chemosphere* **2000,** *41*, (1-2), 271-282.

97. Pickhardt, P. C.; Folt, C. L.; Chen, C. Y.; Klaue, B.; Blum, J. D., Impacts of zooplankton composition and algal enrichment on the accumulation of mercury in an experimental freshwater food web. *Science of the Total Environment* **2005,** *339*, (1-3), 89-101.

98. Blaby-Haas, C. E.; Merchant, S. S., The ins and outs of algal metal transport. *Biochimica et Biophysica Acta - Molecular Cell Research* **2012,** *1823*, (9), 1531-1552.

99. Zhong, H.; Wang, W. X., Controls of dissolved organic matter and chloride on mercury uptake by a marine diatom. *Environmental Science and Technology* **2009,** *43*, (23), 8998-9003.

100. Moye, H. A.; Miles, C. J.; Phlips, E. J.; Sargent, B.; Merritt, K. K., Kinetics and uptake mechanisms for monomethylmercury between freshwater algae and water. *Environmental Science and Technology* **2002,** *36*, (16), 3550-3555.

101. Miles, C. J.; Moye, H. A.; Phlips, E. J.; Sargent, B., Partitioning of monomethylmercury between freshwater algae and water. *Environmental Science & Technology* **2001,** *35*, (21), 4277-4282.

102. Kosakowska, A.; Falkowski, L.; Lewandowska, J., Effect of amino acids on the toxicity of heavy metals to phytoplankton. *Bulletin of Environmental Contamination and Toxicology* **1988,** *40*, (4), 532-538.

103. Watras, C. J.; Back, R. C.; Halvorsen, S.; Hudson, R. J. M.; Morrison, K. A.; Wente, S. P., Bioaccumulation of mercury in pelagic freshwater food webs. *Science of the Total Environment* **1998,** *219*, (2-3), 183-208.

104. Meissner, J.; Krauss, J. H.; Jurgens, U. J.; Weckesser, J., Absence of a characteristic cell wall lipopolysaccharide in the phototrophic bacterium *Chloroflexus aurantiacus*. *Journal of Bacteriology* **1988,** *170*, (7), 3213-3216.

105. Meissner, J.; Pfennig, N.; Krauss, J. H.; Mayer, H.; Weckesser, J., Lipopolysaccharides of *Thiocyststis violacea*, *Thiocapsa pfennigii*, and *Chromatium tepidum*, species of the familia Chromatiaceae. *Journal of Bacteriology* **1988,** *170*, (7), 3217-3222.

106. Flammann, H. T.; Weckesser, J., Characterization of the cell wall and outer memebrane of *Rhodopseudomonas capsulata*. *Journal of Bacteriology* **1984,** *159*, (1), 191-198.

107. Beck, H.; Hegeman, G. D.; White, D., Fatty acid and lipopolysaccharide analyses of 3 *Heliobacterium* sp. *FEMS Microbiology Letters* **1990,** *69*, (3), 229-232.

108. Glass, J. B.; Wolfe-Simon, F.; Anbar, A. D., Coevolution of metal availability and nitrogen assimilation in cyanobacteria and algae. *Geobiology* **2009,** *7*, (2), 100-123.

109. Colica, G.; Caparrotta, S.; Bertini, G.; De Philippis, R., Gold biosorption by exopolysaccharide producing cyanobacteria and purple nonsulphur bacteria. *Journal of Applied Microbiology* **2012,** *113*, (6), 1380-1388.

110. Italiano, F.; Buccolieri, A.; Giotta, L.; Agostiano, A.; Valli, L.; Milano, F.; Trotta, M., Response of the carotenoidless mutant *Rhodobacter sphaeroides* growing cells to cobalt and nickel exposure. *International Biodeterioration & Biodegradation* **2009,** *63*, (7), 948-957.

111. Buccolieri, A.; Italiano, F.; Dell'Atti, A.; Buccolieri, G.; Giotta, L.; Agostiano, A.; Milano, F.; Trotta, M., Testing the photosynthetic bacterium *Rhodobacter sphaeroides* as heavy metal removal tool. *Annali di Chimica* **2006,** *96*, (3-4), 195-203.

112. Rooney, J. P. K., The role of thiols, dithiols, nutritional factors and interacting ligands in the toxicology of mercury. *Toxicology* **2007,** *234*, (3), 145-156.

113. Ahner, B. A.; Morel, F. M., Phytochelatin production in marine algae. 2. Induction by various metals. *Limnology and Oceanography* **1995,** *40*, 658-658.

114. Ahner, B. A.; Shing, K.; Morel, F. M., Phytochelatin production in marine algae. 1. An interspecies comparison. *Limnology and Oceanography* **1995,** *40*, 649-649.

115. Ahner, B. A.; Wei, L.; Oleson, J. R.; Ogura, N., Glutathione and other low molecular weight thiols in marine phytoplankton under metal stress. *Marine Ecology Progress Series* **2002,** *232*, 93-103.

116. Rauser, W. E., Phytochelatins. *Annual Review of Biochemistry* **1990,** *59*, (1), 61-86.

117. Kawakami, S. K.; Gledhill, M.; Achterberg, E. P., Production of phytochelatins and glutathione by marine phytoplankton in response to metal stress. *Journal of Phycology* **2006,** *42*, (5), 975-989.

118. Cobbett, C.; Goldsbrough, P., Phytochelatins and metallothioneins: Roles in heavy metal detoxification and homeostasis. In 2002; Vol. 53, pp 159-182.

119. Morelli, E.; Ferrara, R.; Bellini, B.; Dini, F.; Di Giuseppe, G.; Fantozzi, L., Changes in the non-protein thiol pool and production of dissolved gaseous mercury in the marine diatom *Thalassiosira weissflogii* under mercury exposure. *Science of the Total Environment* **2009,** *408*, (2), 286-293.

120. Wei, L.; Donat, J. R.; Fones, G.; Ahner, B. A., Interactions between Cd, Cu, and Zn influence particulate phytochelatin concentrations in marine phytoplankton: Laboratory results and preliminary field data. *Environmental science & technology* **2003,** *37*, (16), 3609-3618.

121. Kelly, D.; Budd, K.; Lefebvre, D. D., Mercury analysis of acid- and alkaline-reduced biological samples: Identification of meta-cinnabar as the major biotransformed compound in algae. *Applied and Environmental Microbiology* **2006,** *72*, (1), 361-367.

122. Benoit, J. M.; Gilmour, C. C.; Mason, R. P.; Heyes, A., Sulfide controls on mercury speciation and bioavailability to methylating bacteria in sediment pore waters. *Environmental Science and Technology* **1999,** *33*, (6), 951-957.

123. Gadd, G. M., Metals, minerals and microbes: Geomicrobiology and bioremediation. *Microbiology* **2010,** *156*, (3), 609-643.

124. Röderer, G., Differential toxic effects of mercuric chloride and methylmercuric chloride on the freshwater alga *Poterioochromonas malhamensis*. *Aquatic Toxicology* **1983,** *3*, (1), 23-34.

125. De Filippis, L. F.; Hampp, R.; Ziegler, H., The effects of sublethal concentrations of zinc, cadmium and mercury on *Euglena*. II. Respiration, photosynthesis and photochemical activities. *Archives of Microbiology* **1981,** *128*, (4), 407-411.

126. Kukarskikh, G. L.; Graevskaia, E. E.; Krendeleva, T. E.; Timofeedv, K. N.; Rubin, A. B., Effect of methylmercury on primary photosynthesis processes in green microalgae *Chlamydomonas reinhardtii*. *Biofizika* **2003,** *48*, (5), 853-859.

127. Antal, T. K.; Graevskaya, E. E.; Matorin, D. N.; Volgusheva, A. A.; Osipov, V. A.; Krendeleva, T. E.; Rubin, A. B., Assessment of the effects of methylmercury and copper ions on primary processes of photosynthesis in green microalga *Chlamydomonas moewusii* by analysis of the kinetic curves of variable chlorophyll fluorescence. *Biophysics* **2009,** *54*, (4), 481-485.

128. Wu, Y.; Wang, W.-X., Accumulation, subcellular distribution and toxicity of inorganic mercury and methylmercury in marine phytoplankton. *Environmental Pollution* **2011,** *159*, (10), 3097-3105.

129. Matson, R. S.; Mustoe, G. E.; Chang, S. B., Mercury inhibition on lipid biosynthesis in freshwater algae. *Environmental Science & Technology* **1972,** *6*, (2), 158-160.

130. Ahamad, Z. H.; Shuhanija, S. N., Physiological and biochemical responses of a Malaysian red alga, *Gracilaria manilaensis* treated with copper, lead and mercury. *Journal of Environmental Research And Development Vol* **2013,** *7*, (3).

131. Kojima, Y.; Niinomi, Y.; Tsuboi, S.; Hiyama, T.; Sakurai, H., Destruction of photosystem I iron-sulfur centers of spinach and *Anacystis nidulan*s by mercurials. *The botanical magazine = Shokubutsu-gaku-zasshi* **1987,** *100*, (3), 243-253.

132. Murthy, S. D. S.; Sabat, S. C.; Mohanty, P., Mercury-induced inhibition of photosystem II activity and changes in the emission of fluorescence from phycobilisomes in intact cells of the cyanobacterium, *Spirulina platensis*. *Plant and Cell Physiology* **1989,** *30*, (8), 1153-1157.

133. Graevskaya, E. E.; Antal, T. K.; Matorin, D. N.; Voronova, E. N.; Pogosyan, S. I.; Rubin, A. B. In *Evaluation of diatomea algae Thalassiosira weissflogii sensitivity to chloride mercury and methylmercury by chlorophyll fluorescence analysis*, 2003; 2003; pp 569-572.

134. Nicolardi, V.; Cai, G.; Parrotta, L.; Puglia, M.; Bianchi, L.; Bini, L.; Gaggi, C., The adaptive response of lichens to mercury exposure involves changes in the photosynthetic machinery. *Environmental Pollution* **2012,** *160*, (1), 1-10.

135. Zhang, D. Y.; Deng, C. N.; Pan, X. L., Excess Ca2+ does not alleviate but increases the toxicity of Hg2+ to photosystem II in *Synechocystis* sp (Cyanophyta). *Ecotoxicology and Environmental Safety* **2013,** *97*, 160-165.

136. Murthy, S.; Mohanty, P., Mercury ions inhibit photosynthetic electron transport at multiple sites in the cyanobacterium *Synechococcus* 6301. *Journal of biosciences* **1993,** *18*, (3), 355-360.

137. Bird, L. J.; Coleman, M. L.; Newman, D. K., Iron and copper act synergistically to delay anaerobic growth of bacteria. *Applied and Environmental Microbiology* **2013,** *79*, (12), 3619-3627.

138. Poulain, A. J.; Newman, D. K., *Rhodobacter capsulatus* catalyzes light-dependent Fe(II) oxidation under anaerobic conditions as a potential detoxification mechanism. *Applied and Environmental Microbiology* **2009,** *75*, (21), 6639-6646.

139. Giotta, L.; Agostiano, A.; Italiano, F.; Milano, F.; Trotta, M., Heavy metal ion influence on the photosynthetic growth of *Rhodobacter sphaeroides*. *Chemosphere* **2006,** *62*, (9), 1490-1499.

140. Asztalos, E.; Italiano, F.; Milano, F.; Maróti, P.; Trotta, M., Early detection of mercury contamination by fluorescence induction of photosynthetic bacteria. *Photochemical and Photobiological Sciences* **2010,** *9*, (9), 1218-1223.

141. Marteyn, B.; Sakr, S.; Farci, S.; Bedhomme, M.; Chardonnet, S.; Decottignies, P.; Lemaire, S. D.; Cassier-Chauvat, C.; Chauvat, F., The *Synechocystis* PCC6803 MerA-like enzyme operates in the reduction of both mercury and uranium under the control of the glutaredoxin 1 enzyme. *Journal of Bacteriology* **2013,** *195*, (18), 4138-4145.

142. Ben-Bassat, D.; Mayer, A. M., Volatilization of mercury by algae. *Physiologia Plantarum* **1975,** *33*, (2), 128-132.

143. Ben-Bassat, D.; Mayer, A. M., Reduction of mercury chloride by *Chlorella*: Evidence for a reducing factor. *Physiologia Plantarum* **1977,** *40*, (3), 157-162.

144. Deng, L.; Wu, F.; Deng, N.; Zuo, Y., Photoreduction of mercury(II) in the presence of algae, *Anabaena cylindrical*. *Journal of Photochemistry and Photobiology B: Biology* **2008,** *91*, (2-3), 117-124.

145. Deng, L.; Fu, D.; Deng, N., Photo-induced transformations of Hg(II) species in the presence of algae, *Chlorella vulgaris*. *Journal of Hazardous Materials* **2009,** *164*, (2-3), 798-805.

146. Deng, L.; Deng, N.; Mou, L.; Zhu, F., Photo-induced transformations of Hg(II) species in the presence of *Nitzschia hantzschiana*, ferric ion, and humic acid. *Journal of Environmental Sciences* **2010,** *22*, (1), 76-83.

147. Pickhardt, P. C.; Folt, C. L.; Chen, C. Y.; Klaue, B.; Blum, J. D., Algal blooms reduce the uptake of toxic methylmercury in freshwater food webs. *Proceedings of the National Academy of Sciences of the United States of America* **2002,** *99*, (7), 4419-4423.

148. Baeyens, W.; Leermakers, M., Elemental mercury concentrations and formation rates in the Scheldt estuary and the North Sea. *Marine Chemistry* **1998,** *60*, (3–4), 257-266.

149. Rolfhus, K. R.; Fitzgerald, W. F., Mechanisms and temporal variability of dissolved gaseous mercury production in coastal seawater. *Marine Chemistry* **2004,** *90*, (1–4), 125-136.

150. Kim, J. P. Volatilization and efflux of mercury from biologically productive ocean regions. 1987.

151. Mason, R. P.; Morel, F. M. M.; Hemond, H. F., The role of microorganisms in elemental mercury formation in natural waters. *Water, air, and soil pollution* **1995,** *80*, (1-4), 775-787.

152. Peretyazhko, T.; Charlet, L.; Muresan, B.; Kazimirov, V.; Cossa, D., Formation of dissolved gaseous mercury in a tropical lake (Petit-Saut reservoir, French Guiana). *Science of the Total Environment* **2006,** *364*, (1-3), 260-271.

153. Kim, J.; Fitzgerald, W., Gaseous mercury profiles in the tropical Pacific Ocean. *Geophysical Research Letters* **1988,** *15*, (1), 40-43.

154. Barkay, T.; Kritee, K.; Boyd, E.; Geesey, G., A thermophilic bacterial origin and subsequent constraints by redox, light and salinity on the evolution of the microbial mercuric reductase. *Environmental Microbiology* **2010,** *12*, (11), 2904-2917.

155. Ercal, N.; Gurer-Orhan, H.; Aykin-Burns, N., Toxic metals and oxidative stress part I: mechanisms involved in metal-induced oxidative damage. *Current topics in medicinal chemistry* **2001,** *1*, (6), 529-539.

156. Wang, S.; Li, B.; Zhang, M.; Xing, D.; Jia, Y.; Wei, C., Bioaccumulation and trophic transfer of mercury in a food web from a large, shallow, hypereutrophic lake (Lake Taihu) in China. *Environmental Science and Pollution Research* **2012,** *19*, (7), 2820-2831.

157. Hughes, C.; Malin, G.; Turley, C. M.; Keely, B. J.; Nightingale, P. D.; Liss, P. S., The production of volatile iodocarbons by biogenic marine aggregates. *Limnology and Oceanography* **2008,** *53*, (2), 867-872.

158. Tsui, M. T. K.; Finlay, J. C.; Balogh, S. J.; Nollet, Y. H., In situ production of methylmercury within a stream channel in Northern California. *Environmental Science and Technology* **2010,** *44*, (18), 6998-7004.

159. Deng, G. F.; Zhang, T. W.; Yang, L. M.; Wang, Q. Q., Studies of biouptake and transformation of mercury by a typical unicellular diatom *Phaeodactylum tricornutum*. *Chinese Science Bulletin* **2013,** *58*, (2), 256-265.

160. Pongratz, R.; Heumann, K. G., Production of methylated mercury and lead by polar macroalgae - A significant natural source for atmospheric heavy metals in clean room compartments. *Chemosphere* **1998,** *36*, (9), 1935-1946.

161. Allakhverdiev, S. I.; Tomo, T.; Shimada, Y.; Kindo, H.; Nagao, R.; Klimov, V. V.; Mimuro, M., Redox potential of pheophytin a in photosystem II of two cyanobacteria having the different special pair chlorophylls. *Proceedings of the National Academy of Sciences of the United States of America* **2010,** *107*, (8), 3924-3929.

162. Nelson, N.; Yocum, C. F., Structure and function of photosystems I and II. In *Annual Review of Plant Biology*, 2006; Vol. 57, pp 521-565.

163. Scholz, F.; Lovrić, M., The standard potentials of the electrode “dissolved atomic mercury/dissolved mercury ions". *Electroanalysis* **1996,** *8*, (11), 1075-1076.

164. Agalidis, I.; Ivancich, A.; Mattioli, T. A.; ReissHusson, F., Characterization of the *Rhodocyclus tenuis* photosynthetic reaction center. *Biochimica Et Biophysica Acta-Bioenergetics* **1997,** *1321*, (1), 31-46.

165. Heathcote, P.; Jones, M. R.; Fyfe, P. K., Type I photosynthetic reaction centres: structure and function. *Philosophical Transactions of the Royal Society of London Series B-Biological Sciences* **2003,** *358*, (1429), 231-243.

166. Krabbenhoft, D. P.; Sunderland, E. M., Global change and mercury. *Science* **2013,** *341*, (6153), 1457-1458.

167. Amyot, M.; Southworth, G.; Lindberg, S. E.; Hintelmann, H.; Lalonde, J. D.; Ogrinc, N.; Poulain, A. J.; Sandilands, K. A., Formation and evasion of dissolved gaseous mercury in large enclosures amended with 200HgCl2. *Atmospheric Environment* **2004,** *38*, (26), 4279-4289.

168. Luengen, A. C.; Flegal, A. R., Role of phytoplankton in mercury cycling in the San Francisco Bay estuary. *Limnology and Oceanography* **2009,** *54*, (1), 23-40.

169. Amos, H. M.; Jacob, D. J.; Streets, D. G.; Sunderland, E. M., Legacy impacts of all-time anthropogenic emissions on the global mercury cycle. *Global Biogeochemical Cycles* **2013,** *27*, (2), 410-421.

2.8 FIGURE AND CAPTION

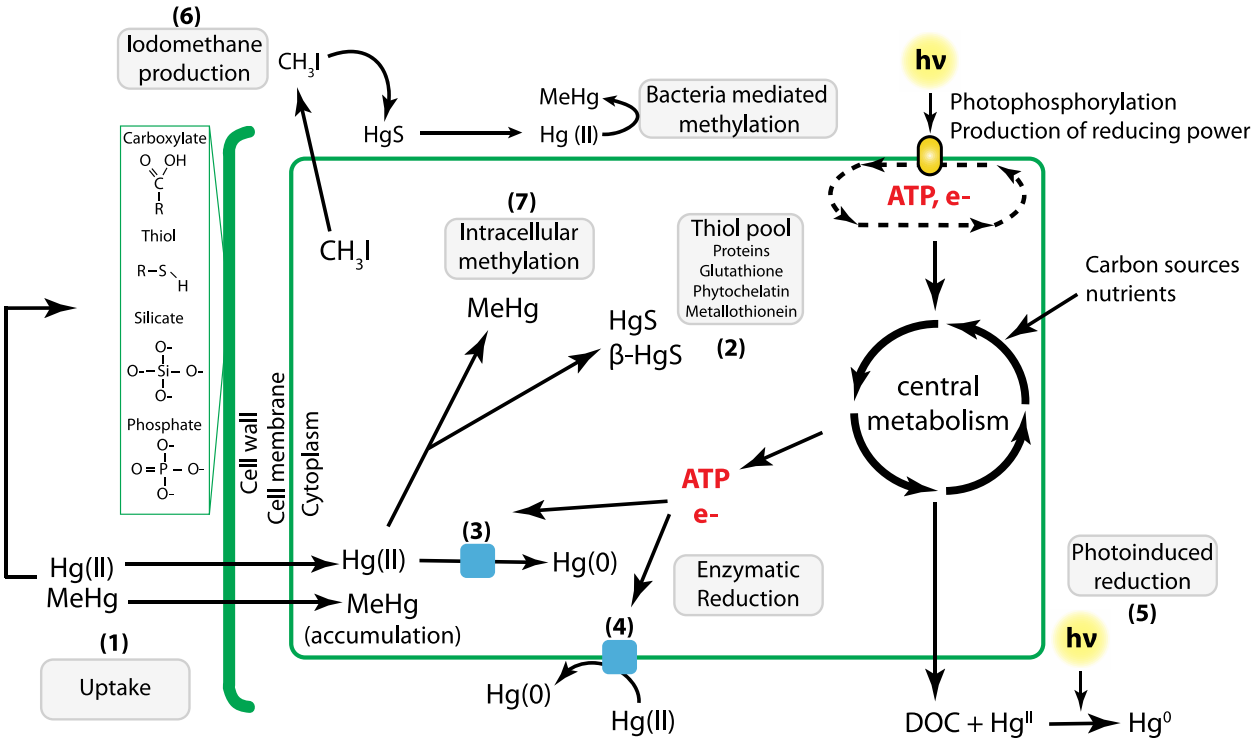

Figure 2.1: Phototrophic Hg transformations: (**1**) Hg^{II} and MeHg uptake and interaction with cell walls; (**2**) Hg^{II} sequestration via the thiol pool and production of HgS; (**3**) enzymatically mediated intracellular Hg^{II} reduction; (**4**) enzymatically mediated extracellular Hg^{II} reduction; (**5**) Hg^{II} reduction via the formation of photoreactive compounds with photosynthetic exudates (DOC stands for dissolved organic carbon); (**6**) HgS species solubilization via ICH_3 production and subsequent methylation by epiphytic bacteria; (**7**) intracellular methylation of Hg^{II}.

Chapter 3: Shining light on recent advances in microbial mercury cycling

Daniel S. Grégoire [a] & Alexandre J. Poulain [a]

a - Biology Department, University of Ottawa, 30 Marie Curie, Ottawa, ON, K1N 6N5, Canada.

A modified version of this literature review was originally published as: **Grégoire, D.S.;** Poulain, A.J., Shining a light on recent advances in microbial mercury cycling, *FACETS* **2018,** *3*, (1), 858-879.

Direct link: http://www.facetsjournal.com/doi/10.1139/facets-2018-0015

3.1 ABSTRACT

Mercury (Hg) is a global pollutant emitted primarily as gaseous Hg^0 that deposits into aquatic and terrestrial ecosystems following its oxidation to Hg^{II}. From that point, microbes play a key role in determining Hg's fate in the environment by participating in sequestration, oxidation, reduction and methylation reactions. A wide diversity of chemotrophic and phototrophic microbes occupying oxic and anoxic habitats are known to participate directly in Hg cycling. Over the last few years, new findings have come to light that have greatly improved our mechanistic understanding of microbe-mediated Hg cycling pathways in the environment. In this review, we summarize recent advances in microbe-mediated Hg cycling and take the opportunity to compare the relatively well-studied chemotrophic pathways to poorly understood phototrophic pathways. We present how the use of genomic and analytical tools can be used to understand Hg transformations and the physiological context of recently discovered cometabolic Hg transformations supported in anaerobes and phototrophs. Finally, we propose a conceptual framework that emphasizes the role phototrophs play in environmental Hg redox cycling and the importance of better characterizing such pathways in the face of environmental change currently underway.

3.2 INTRODUCTION

Mercury (Hg) is a global pollutant emitted from natural sources such as volcanic activity and forest fires and anthropogenic sources such as mining and coal combustion [1]. Hg is emitted primarily in its elemental and highly volatile form Hg^0, which can travel in the atmosphere for up to a year before being depositing into aquatic and terrestrial ecosystems as oxidized Hg^{II} [2]. From that point, Hg can be subject to a variety of transformations including burial into sediments; reduction, which results in Hg^0 re-emission to the atmosphere; and methylation, which converts inorganic Hg to toxic monomethylmercury (MeHg) that bioaccumulates in animals [3] and plants such as rice [4].

Microbes play a key role in Hg transformations. They can produce or degrade MeHg, reduce Hg^{II}, oxidize Hg^0 and sequester a variety of Hg chemical species [as summarized in [5] and [6]]. Generally speaking, microbial Hg transformations occur through cometabolic processes (e.g., encoded by *hgcAB* gene cluster) or dedicated detoxification strategies (e.g., encoded by the *mer*-operon). Hg sequestration, can occur through dedicated pathways [e.g. phytochelatins binding Hg [7, 8]] or cometabolic processes [e.g. HgS formation during photosynthesis [9]]. Indeed, a wide diversity of microbes can mediate Hg cycling pathways in a variety of habitats: aerobic, anaerobic, chemotrophic and phototrophic microbes all influence the fate of Hg in the environment.

In an earlier review, we synthesized the state of knowledge on Hg transformations mediated by phototrophic microbes [6]. We highlighted that phototrophic Hg cycling pathways were poorly understood compared with their chemotrophic counterparts. We also discussed why this was an important knowledge gap to address because of the drastic changes predicted to occur in phototrophic communities in

response to global environmental change such as the increased frequency, magnitude and duration of phytoplankton blooms [10].

Although the environmental contributions of phototrophs to environmental Hg cycling remain understudied compared with their chemotrophic counterparts, considerable research has been done in recent years to better understand the role of phototrophs in the global Hg cycle. Here, we offer an update to our initial literature review comparing chemotrophic and phototrophic Hg cycling pathways including 68 research papers published since 2014 [6]. Our objective with this review is to summarize the recent advances in our understanding of chemotrophic and phototrophic Hg cycling pathways. As part of this, we highlight outstanding knowledge gaps pertaining to microbially mediated Hg cycling emphasizing recent efforts that have helped better understand the role of phototrophs in Hg cycling. Ultimately, we aim to provide recommendations on how to better characterize the environmental and ecological context of microbial Hg cycling in future research.

3.3 CHEMOTROPHIC MERCURY TRANSFORMATIONS

3.3.1 Chemotrophic mercury methylation

Chemotrophic Hg methylation continues to be the most studied microbially mediated Hg transformation, which is unsurprising given the health concerns surrounding MeHg. At the time of our initial review, the discovery of the *hgcAB* gene cluster encoding for Hg methylation had just been published [11]. Since this transformational finding in the field of Hg research, there has been a surge in the number of studies investigating the physiological and environmental controls of Hg methylation.

On the mechanistic front, computer modeling has shown that the corrinoid protein encoded by *hgcA* initiates a key step in MeHg formation by transferring a negatively charged methyl carbanion to an Hg^{II} substrate [12]. This process is thought to occur on the inner side of the cell membrane based on observations in spheroplasts (i.e. bacteria partially/wholly devoid of a cell wall) generated from well-characterized Hg methylating bacteria [13]. With respect to the physiology of Hg methylation, gene deletions targeting *hgcAB* in *Geobacter sulfurreducens* PCA, a well-known Hg methylator with proven Hg redox cycling capabilities, resulted in increased Hg uptake, Hg^{II} reduction and Hg^{0} oxidation [14, 15]. In contrast, deleting the genes encoding for electron transport machinery essential to Hg^{II} reduction (e.g. encoding for cytochrome c synthesis) in *G. sulfurreducens* increased the abundance of proteins involved in the metabolism of C1 compounds potentially involved in Hg methylation [15]. These studies suggest that Hg methylation and Hg reduction can compete for common Hg or metabolic substrates inside the cell and support the presence of common physiological controls for both transformations. Further physiological characterization of strains capable of a suite of Hg transformations are required to identify the potential metabolic coupling points that exist for competing Hg transformations.

The discovery of the *hgcAB* gene cluster has revealed a broader diversity of microbes that can potentially methylate Hg compared to what was known four years ago [16]. Previously, representatives in sulphate-reducing bacteria (SRB) [17, 18], iron reducing bacteria [19] and methanogens [20-22], were known to methylate Hg. Homologues for *hgcAB* have now been identified in representatives of the phyla Chloroflexi and Firmicutes [23, 24]; a compilation of microbial strains harbouring the *hgcAB* sequence has been published

elsewhere [25]. Most recently, robust Hg methylation was demonstrated in several cultured methanogen strains [26]. Such studies exemplify how *hgcAB* genes can be used to identify Hg methylators across diverse clades of microbes and gain insight into the environmental controls of Hg methylation that exist in a variety of habitats.

Mining existing (meta)genomic information for *hgcAB* sequences has revealed several new environments that can potentially support Hg methylation including invertebrate digestive tracts, permafrost soil, hypoxic coastal areas, soda lakes and thermal springs [16]. In addition, a number of field studies have evaluated the presence or quantified the abundance of *hgcA* gene or *hgcAB* genes in habitats including wetland sediments [24, 27, 28], wastewater treatment plants [29], rivers near chlor-alkali plants [30], lake sediments [31], river biofilms [32], hydroelectric dam sediments [33], rice paddies [34, 35] and Antarctic sea ice [36]. If the number of studies cited above is any indication, the number of habitats that can support Hg methylation will continue to grow, which will help identify novel and potentially overlooked Hg methylation hotspots in the environment.

Several of the above-mentioned studies have assessed the distribution the *hgcAB* gene cluster alongside the abundance of marker genes used as proxies for microbial metabolisms that support Hg methylation. Studies using genes such as the *dsrAB* genes [encoding for subunits of the dissimilatory sulphite reductase (EC 1.8.99.5)] and the *mcrA* gene [encoding the methyl-coenzyme M reductase (EC: 3.1.21)] as proxies for sulphate reduction and methane cycling, respectively, have linked the abundance of Hg methylation genes to different metabolic functional groups [27, 29, 31, 32, 36]. These studies have led to the discovery that syntrophic microbes, such as those that rely on interspecies hydrogen and acetate transfer following propionate fermentation for growth, play an

important role in Hg methylation [27, 29] in environments depleted in sulphate and iron (e.g. terminal electron acceptors) [37]. The findings concerning syntrophs highlight the importance of moving away from studies that use single model organisms to better address how complex microbial assemblages can influence MeHg production in the environment.

Despite the surge in studies investigating Hg methylation in microbes, whether a physiological purpose for this Hg transformation exists remains unclear. Hg methylation was once thought to be a detoxification strategy as studied in the fungus *Neurospora crassa* [38]. However, experimental evidence in other microbes, including bacteria and archaea, are currently lacking. Much of the evidence published to date supports that Hg methylation is a cometabolic accidental process. In support of cometabolic Hg methylation, recent studies have shown that organic carbon source composition [30, 39], electron acceptor availability [29, 37], and salinity [30] appear to control the distribution *hgcAB* genes. With some of the genetic determinants for Hg methylation now in hand, the field is ripe to explore the physiological and evolutionary context of Hg methylation in a variety of model organisms.

Despite the recent emphasis on the genetic basis of Hg methylation, research addressing the fundamental aspects of Hg bioavailability to methylators continues to expand. Previously, it was thought that Hg methylation was limited by availability of inorganic Hg substrates such as HgS, which was considered poorly bioavailable to methylators in sulphidogenic environments [40]. The importance of HgS as a substrate for methylation has recently been revisited in the context of how HgS nanoparticle formation controls Hg bioavailability to methylators under anoxic conditions. It has been shown

that HgS particles tend to agglomerate, becoming more crystalline and less bioavailable as they age in the presence of dissolved organic matter (DOM), which can decrease Hg methylation [41]. In contrast, it has also been shown that methylation of HgS can increase in the presence of DOM as a function of thiol content, preventing large and poorly bioavailable HgS aggregates from forming [42, 43]. Aside from thiols, it has been suggested that amine, and to a lesser degree, carboxyl functional groups, can also control HgS aggregation once thiols binding sites have been saturated at high Hg to DOM ratios [44]. These studies suggest that the controls on HgS nanoparticle formation are complex and reveal the transient nature of how HgS species exert dynamic controls on Hg bioavailability to Hg methylators.

The bioavailability and toxicity of Hg are controlled, in part, by its affinity for thiol-bearing molecules such as cysteine. For the sake of brevity, we have omitted discussing mechanisms for Hg uptake and toxicity in this section as these topics have been recently reviewed elsewhere [6, 45-47]. Instead we briefly focus on recent work addressing the role of DOM and thiol-bearing ligands in mediating Hg bioavailability to Hg methylators.

In a recent study using the model Hg methylating bacterium *G. sulfurreducens* PCA, cysteine inhibited Hg methylation at low concentrations (0.01 to 0.1 µM) but stimulated Hg methylation at higher concentrations (100 to 1000 µM) when experiments were run for 144 hours vs 4 hours [48]. One potential explanation provided for this trend was that thiols mobilized Hg from binding sites on the cell membrane to the cytoplasm, where Hg was more bioavailable for methylation [49]. The role of functional groups in the cell membrane was recently highlighted in a study comparing Hg methylation in

Desulfovibrio desulfuricans ND132 and *G. sulfurreducens* in the presence of two sources of DOM (one of aquatic origin with low aromaticity and the other of terrestrial origin with relatively higher aromaticity) [50]. In this study, MeHg production by *D. desulfuricans* increased with DOM concentration, whereas MeHg production in *G. sulfurreducens* decreased [50]. Another study examining Hg stable isotope fractionation during Hg methylation in *D. desulfuricans* and *G. sulfurreducens* demonstrated that the same strains accessed different intracellular and extracellular pools of Hg during methylation [51]. These studies highlight that strain specific characteristics can have a considerable impact on Hg uptake and subsequent methylation. Although the exact nature of the differences in characteristics has yet to be properly defined, they are clearly important to consider when extending conclusions drawn from a given model Hg methylator to microbial communities in the environment.

3.3.2 Chemotrophic methylmercury demethylation

Compared to Hg methylation, MeHg demethylation has been relatively understudied, although new mechanistic details have emerged for both reductive demethylation (RD) and oxidative demethylation (OD) pathways. Microbes capable of RD harbour the *mer* operon, which is a series of genes encoding dedicated Hg scavenging, transport and detoxification machinery [52, 53]. The *mer* operon's expression is induced as a function of intracellular Hg concentration and RD is carried out thanks to the presence of ***merB*****,** which encodes an organomercury lyase (e.g. MerB) that cleaves MeHg into inorganic Hg^{II} and CH_4 [53]. Hg^{II} is subsequently reduced to Hg^0 via the mercuric reductase MerA and CH_4 and Hg^0 can evade the cell [52]. In contrast to RD, OD occurs in the absence of

dedicated Hg detoxification machinery and is a non-specific cometabolic process tied to C1 compound metabolism that results in the production of Hg^{II} and CO_2 [46, 54].

Recent work on MerB has shown that conserved cysteine and aspartic acid residues are essential for releasing Hg from MerB's active site following the cleaving of the methyl group [55]. When a serine residue was present in place of aspartic acid, MerB lost its specificity for MeHg and was also able to bind copper (Cu), although resupplying MerB with Hg successfully removed Cu from the enzyme's active site [56]. These findings demonstrate that MeHg can outcompete Cu for the binding site on MerB, but also highlight functional parallels that may exist between RD and copper homeostasis that merit further investigation.

Despite MeHg formation occurring predominantly in anoxic environments, broad Hg resistance strategies relying on MerB have largely been associated with aerobes. Recent work with the model anaerobe *Geobacter bemidjiensis* Bem suggests that strategies similar to those encoded by the *mer* operon may be present in anaerobes providing them with a means for RD [57]. *G. bemidjiensis* supported a suite of Hg transformation pathways including Hg methylation, Hg^{II} reduction via a MerA-like mechanism, and Hg^0 oxidation [57]. The latter finding is interesting because to the best of our knowledge very few complete *mer* operons have yet to be reported for obligate anaerobes. Although these are not the first observations that anaerobes can mediate several Hg transformations, they do provide an interesting basis from which to investigate the physiological controls of competing Hg transformations that may occur simultaneously.

Similar to the work done on Hg methylation, new studies have addressed how thiol-bearing ligands affect RD. In contrast to inorganic Hg, thiol-bearing ligands had little effect on MeHg bioavailability in bacteria capable of RD (*Escherichia coli* and *Pseudomonas stutzeri*) [58]. The same study found a considerable difference in MeHg demethylation rates for the two strains despite comparable bioavailability among the different MeHg complexes tested [58]. Similar to what was suggested for Hg methylators, the authors attributed the contrasting results to differences in MeHg bioavailability associated with strain specific characteristics [58]. Although the authors demonstrated that non-specific binding of MeHg to heat-killed cells rendered a portion of MeHg unavailable for demethylation, the exact nature of these binding sites was not further discussed [58].

A newly discovered OD pathway in methanotrophs serendipitously provides additional links between Cu metabolism and MeHg demethylation. Methanobactin, a Cu chaperone molecule synthesized by methanotrophs, was essential for OD [59, 60]. Recent findings in the model methanotroph *Methylosinus trichosporium* OB3b showed that MeHg demethylation was dependent on the activity of methanol dehydrogenase [60], further supporting a link between C1 metabolism and OD [46]. Given that C1 metabolism is also tied to Hg methylation, these results suggest that the availability of C1 compounds in the environment plays an important role in mediating MeHg accumulation. That being said, when considering the role of methanotrophs in OD and its relevance to the environment, one must remember that in most environments where methanotrophs are active, MeHg degradation via OD could be overwhelmed by the large availability of other reduced C1 compounds (e.g., methane). The environmental relevance of this type

of OD remains to be determined.

At the environmental scale, a number of studies have measured MeHg demethylation [many of which were summarized in [25]]; however, few of these studies explicitly discuss the direct contribution of microbes to demethylation. The fact that many of these systems are net MeHg sources makes it difficult to investigate the mechanisms supporting MeHg destruction beyond the laboratory scale. Further investigations into the mechanisms of biotic MeHg sinks may yield important clues to mitigating MeHg exposure in the environment. To the best of our knowledge, only one recent study fitting this description has been published. In this work, Kronberg et al. showed that methanogens are important contributors to OD in a wetland ecosystem known to be a sink for MeHg [61]. Together with previous work on methanogens, these findings frame methane cycling microbes as key players in controlling MeHg levels in the environment.

3.3.3 Chemotrophic mercury reduction

The mercuric reductase MerA encoded by the *mer* operon continues to be one of the best-studied chemotrophic Hg reduction strategies. Recently, it has been shown that sulphur-oxidizing bacteria carrying *merA* were not only able to reduce HgS minerals in aquatic environments, but also use HgS as a sulphur source [62]. Although it is well established that MerA relies on the use of nicotinamide adenine dinucleotide phosphate (NADPH) as a redox cofactor for Hg^{II} reduction [52], the link between *mer*-mediated reduction and the redox state of the cell is rarely discussed. Recent work with *Thermus thermophilus* HB27 revealed important links between cellular redox balance, Hg sequestration and MerA

activity [63]. *T. thermophilus* (alongside other representatives of the *Thermus* genus) harboured genes upstream of *merA* in the *mer* operon encoding for the synthesis of low molecular weight thiols that buffered Hg toxicity prior to Hg^{II} reduction [63]. The synthesis of cellular redox buffering compounds proved essential to supporting this Hg detoxification strategy [63].

Perhaps by further investigating the influence of redox homeostasis on *mer*-mediated reduction we can gain insights into how such Hg detoxification strategies evolved across different redox conditions throughout Earth's history [64]. Therein may lay an explanation for the observation of a MerA-like reductase in the obligate anaerobe *G. bemidjiensis* despite such strategies being largely absent in anaerobes (see the previous section). Perhaps such pathways only occur under specific redox conditions in the environment that support anaerobic metabolism optimized for cell growth and Hg detoxification.

Anaerobes such as dissimilatory metal reducing bacteria continue to be studied with respect to non-*mer*-mediated Hg reduction pathways. As previously mentioned, work with *G. sulfurreducens* has shown that Hg^{II} reduction increased following the deletion of *hgcAB* [14], as did the abundance of cytochrome-c proteins supporting Hg^{II} reduction [15], supporting a physiological link for both of these Hg transformations. Recently, it has also been shown that Hg^{II} reduction increased as a function of electron transfer from *Shewanella oneidensis* MR-1 to natural organic matter (NOM), which led to the formation of free radicals that could reduce Hg^{II} [65].

Novel non-*mer*-mediated pathways have also recently been discovered in previously untested model organisms. Magnetotactic bacteria are now known to reduce Hg^{II} during microaerophilic growth via coupled redox reactions with biogenic magnetite in the membrane of the magnetosome [66]. Our own research has revealed that Hg^{II} reduction is supported in obligate anaerobes from the order Clostridiales. We observed that Hg^{II} reduction was dependent on the ability of cells to produce reduced redox cofactors (possibly ferredoxin) via fermentation when pyruvate was used as a carbon source [67]. Given that *merA* was absent in these strains, our results support that cells reduced Hg because of its electrophilic nature allowing cells to transfer electrons from reduced redox cofactors to Hg during fermentative growth [67]. This finding suggests that fermentative Hg reduction may be an important pathway for Hg redox cycling in environments devoid of light and electron acceptors [67]. Given that fermentative microbes occupy a niche similar to chemotrophic Hg methylators [68], such pathways may also influence the accumulation of MeHg. However, the contributions of fermenters to Hg^{II} reduction and the potential influence of such pathways on Hg availability to methylators have yet to be investigated.

3.3.4 Chemotrophic mercury oxidation

Hg oxidation still remains one of the most poorly understood chemotrophic Hg transformations, with the first mechanistic details having only just recently been published. Following the seminal work demonstrating Hg^0 oxidation via redox reactions with thiols in the cell membranes of anaerobes [69], additional evidence has emerged supporting the presence of a similar pathway in other obligate and facultative anaerobes

[57, 70, 71]. It has also been shown that dead cell material bearing intact thiol groups can catalyze Hg^0 oxidation offering a potentially important route for delivering freshly oxidized Hg^{II} to anoxic environments [70]. Hg^0 oxidation is thought to be more important in situations where thiol binding site availability is high relative to low extracellular Hg concentration [71]. Given the ubiquitous nature of thiols in bacterial membranes [72], Hg^0 oxidation by anaerobes is likely widespread in environments such as waterlogged soils [73, 74] and anoxic lake sediments [75] where Hg^0 can dominate Hg speciation. When considered alongside the growing evidence for anaerobic Hg^{II} reduction, these findings show that anaerobes are poised to be key players in controlling MeHg production in anoxic systems by catalyzing a dynamic anaerobic redox cycle.

3.4 PHOTOTROPHIC MICROBIAL MERCURY TRANSFORMATIONS

As outlined in our previous review, there is a growing body of evidence suggesting oxygenic and anoxygenic phototrophs can participate in Hg transformations in the environment [6]. Phototroph-mediated Hg cycling pathways stand to be important in environments where abiotic photochemical Hg transformations are limited [76]. Such habitats could include the metalimnion of thermally stratified lakes [76], microbial mats [77, 78] and photic surface sediments [79, 80] where phototrophs thrive at low visible light intensities. Despite the potential for phototrophs to directly influence Hg speciation, considerably fewer studies have addressed phototrophic Hg cycling in recent years compared with the large body of work that exist on chemotrophs. However, recent

research at the laboratory scale has advanced our mechanistic understanding of Hg uptake, toxicity, and transformation in a variety of phototrophic organisms.

3.4.1 Phototrophic mercury uptake studies

In our initial review, we detailed the existing body of work on the passive and active Hg uptake pathways in phototrophs [6]. At that time, all the information available on Hg uptake in phototrophs was derived from oxygenic phototrophs such as algae, cyanobacteria, and diatoms. Since then, new mechanistic details have emerged on the uptake of Hg in the model green alga *Chlamydomonas reinhardtii* and for the first time, in anoxygenic phototrophic purple non-sulphur bacteria (PNSB).

Transcriptomic evidence has suggested that *C. reinhardtii* can actively take up inorganic Hg complexes through divalent metal transporters, and organic Hg complexes through amino acid transporters [81], although this was not directly experimentally tested. A similar mechanism was proposed for model PNSB whereby Hg uptake occurred via Ca^{2+} transport channels as an active process [82]. These findings echo those for chemotrophic anaerobes where active uptake of Hg occurred through Zn^{2+} or Mn^{2+} transporters [13, 83]. These studies suggest that Hg uptake via divalent cation transporters is supported across diverse microbial metabolisms. Given the high metal requirements associated with phototrophy, Hg uptake via metal transporters is possibly important and may exert a strong influence on downstream Hg transformations.

Whereas the effects of DOM on Hg bioavailability to chemotrophs have been extensively studied, there is little information available for phototrophs [84]. Microbial phototrophy is not limited to autotrophy. Strategies such as a mixotrophy, where cells use light for energy and a diverse carbon pool for biosynthesis, could lead to Hg uptake via the shuttling of Hg-DOM complexes into cells [85]. To the best of our knowledge, the contributions of mixotrophs to Hg uptake in aquatic food webs have only recently been addressed [86, 87]. In these studies, the authors showed that mixotrophic ciliates could incorporate Hg through passive diffusion and active uptake linked to bacterivory [86, 87]. Despite mixotrophy being widespread in the environment [88] the potential implications of mixotrophy on Hg accumulation in aquatic and terrestrial food webs remain largely unexplored.

3.4.2 Phototrophic mercury methylation

The majority of studies addressing the role of phototrophs in controlling MeHg's fate focus on bioaccumulation in food webs and fewer studies directly address how phototrophic communities affect Hg speciation in the environment. Most of the recent work has been conducted on periphytic communities. These studies face the challenge of distinguishing the direct involvement of phototrophs in Hg methylation from the indirect role that they have (as primary producers) in supplying nutrients to chemotrophic Hg methylators in the periphytic matrix [89, 90]. In most cases, MeHg production increased under conditions of higher photosynthetic activity [36, 91-93] but recent work emphasized the importance of considering diel periphytic dynamics in MeHg production [90].

Currently, there is very little support for phototrophs participating directly in Hg methylation. Aside from the initial research cited in our first review [94, 95], only one new study has emerged investigating the potential for direct methylation in the cyanobacterium *Nostoc paludosum* that showed no MeHg production [96].

Microbial strains in the phylum Chloroflexi, which includes representatives of the anoxygenic phototrophic green non-sulphur bacteria, are now known to host the *hgcAB* gene cluster. However, the gene sequences found to date belong to the chemotrophic Dehalococcoidaceae family [16, 24, 27]. With the increasing diversity of habitats being investigated for Hg methylation, perhaps a phototrophic representative harbouring the *hgcAB* gene cluster capable of methylation may soon be uncovered.

3.4.3 Phototrophic methylmercury demethylation

Previously, there was little to no mechanistic data available for direct phototroph-mediated MeHg demethylation [6]. Recently, Kritee et al. used Hg stable isotope fractionation in *Isochrysis galbana* to demonstrate MeHg demethylation in algal cells [97]. In this study, cells preferentially demethylated lighter MeHg isotopes resulting in a pool of isotopically light Hg^{II} [97]. In addition, MeHg demethylation resulted in a positive odd-isotope mass independent signature that was characteristic of photochemical destruction of MeHg and similar to the Hg isotope signature observed in a variety of marine and freshwater fish [97]. This study highlights the power of Hg stable isotope fractionation to track phototroph-mediated Hg transformations at the environmental scale.

3.4.4 Phototrophic mercury reduction

Most of the previous evidence for phototroph-mediated Hg reduction stemmed from observations and experiments performed with oxygenic phototrophs [6]. Recent work on anoxygenic phototrophic PNSB [98] and Heliobacteria [67] has provided some of the first mechanistic details for anaerobic phototrophic Hg reduction.

Our work with PNSB demonstrated that Hg^{II} was preferentially reduced during photoheterotrophic growth on reduced organic carbon substrate (e.g. using light as an energy source and generating biomass using an organic carbon source) [98]. Under controlled laboratory conditions, we showed that PNSB derived an advantage from sublethal Hg exposure, which we attributed to the ability of Hg to act as an electron sink during phototrophic growth [98]. Large peaks of Hg^0 have been reported in the metalimnion of lakes [76] and anoxygenic phototrophs such as PNSB thrive in environments such as the thermoclines and chemoclines of stratified aquatic ecosystems [99] and microbial mats [100]. These metabolically versatile microbes stand to be important players in Hg redox cycling in environments where light is attenuated and reduced organic carbon is available. Such habitats are often located at redox interfaces that act as gateways to Hg methylation sites.

Following up on our work with anoxygenic phototrophs, we further discovered that Heliobacteria, a family of spore-forming fermentative photoheterotrophs of the order Clostridiales, were among the most efficient Hg reducers reported to date [67]. No apparent dedicated Hg reduction machinery (i.e., *mer* operon determinants) was found in the genome of *Heliobacterium modesticaldum* Ice1, and Hg^{II} reduction most likely occurred as a cometabolic process related to the availability of reduced redox cofactors (e.g., ferredoxin) [67]. The fact that cometabolic Hg reduction was observed in two

phylogenetically and ecologically distinct groups of anoxygenic phototrophs suggest that such pathways may be widespread in anoxic habitats offering phototrophs a means of detoxifying Hg without dedicated enzymatic machinery.

The use of stable Hg isotopes has recently provided unique insights into oxygenic phototrophic Hg reduction. In the same study addressing MeHg demethylation in *I. galbana*, cells reduced lighter Hg^{II} isotopes with the strongest fractionation signature occurring within the intracellular pool of Hg^{II} [97]. The authors also observed mass-independent fractionation signatures suggesting that Hg was reduced by free radicals inside the cell following binding to thiol functional groups [97, 101]. The prevalence of free radical formation during oxygenic photosynthesis is such that algal cells could be seen as small photoreactors hosting Hg photoreduction. Indeed, this study represents a fascinating case of intracellular metal photoreduction that blurs the lines between abiotic and biotic transformations.

The presence of putative *merA* homologues in the genomes of some anoxygenic phototrophs [102, 103] highlights an interesting question regarding Hg tolerance in phototrophs: Do cells preferentially detoxify Hg via cometabolic processes or through the use of dedicated reductases? Currently, it seems that phototrophic Hg reduction occurs mostly as a cometabolic process that relies on core metabolic machinery rather than *mer*-like determinants, which are largely absent in phototrophs. However, very few studies have been published on the subject and the presence of such pathways has only been identified for a small number of model organisms. By exploring this question further, we will be able to better define the physiological mechanisms supporting phototrophic Hg

metabolism. The increasing availability of microbial genomes and genetic tractability of anoxygenic phototrophs should help address this question in future research.

Clearly, phototrophs are more than just an entry point for Hg into food webs. The mechanistic findings mentioned in this section frame photosynthetic redox homeostasis as a metabolic process coupled with Hg reduction. These mechanistic studies further demonstrate that phototrophs can directly impact the substrate of Hg available to methylators via Hg redox cycling. How such interactions play out in the environment remains elusive, however.

3.4.5 Phototrophic mercury oxidation

At present, there is a lack of studies addressing Hg^0 oxidation in phototrophs. This could be related to the challenges associated with working with volatile Hg^0 as a substrate. We speculate that anoxygenic phototrophic bacteria could potentially oxidize Hg^0 through thiol-related mechanisms similar to those outlined in chemotrophic anaerobes based on the fact that Hg is known to bind to thiols in the photosynthetic reaction center of PNSB [104, 105]. Currently, the presence of such pathways has yet to be investigated and Hg^0 oxidation in phototrophs has yet to be demonstrated.

3.4.6 Mercury toxicity to phototrophs

Phototrophs appear to mitigate Hg toxicity either via intracellular sequestration or elimination from the cell (e.g., via efflux or evasion). Sequestration strategies come in the form of dedicated chelating molecules such as phytochelatins and metallothioneins [7, 8]

and the production of HgS [9], all of which prevent Hg from binding to sensitive target sites inside of the cell.

Inside the cell, inorganic and organic Hg^{II} complexes can interact with a number of proteins that are essential for supporting photosynthetic metabolism. Hg's toxicity is attributable to Hg's affinity for thiols bonds [106] and its ability to substitute for cations that serve as cofactors in enzymatic reactions essential to capturing light energy [107-109]. By disrupting protein function, Hg can inhibit electron transport and the ability of cells to generate ATP thereby inhibiting cell growth [110-112]. Although toxicological studies continue to emerge evaluating the ranges of Hg concentrations tolerated by different model phototrophs [113-116], very few offer new mechanistic insights [6]. In addition, the impact of Hg^0 on photosynthetic metabolic machinery remains unexplored despite recent evidence demonstrating that Hg^0 interacts with thiols in bacterial cell membranes [69, 70].

The recent transcriptomic work with *C. reinhardtii* has provided insights into the genetic response of green algae to Hg toxicity [81, 117]. Hg exposure led to the disruption of genes involved in motility, cell division, energy metabolism, amino acid production, lipid oxidation, metal transport and antioxidant enzyme synthesis [81]. Although the apparent negative effects on gene regulation did not always manifest as a physiological response [81, 117], the authors saw increased photosynthetic efficiency when small levels of MeHg were present [117]. These results suggested a possible hormetic effect derived from MeHg exposure that merits further investigation. Based on our own observations in PNSB, there is precedence for sublethal exposure to Hg providing a physiological advantage during phototrophic growth by acting as an electron sink [98]. Whether such a pathway is

supported in oxygenic phototrophs has yet to be tested and the importance of beneficial or hormetic responses to Hg in the environment remains to be evaluated.

At the time of publishing our 2014 review paper, very little mechanistic information was available on Hg toxicity in anoxygenic phototrophs. This has changed in recent years. Work with PNSB showed that large amounts of Hg^{II} can bind to the photosynthetic reaction center (PS-RC) [104] and that the vast majority of Hg supplied to PNSB was bound to weak binding sites, rather than to high affinity thiol-bearing sites [105]. Although the exact chemical nature of the weak binding sites were not further discussed, one can speculate that these binding sites may have been carboxyl groups that have a lower affinity for Hg [118-120] and are known to be present in the PS-RC [121]. Sipka et al., also demonstrated that Hg toxicity was attributable to a small number of strong thiol-bearing Hg binding sites that disrupted cyclical phosphorylation by inhibiting inter-quinone electron transfer and proton translocation [105]. Despite the sensitivity of electron transport machinery to Hg, model PNSB strains could tolerate µM levels of Hg before damage to photosynthetic membranes became apparent [122].

These new findings illustrate that Hg targets may be similar between oxygenic anoxygenic phototrophs, which is unsurprising given the evolutionary parallels between some components of their photosynthetic machinery. Although the availability of genomic information frame PNSB as excellent models to study Hg toxicity in anoxygenic phototrophs, the response of other clades to Hg has yet to be characterized. For instance, we know very little of Hg interactions with green (non)-sulphur bacteria, aerobic anoxygenic photosynthetic bacteria, Heliobacteria or purple sulphur bacteria. This information would be useful in revealing the evolutionary and physiological context

shaping the response to Hg toxicity among phylogenetically distinct clades of phototrophs. Indeed, the absence of dedicated Hg resistance strategies such as the *mer* operon among anaerobes and phototrophs is puzzling. There appears to be a tight coupling between the presence of oxygen and the evolution of the *mer* operon [64]. Anaerobic and anoxygenic phototrophic metabolisms predate the rise of oxygen on planet Earth and cometabolic processes such as sequestration or the use of excess reducing power to catalyze Hg reduction may have been sufficient to cope with Hg toxicity in the absence of oxygen.

3.5 CONCLUDING REMARKS

Over the last four years, we have observed a shift in the field of research addressing microbial Hg transformations. Investigations into chemotrophic Hg methylation still dominate the literature thanks largely to the discovery of the *hgcAB* gene cluster. With powerful molecular tools in hand, one important frontier in our field is to identify the native function of this gene cluster and the possible role(s) associated with Hg methylation. In addition to gaining fundamental insights into the process, such mechanistic insights may reveal strategies that could help manage Hg pollution.

Important mechanistic details on anaerobic and phototrophic Hg cycling have also emerged leading us to reconsider the environmental contributions of anaerobic Hg redox cycling pathways. One such contribution is summarized in **Fig 3.1**, highlighting a possible role for phototrophs in catalyzing Hg reduction at redox interfaces within a stratified lake ecosystem.

Once deposited into aquatic ecosystems, aqueous Hg speciation is altered such that ageing of Hg complexes occurs, typically leading to low Hg bioavailability over time (**Fig 3.1A-(1**)). Redox processes catalyzing the transformation of Hg complexes control the delivery of bioavailable Hg to anoxic zones. This occurs by resetting Hg speciation, i.e., remobilizing Hg initially present as poorly bioavailable complexes (e.g., Hg-DOM or Hg-particles) to more mobile and bioavailable species (e.g., Hg^0, **Fig 3.1A-(2)** and **3.1B**). This can occur by anaerobic or photobiological redox processes targeting Hg and described in this review, or via heterotrophic or photochemical degradation of the organic ligands to which Hg is bound. Given the increasing importance of anaerobes in Hg^0 oxidation and anoxygenic phototrophs in Hg^{II} reduction, these groups can provide a fresh supply of bioavailable Hg to sites conducive to Hg methylation (**Fig 3.1A-(3)** and **3.1B**).

This conceptual redox wheel [85] is meant to highlight the potential for highly dynamic yet cryptic Hg redox cycling (**Fig 3.1B**). We use the word cryptic here to highlight the fact that no net Hg^0 accumulation may be observed but its production and rapid oxidation may represent an essential step in controlling Hg mobility at, and across, redox interfaces. Furthermore, this conceptual framework illustrates how phototrophs (or other anaerobes) can participate in Hg transformation well beyond their role as MeHg accumulators at the base of food webs. Note that such processes can occur in any stratified environment, whether it is within the metalimnion of lakes, microbial mats or periphytic communities (**Fig 3.1**).

Although lab studies have afforded the controlled conditions necessary to elucidate new mechanisms for phototrophic Hg transformations, these pathways continue to be understudied in the environment. This knowledge gap will become increasingly important to address in the face of predicted environmental change. Increases in temperature, prolonged ice-free seasons and more intense water column stratification will have a dramatic impact on phototroph dynamics that, in turn, exert important controls on environmental chemistry and metal speciation. Indeed, there stand to be far-reaching impacts on global Hg cycling stemming from changes in phototrophic communities that occupy broad niches in oxic and anoxic habitats.

3.6 FUNDING

Our work was funded by NSERC Discovery and Accelerator grants, CFI funding to AJP and NSERC graduate scholarship to DSG.

3.7 ACKNOWLEDGMENTS

This paper has been improved thanks to the work of three reviewers to whom we are grateful. We also would like to thank Tamar Barkay and Britt D. Hall for comments on an earlier version of this manuscript and Cindy Gilmour for her continued insights on the role of microbes in Hg cycling.

3.8 AUTHOR CONTRIBUTIONS

DSG and AJP conceived and designed the study. DSG and AJP performed the experiments/collected the data. DSG and AJP analyzed and interpreted the data. DSP and AJP contributed resources. DSG and AJP drafted or revised the manuscript.

3.9 REFERENCES

1. Obrist, D.; Kirk, J. L.; Zhang, L.; Sunderland, E. M.; Jiskra, M.; Selin, N. E., A review of global environmental mercury processes in response to human and natural perturbations: Changes of emissions, climate, and land use. *Ambio* **2018,** *47*, (2), 116-140.

2. Selin, N. E.; Jacob, D. J.; Park, R. J.; Yantosca, R. M.; Strode, S.; Jaegle, L.; Jaffe, D., Chemical cycling and deposition of atmospheric mercury: Global constraints from observations. *Journal of Geophysical Research-Atmospheres* **2007,** *112*, (D2).

3. Sunderland, E. M., Mercury exposure from domestic and imported estuarine and marine fish in the U.S. seafood market. *Environmental Health Perspectives* **2007,** *115*, (2), 235-242.

4. Zhang, H.; Feng, X. B.; Larssen, T.; Qiu, G. L.; Vogt, R. D., In inland China, rice, rather than fish, is the major pathway for methylmercury exposure. *Environmental Health Perspectives* **2010,** *118*, (9), 1183-1188.

5. Barkay, T.; Wagner-Dobler, I., Microbial transformations of mercury: Potentials, challenges, and achievements in controlling mercury toxicity in the environment. In *Advances in Applied Microbiology, Vol 57*, Laskin, A. I.; Bennett, J. W.; Gadd, G. M., Eds. 2005; Vol. 57, pp 1-52.

6. Grégoire, D. S.; Poulain, A. J., A little bit of light goes a long way: The role of phototrophs on mercury cycling. *Metallomics* **2014,** *6*, (3), 396-407.

7. Rauser, W. E., Phytochelatins. *Annual Review of Biochemistry* **1990,** *59*, (1), 61-86.

8. Kawakami, S. K.; Gledhill, M.; Achterberg, E. P., Production of phytochelatins and glutathione by marine phytoplankton in response to metal stress. *Journal of Phycology* **2006,** *42*, (5), 975-989.

9. Kelly, D. J. A.; Budd, K.; Lefebvre, D. D., Biotransformation of mercury in pH-stat cultures of eukaryotic freshwater algae. *Archives of Microbiology* **2007,** *187*, (1), 45-53.

10. Krabbenhoft, D. P.; Sunderland, E. M., Global change and mercury. *Science* **2013,** *341*, (6153), 1457-1458.

11. Parks, J. M.; Johs, A.; Podar, M.; Bridou, R.; Hurt Jr, R. A.; Smith, S. D.; Tomanicek, S. J.; Qian, Y.; Brown, S. D.; Brandt, C. C.; Palumbo, A. V.; Smith, J. C.; Wall, J. D.; Elias, D. A.; Liang, L., The genetic basis for bacterial mercury methylation. *Science* **2013,** *339*, (6125), 1332-1335.

12. Zhou, J.; Riccardi, D.; Beste, A.; Smith, J. C.; Parks, J. M., Mercury methylation by HgcA: Theory supports carbanion transfer to Hg(II). *Inorganic Chemistry* **2014,** *53*, (2), 772-777.

13. Schaefer, J. K.; Szczuka, A.; Morel, F. M. M., Effect of divalent metals on Hg(II) uptake and methylation by bacteria. *Environmental Science and Technology* **2014,** *48*, (5), 3007-3013.

14. Lin, H.; Hurt, R. A.; Johs, A.; Parks, J. M.; Morrell-Falvey, J. L.; Liang, L.; Elias, D. A.; Gu, B., Unexpected effects of gene deletion on interactions of mercury with the methylation-deficient mutant Δ*hgcAB*. *Environmental Science and Technology Letters* **2014,** *1*, (5), 271-276.

15. Qian, C.; Johs, A.; Chen, H.; Mann, B. F.; Lu, X.; Abraham, P. E.; Hettich, R. L.; Gu, B., Global proteome response to deletion of genes related to mercury methylation and dissimilatory metal reduction reveals changes in respiratory metabolism in *Geobacter sulfurreducens* PCA. *Journal of Proteome Research* **2016,** *15*, (10), 3540-3549.

16. Podar, M.; Gilmour, C. C.; Brandt, C. C.; Soren, A.; Brown, S. D.; Crable, B. R.; Palumbo, A. V.; Somenahally, A. C.; Elias, D. A., Global prevalence and distribution of

genes and microorganisms involved in mercury methylation. *Science Advances* **2015,** *1*, 1-13.

17. Choi, S. C.; Chase Jr, T.; Bartha, R., Metabolic pathways leading to mercury methylation in *Desulfovibrio desulfuricans* LS. *Applied and Environmental Microbiology* **1994,** *60*, (11), 4072-4077.

18. Choi, S. C.; Chase Jr, T.; Bartha, R., Enzymatic catalysis of mercury methylation by *Desulfovibrio desulfuricans* LS. *Applied and Environmental Microbiology* **1994,** *60*, (4), 1342-1346.

19. Fleming, E. J.; Mack, E. E.; Green, P. G.; Nelson, D. C., Mercury methylation from unexpected sources: Molybdate-inhibited freshwater sediments and an iron-reducing bacterium. *Applied and Environmental Microbiology* **2006,** *72*, (1), 457-464.

20. Han, S.; Narasingarao, P.; Obraztsova, A.; Gieskes, J.; Hartmann, A. C.; Tebo, B. M.; Allen, E. E.; Deheyn, D. D., Mercury speciation in marine sediments under sulfate-limited conditions. *Environmental Science and Technology* **2010,** *44*, (10), 3752-3757.

21. Hamelin, S.; Amyot, M.; Barkay, T.; Wang, Y.; Planas, D., Methanogens: Principal methylators of mercury in lake periphyton. *Environmental Science and Technology* **2011,** *45*, (18), 7693-7700.

22. Yu, R.-Q.; Reinfelder, J. R.; Hines, M. E.; Barkay, T., Mercury methylation by the methanogen *Methanospirillum hungatei*. *Applied and Environmental Microbiology* **2013,** *79*, (20), 6325-6330.

23. Christensen, G. A.; Wymore, A. M.; King, A. J.; Podar, M.; Hurt, R. A.; Santillan, E. U.; Soren, A.; Brandt, C. C.; Brown, S. D.; Palumbo, A. V.; Wall, J. D.; Gilmour, C. C.; Elias, D. A., Development and validation of broad-range qualitative and

clade-specific quantitative molecular probes for assessing mercury methylation in the environment. *Applied and Environmental Microbiology* **2016,** *82*, (19), 6068-6078.

24. Schaefer, J. K.; Kronberg, R. M.; Morel, F. M. M.; Skyllberg, U., Detection of a key Hg methylation gene, *hgcA*, in wetland soils. *Environmental Microbiology Reports* **2014,** *6*, (5), 441-447.

25. Paranjape, A. R.; Hall, B. D., Recent advances in the study of mercury methylation in aquatic systems. *FACETS* **2017,** *2*, (1), 85-119.

26. Gilmour, C. C.; Bullock, A. L.; McBurney, A.; Podar, M.; Elias, D. A., Robust mercury methylation across diverse methanogenic Archaea. *mBio* **2018,** *9*, (2).

27. Bae, H. S.; Dierberg, F. E.; Ogram, A., Syntrophs dominate sequences associated with the mercury methylation-related gene *hgcA* in the water conservation areas of the Florida Everglades. *Applied and Environmental Microbiology* **2014,** *80*, (20), 6517-6526.

28. Graham, E. B.; Gabor, R. S.; Schooler, S.; McKnight, D. M.; Nemergut, D. R.; Knelman, J. E., Oligotrophic wetland sediments susceptible to shifts in microbiomes and mercury cycling with dissolved organic matter addition. *PeerJ* **2018,** *6*, e4575.

29. Bravo, A. G.; Zopfi, J.; Buck, M.; Xu, J.; Bertilsson, S.; Schaefer, J. K.; Poté, J.; Cosio, C., Geobacteraceae are important members of mercury-methylating microbial communities of sediments impacted by waste water releases. *ISME Journal* **2018**, 1-11.

30. Bravo, A. G.; Loizeau, J. L.; Dranguet, P.; Makri, S.; Björn, E.; Ungureanu, V. G.; Slaveykova, V. I.; Cosio, C., Persistent Hg contamination and occurrence of Hg-methylating transcript (*hgcA*) downstream of a chlor-alkali plant in the Olt River (Romania). *Environmental Science and Pollution Research* **2016,** *23*, (11), 10529-10541.

31. Ma, M.; Du, H. X.; Wang, D. Y.; Kang, S. C.; Sun, T., Biotically mediated mercury methylation in the soils and sediments of Nam Co Lake, Tibetan Plateau. *Environmental Pollution* **2017,** *227*, 243-251.

32. Dranguet, P.; Le Faucheur, S.; Cosio, C.; Slaveykova, V. I., Influence of chemical speciation and biofilm composition on mercury accumulation by freshwater biofilms. *Environmental Science-Processes & Impacts* **2017,** *19*, (1), 38-49.

33. Ma, M.; du, H.; Wang, D.; Sun, T., Mercury methylation in the soils and sediments of Three Gorges Reservoir Region. *Journal of Soils and Sediments* **2017**, 1-10.

34. Su, Y. B.; Chang, W. C.; Hsi, H. C.; Lin, C. C., Investigation of biogeochemical controls on the formation, uptake and accumulation of methylmercury in rice paddies in the vicinity of a coal-fired power plant and a municipal solid waste incinerator in Taiwan. *Chemosphere* **2016,** *154*, 375-384.

35. Vishnivetskaya, T. A.; Hu, H.; Van Nostrand, J. D.; Wymore, A.; Xu, X.; Qiu, G.; Feng, X.; Zhou, J.; Brown, S. D.; Brandt, C. C.; Podar, M.; Gu, B.; Elias, D. A., Microbial community structure with trends in methylation gene diversity and abundance in mercury-contaminated rice paddy soils in Guizhou, China. *Environmental Science: Processes & Impacts* **2018,** *20*, (4), 673-685.

36. Gionfriddo, C. M.; Tate, M. T.; Wick, R. R.; Schultz, M. B.; Zemla, A.; Thelen, M. P.; Schofield, R.; Krabbenhoft, D. P.; Holt, K. E.; Moreau, J. W., Microbial mercury methylation in Antarctic sea ice. *Nature microbiology* **2016,** *1*, (10), 16127.

37. Yu, R.-Q.; Reinfelder, J. R.; Hines, M. E.; Barkay, T., Syntrophic pathways for microbial mercury methylation. *The ISME Journal* **2018**.

38. Landner, L., Biochemical model for the biological methylation of mercury suggested from methylation studies *in vivo* with *Neurospora crassa*. *Nature* **1971,** *230*, (5294), 452-454.

39. Christensen, G. A.; Somenahally, A. C.; Moberly, J. G.; Miller, C. M.; King, A. J.; Gilmour, C. C.; Brown, S. D.; Podar, M.; Brandt, C. C.; Brooks, S. C.; Palumbo, A. V.; Wall, J. D.; Elias, D. A., Carbon amendments alter microbial community structure and net mercury methylation potential in sediments. *Applied and Environmental Microbiology* **2018,** *84*, (3).

40. Liu, J.; Valsaraj, K. T.; Delaune, R. D., Inhibition of mercury methylation by iron sulfides in an anoxic sediment. *Environmental Engineering Science* **2009,** *26*, (4), 833-840.

41. Pham, A. L. T.; Morris, A.; Zhang, T.; Ticknor, J.; Levard, C.; Hsu-Kim, H., Precipitation of nanoscale mercuric sulfides in the presence of natural organic matter: Structural properties, aggregation, and biotransformation. *Geochimica et Cosmochimica Acta* **2014,** *133*, 204-215.

42. Graham, A. M.; Aiken, G. R.; Gilmour, C. C., Effect of dissolved organic matter source and character on microbial Hg methylation in Hg-S-DOM solutions. *Environmental Science & Technology* **2013,** *47*, (11), 5746-5754.

43. Graham, A. M.; Cameron-Burr, K. T.; Hajic, H. A.; Lee, C.; Msekela, D.; Gilmour, C. C., Sulfurization of dissolved organic matter increases Hg-sulfide-dissolved organic matter bioavailability to a Hg-methylating bacterium. *Environmental Science & Technology* **2017,** *51*, (16), 9080-9088.

44. Mazrui, N.; Seelen, E.; King'ondu, C. K.; Thota, S.; Awino, J.; Rouge, J.; Zhao, J.; Mason, R. P., The precipitation, growth and stability of mercury sulfide nanoparticles formed in the presence of marine dissolved organic matter. *Environmental Science: Processes & Impacts* **2018**.

45. Parks, J. M.; Smith, J. C., Modeling mercury in proteins. In *Computational Approaches for Studying Enzyme Mechanism, Pt B*, Voth, G. A., Ed. 2016; Vol. 578, pp 103-122.

46. Hsu-Kim, H.; Kucharzyk, K. H.; Zhang, T.; Deshusses, M. A., Mechanisms regulating mercury bioavailability for methylating microorganisms in the aquatic environment: A critical review. *Environmental Science and Technology* **2013,** *47*, (6), 2441-2456.

47. Mahbub, K. R.; Krishnan, K.; Naidu, R.; Andrews, S.; Megharaj, M., Mercury toxicity to terrestrial biota. *Ecological Indicators* **2017,** *74*, (Complete), 451-462.

48. Lin, H.; Lu, X.; Liang, L. Y.; Gu, B. H., Cysteine inhibits mercury methylation by *Geobacter sulfurreducens* PCA mutant Δ*omcBESTZ*. *Environmental Science & Technology Letters* **2015,** *2*, (5), 144-148.

49. Liu, Y. R.; Lu, X.; Zhao, L. D.; An, J.; He, J. Z.; Pierce, E. M.; Johs, A.; Gu, B. H., Effects of cellular sorption on mercury bioavailability and methylmercury production by *Desulfovibrio desulfuricans* ND132. *Environmental Science & Technology* **2016,** *50*, (24), 13335-13341.

50. Zhao, L. D.; Chen, H. M.; Lu, X.; Lin, H.; Christensen, G. K.; Pierce, E. M.; Gu, B. H., Contrasting effects of dissolved organic matter on mercury methylation by

Geobacter sulfurreducens PCA and *Desulfovibrio desulfuricans* ND132. *Environmental Science & Technology* **2017,** *51*, (18), 10468-10475.

51. Janssen, S. E.; Schaefer, J. K.; Barkay, T.; Reinfelder, J. R., Fractionation of mercury stable isotopes during microbial methylmercury production by iron- and sulfate-reducing bacteria. *Environmental Science & Technology* **2016,** *50*, (15), 8077-8083.

52. Barkay, T.; Miller, S. M.; Summers, A. O., Bacterial mercury resistance from atoms to ecosystems. *FEMS microbiology reviews* **2003,** *27*, (2-3), 355-384.

53. Parks, J. M.; Guo, H.; Momany, C.; Liang, L.; Miller, S. M.; Summers, A. O.; Smith, J. C., Mechanism of Hg-C protonolysis in the organomercurial lyase MerB. *Journal of the American Chemical Society* **2009,** *131*, (37), 13278-13285.

54. Oremland, R. S.; Culbertson, C. W.; Winfrey, M. R., Methylmercury decomposition in sediments and bacterial cultures: Involvement of methanogens and sulfate reducers in oxidative demethylation. *Applied and Environmental Microbiology* **1991,** *57*, (1), 130-137.

55. Silva, P. J.; Rodrigues, V., Mechanistic pathways of mercury removal from the organomercurial lyase active site. *PeerJ* **2015,** *2015*, (7).

56. Wahba, H. M.; Lecoq, L.; Stevenson, M.; Mansour, A.; Cappadocia, L.; Lafrance-Vanasse, J.; Wilkinson, K. J.; Sygusch, J.; Wilcox, D. E.; Omichinski, J. G., Structural and biochemical characterization of a copper-binding mutant of the organomercurial lyase MerB: Insight into the key role of the active site aspartic acid in Hg-carbon bond cleavage and metal binding specificity. *Biochemistry* **2016,** *55*, (7), 1070-1081.

57. Lu, X.; Liu, Y.; Johs, A.; Zhao, L.; Wang, T.; Yang, Z.; Lin, H.; Elias, D. A.; Pierce, E. M.; Liang, L.; Barkay, T.; Gu, B., Anaerobic mercury methylation and

demethylation by *Geobacter bemidjiensis* Bem. *Environmental Science and Technology* **2016,** *50*, (8), 4366-4373.

58. Ndu, U.; Barkay, T.; Schartup, A. T.; Mason, R. P.; Reinfelder, J. R., The effect of aqueous speciation and cellular ligand binding on the biotransformation and bioavailability of methylmercury in mercury-resistant bacteria. *Biodegradation* **2016,** *27*, (1), 29-36.

59. Baral, B. S.; Bandow, N. L.; Vorobev, A.; Freemeier, B. C.; Bergman, B. H.; Herdendorf, T. J.; Fuentes, N.; Ellias, L.; Turpin, E.; Semrau, J. D.; DiSpirito, A. A., Mercury binding by methanobactin from *Methylocystis* strain SB2. *Journal of Inorganic Biochemistry* **2014,** *141*, 161-169.

60. Lu, X.; Gu, W. Y.; Zhao, L. D.; Ul Haque, M. F.; DiSpirito, A. A.; Semrau, J. D.; Gu, B. H., Methylmercury uptake and degradation by methanotrophs. *Science Advances* **2017,** *3*, (5).

61. Kronberg, R.-M.; Schaefer, J. K.; Björn, E.; Skyllberg, U., Mechanisms of methylmercury net degradation in alder swamps: The role of methanogens and abiotic processes. *Environmental Science & Technology Letters* **2018**.

62. Vazquez-Rodriguez, A. I.; Hansel, C. M.; Zhang, T.; Lamborg, C. H.; Santelli, C. M.; Webb, S. M.; Brooks, S. C., Microbial- and thiosulfate-mediated dissolution of mercury sulfide minerals and transformation to gaseous mercury. *Frontiers in Microbiology* **2015,** *6*.

63. Norambuena, J.; Wang, Y.; Hanson, T.; Boyd, J. M.; Barkay, T., Low-molecular-weight thiols and thioredoxins are important players in Hg(II) resistance in *Thermus thermophilus* HB27. *Applied and Environmental Microbiology* **2018,** *84*, (2).

64. Barkay, T.; Kritee, K.; Boyd, E.; Geesey, G., A thermophilic bacterial origin and subsequent constraints by redox, light and salinity on the evolution of the microbial mercuric reductase. *Environmental Microbiology* **2010,** *12*, (11), 2904-2917.

65. Lee, S.; Kim, D. H.; Kim, K. W., The enhancement and inhibition of mercury reduction by natural organic matter in the presence of *Shewanella oneidensis* MR-1. *Chemosphere* **2018,** *194*, 515-522.

66. Liu, S.; Wiatrowski, H. A., Reduction of Hg(II) to Hg(0) by biogenic magnetite from two magnetotactic bacteria. *Geomicrobiology Journal* **2018,** *35*, (3), 198-208.

67. Grégoire, D. S.; Lavoie, N. C.; Poulain, A. J., Heliobacteria reveal fermentation as a key pathway for mercury reduction in anoxic environments. *Environmental Science and Technology* **2018,** *52*, 4145-4153.

68. Desrochers, K. A. N.; Paulson, K. M. A.; Ptacek, C. J.; Blowes, D. W.; Gould, W. D., Effect of electron donor to sulfate ratio on mercury methylation in floodplain sediments under saturated flow conditions. *Geomicrobiology Journal* **2015,** *32*, (10), 924-933.

69. Colombo, M. J.; Ha, J.; Reinfelder, J. R.; Barkay, T.; Yee, N., Anaerobic oxidation of Hg(0) and methylmercury formation by *Desulfovibrio desulfuricans* ND132. *Geochimica et Cosmochimica Acta* **2013,** *112*, 166-177.

70. Colombo, M. J.; Ha, J.; Reinfelder, J. R.; Barkay, T.; Yee, N., Oxidation of Hg(0) to Hg(II) by diverse anaerobic bacteria. *Chemical Geology* **2014,** *363*, 334-340.

71. Lin, H.; Morrell-Falvey, J. L.; Rao, B.; Liang, L.; Gu, B., Coupled mercury-cell sorption, reduction, and oxidation on methylmercury production by *Geobacter*

sulfurreducens PCA. *Environmental Science and Technology* **2014,** *48*, (20), 11969-11976.

72. Yu, Q.; Szymanowski, J.; Myneni, S. C. B.; Fein, J. B., Characterization of sulfhydryl sites within bacterial cell envelopes using selective site-blocking and potentiometric titrations. *Chemical Geology* **2014,** *373*, 50-58.

73. Mazur, M. E. E.; Eckley, C. S.; Mitchell, C. P. J., Susceptibility of soil bound mercury to gaseous emission as a function of source depth: An enriched isotope tracer investigation. *Environmental Science & Technology* **2015,** *49*, (15), 9143-9149.

74. Poulin, B. A.; Aiken, G. R.; Nagy, K. L.; Monceau, A.; Krabbenhoft, D. P.; Ryan, J. N., Mercury transformation and release differs with depth and time in a contaminated riparian soil during simulated flooding. *Geochimica Et Cosmochimica Acta* **2016,** *176*, 118-138.

75. Bouffard, A.; Amyot, M., Importance of elemental mercury in lake sediments. *Chemosphere* **2009,** *74*, (8), 1098-1103.

76. Poulain, A. J.; Amyot, M.; Findlay, D.; Telor, S.; Barkay, T.; Hintelmann, H., Biological and photochemical production of dissolved gaseous mercury in a boreal lake. *Limnology and Oceanography* **2004,** *49*, (6), 2265-2275.

77. Polerecky, L.; Bachar, A.; Schoon, R.; Grinstein, M.; Jorgensen, B. B.; de Beer, D.; Jonkers, H. M., Contribution of *Chloroflexus* respiration to oxygen cycling in a hypersaline microbial mat from Lake Chiprana, Spain. *Environmental Microbiology* **2007,** *9*, (8), 2007-2024.

78. Dupraz, C.; Visscher, P. T., Microbial lithification in marine stromatolites and hypersaline mats. *Trends in Microbiology* **2005,** *13*, (9), 429-438.

79. Sloth, N. P.; Riemann, B.; Nielsen, L. P.; Blackburn, T. H., Resilience of pelagic and benthic microbial communities to sediment resuspension in a coastal ecosystem, Knebel Vig, Denmark. *Estuarine Coastal and Shelf Science* **1996,** *42*, (4), 405-415.

80. Rossi, F.; Potrafka, R. M.; Pichel, F. G.; De Philippis, R., The role of the exopolysaccharides in enhancing hydraulic conductivity of biological soil crusts. *Soil Biology & Biochemistry* **2012,** *46*, 33-40.

81. Beauvais-Fluck, R.; Slaveykova, V. I.; Cosio, C., Cellular toxicity pathways of inorganic and methyl mercury in the green microalga *Chlamydomonas reinhardtii*. *Scientific Reports* **2017,** *7*.

82. Kis, M.; Sipka, G.; Maroti, P., Stoichiometry and kinetics of mercury uptake by photosynthetic bacteria. *Photosynthesis Research* **2017,** *132*, (2), 197-209.

83. Stenzler, B.; Hinz, A.; Ruuskanen, M.; Poulain, A. J., Ionic strength differentially affects the bioavailability of neutral and negatively charged inorganic Hg complexes. *Environmental Science & Technology* **2017,** *51*, (17), 9653-9662.

84. Zhong, H.; Wang, W. X., Controls of dissolved organic matter and chloride on mercury uptake by a marine diatom. *Environmental Science and Technology* **2009,** *43*, (23), 8998-9003.

85. Chiasson-Gould, S. A.; Blais, J. M.; Poulain, A. J., Dissolved organic matter kinetically controls mercury bioavailability to bacteria. *Environmental Science & Technology* **2014,** *48*, (6), 3153-3161.

86. Cárdenas, C. S.; Diéguez, M. C.; Guevara, S. R.; Marvin-DiPasquale, M.; Queimaliños, C. P., Incorporation of inorganic mercury (Hg2+) in pelagic food webs of

ultraoligotrophic and oligotrophic lakes: The role of different plankton size fractions and species assemblages. *Science of the Total Environment* **2014,** *494*, 65-73.

87. Soto Cárdenas, C.; Gerea, M.; Queimaliños, C.; Ribeiro Guevara, S.; Diéguez, M. C., Inorganic mercury (Hg2+) accumulation in autotrophic and mixotrophic planktonic protists: Implications for Hg trophodynamics in ultraoligotrophic Andean Patagonian lakes. *Chemosphere* **2018,** *199*, 223-231.

88. Raven, J. A., Contributions of anoxygenic and oxygenic phototrophy and chemolithotrophy to carbon and oxygen fluxes in aquatic environments. *Aquatic Microbial Ecology* **2009,** *56*, (2-3), 177-192.

89. Lanza, W. G.; Acha, D.; Point, D.; Masbou, J.; Alanoca, L.; Amouroux, D.; Lazzaro, X., Association of a specific algal group with methylmercury accumulation in periphyton of a tropical high-altitude Andean lake. *Archives of Environmental Contamination and Toxicology* **2017,** *72*, (1), 1-10.

90. Bouchet, S.; Goñi-Urriza, M.; Monperrus, M.; Guyoneaud, R.; Fernandez, P.; Heredia, C.; Tessier, E.; Gassie, C.; Point, D.; Guédron, S.; Acha, D.; Amouroux, D., Linking microbial activities and low molecular weight thiols to Hg methylation in biofilms and periphyton from high altitude tropical lakes (Bolivian altiplano). *Environmental Science & Technology* **2018**.

91. Gentes, S.; Taupiac, J.; Colin, Y.; Andre, J. M.; Guyoneaud, R., Bacterial periphytic communities related to mercury methylation within aquatic plant roots from a temperate freshwater lake (South-Western France). *Environmental Science and Pollution Research* **2017,** *24*, (23), 19223-19233.

92. Olsen, T. A.; Brandt, C. C.; Brooks, S. C., Periphyton biofilms influence net methylmercury production in an industrially contaminated system. *Environmental Science & Technology* **2016,** *50*, (20), 10843-10850.

93. Lazaro, W. L.; Diez, S.; da Silva, C. J.; Ignacio, A. R. A.; Guimaraes, J. R. D., Seasonal changes in peryphytic microbial metabolism determining mercury methylation in a tropical wetland. *Science of the Total Environment* **2018,** *627*, 1345-1352.

94. Deng, G. F.; Zhang, T. W.; Yang, L. M.; Wang, Q. Q., Studies of biouptake and transformation of mercury by a typical unicellular diatom *Phaeodactylum tricornutum*. *Chinese Science Bulletin* **2013,** *58*, (2), 256-265.

95. Pongratz, R.; Heumann, K. G., Production of methylated mercury and lead by polar macroalgae - A significant natural source for atmospheric heavy metals in clean room compartments. *Chemosphere* **1998,** *36*, (9), 1935-1946.

96. Franco, M. W.; Mendes, L. A.; Windmöller, C. C.; Moura, K. A. F.; Oliveira, L. A. G.; Barbosa, F. A. R., Mercury methylation capacity and removal of Hg species from aqueous medium by Cyanobacteria. *Water, Air, & Soil Pollution* **2018,** *229*, (4), 127.

97. Kritee, K.; Motta, L. C.; Blum, J. D.; Tsui, M. T.-K.; Reinfelder, J. R., Photomicrobial visible light-induced magnetic mass independent fractionation of mercury in a marine microalga. *ACS Earth and Space Chemistry* **2017**.

98. Grégoire, D. S.; Poulain, A. J., A physiological role for Hg(II) during phototrophic growth. *Nature Geoscience* **2016,** *9*, (2), 121-125.

99. Schütte, U. M. E.; Cadieux, S. B.; Hemmerich, C.; Pratt, L. M.; White, J. R., Unanticipated geochemical and microbial community structure under seasonal ice cover in a dilute, dimictic Arctic lake. *Frontiers in Microbiology* **2016,** *7*, (1035).

100. Schneider, D.; Arp, G.; Reimer, A.; Reitner, J.; Daniel, R., Phylogenetic analysis of a microbialite-forming microbial mat from a hypersaline lake of the Kiritimati Atoll, Central Pacific. *Plos One* **2013,** *8*, (6).

101. Zheng, W.; Hintelmann, H., Isotope fractionation of mercury during Its photochemical reduction by low-molecular-weight organic compounds. *The Journal of Physical Chemistry A* **2010,** *114*, (12), 4246-4253.

102. Mukkata, K.; Kantachote, D.; Wittayaweerasak, B.; Techkarnjanaruk, S.; Mallavarapu, M.; Naidu, R., Distribution of mercury in shrimp ponds and volatilization of Hg by isolated resistant purple non-sulfur bacteria. *Water, Air, and Soil Pollution* **2015,** *226*, (5).

103. Pérez, V.; Dorador, C.; Molina, V.; Yáñez, C.; Hengst, M., *Rhodobacter* sp. Rb3, an aerobic anoxygenic phototroph which thrives in the polyextreme ecosystem of the Salar de Huasco, in the Chilean Altiplano. *Antonie van Leeuwenhoek* **2018**.

104. Asztalos, E.; Sipka, G.; Kis, M.; Trotta, M.; Maróti, P., The reaction center is the sensitive target of the mercury(II) ion in intact cells of photosynthetic bacteria. *Photosynthesis Research* **2012,** *112*, (2), 129-140.

105. Sipka, G.; Kis, M.; Maróti, P., Characterization of mercury(II)-induced inhibition of photochemistry in the reaction center of photosynthetic bacteria. *Photosynthesis Research* **2017**, 1-14.

106. Rooney, J. P. K., The role of thiols, dithiols, nutritional factors and interacting ligands in the toxicology of mercury. *Toxicology* **2007,** *234*, (3), 145-156.

107. Singh, R.; Srivastava, P. K.; Singh, V. P.; Dubey, G.; Prasad, S. M., Light intensity determines the extent of mercury toxicity in the cyanobacterium *Nostoc muscorum*. *Acta Physiologiae Plantarum* **2012,** *34,* (3), 1119-1131.

108. Matson, R. S.; Mustoe, G. E.; Chang, S. B., Mercury inhibition on lipid biosynthesis in freshwater algae. *Environmental Science & Technology* **1972,** *6,* (2), 158-160.

109. Zhang, D. Y.; Deng, C. N.; Pan, X. L., Excess Ca2+ does not alleviate but increases the toxicity of Hg2+ to photosystem II in *Synechocystis* sp (Cyanophyta). *Ecotoxicology and Environmental Safety* **2013,** *97,* 160-165.

110. Murthy, S.; Mohanty, P., Mercury ions inhibit photosynthetic electron transport at multiple sites in the cyanobacterium *Synechococcus* 6301. *Journal of biosciences* **1993,** *18,* (3), 355-360.

111. Kukarskikh, G. P.; Graevskaya, E. E.; Krendeleva, T. E.; Timofeev, K. N.; Rubin, A. B., Effect of methylmercury on primary photosynthetic processes in the green microalga *Chlamydomonas reinhardtii*. *Biophysics* **2003,** *48,* (5), 795-801.

112. Antal, T. K.; Graevskaya, E. E.; Matorin, D. N.; Volgusheva, A. A.; Osipov, V. A.; Krendeleva, T. E.; Rubin, A. B., Assessment of the effects of methylmercury and copper ions on primary processes of photosynthesis in green microalga *Chlamydomonas moewusii* by analysis of the kinetic curves of variable chlorophyll fluorescence. *Biophysics* **2009,** *54,* (4), 481-485.

113. Chen, H. W.; Huang, W. J.; Wu, T. H.; Hon, C. L., Effects of extracellular polymeric substances on the bioaccumulation of mercury and its toxicity toward the cyanobacterium *Microcystis aeruginosa*. *Journal of Environmental Science and Health -*

Part A Toxic/Hazardous Substances and Environmental Engineering **2014,** *49*, (12), 1370-1379.

114. Nowicka, B.; Pluciński, B.; Kuczyńska, P.; Kruk, J., Physiological characterization of *Chlamydomonas reinhardtii* acclimated to chronic stress induced by Ag, Cd, Cr, Cu and Hg ions. *Ecotoxicology and Environmental Safety* **2016,** *130*, 133-145.

115. Zhu, X. F.; Zou, D. H.; Huang, Y. H.; Cao, J. M.; Sheng, G. C.; Wang, G. X., Physiological responses of *Hizikia fusiformis* (Phaeophyta) to mercury exposure. *Botanica Marina* **2015,** *58*, (2), 93-101.

116. Mu, W.; Jia, K.; Liu, Y.; Pan, X.; Fan, Y., Response of the freshwater diatom *Halamphora veneta* (Kützing) Levkov to copper and mercury and its potential for bioassessment of heavy metal toxicity in aquatic habitats. *Environmental Science and Pollution Research* **2017,** *24*, (34), 26375-26386.

117. Beauvais-Fluck, R.; Slaveykova, V. I.; Cosio, C., Transcriptomic and physiological responses of the green microalga *Chlamydomonas reinhardtii* during short-term exposure to subnanomolar methylmercury concentrations. *Environmental Science & Technology* **2016,** *50*, (13), 7126-7134.

118. Jiang, T.; Skyllberg, U.; Wei, S. Q.; Wang, D. Y.; Lu, S.; Jiang, Z. M.; Flanagan, D. C., Modeling of the structure-specific kinetics of abiotic, dark reduction of Hg(II) complexed by O/N and S functional groups in humic acids while accounting for time-dependent structural rearrangement. *Geochimica Et Cosmochimica Acta* **2015,** *154*, 151-167.

119. Gu, B.; Bian, Y.; Miller, C. L.; Dong, W.; Jiang, X.; Liang, L., Mercury reduction and complexation by natural organic matter in anoxic environments. *Proceedings of the National Academy of Sciences of the United States of America* **2011,** *108*, (4), 1479-1483.

120. Mishra, B.; O'Loughlin, E. J.; Boyanov, M. I.; Kemner, K. M., Binding of Hg(II) to high-affinity sites on bacteria inhibits reduction to Hg(0) by mixed Fe(II)/(III) phases. *Environmental Science & Technology* **2011,** *45*, (22), 9597-9603.

121. Knox, P. P.; Gorokhov, V. V.; Korvatovskiy, B. N.; Lukashev, E. P.; Goryachev, S. N.; Paschenko, V. Z.; Rubin, A. B., The effect of light and temperature on the dynamic state of *Rhodobacter sphaeroides* reaction centers proteins determined from changes in tryptophan fluorescence lifetime and P(+)Q(A)(-) recombination kinetics. *Journal of Photochemistry and Photobiology B-Biology* **2018,** *180*, 140-148.

122. Kis, M.; Sipka, G.; Asztalos, E.; Rázga, Z.; Maróti, P., Purple non-sulfur photosynthetic bacteria monitor environmental stresses. *Journal of Photochemistry and Photobiology B: Biology* **2015,** *151*, 110-117.

3.10 FIGURE AND CAPTION

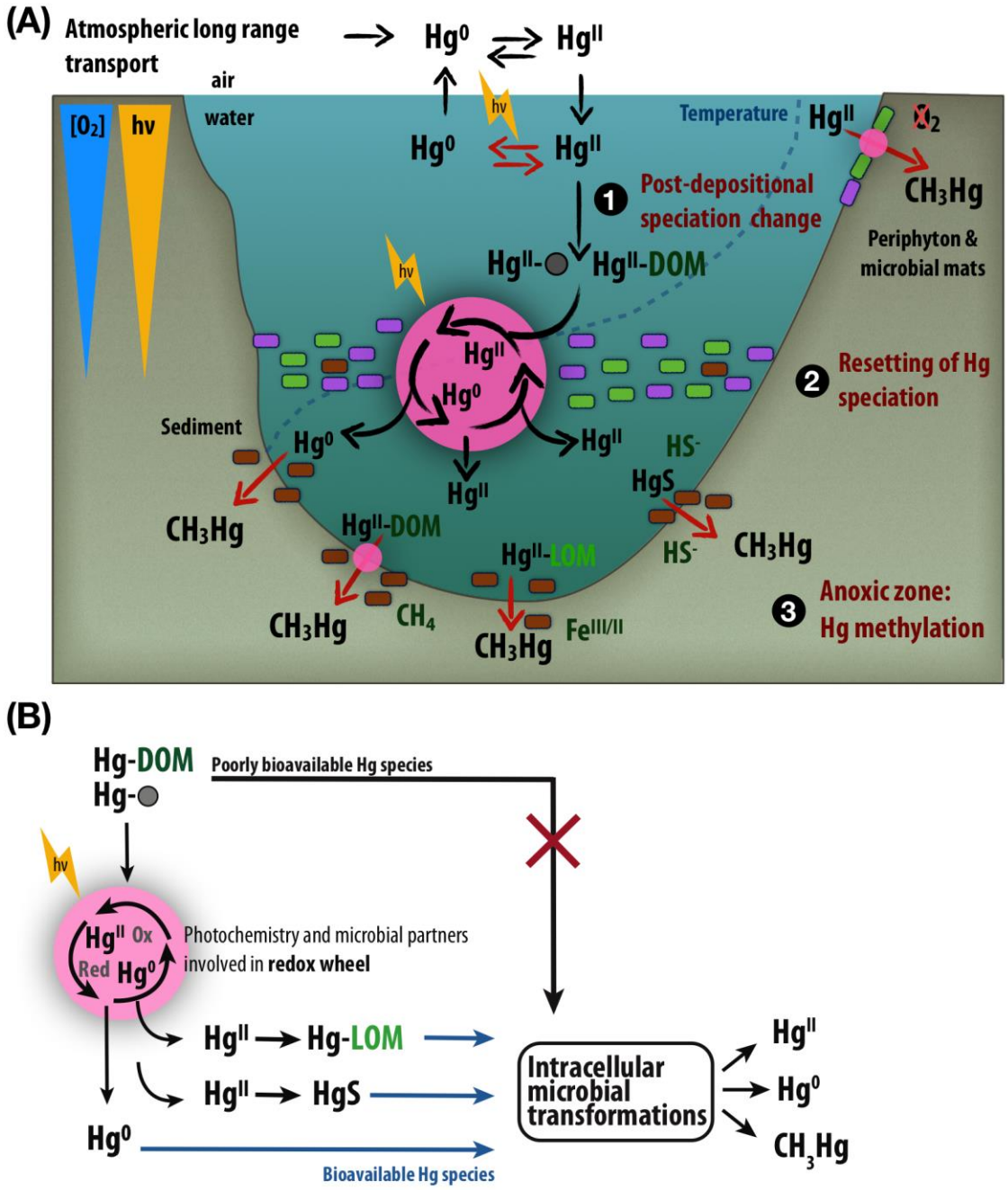

(Figure caption provided on the following page)

Figure 3.1: Conceptual summary for the possible role of phototrophic and anaerobic microbes in controlling Hg bioavailability. Numbers refer to descriptions made in the **Concluding remarks** section of the text. The pink disks highlight sites where Hg speciation can be reset via redox processes that directly affect Hg (see text) or the ligands to which Hg is bound (e.g., via heterotrophy or DOM photo-transformation). These processes can occur under oxic or anoxic conditions and be catalyzed by light, microbes or both. At the ecosystem scale (**A**): anoxygenic phototrophs are coloured in green and purple, Hg methylators are coloured in brown, dissolved organic matter has been abbreviated as DOM, labile organic matter available to microbes is abbreviated as LOM and particulate matter is denoted by small grey circles. Hg-DOM represents poorly bioavailable Hg complexes formed with organic matter ligands of a large size. Hg-LOM represents highly bioavailable Hg complexes formed with labile organic matter ligands; these labile organic matter ligands can shuttle Hg inside the cell. Lightning bolts represent light energy (hv) required for photobiological or photochemical processes. Inverted blue and yellow triangles represent oxygen and light energy gradients, respectively. HS^- (sulphide), CH_4 (methane) and $Fe^{II/III}$ (iron oxides) are meant to represent some of the anaerobic metabolisms known to be involved in Hg metabolism: sulphatoreduction, methanogenesis and ferroreduction, respectively. (**B**) was adapted from Chiasson-Gould et al. 2014 and represents the redox wheel in the context of the diversity of Hg species available for microbial transformations.

Chapter 4: A physiological role for Hg^{II} during phototrophic growth

Daniel S. Grégoire [a] & Alexandre J. Poulain [a]

a - Biology Department, University of Ottawa, 30 Marie Curie, Ottawa, ON, K1N6N5, Canada.

Research highlights:

- First study to explore how anoxygenic phototrophic purple non-sulphur bacteria can contribute to Hg redox cycling
- Tested whether Hg^{II} reduction occurs because of a redox imbalance incurred during photoheterotrophic growth
- Hg reduction was only associated with photoheterotrophic metabolism and was favoured under conditions that generated a redox imbalance
- Cells were able to reduce up to 20 % of the initial Hg^{II} supplied, achieving rates of Hg^0 production observed in previously published environmental studies
- Phototrophically-grown cells benefited from sublethal levels of Hg (200 nM)
- Findings are the first to directly link photosynthetic metabolism to Hg reduction and suggest that Hg^{II} can act as an electron sink during phototrophic growth

A modified version of this chapter was originally published as: **Grégoire, D.S**.; Poulain, A.J., A physiological role for Hg(II) during phototrophic growth. *Nature Geoscience* **2016,** *9***,** (2)**,** 121-125. **Direct link:** https://www.nature.com/articles/ngeo2629

N.B. Supporting information for this chapter can be found in **Appendix A**

4.1 ABSTRACT

The bioaccumulation of toxic monomethylmercury (MMHg) is influenced by redox reactions that determine the mercury (Hg) substrate – Hg^{II} or Hg^0 – available for methylation [1, 2]. Phototrophs can reduce Hg^{II} to Hg^0 [3]. This reduction has been linked to a mixotrophic lifestyle [4], in which microbes gain energy photosynthetically but acquire diverse carbon compounds for biosynthesis from the environment. Photomixotrophs must maintain redox homeostasis to disperse excess reducing power due to the accumulation of reduced enzyme cofactors [5]. Here we exposed purple bacteria growing in a bioreactor to Hg^{II} and monitored Hg^0 concentrations. We show that phototrophs use Hg^{II} as an electron sink to maintain redox homeostasis. Hg^0 concentrations increased only when bacteria grew phototrophically, and when bacterial enzyme cofactor ratios indicated the presence of an intracellular redox imbalance. Under such conditions, bacterial growth rates increased with increasing Hg^{II} concentrations; when alternative electron sinks were added, Hg^0 production decreased. We conclude that Hg can fulfill a physiological function in bacteria, and that photomixotrophs can modify the availability of Hg to methylation sites.

4.2 INTRODUCTION

Hg is a contaminant globally distributed via the atmosphere that not only persists in the environment but is also biomagnified through aquatic food webs, particularly in its methylated form MMHg [6]. Redox reactions control Hg cycling by affecting the Hg substrate available for methylation [7, 8]. So far, much of the work on microbially-mediated Hg redox cycling has focused on chemotrophs [3]. Few laboratory studies have addressed the role of phototrophs and even then, only algae and cyanobacteria (that is, oxygenic photolithoautotrophs) have been investigated. In the environment, increased Hg^0 production has been associated with phytoplankton blooms in freshwater [4, 7, 9, 10] and marine systems [11]. Thus far, research has shown that oxygenic phototrophs can indirectly contribute to Hg redox cycling via the excretion of (photo)reactive compounds [12] but support for a direct coupling between Hg and phototrophic metabolism remains elusive [13]. Indeed, except for recent work demonstrating the presence of a mercuric reductase-like enzyme in a cyanobacterium [14], other pathways for phototroph-mediated Hg redox cycling remain poorly understood. Although it has been shown that some anoxygenic phototrophs can indirectly influence MMHg production by affecting the sulphur cycle [15], their potential to contribute directly to Hg redox cycling has yet to be explored. These are important knowledge gaps to address because anoxygenic phototrophs thrive under anoxic conditions that are also conducive to the production of MMHg and because phototrophs stand as key ecological players in aquatic ecosystems, acting as an entry point for Hg in food webs [16]. There is an increasing need to fully understand how phototrophs affect Hg cycling given continued anthropogenic Hg inputs to aquatic

ecosystems and considerable shifts in the ecological dynamics of phototrophic communities predicted to occur in the face of ongoing environmental change [17].

Our work was motivated by field studies suggesting that Hg^0 production was dependent on the mixotrophic status of organisms present in phytoplankton blooms (that is, their ability to use a variety of energy and carbon sources) [4]. In this study, we selected purple non-sulphur bacteria (PNSB) as model organisms to investigate how a phototrophic lifestyle can affect Hg redox cycling and thus its mobility and toxicity in the environment. PNSB were chosen because they are ubiquitous in the environment, exhibit tremendous metabolic diversity and because their preferred mode of growth is via photoheterotrophic metabolism [18].

During photoheterotrophic growth, microbes accrue excess reducing power in the form of NAD(P)H and typically maintain redox homeostasis by shuttling excess reducing power onto exogenous electron acceptors such as inorganic carbon or dimethylsulphoxide (DMSO) [5, 19]. With this mechanism in mind, we hypothesized that the ability of phototrophs to reduce Hg^{II} is directly dependent on their ability to maintain redox homeostasis. We predicted that the magnitude of Hg reduction is positively associated with acquiring increasingly reduced carbon sources and that chemotrophic growth will not be associated with any Hg^0 production, given that all reducing power is expected to be used for the energetic and biosynthetic needs of the cells.

4.3 METHODS

4.3.1 Strains and culture conditions

Strains were grown aerobically and chemotrophically in liquid 0.3 % yeast peptone (0.3 % yeast extract and 0.3 % peptone) (YP) medium (*Rhodobacter capsulatus* SB1003 and *Rhodopseudomonas palustris* TIE-1) or Lysogeny broth (LB) (*Rhodobacter sphaeroides* 2.4.1), overnight, and transferred into anoxic minimal salts medium for freshwater cultures (herein referred to as FEM)[20]. All strains can be obtained from the American Type Culture Collection (ATCC) (catalogue numbers are ATCC BAA-309, ATCC 17023, and ATCC 17001 for *R capsulatus* SB1003, *R. sphaeroides* 2.4.1 and *Rp. palustris* TIE-1, respectively). Media were modified by substituting 25 mM of MOPS buffer in place of HCO_3^- and amended with an organic carbon source. In the case of *R. capsulatus*, one of several potential exogenous electron acceptors was supplied (see **Appendix A, Table A1,** for the full list of carbon sources and exogenous electron acceptor combinations and their redox potentials). To test whether the oxidation of butyrate to CO_2, polyhydroxybutyrate (PHB) and biomass, coupled to reduction of Hg^{II} was favourable under standard conditions, we calculated ΔG^0 derived from reduction potentials. The ΔG was also estimated for an environmentally relevant range of concentrations of the reactants and products (see **Table A2** for reagent and product concentrations, **Table A3** for ΔG^0, and see **Table A4** for ΔG). The oxidation of butyrate to CO_2, biomass or PHB coupled to the oxidation of Hg^{2+} to Hg^0 remains favourable in all environmental conditions tested.

Cultures destined for the bioreactor were grown either phototrophically at 28°C, in crimped serum vials, with the headspace exchanged with argon and received a visible irradiance of 20 µmol photon $m^{-2}s^{-1}$ from a 60 W incandescent light source that emitted light primarily in the near-red to red spectrum (600 to 700 nm), or chemotrophically, aerobically, in the dark, in 250 mL sterile flasks shaken continuously at a speed of 200 rotations per minute. Cells were grown to late exponential phase and added to the bioreactor as a 10 % inoculum in a final volume of 560 mL (sterile medium had 620 mL to account for lack of inoculum). *R. capsulatus* supplied with 30 mM acetate, 15 mM butyrate (concentrations normalized for total carbon available) or 15 mM butyrate with 10 or 20 mM HCO_3^- was used for [NADH]/[NAD]+ measurements and grown using the same method as described above for phototrophic cultures. *R. capsulatus* was also used in Hg and HCO_3^- growth assays. Cells used in HCO_3^- assays were initially transferred as a 10% inoculum from 0.3% YP to FEM with 15 mM butyrate, grown to mid-exponential phase and transferred into fresh FEM with 15 mM butyrate amended with 10 mM HCO_3^- (or not). For Hg exposure growth assays, 2.5 mL of each 0.3 % YP culture of *R. capsulatus* was washed three times with FEM containing 1 mM butyrate before being resuspended in the same medium, exposed to 0, 200 or 400 nM of $HgCl_2$ and incubated in the same conditions as mentioned above for phototrophic growth. All growth assays were performed in Balch tubes to facilitate spectrophotometric measurements at O.D. $_{600\ nm}$ (where O.D. is optical density) using a Spectronic 20D+ (Fisher Scientific).

4.3.2 Bioreactor setup and elemental mercury measurements

All glassware used in the bioreactor setup was made of borosilicate glass and all connecting lines were made of ¼" PTFE. All components were manipulated using clean trace element analysis handling techniques and assembled under sterile conditions. The bioreactor components formed a closed system comprised of a gas supply connected to a bubbler that fed into the medium contained in a 1 L three-neck spherical flask where the two other necks were sealed with sterilized rubber septa used for subsampling. A line connected to an opening in the headspace of the bubbler was attached to a 1 L vessel kept at 12°C that collected condensation and allowed gas accumulated in the headspace of the reactor to flow through to a Tekran 2537B Hg^0 analyzer (Tekran instruments, Toronto, ON, Canada) (**Fig A1**). The Tekran 2537B measured Hg^0 in real time via cold-vapour atomic fluorescence spectroscopy (CVAFS) based on Hg^0's peak fluorescence emission at 253.7 nm. The reactor was continuously sparged with Hg^0-free atmospheric air (for aerobic chemotrophic assays) or ultra high purity argon (for anaerobic phototrophic assays) at a rate of 0.5 L min^{-1} for 60 minute sampling periods. In addition to setting the sample flow on the Tekran 2537B Hg^0 analyzer, gas flow was controlled by using two Tekran Hg^0-free air units: one operated automatically used for the regular calibration and cleaning of the instrument, and the other operated manually following the completion of clean cycles on the Tekran 2537B that regulated airflow to the bioreactor. Both contained two activated carbon Hg^0 filters and in-line pressure regulators to ensure consistent flow.

Growth conditions for bioreactor experiments were identical to those supplied during culture incubation unless otherwise noted in **Table A1**. Temperature was maintained using a water bath set to 28°C. Light was supplied using a 200 W incandescent light bulb with a visible light intensity being maintained at 20 µmol photon $m^{-2}s^{-1}$ by means of multiple layers of dark screens. Peak irradiance for this light source occurred in the near-red to red spectrum (600 to 700 nm). Darkness was maintained for chemotrophic growth by wrapping the reactor in aluminum foil.

The reactor was purged of trace atmospheric Hg^0 for 30 minutes, after which the live or dead cell inoculum and the desired exogenous electron acceptor were added using sterile 18 G needles and syringes. The reactor was further purged until Hg^0 readings between 0 and 0.1 ng m^{-3} were obtained, after which the $HgCl_2$ spike was added from a 250 nM working solution prepared fresh daily to a final concentration of 250 pM and Hg^0 production was monitored for 48h. The initial Hg^0 measurements immediately following the Hg spikes were consistently high and skewed the long-term trends in Hg^0 loss. As such, these measurements were omitted from **Fig 4.1** and **4.2**.

4.3.3 Bioreactor subsampling for total mercury mass balance and cell density

Samples were withdrawn with sterile stainless steel 18 G needles and syringes throughout each experiment to measure total Hg (THg) and cell density via viable plate count. Before assembly, the weight of the empty spherical flask and condensation trap, were recorded, as was the weight of the spherical flask full of growth medium. All containers used for containing the live or dead cell inoculums, bioreactor subsamples and exogenous electron acceptor spiking solutions were weighed before and after to account for changes

in weight of the reactor. All samples used for THg analyses were conserved with BrCl and stored in the dark at 4°C [21]. Samples were taken in triplicate for quality control after sparging the reactor of trace atmospheric Hg^0 to verify for potential contamination in the medium prior to spiking. The reactor was subsampled in triplicate following the addition of the Hg spike to measure THg at the beginning of the experiment (herein referred to as T_0). After 48h, the reactor was subsampled again in triplicate to quantify THg at the end of the experiment (herein referred to as T_f), and after disassembly the masses of the spherical flask and condensation trap were re-recorded. For treatments where live or heat-killed cells were supplied, the spherical flask was rinsed with 100 mL of 10 % trace element grade HCl from which triplicate samples were taken. The rinse and sampling steps were repeated twice more to ensure all Hg adsorbed to the walls of the reactor was accounted for. In the case of sterile medium, the first rinse was performed by filling the reactor with 500 mL of 10% HCl and soaking it for 24h before subsampling, owing to the strong adsorption of Hg to the walls of the reactor. Subsequent rinsing and sampling were performed the same was as describe above.

Total Hg analyses were performed using EPA method 1631 [21]. This method involves conserving all Hg in solution with the strong oxidizing agent BrCl, which is subsequently degraded with hydroxylamine prior to addition of $SnCl_2$ upon sample analysis to reduce all the Hg^{II} to Hg^0. Afterwards, this Hg^0 is concentrated onto gold traps and the concentration is measured via CVAFS at 253.7 nm. The average values from each set of triplicate samples were used to perform the mass balance (**Fig A2**). Hg removed from cell growth subsampling was estimated using the concentration at the beginning of the experiment. Total volume was approximated assuming the density of

water (i.e., 1 g = 1 mL). Total Hg recovery (%) was calculated by multiplying the following ratio by 100:

$$THg\ recovered = (N_f + N_t + N_g + Hg^0)/N_i \times 100$$

Where:

N_f = [THg] taken at the end of the experiment

x volume of medium in the reactor at the end of the experiment

N_t= sum of ([THg] of HCl rinses 1, 2 and 3

x volume of each HCl rinse)

N_g = [THg] at the beginning of the experiment

x volume subsampled for growth measurement

Hg^0 = cumulative Hg^0 production recorded by the Tekran 2537B

N_i = [THg] taken at the beginning of the experiment

x volume of medium in the reactor at the beginning of the experiment

The amount of water recovered was verified for each assay to ensure that there was no loss of medium and to corroborate the THg mass balance results. Total water recoveries were determined by summing the mass removed or added to the reactor, dividing it by the mass of medium in the full reactor before starting the experiment and multiplying it by 100.

4.3.4 [NADH]/[NAD+] measurements

Cultures were subsampled upon reaching stationary phase and [NADH]/[NAD]+ measurements were performed in biological triplicates under anaerobic conditions according to the method outlined by Kern *et al*. [22] using a Synergy HTX 96-well plate reader (Bio-tek, Winooski, VT, USA). This method involved extracting NAD(P)H and $NAD(P)^+$ with HCl and NaOH, respectively. The concentrations of redox cofactors were then measured using an enzymatic colorimetric assay with a redox sensitive dye. The rate at which the dye was converted to its reduced form (as measured by absorbance at 570 nm) was used to calculate the initial concentration of each redox cofactor based on a standard curves included in each assay. Results were presented as boxplots where the boxes represent the first and third quartile; the bars represent the median value, and the whiskers the minima and maxima for each treatment.

4.3.5 Growth assay indices calculation and bioreactor cell density estimation

Lag phase durations for Hg exposure and HCO_3^- growth assays were extracted by fitting a four-parameter logistic model in Sigmaplot and calculating the first derivative between each pair of points in chronological order. Lag phase was deemed complete once the first derivative yielded a consistently positive value (i.e. representative of an inflexion point and a positive slope value for $O.D._{600nm}$ over time). Maximum growth rate was calculated as the maximum slope of $O.D._{600nm}$ over time during mid-exponential phase, determined by comparing each pair of points in chronological order. Growth rates for Hg-exposed cultures were also calculated by fitting a natural logarithmic curve or a linear regression to cell growth data from which the slope coefficient for each model was used as an index

for growth rate. These calculations were used to verify that the conclusions obtained using the pairwise comparison were not from sampling errors. Yield was determined as the maximum O.D. $_{600nm}$ value reached over the course of each experiment. Results were presented as boxplots where the boxes represent the first and third quartile; the bars represent the median value, and the whiskers the minima and maxima for each treatment.

For bioreactor experiments, the rates of Hg^0 production normalized per cell for phototrophically grown cultures were determined based on cell numbers averaged for the entire experiment, as they did not vary over time. Chemotrophically grown cultures showed substantial growth and cell numbers were estimated by fitting a four-parameter logistic equation in Sigmaplot for the concentrations obtained by viable plate count. Each Hg^0 measurement was normalized for the corresponding time point in each fitted model.

4.3.6 Statistical analyses

All statistical analyses were performed in R [23]. One-way ANOVA's using the partial sum of squares were used to compare the mean [NADH]/[NAD]+ ratios and one-way ANOVA's using sequential sum of squares were used to compare the growth indices from growth assay experiments. Multiple comparisons were subsequently performed using the Tukey HSD *post hoc* test with the significance threshold set to $p<0.05$.

4.3.7 Thermodynamic calculations

To estimate whether the reduction of Hg^{II} in the presence of butyrate was thermodynamically favourable, we calculated the free energy associated with the reactions coupling butyrate oxidation to Hg^{II} reduction. The substrates acetate and

butyrate can be converted to acetylCoA and generate NADH via a modified version of the tricarboxylic acid (TCA) cycle, but butyrate can also be converted into polyhydroxybutyrate (PHB) – a storage molecule – via an oxidative pathway, generating additional reducing power. As such, the electron donors do not undergo simple one-step oxidation, thus making it difficult to identify the proper redox partners. NADH is one of the main electron carriers involved in these reactions. The redox potential of NAD^+/NADH (E^0 = -0.32V) is very close to that of several reduced carbon substrates coupled to HCO_3^-, including acetate (-0.28V), butyrate (-0.35V), butanol (-0.3V); the oxidation of these substrates often consumes energy and is catalyzed by enzymes.

The redox reaction does not proceed (or is too slow to proceed) directly between butyrate and Hg^{2+}, as our abiotic controls showed no Hg^0 production and our killed controls also showed virtually no Hg^0 production, meaning that live cells are required to catalyze the reaction (**Fig 4.1 d, e**). It is likely that enzyme(s) using NADH act(s) as a redox intermediate in the reaction, but the site of reduction and the nature of the enzyme(s) involved remain unclear. The reduction potential of NAD^+/NADH is such that under standard conditions, electrons are predicted to flow from NADH to Hg^{2+}, DMSO, or used by enzymes of the Calvin-Benson-Bassham cycle to fix CO_2.

$$E^{0'}_{Hg^{2+}/Hg^0} = +0.8V$$

$$E^{0'}_{DMSO/DMS} = +0.16V$$

$$E^{0'}_{NAD^+/NADH} = -0.32V$$

$$E^{0'}_{CO2/butyrate} = -0.35V$$

We present three different scenarios for the oxidation of butyrate involving the reduction of Hg^{2+} and DMSO, where butyrate can be oxidized to CO_2, to PHB or assimilated into biomass, as shown in the reactions below.

Reactions involving the reduction of Hg^{2+} and DMSO:

$$Hg^{2+} + \mathbf{2e^-} \rightarrow Hg^0; \quad E^{0\prime}_{Hg^{2+}/Hg^0} = +0.8V \ (\mathbf{1})$$

$$(CH_3)_2SO + 2H+ + \mathbf{2e^-} \rightarrow (CH_3)_2S + H_2O; \quad E^{0\prime}_{DMSO/DMS} = +0.16V \ (\mathbf{2})$$

Reactions involving butyrate: $E^{0\prime}_{CO_2/\ C_4H_8O_2} = -0.35V$

$$4CO_2 + 20H^+ + \mathbf{20e^-} \rightarrow C_4H_8O_2 + 6H_2O \ (\mathbf{3})$$

$$(C_4H_6O_2)n + 2nH^+ + \mathbf{2ne^-} \rightarrow n(C_4H_8O_2) \ (\mathbf{4})$$

$$CH_{1.8}N_{0.18}O_{0.38} + 0.48H_2O + 2.72H^+ + \mathbf{2.72e^-} \rightarrow C_4H_8O_2 + 0.72NH_4^+ \ (\mathbf{5})$$

An example of the half reactions with Hg^{2+}/Hg^0 and CO_2/butyrate:

$$C_4H_8O_2 + 6H_2O \rightarrow 4CO_2 + 20H^+ + \mathbf{20e^-} \qquad E^0(V) = +0.35\ V$$

$$+ \quad 10Hg^{2+} + 20e^- \rightarrow 10Hg^0 \qquad E^0(V) = +0.8\ V$$

Overall reaction:

$$C_4H_8O_2 + 10Hg^{2+} + 6H_2O \rightarrow 4CO_2 + 10Hg^0 + 20H^+ \qquad \Delta E^0(V) = 1.15\ V$$

$$\Delta G^0 = -nF(\Delta E^0)$$

$$\Delta G^0 = -20 \times 96.485\ kJ.\ V^{-1}.mol^{-1} \times 1.15\ V;\ \Delta G^0 = -2219.2\ kJ.mol^{-1}$$

The ΔG^0 values for each reaction can be found in **Table A3** and **Table A4**. The oxidation of butyrate coupled to the reduction of Hg or DMSO was predicted to be favourable under standard conditions ($\Delta G^0<0$).

We also estimated ΔG using the ΔG^0 calculated under standard conditions and defining conservative environmental conditions with respect to the concentrations of reactants and products (see **Table A2**) of the three scenarios described above.

Details of the calculation are:

$$G = G^0 + RT\ln Q$$

Where for the reaction $aA + bB \rightarrow cC + dD$

$$Q = [C]^c \times [D]^d / [B]^b \times [A]^a$$

With:

$$R = 8.314 \times 10^{-3}\ kJ\ K^{-1}\ mol^{-1}$$

$$T = 283\ K\ (or\ 10\ °C)$$

We do not know all of the possible redox intermediates involved in the reaction that eventually lead to Hg^{II} reduction. We speculate that some reactions will require energy to proceed and the ΔG values provided here should therefore be seen as overestimations. We ran this simulation using a range of values covering two orders of magnitude for reactants and/or products in order to test for the sensitivity of the analysis. The oxidation of butyrate to CO_2, biomass or PHB coupled to the reduction of Hg^{2+} to Hg^0 remains favourable in all environmental conditions tested.

4.4 RESULTS AND DISCUSSION

4.4.1 Hg^{II} reduction only occurs during phototrophic metabolism

In nature, photomixotrophy is a widespread strategy that enables microbes to derive energy from light, while accessing a diverse pool of inorganic and organic carbon sources [18]. In our study, we compared the use of two carbon sources differing in their oxidation state that are naturally occurring in the environment. Our phototrophic models (*Rhodobacter capsulatus*, *Rhodobacter sphaeroides* and *Rhodopseudomonas palustris*) only reduced Hg^{II} to Hg^0 when grown phototrophically, regardless of the organic carbon source supplied (**Fig 4.1**); chemotropically grown cells did not reduce Hg^{II} (**Fig 4.1**). When grown phototrophically on butyrate (the most reduced carbon source used), Hg^0 production was greater than when grown on acetate (the most oxidized carbon source used) for all three strains tested (**Fig 4.1a-c**). Autoclaved killed controls resulted in a 11-fold decrease in Hg^0 production (2.29 pmol) whereas abiotic controls resulted in a 22-fold decrease (1.18 pmol) (**Fig 4.1d, e**). The difference between autoclaved and sterile treatments could be associated with the presence of reduced cell material and/or metabolic exudates released during the autoclaving step that may contribute indirectly to Hg^0 production [12]. Our experiments were performed at a visible light intensity (20 µmol photon $m^{-2}s^{-1}$) corresponding to levels that are sufficient for phototrophic growth but insufficient to catalyze abiotic photoreduction[4] (**Fig 4.1e**).

4.4.2 Hg^{II} reduction competes with known redox homeostasis pathways

To further test our hypothesis, we supplied known electron sinks to *R. capsulatus* during photoheterotrophic growth on butyrate and predicted that they would compete with Hg^{II} for reducing power thereby decreasing Hg^0 production. Such electron sinks (that is, HCO_3^-, DMSO) have been shown in previous studies to alleviate the stress associated with redox imbalance and their presence enabled growth on reduced carbon [19, 24]. Supplying HCO_3^- and DMSO greatly decreased Hg^0 production (up to 80% for $[HCO_3^-]$ = 20mM and 85% for [DMSO] = 20 mM) (**Fig 4.2** and **Fig A3**). This decrease in Hg^0 production shows that Hg^{II}, HCO_3^- and DMSO compete for the pool of excess reducing power within the cell, especially when these electron sinks are provided at mM levels (**Fig 4.2**). In fact, the highest rates were observed in the presence of $[HCO_3^-]$ = 100 µM, suggesting that cellular pathways possibly involved in Hg^{II} reduction are stimulated by small amounts of HCO_3^-; a small decrease in cumulative Hg^0 production was observed in the presence of [DMSO] = 1nM (**Fig 4.2**). When cells were supplied with other potential oxidants, such as NO_3^- or Fe^{III}, for which no dedicated reduction pathways are known to exist in *R. capsulatus*, Hg^0 production was not inhibited (**Fig A4**). These results support our initial hypothesis and show that excess reducing power accrued during photoheterotrophic growth is associated with Hg^{II} reduction.

The competition observed between Hg^{II}, HCO_3^- and DMSO provides the basis for determining the sites of Hg reduction. Inorganic carbon and DMSO reduction both derive reducing power from the ubiquinone (UQ) pool, which receives electrons from reducing power generated through the oxidation of organic matter and/or ATP-consuming reverse electron flow [25]. The UQ pool is not sufficiently electronegative to reduce NAD+

directly, [-0.1V < E^0(UQ/ UQH_2) < 0.1 V versus E^0 (NAD+/NADH)= -0.32 V], but it could potentially serve as an electron donor to Hg^{II} [0.7V < E^0(Hg^{2+}/ Hg^0) < 0.85V] or Hg^I [present as Hg_2^{2+} E^0(Hg_2^{2+}/Hg^0) = 0.4 V] [26]. Whereas under standard conditions, the reduction potential of Hg^{II}/Hg^0 is very favourable to Hg^{II} reduction (see **Appendix A**), this value is expected to decrease once Hg^{II} binds to thiols [27], possibly affecting the ability of Hg to act as an electron acceptor. Alternatively, NADH could potentially reduce Hg^{II} through the activity of nonspecific reductases. One of the few studies addressing Hg toxicity in PNSB also showed that Hg^{II} induces toxicity partially through interactions with the UQ pool indicating a precedence for Hg^{II}-quinone interactions [28].

4.4.3 Hg^{II} reduction occurs under conditions where there is a redox imbalance

To establish the physiological basis of our proposed mechanism, we compared the ratios of [NADH]/[NAD+] for cells grown on butyrate to those grown on acetate. These ratios are typically used as proxies to evaluate redox imbalance [29]. Cells grown solely on butyrate had a higher mean [NADH]/[NAD+] ratio compared to those grown on acetate (0.78 ± 0.06 vs. 0.42 ± 0.26) and differed significantly when compared to cells grown on butyrate supplied with 10 and 20 mM HCO_3^- (0.13 ± 0.02 and 0.17 ± 0.05, respectively) (**Fig 4.3**). These ratios are well within the range of what can be expected when studying microbial redox imbalance [29] and confirm previous work where PNSB use HCO_3^- to maintain redox homeostasis [5]. We were unable to test how Hg^{II} affected this ratio due to our inability to harvest enough biomass and extract enzymatic redox cofactors at Hg concentrations required to create an effect comparable to that of HCO_3^-.

4.4.4 Hg^{II} can act an electron sink during phototrophic growth

Having demonstrated that Hg^{II} reduction depends on the availability of excess reducing power, we tested whether Hg^{II} could fulfill a physiological function by acting as an electron sink, and thus favour growth. With this aim, phototrophically grown cultures were supplied with sublethal concentrations of Hg^{II} ($\leq$ 400 nM). The growth rate of *R. capsulatus* was 1.5-fold higher in the presence of 200 nM Hg and differed significantly from that of controls grown in the absence of Hg (0.061 ± 0.005 vs. 0.039 ± 0.012 hr^{-1}) (**Fig 4.4a**) and this conclusion was supported regardless of the method used to calculate growth rate (**Fig A5**). Furthermore, the lag phase duration and yield were consistent with a beneficial role of Hg^{II} with lag phase duration decreasing 3-fold, and yield increasing 1.25-fold in the presence of $[Hg^{II}]$ = 200 nM (**Fig 4.4 c, e**). Supplying HCO_3^- and not Hg^{II} to butyrate-grown cells yielded similar results (**Fig 4.4 b, d, f**). We show that Hg offered a physiological advantage, but the small effect size observed is most likely associated to the toxic, yet sublethal, nature of Hg^{II} at concentrations greater than 200 nM.

4.4.5 Environmental and evolutionary context of phototrophic Hg^{II} reduction

The rates of Hg^0 production reported during our experiments are comparable to those determined for abiotic photoreduction in boreal lakes, and in line with $[Hg^0]$ and Hg^0 production rates observed during metalimnetic incubations (**Table A5**). When normalized for incoming irradiance, our results also suggest that PNSB are more efficient at reducing Hg^{II} per mol of photon received compared to abiotic photoreduction (**Table A6**). Interestingly, the rates observed for anoxygenic phototrophs were comparable to those of the chemotrophic anaerobes *Shewanella oneideinsis* MR-1 and *Geobacter sulfurreducens*

PCA (**Table A5**). Whereas photochemical reactions may rule Hg redox cycling at the surface of lakes and therefore control its evasion to the atmosphere, anoxygenic phototrophs are poised to catalyze Hg^{II} reduction deeper in the water column where light energy alone cannot account for Hg phototransformation [4, 7, 9, 30]. This occurs under anoxic conditions that are also conducive to the production of the toxic MMHg and as such directly affect its availability to food webs.

Hg^{II} reduction to Hg^0 in biological systems is often thought of as a detoxification mechanism that leads to the formation of a less toxic, readily evaded species, Hg^0. We suggest that phototrophic cells using Hg^{II} as an electron sink not only benefit from Hg reduction to maintain low intracellular Hg levels but also benefit from Hg's reduction potential to maintain redox homeostasis. Insights into the evolutionary path of Hg reduction by phototrophs may be gained when considering the well-known chemotrophic *mer* operon. It has been proposed that this operon evolved among thermophilic bacteria thriving in hydrothermal environments with high Hg levels [31]. It is difficult to reconstruct the evolution of the *mer* operon over geological times, except when considering Earth's oxygenation, which may have supported the operon's diversification [31]. Strikingly, no *mer* operons were reported in the genomes of the purple bacteria investigated (one putative MerA homologue was found in the genome of *Rhodobacter sphaeroides* 2.4.1) and very few studies report functional *mer*-determinants in obligate anaerobes or oxygenic phototrophs [14]. Available oxygen and Hg levels both fluctuated greatly over geological time scales [32, 33], but ample light was available [34]. The ability of anoxygenic phototrophs to use Hg reduction both as detoxification and a redox homeostasis strategy may have conferred as yet unsuspected growth or survival advantages. Further

investigations into the geobiology of phototrophs may lead to the discovery of molecular markers that will shed light on the evolutionary path of a phototrophic lifestyle, possibly relying on one of the most unexpected elements, the toxic metal mercury.

4.5 ACKNOWLEDGMENTS

Our work was funded by NSERC Discovery and Accelerator grants as well as CFI funding to AJP and an NSERC CGS D Scholarship to DSG. This work was inspired by discussions with Marc Amyot, Tamar Barkay and Dianne Newman on the photobiology of metals and its evolution through geological times. We are thankful for all three PNSB strains that were a gift from Dianne K. Newman. We thank Alexa Price-Whelan and Susanne Kern for help and guidance with [NADH]/[NAD+] assays and we thank Emmanuel Yumvihoze and Aurélien Dommergue for their help with Hg analyses.

4.6 AUTHOR CONTRIBUTIONS

AJP initiated the study; AJP and DSG designed the experiments and DSG carried them out and AJP and DSG performed data analyses; AJP and DSG wrote the manuscript.

4.7 REFERENCES

1. Hu, H.; Lin, H.; Zheng, W.; Tomanicek, S. J.; Johs, A.; Feng, X.; Elias, D. A.; Liang, L.; Gu, B., Oxidation and methylation of dissolved elemental mercury by anaerobic bacteria. *Nature Geoscience* **2013,** *6*, 751-754.

2. Colombo, M. J.; Ha, J.; Reinfelder, J. R.; Barkay, T.; Yee, N., Anaerobic oxidation of Hg(0) and methylmercury formation by *Desulfovibrio desulfuricans* ND132. *Geochimica et Cosmochimica Acta* **2013,** *112*, 166-177.

3. Grégoire, D. S.; Poulain, A. J., A little bit of light goes a long way: The role of phototrophs on mercury cycling. *Metallomics* **2014,** *6*, (3), 396-407.

4. Poulain, A. J.; Amyot, M.; Findlay, D.; Telor, S.; Barkay, T.; Hintelmann, H., Biological and photochemical production of dissolved gaseous mercury in a boreal lake. *Limnology and Oceanography* **2004,** *49*, (6), 2265-2275.

5. McKinlay, J. B.; Harwood, C. S., Carbon dioxide fixation as a central redox cofactor recycling mechanism in bacteria. *Proceedings of the National Academy of Sciences of the United States of America* **2010,** *107*, (26), 11669-11675.

6. Morel, F. M. M.; Kraepiel, A. M. L.; Amyot, M., The chemical cycle and bioaccumulation of mercury. *Annual Review of Ecology and Systematics* **1998,** *29*, 543-566.

7. Amyot, M.; Mierle, G.; Lean, D.; McQueen, D. J., Effect of solar radiation on the formation of dissolved gaseous mercury in temperate lakes. *Geochimica et Cosmochimica Acta* **1997,** *61*, (5), 975-987.

8. Fitzgerald, W. F.; Lamborg, C. H.; Hammerschmidt, C. R., Marine biogeochemical cycling of mercury. *Chemical Reviews* **2007,** *107*, (2), 641-662.

9. Vandal, G. M.; Fitzgerald, W. F.; Rolfhus, K. R.; Lamborg, C. H., Modeling the elemental mercury cycle in Pallette Lake, Wisconsin, USA. *Water, air, and soil pollution* **1995,** *80*, (1-4), 529-538.

10. Mason, R. P.; Morel, F. M. M.; Hemond, H. F., The role of microorganisms in elemental mercury formation in natural waters. *Water, air, and soil pollution* **1995,** *80*, (1-4), 775-787.

11. Baeyens, W.; Leermakers, M., Elemental mercury concentrations and formation rates in the Scheldt estuary and the North Sea. *Marine Chemistry* **1998,** *60*, (3–4), 257-266.

12. Lanzillotta, E.; Ceccarini, C.; Ferrara, R.; Dini, F.; Frontini, F. P.; Banchetti, R., Importance of the biogenic organic matter in photo-formation of dissolved gaseous mercury in a culture of the marine diatom *Chaetoceros* sp. *Science of the Total Environment* **2004,** *318*, (1-3), 211-221.

13. Ben-Bassat, D.; Mayer, A. M., Volatilization of mercury by algae. *Physiologia Plantarum* **1975,** *33*, (2), 128-132.

14. Marteyn, B.; Sakr, S.; Farci, S.; Bedhomme, M.; Chardonnet, S.; Decottignies, P.; Lemaire, S. D.; Cassier-Chauvat, C.; Chauvat, F., The *Synechocystis* PCC6803 MerA-like enzyme operates in the reduction of both mercury and uranium under the control of the glutaredoxin 1 enzyme. *Journal of Bacteriology* **2013,** *195*, (18), 4138-4145.

15. Cleckner, L. B.; Gilmour, C. C.; Hurley, J. P.; Krabbenhoft, D. P., Mercury methylation in periphyton of the Florida Everglades. *Limnology and Oceanography* **1999,** *44*, (7), 1815-1825.

16. Mason, R. P.; Reinfelder, J. R.; Morel, F. M. M., Uptake, toxicity, and trophic transfer of mercury in a coastal diatom. *Environmental Science and Technology* **1996,** *30*, (6), 1835-1845.

17. Krabbenhoft, D. P.; Sunderland, E. M., Global change and mercury. *Science* **2013,** *341*, (6153), 1457-1458.

18. Raven, J. A., Contributions of anoxygenic and oxygenic phototrophy and chemolithotrophy to carbon and oxygen fluxes in aquatic environments. *Aquatic Microbial Ecology* **2009,** *56*, (2-3), 177-192.

19. Richardson, D. J.; King, G. F.; Kelly, D. J.; McEwan, A. G.; Ferguson, S. J.; Jackson, J. B., The role of auxiliary oxidants in maintaining redox balance during

phototrophic growth of *Rhodobacter capsulatus* on propionate or butyrate. *Archives of Microbiology* **1988,** *150*, (2), 131-137.

20. Croal, L. R.; Johnson, C. M.; Beard, B. L.; Newman, D. K., Iron isotope fractionation by Fe(II)-oxidizing photoautotrophic bacteria. *Geochimica et Cosmochimica Acta* **2004,** *68*, (6), 1227-1242.

21. EPA, U., Method 1631, Revision E: Mercury in water by oxidation, purge and trap, and cold vapor atomic fluorescence spectrometry. In US Environmental Protection Agency Washington, DC: 2002.

22. Kern, S. E.; Price-Whelan, A.; Newman, D. K., Extraction and Measurement of NAD (P)+ and NAD (P) H. In *Pseudomonas Methods and Protocols*, Springer: 2014; pp 311-323.

23. R Core Team *R: A Language and Environment for Statistical Computing*, R Foundation for Statistical Computing: 2014.

24. Ferguson, S. J.; Jackson, J. B.; McEwan, A. G., Anaerobic respiration in the Rhodospirillaceae: characterisation of pathways and evaluation of roles in redox balancing during photosynthesis. *FEMS Microbiology Letters* **1987,** *46*, (2), 117-143.

25. Klemme, J. H., Studies on the mechanism of NAD-photoreduction by chromatophores of the facultative phototroph, *Rhodopseudomonas capsulata*. *Zeitschrift fur Naturforschung. Teil B: Chemie, Biochemie, Biophysik, Biologie* **1969,** *24*, (1), 67-76.

26. Scholz, F.; Lovrić, M., The standard potentials of the electrode “dissolved atomic mercury/dissolved mercury ions". *Electroanalysis* **1996,** *8*, (11), 1075-1076.

27. Gopinath, E.; Kaaret, T. W.; Bruice, T. C., Mechanism of mercury(II) reductase and influence of ligation on the reduction of mercury(II) by a water soluble 1,5-

dihydroflavin. *Proceedings of the National Academy of Sciences of the United States of America* **1989,** *86*, (9), 3041-3044.

28. Asztalos, E.; Sipka, G.; Kis, M.; Trotta, M.; Maróti, P., The reaction center is the sensitive target of the mercury(II) ion in intact cells of photosynthetic bacteria. *Photosynthesis Research* **2012,** *112*, (2), 129-140.

29. Price-Whelan, A.; Dietrich, L. E. P.; Newman, D. K., Pyocyanin alters redox homeostasis and carbon flux through central metabolic pathways in *Pseudomonas aeruginosa* PA14. *Journal of Bacteriology* **2007,** *189*, (17), 6372-6381.

30. Peretyazhko, T.; Charlet, L.; Muresan, B.; Kazimirov, V.; Cossa, D., Formation of dissolved gaseous mercury in a tropical lake (Petit-Saut reservoir, French Guiana). *Science of the Total Environment* **2006,** *364*, (1-3), 260-271.

31. Barkay, T.; Kritee, K.; Boyd, E.; Geesey, G., A thermophilic bacterial origin and subsequent constraints by redox, light and salinity on the evolution of the microbial mercuric reductase. *Environmental Microbiology* **2010,** *12*, (11), 2904-2917.

32. Anbar, A. D., Elements and Evolution. *Science* **2008,** *322*, (5907), 1481-1483.

33. Grasby, S. E.; Sanei, H.; Beauchamp, B.; Chen, Z., Mercury deposition through the Permo–Triassic Biotic Crisis. *Chemical Geology* **2013,** *351*, 209-216.

34. Glass, J. B.; Wolfe-Simon, F.; Anbar, A. D., Coevolution of metal availability and nitrogen assimilation in cyanobacteria and algae. *Geobiology* **2009,** *7*, (2), 100-123.

4.8 FIGURES AND CAPTIONS

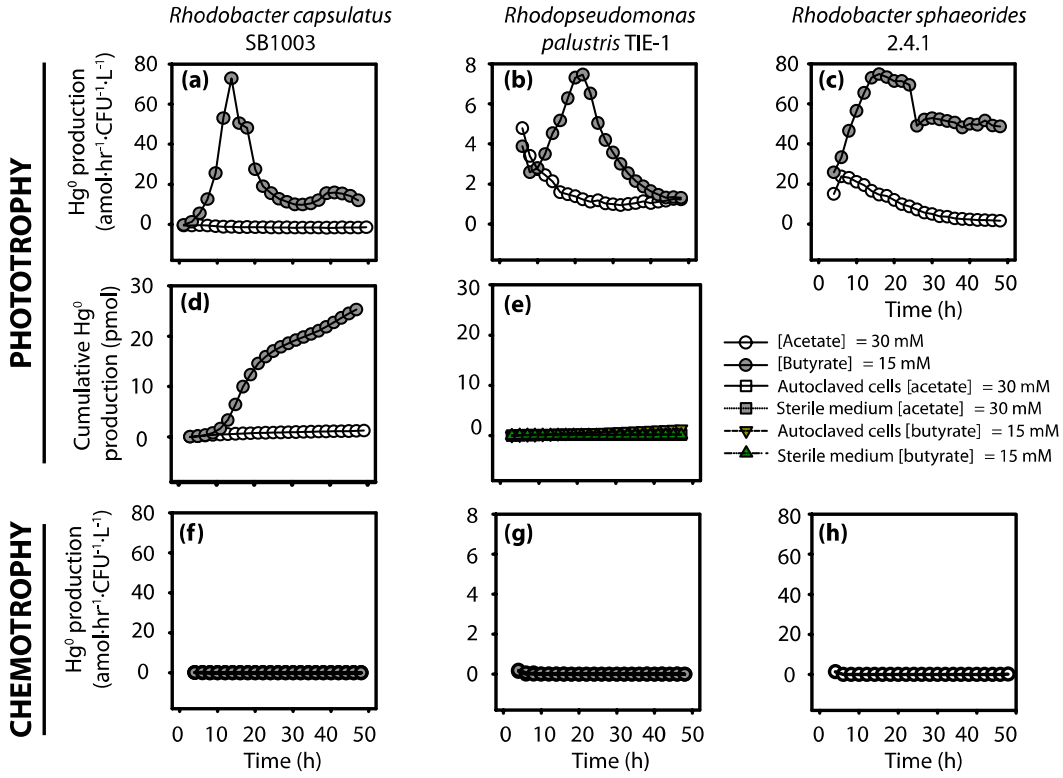

Figure 4.1: Hg^{II} reduction by purple non-sulphur bacteria grown phototrophically or chemotrophically on acetate or butyrate. **a-c** Hg^0 production normalized for cell density for phototrophically grown *R. capsulatus* (**a**), *R. palustris* (**b**) and *R. sphaeroides* (**c**). **d, e** Cumulative production for *R. capsulatus* (**d**) and phototrophic autoclaved cells and sterile medium controls (**e**). **f-h** Hg^0 production normalized for cell density for chemotrophically grown *R. capsulatus* (**f**), *R. palustris* (**g**) and *R. sphaeroides* (**h**). Results are representative cases of replicated experiments, but each data point was recorded once per time step by the instrument and as such no error bars are included.

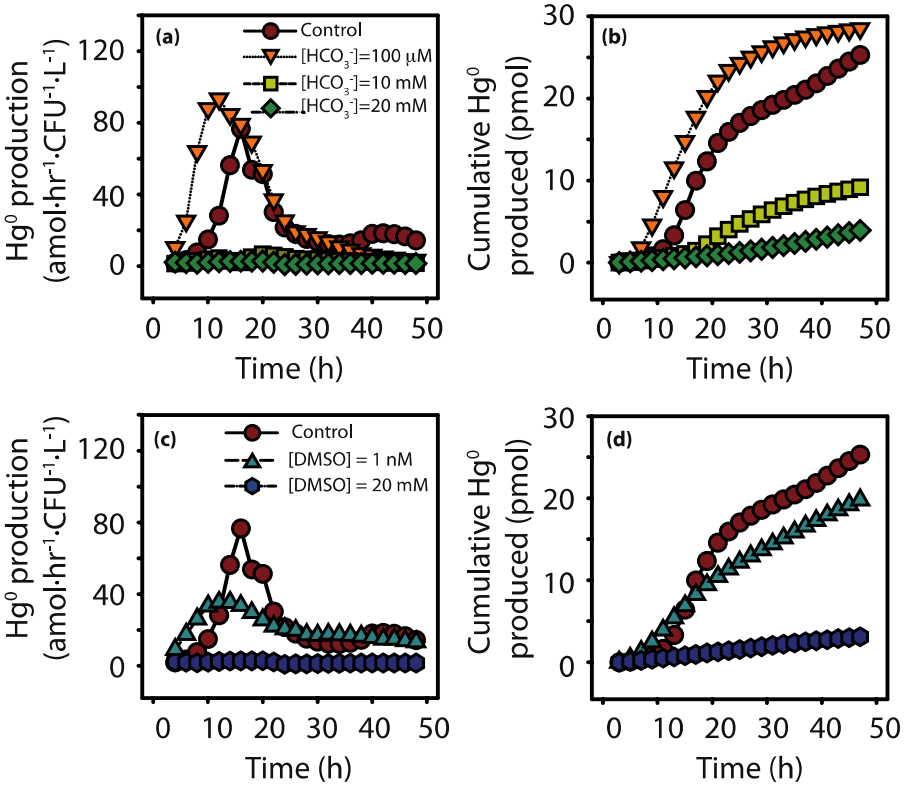

Figure 4.2: Hg^{II} reduction by *R. capsulatus* grown phototrophically on butyrate and supplied with competing electron sinks. The competing electron sinks and the concentrations at which they were supplied are: 100 µM, 10 and 20 mM of HCO_3^-; 1 nM and 20 mM DMSO; control indicates no competing electron sink. **a, c** Hg^0 production normalized for cell density for HCO_3^- (**a**) and DMSO (**c**). **b, d** Cumulative Hg^0 production for HCO_3^- (**b**) and DMSO (**d**). These results are representative cases of replicated experiments, but each data point was recorded once per time step by the instrument and as such no error bars are included.

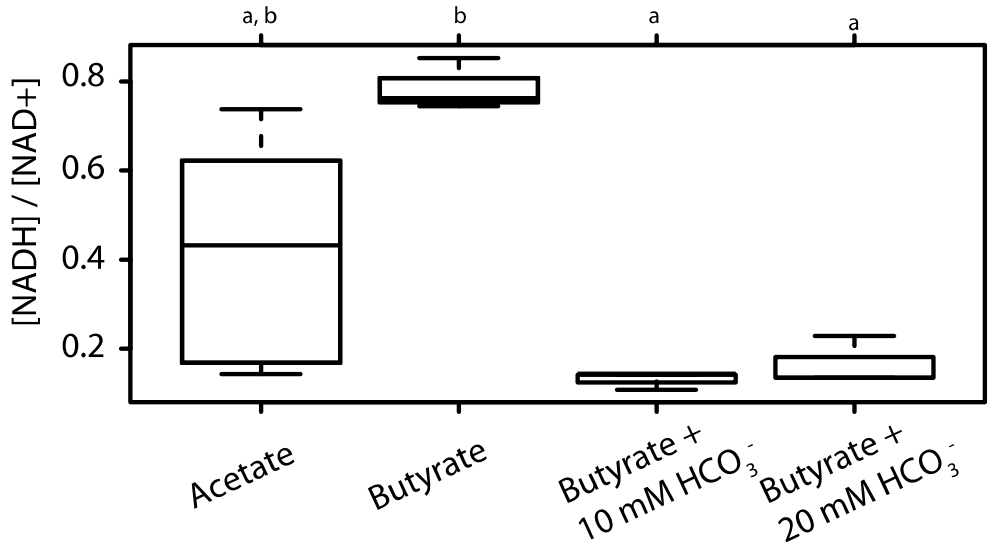

Figure 4.3: [NADH]/[NAD$^+$] for *R. capsulatus* grown phototrophically on butyrate or acetate in the presence of HCO_3^-. Cells were supplied with 30 mM acetate (n=6), 15 mM butyrate (n=3), or 15 mM butyrate with 10 (n=3) and 20 mM HCO_3^- (n=3). The bottom and top of the boxes show the first and third quartiles, respectively, the bar in the middle shows the median and the whiskers show the minimum and maximum for each treatment. Carbon source and HCO_3^- had a significant effect on [NADH]/[NAD_+] ($p<0.01$). Letters that are not shared between treatments indicate a significant difference according to the Tukey HSD test ($p<0.05$).

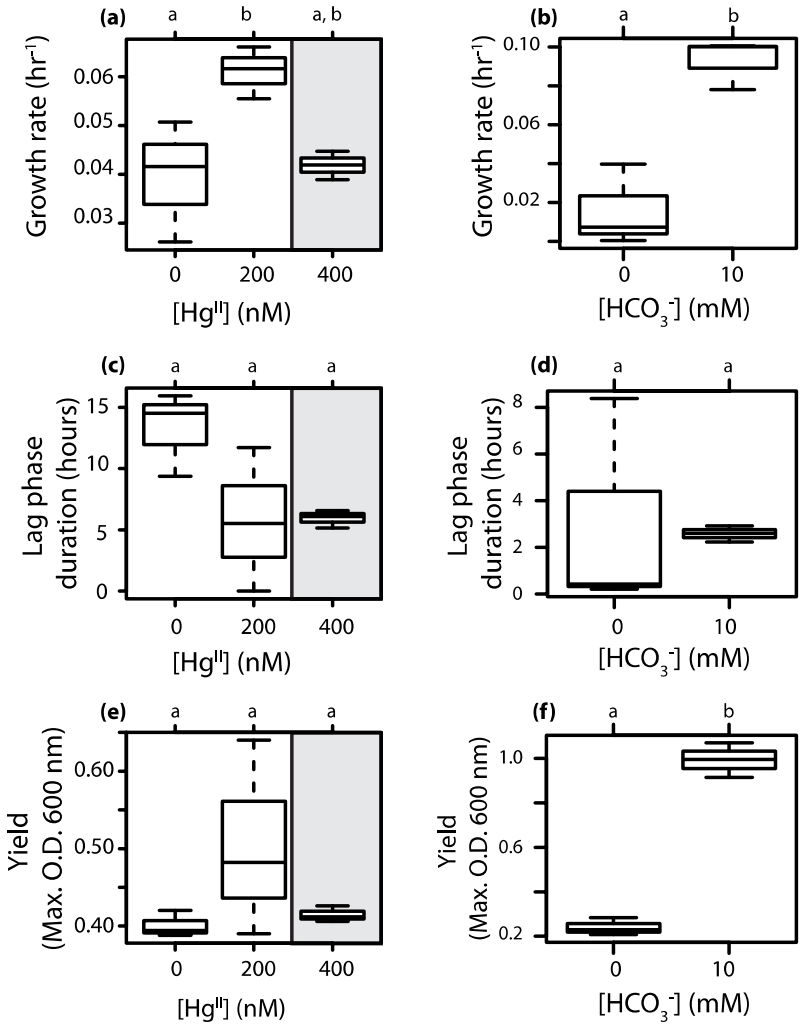

Figure 4.4: Comparison of Hg^{II} and HCO_3^- as electron sinks for *R. capsulatus* grown phototrophically. Growth parameters are presented for cells grown on 1 mM (**a, c, e**) and 15 mM butyrate (**b, d, f**) (n = 3). The bottom and top of the boxes show the first and third quartiles, respectively, the bar in the middle shows the median and the whiskers show the minimum and maximum for each treatment. Shaded areas represent toxic but sublethal [Hg]. [Hg] had a significant effect on growth rate ($p<0.05$) while [HCO_3^-] had a significant effect on growth rate ($p<0.01$) and yield ($p<0.001$). Letters not shared between treatments indicate a significant ($p<0.05$) difference based on Tukey HSD test.

Chapter 5: Heliobacteria reveal fermentation as a key pathway for mercury reduction in anoxic environments

Daniel S. Grégoire [a], Noémie C. Lavoie [a] & Alexandre J. Poulain [a]

a- Biology Department, University of Ottawa, 30 Marie Curie, Ottawa, ON, K1N 6N5, Canada.

Research highlights:

- This study explored whether obligate anaerobic phototrophic and fermentative bacteria from terrestrial environments can participate in Hg redox cycling
- *Heliobacterium modesticaldum* Ice1, an obligate anaerobe capable of photoheterotrophic and fermentative growth, was used as a model organism
- *H. modesticaldum* reduced 55% to 75% of the initial Hg^{II} supplied during phototrophic and fermentative growth, respectively
- Hg reduction relied on the ability of cells to generate reduced redox cofactors
- Similar mechanism for Hg reduction observed in the obligate fermenter *Clostridium acetobutylicum* ATCC824
- Findings suggests a wide diversity of phototrophs and fermenters can participate in Hg redox cycling in anoxic terrestrial habitats

Reprinted with permission from: **Grégoire, D. S**., Lavoie, N. C. & Poulain, A. J., Heliobacteria reveal fermentation as a key pathway for mercury reduction in anoxic environments. *Environmental Science and Technology* **2018,** *52***,** 4145-415.

N.B. Supporting information for this chapter can be found in **Appendix B**

5.1 ABSTRACT

The accumulation of mercury (Hg) in rice, a dietary staple for over half of the world's population, is rapidly becoming a global food safety issue. Rice paddies support the anaerobic production of toxic methylmercury that accumulates in plant tissue, however the microbial controls of Hg cycling in anoxic environments remain poorly understood. In this study, we reveal a novel reductive Hg metabolism in a representative of the family Heliobacteria (*Heliobacterium modesticaldum* Ice1) that we confirm in model chemotrophic anaerobes. Heliobacteria served as our initial model because they are a family of spore-forming fermentative photoheterotrophs commonly isolated from terrestrial environments. We observed that *H. modesticaldum* reduced up to 75% of Hg^{II} under phototrophic or fermentative conditions. Fermentative Hg^{II} reduction relied on the ability of cells to oxidize pyruvate whereas phototrophic Hg^{II} reduction could be supported even in the absence of a carbon source. Inhibiting pyruvate fermentation eliminated Hg^{II} reduction in all chemotrophic strains tested, whereas phototrophic cells remained unaffected. Here we propose a non-*mer* operon dependent mechanism for Hg^0 production in anoxic environments devoid of light where external electron acceptors are limited. These mechanistic details provide the foundation for novel bioremediation strategies to limit the negative impacts of Hg pollution.

5.2 INTRODUCTION

Mercury (Hg) is a global pollutant that causes severe neurological damage in humans who become exposed to it through diet [1]. Although all chemical species of Hg are toxic, methylmercury (MeHg) is the most concerning because it bioaccumulates in the tissues of plants [2] and animals [1]. Whereas fish consumption has long been thought of as the primary route of Hg exposure for humans, contaminated rice is becoming an emerging health concern in countries facing Hg pollution issues where rice is a dietary staple [2, 3].

Rice paddies are often flooded, leading to prolonged periods of anoxia and are rich with nutrients that stimulate the metabolism of iron and sulphate reducers, fermentative bacteria and methanogenic archaea [4]. These groups of microbes are directly responsible for Hg methylation and make rice paddies methylation hotspots [3, 5-9]. Similar hotspots can be found in other surface and near subsurface environments such as sediments [10] and groundwater [11]. To mitigate risks of Hg exposure in these environments, it is important to characterize the pathways that control the availability of inorganic Hg substrate for methylation [12, 13].

Hg redox transformations control Hg's fate and can limit Hg availability by reducing Hg^{II} to Hg^{0} that readily evades to the atmosphere [1]. Despite Hg^{0} being a dominant chemical species in anoxic environments [14, 15], Hg^{II} reduction pathways remain poorly characterized. Anoxic Hg^{II} reduction can occur abiotically, via redox reactions with iron-bearing minerals [16, 17] and dissolved organic matter [18]. Biological pathways catalyzed by dissimilatory metal reducing bacteria [19, 20] and anoxygenic photosynthetic purple non-sulphur bacteria (PNSB) can also contribute to anaerobic Hg^{II} reduction [21]. Strikingly, very few studies report functional *mer* operon determinants (genes encoding

enzymes for Hg scavenging, transport and reduction) in obligate anaerobes [22] and only homologues to the mercuric reductase MerA (encoded by *merA*) have been reported in the genome of an oxygenic phototroph [23].

The recent finding that PNSB couple Hg^{II} reduction to maintaining redox homeostasis (i.e., the recycling of redox cofactors) during photoheterotrophic growth suggests these types of pathways may be widespread among other anaerobes [21]. PNSB, which can derive energy from light and the oxidation of organic carbon, recycle the pool of redox cofactors by reducing exogenous electron acceptors (e.g., DMSO and CO_2) [24]. Chemotrophs such as fermenters rely on similar strategies (e.g. reduction of protons, the fixation of nitrogen gas) or the use of endogenous organic electron acceptors to maintain an optimal ratio of redox cofactors. Fermentation often co-occurs with sulphate reduction in Hg methylation hotspots [25] and some fermenters have been identified as Hg methylators [4]. Yet, whether fermentation can lead to Hg^{II} reduction remains to be tested. The potential contribution of anaerobic metabolism to Hg redox cycling is important to address, as it will directly impact the availability of inorganic Hg substrate for methylation in anoxic environments [12, 13].

Our first objective is to elucidate the mechanism for Hg redox cycling using a model organism from the Heliobacteria family (order Clostridiales), a family characterized as metabolically versatile terrestrial spore forming photoheterotrophs [26]. We elected to work with a model Heliobacteria because many representatives from this family have been isolated from rice paddies and contribute to their ecology [26-28]. Here, we test whether *Heliobacterium modesticaldum* Ice1, one of the best studied members of the Heliobacteria and for which there exists a sequenced genome, can reduce Hg^{II} during

photoheterotrophic growth. *H. modesticaldum* can also grow fermentatively in the dark [29]. Our second objective was therefore to test whether Hg^{II} reduction also occurs during fermentative growth providing a means for Hg redox cycling in anoxic systems devoid of light and terminal electron acceptors. We also compare the potential of *H. modesticaldum* to produce Hg^0 to that of other obligate chemotrophic anaerobes: *Clostridium acetobutylicum* ATCC 824 (a known fermenter with untested Hg^0 production ability) [30] and *Geobacter sulfurreducens* PCA (a strain growing via anaerobic respiration [31] known to produce Hg^0 [19, 20]) in an effort to expand our knowledge on Hg^{II} reduction for different anaerobic metabolisms.

In this study, by carefully manipulating growth conditions and using specific metabolic inhibitors, we provide the first evidence of fermentative Hg^0 production and discuss its importance in the context of Hg cycling in anoxic environments.

5.3 METHODS

5.3.1 Strains, culture conditions and Hg growth assays

All manipulations with cell cultures were performed under anaerobic conditions by working in a Coy anaerobic glove box under 98% N_2/2% H_2 atmosphere or by using sterile anaerobic technique on a bench top where equipment was sparged with N_2 gas prior to use. All obligate anaerobe strains were revived in the anaerobic glove box from cryostocks kept at -80°C. Tubes were then crimped shut and had their headspace replaced with 100 % N_2.

The following strains were used in this study: *Heliobacterium modesticaldum* Ice1, *Clostridium acetobutylicum* ATCC 824, *Geobacter sulfurreducens* PCA and *Escherichia coli* K-12. All strains were obtained from the Deutsche Sammlung von Mikrooganismen und Zellkulturen (DSMZ) collection (DSM-9504, DSM-792, DSM-12127 and DSM-18039, for *H. modesticaldum* Ice1, *C. acetobutylicum* ATCC 824, *G. sulfurreducens* PCA and *E.coli* K-12, respectively). For phototrophic growth of *H. modesticaldum*, cells were supplied with constant illumination at a visible light intensity of 80 µmol photon m^{-2} s^{-1} with a light source emitting peak irradiance in the near-red to red (600 to 700 nm) at 50°C whereas chemotrophic cells were grown at the same temperature in the dark in line with previous work [32]. *C. acetobutylicum* and *E. coli* were grown at 37°C whereas *G. sulfurreducens* was grown at 28°C, all chemotrophically in the dark. Details on the growth media and environmental conditions supplied are provided in **Table B1**. Additional information on cell culturing protocols and preparation of reagents are provided in **Appendix B**.

All bioreactor assays were performed at a final [Hg] = 250 pM. Selected assays testing for Hg^{II} possibly acting as an electron sink and thus enabling growth were carried out at [Hg] = 500 nM. Hg growth assays were carried out under the same phototrophic and chemotrophic conditions mentioned above.

5.3.2 Bioreactor setup and elemental Hg measurements

Please refer to the methods section of Grégoire and Poulain (2016) [21] for a schematic of the bioreactor setup employed and the Hg^0 sampling methodology. Light was supplied using a 200 W incandescent light bulb with a visible light intensity maintained at 20

μmol photon $m^{-2}s^{-1}$ by means of multiple layers of dark screens. Peak irradiance for this light source occurred in the near-red to red spectrum (600 to 700 nm). The only modifications to this method are the growth conditions supplied in the bioreactor that are summarized in the previous section **Strains, culture conditions and Hg growth assays** and **Table B1**.

Each single bioreactor experiment required one week to be fully completed, with little overlap allowed between experiments as we relied on a single continuous Hg^0 analyzer (Tekran 2537). We performed a total of 53 bioreactor experiments to support the conclusions presented in this paper. The details of replicated experiments and associated metadata are presented in **Table B2**.

5.3.3 Bioreactor subsampling for total Hg mass balance and cell density

Total Hg analyses in solution were performed using EPA method 1631. This method involves conserving all Hg in solution with the strong oxidizing agent BrCl, which is subsequently degraded with hydroxylamine prior to addition of $SnCl_2$ upon sample analysis to reduce all the Hg^{II} to Hg^0. Afterwards, this Hg^0 is concentrated onto gold traps and the concentration is measured via CVAFS at 253.7 nm. Total Hg mass balance and bioreactor subsampling were performed following the methodology from Grégoire and Poulain (2016) [21] with the following modification: cell growth was monitored via changes in $O.D._{600nm}$. We performed mass balance experiments and measured total Hg amounts (**Fig B1**) and recoveries (**Fig B2**) for experiments with *H. modesticaldum* to corroborate our Hg^0 measurements. The average quantity of Hg recovered at the end of the experiment was 170.12 ± 18.92 pmol and the average quantity measured at the

beginning of the experiments was 177.18 ± 12.84 pmol (**Fig B1**). The average percent Hg recovered was 97.94 ± 7.92 % (**Fig B2**).

5.3.4 HPLC measurements of pyruvate and acetate

H. modesticaldum cultures grown chemotrophically in PYE with 0.2 g L^{-1} yeast extract were employed to measure pyruvate consumption and acetate production. Compounds were detected using high performance liquid chromatography coupled with a photodiode array detector (HPLC-DAD). Additional details on the HPLC setup are provided in **Appendix B.**

5.3.5 Statistical analyses

All essential statistical information is provided in the figure captions. Additional details on the statistical tests employed are provided in **Appendix B**. The software package used for comparison of means was R v 3.4.2 and the software package used for fitting non-linear regressions was Sigmaplot v 12.5

5.4 RESULTS & DISCUSSION

5.4.1 Hg^0 production occurs phototrophically and chemotrophically

To test whether *H. modesticaldum* reduced Hg^{II} by using it as an electron acceptor during photoheterotrophic growth, we compared biotic and abiotic Hg^0 production under phototrophic and chemotrophic (fermentative) growth conditions (**Table B2**). We predicted that more Hg^0 would be produced when *H. modesticaldum* was grown

phototrophically compared to cells grown chemotrophically because PNSB only reduced Hg phototrophically [21].

Contrary to our predictions, we repeatedly observed 15 % more Hg^0 produced during chemotrophic vs. phototrophic growth (**Fig 5.1** and **Table B2**). Autoclaved and sterile medium treatments produced 95 % less Hg^0 (< 6 pmol) than live cells, regardless of the conditions supplied (**Fig 5.1** and **Table B2**). Hg^0 production by phototrophic cells showed a single peak early on in the experiment (**Fig 5.1A**). In contrast, chemotrophic cells produced two distinct peaks 20 to 24 h apart (**Fig 5.1D**) with the second peak occurring in late exponential phase (**Fig 5.1D** and **Fig B3A**). These findings suggest that time was required for cells to re-oxidize some yet unidentified intracellular redox active cofactor, possibly through growth, before Hg^{II} reduction could resume.

In order to explain the occurrence of the second peak and link its presence to cell growth, we performed a series of experiments where cells were supplied with increasing concentrations of yeast extract (YE) in the presence of 20 mM pyruvate. Indeed, *H. modesticaldum* could not grow on pyruvate alone and the addition of YE was necessary for growth (**Fig 5.1F** and **I**). The addition of trace amounts of YE (0.2 $g.L^{-1}$) did not enable growth and did not enhance Hg^{II} reduction beyond what was observed for pyruvate alone (**Fig 5.1H** and **I**). It is only when YE was provided at a concentration of 4 $g.L^{-1}$ that growth was observed, the second peak occurred and Hg^{II} reduction more than doubled reaching 124.46 ± 6.43 pmol (**Fig 5.1** and **Table B2**) which amounts to 75% of the Hg^{II} being converted into Hg^0 (**Fig B1** and **B2**). Our results show that Hg reduction is not solely driven by light reactions in *H. modesticaldum*. We speculate that under chemotrophic conditions the ability of cells to recycle the pool of redox cofactors through

growth leads to optimal Hg^{II} reduction. We cannot exclude that the second peak observed for Hg^0 results from a different mechanism, however.

As previously proposed for PNSB [21], we also tested whether *H. modesticaldum* was able to derive a physiological advantage when supplied with sublethal amounts of Hg^{II} by using it as an electron sink to recycle the pool of reduced cofactors. No physiological advantage was observed except for a small increase in the yield of phototrophically grown cells in the presence of sublethal amounts of Hg (**Fig B3B** and **Fig B4**).

5.4.2 Pyruvate oxidation contributes to dark Hg^{II} reduction

No previous studies have reported on a mechanism for Hg reduction by Heliobacteria or a model fermentative bacterium. This is surprising given the importance of fermentation in nutrient cycling in anoxic environments. To begin elucidating the mechanism supporting our observations, we focused on narrowing down the potential metabolic coupling points involved in Hg^{II} reduction by varying the supply of organic carbon under chemotrophic conditions. Our hypothesis was that chemotrophic Hg^{II} reduction is dependent on the ability of cells to generate reducing power while growing fermentatively.

To first test this hypothesis, we compared Hg^0 production for cells provided with non-fermentable carbon sources to cells provided with a fermentable carbon source. The non-fermentable carbon source treatments were YE alone, acetate alone or a no carbon control; the fermentable carbon source was pyruvate [29] (**Table B1**). Cells provided with non-fermentable carbon sources exhibited up to an 80% decrease in Hg^0 production (<15 pmol) compared to cells supplied with pyruvate (59.51 ± 0.83 pmol,) or pyruvate + YE

(124.46 ± 6.43 pmol) (**Fig 5.2**). These results suggest that chemotrophic Hg^{II} reduction is dependent on a substrate that supports fermentation and that pyruvate metabolism is one key component of chemotrophic Hg^{II} reduction in *H. modesticaldum*.

To test for the importance of pyruvate metabolism in Hg redox cycling we focused on the core metabolic role of the reversible enzyme pyruvate:ferredoxin oxidoreductase (PFOR), an essential enzyme used to generate reducing power for biosynthesis and metabolize carbon substrate used in fermentative ATP production [33]. PFOR reversibly catalyzes the conversion of pyruvate to acetyl-CoA and transfers electrons to the redox cofactor ferredoxin when operating in the oxidative direction. This reaction acts as the primary source of reducing power in *H. modesticaldum* [29, 33]. Acetyl-CoA can be converted to acetyl-phosphate and acetate is generated as a by-product of energy conservation through ATP synthesis [29]. *H. modesticaldum* can only use acetate as a carbon source during phototrophic growth [29, 32].

Based on this metabolic restriction we tested whether Hg^0 production in the dark is dependent on the availability of pyruvate, the oxidation of which is directly tied to generating reducing power via PFOR [29]. We predicted that Hg^0 production would increase as a function of pyruvate concentration.

We first confirmed that the reaction catalyzed by PFOR was carried out under the chemotrophic conditions tested. We observed that pyruvate was rapidly consumed over the time frame of the experiment with ca. 50% being excreted as acetate similar to what has been reported in previous studies [29] (**Fig B5**). Under these conditions, we showed that Hg^0 production increased as a function of pyruvate concentration although the total amount of Hg^0 produced reached a plateau between 20 and 100 mM pyruvate (**Fig 5.2C**).

These results support that chemotrophic Hg^0 production is dependent on pyruvate oxidation for the initial supply of reducing power. However, we suspect that cells eventually became limited in their ability to reduce Hg^{II} even when supplied with ample pyruvate. We attribute the presence of a plateau to the inability of cells to recycle the intracellular pool of redox cofactors via growth. Indeed, H. *modesticaldum* was unable to grow on pyruvate in the absence of YE (**Fig 5.1I** and previous section). These results support that organic carbon oxidation provides reducing power for Hg^{II} reduction during fermentative growth and underscore that Hg^0 production is optimal when cells can recycle the pool of redox cofactors during growth.

Despite growth leading to optimal Hg^{II} reduction, 100% Hg^{II} reduction was never observed (**Fig B2**). With mM levels of pyruvate available for oxidation via PFOR, there should be ample reducing power available to reduce pM amounts of Hg. We suspect that the extent of net Hg reduction can be limited i) by cellular Hg^{II} uptake, ii) the availability of intracellular redox cofactors and iii) the very rapid reoxidation of newly formed Hg^0. Assuming that the Hg reduction observed here is an intracellular process, it is remarkable to observe such high levels of Hg^0 produced in the absence of a dedicated transport system, such as those available to microbes possessing the *mer* operon. Although we suspect that the majority of the reducing power generated by pyruvate oxidation is being employed to maintain cellular functions, we are not yet able to quantify the proportion of reducing power available for Hg reduction due to the low cell density achieved in our bioreactor experiments. The potential for *H. modesticaldum* to oxidize Hg^0 remains to be tested.

5.4.3 *H. modesticaldum* can catalyze light-dependent reduction of Hg^{II}

When grown phototrophically, cells rely on their photosynthetic machinery to produce ATP and reduce ferredoxin [29]. To further explore the role of reducing power availability on Hg^{II} reduction we first tested whether cells irradiated by light in the absence of a carbon source could trigger Hg^{II} reduction. We observed that non-growing (no carbon) irradiated *H. modesticaldum* cells produced nearly as much Hg^0 compared to cells supplied with pyruvate and YE (87.21 ± 10.25 pmol vs. 99.79 ± 3.11 pmol, **Fig 5.2** and **Table B2**). This result contrasts with cells kept in the dark where virtually no Hg^0 was produced (**Fig 5.2**, **Fig B6** and **Table B2**). These results suggest that photoinduced electron transfer maintains a sufficient pool of reducing power that drives Hg^{II} reduction in *H. modesticaldum*. Although our evidence suggests that Hg^{II} reduction depends on the availability of reduced cytoplasmic ferredoxin, we cannot discount that components of *H. modesticaldum'*s electron transport chain participate directly in Hg^{II} reduction. Additional work is required to identify which components of the electron transport chain can reduce Hg^{II}.

5.4.4 Light-dependent Hg^{II} reduction depends on the availability of redox cofactors

As an additional test for the role of reducing power availability in Hg^{II} reduction, we supplied cells with conditions that favour the consumption of reducing power. Indeed, during phototrophic growth on acetate, PFOR is predicted to consume acetate, inorganic carbon (HCO_3^-) and reduced ferredoxin originating from light reactions to produce pyruvate [33]. We compared Hg^0 production for phototrophic cells grown on YE alone, YE + acetate and YE + acetate + HCO_3^- (**Table B1**). Under conditions that favour growth on

acetate and the consumption of reduced ferredoxin, Hg^0 production decreased by ca. 40% compared to the YE only control (52.04 ± 8.52 pmol for YE + acetate, 42.91 ± 0.57 pmol for YE + acetate + HCO_3^- vs. 91.38 ± 1.26 pmol for YE, **Fig 5.2** and **Table B2**).

Our results show that Hg^0 production is enhanced when cells chemotrophically oxidize pyruvate but inhibited when cells phototrophically consume acetate. These findings suggest that Hg^{II} reduction is linked to the activity of enzymes that depend on the availability of redox cofactors.

5.4.5 Inhibiting a key fermentation enzyme affects Hg^0 production

Our next objective was to distinguish the role of a direct involvement of PFOR from that of reduced ferredoxin in Hg reduction. First, we inhibited PFOR activity for phototrophically and chemotrophically grown *H. modesticaldum* cells using nitazoxanide (NTZ), a specific PFOR inhibitor that has previously been used on members of the closely related Clostridia [34] (**Table B1**). Whereas PFOR is essential to maintain the pool of reducing power when cells are growing fermentatively in the dark, it is not the case in the presence of light when oxidized ferredoxin can be reduced by photobiological reactions [29]. We predicted that if Hg^{II} reduction depends on the ability of cells to generate reduced cofactors, compensatory pathways such as light-driven reduction of ferredoxin would maintain a sufficient supply of reducing equivalents for Hg^{II} reduction even when PFOR was inhibited.

The presence of NTZ inhibited chemotrophic Hg^0 production by 88 % compared to controls (7.14 ± 3.83 pmol vs. 66.97 ± 28.64 pmol, **Fig 5.3C, D** and **Table B2**). In contrast, phototrophic Hg^0 production was mostly unaffected for cells supplied with NTZ (74.00 ± 16.99 pmol vs. 82.29 ± 1.50 pmol) (**Fig 5.3A, B** and **Table B2**). Phototrophic cells showed a lag in Hg^0 production with the peak of Hg^0 production occurring 11h later than what was previously observed (**Fig 5.1A** and **Fig 5.3A**). We attribute this lag to the time required to generate a sufficient amount of reducing power, probably in the form of NADH. NADH acts as an electron donor to the heliobacterial photosynthetic transport chain, eventually reducing the pool of ferredoxin via light-induced low potential electrons [35].

Although cells did not grow, NTZ did not arrest all metabolism or trigger cell death because Hg^0 production was observed (ca. 80 pmol), albeit after a considerable lag phase. NTZ is a specific inhibitor of PFOR and we suspect that phototrophic cell growth was inhibited because acetyl-CoA generated as a result of PFOR activity is an essential metabolite (**Fig 5.3B**). In the absence of acetate, PFOR-mediated oxidation of pyruvate is the only known pathway leading to acetyl-CoA production in *H. modesticaldum* [33]. That being said, the ability of uninhibited cells to use PFOR and grow may have afforded them additional means of generating reducing power, possibly explaining the absence of a delay in Hg^0 production.

As an additional test for the role of reduced ferredoxin availability on Hg^{II} reduction, we conducted a series of experiments where we attempted to inhibit the activity of *H. modesticaldum*'s hydrogenase. In *H. modesticaldum*, a [Fe]-hydrogenase is predicted to be responsible for recycling the pool of reduced ferredoxin via proton

reduction and subsequent H_2 production [29, 36]. We predicted that an inhibition of the hydrogenase during chemotrophic growth would increase Hg^0 production because more reduced ferredoxin would be available for Hg^{II} reduction. In support of our prediction a 30% increase in the amount of Hg^0 produced (53.36 ± 0.13 pmol vs. 41.29 ± 5.41 pmol) was observed in the presence of NO_2^- (an inhibitor of [Fe]-hydrogenase) [37, 38] (**Fig B7** and **Table B2**).

These results show that in the absence of PFOR activity (be it through direct inhibition or lack of substrate), cells can continue to reduce Hg^{II} when other means of generating reducing equivalents are available. We propose that ferredoxin is the main electron carrier involved in Hg^{II} reduction, but we cannot rule out the contributions of other reducing equivalents such as NAD(P)H. It is also possible that components of the photosynthetic chain could directly catalyze Hg^{II} reduction before the production of cytosolic reduced ferredoxin, representing an additional means by which *H. modesticaldum* could affect Hg redox cycling. Finally, we can rule out that the mercuric reductase (MerA) is involved in NAD(P)H-mediated Hg reduction in *H. modesticaldum* given that no *mer* operon or MerA homologues have been detected in the genome of *H. modesticaldum*.

5.4.6 Hg reduction is associated with a fermentative lifestyle

We next sought to test whether other anaerobes reduced Hg^{II} through similar means to *H. modesticaldum*. We compared Hg^0 production in an obligate fermenter to that of other model anaerobes who favour anaerobic respiration. To achieve this objective, we repeated experiments with three additional strains possessing genes encoding for PFOR

and who use ferredoxin as a reduced cofactor: *C. acetobutylicum, G. sulfurreducens* and *E. coli* (additional details on the pyruvate metabolism of these strains is provided in **Appendix B**).

First, we performed NTZ exposure experiments with *C. acetobutylicum* and *G. sulfurreducens*. Although both strains differed in the magnitude of Hg^0 produced, NTZ inhibited Hg^{II} reduction in both strains tested (**Fig 5.4**). *C. acetobutylicum* produced 83% more Hg^0 than *G. sulfurreducens* (51.02 pmol vs. 8.46 pmol) achieving total Hg^0 production on the same order of magnitude as *H. modesticaldum* (ca. 70 pmol) (**Fig 5.3** and **Fig 5.4**); this difference in Hg reduction ability between the two strains was also observed when each strain was grown in their own optimal growth medium (**Table B2**). In the presence of NTZ, Hg^0 production decreased by 98% and 62 %, respectively (1.20 pmol and 3.19 pmol) which is comparable to the 88% decrease observed for *H. modesticaldum* (**Fig 5.3** and **Fig 5.4**). Given that NTZ affected Hg^0 production to a similar degree across the model organisms studied, these results suggest that the production of reduced ferredoxin is linked to Hg^{II} reduction across multiple anaerobes.

C. acetobutylicum did not exhibit two distinct peaks and Hg^0 production occurred 14h into the experiment (**Fig 5.4A**). In this case, we attribute the lag in Hg^0 production to the time required for cells to oxidize sufficient amounts of pyruvate to reduce the pool of oxidized ferredoxin. In all cases, growth was very slow (**Fig B8**), which could be due to the presence of DMSO, an essential carrier solvent for the NTZ inhibitor.

The considerably lower Hg^0 production observed in *G. sulfurreducens* may be associated with the slow reaction of its PFOR system, as previously reported [39, 40]. Alternatively, the inability of cells to grow under the conditions tested and thereby recycle the pool of redox cofactors necessary to reduce Hg^{II} may have contributed to the lower values observed.

To test for this, we evaluated the ability of *G. sulfurreducens* to reduce Hg^{II} with and without fumarate as a terminal electron acceptor. The presence of fumarate should enable growth but also the activation of pyruvate dehydrogenase (PDH) [39]. In the presence of fumarate, *G. sulfurreducens* cells were able to grow but Hg^0 production decreased by 50% (**Table B2**). Similarly, Hg^0 production by *E. coli*, which mostly relies on pyruvate formate lyase (PFL) and PDH activity rather than PFOR for pyruvate metabolism, was virtually undetectable (i.e., not different from autoclaved controls), although cells were able to grow (**Table B2**).

These experiments showed that Hg^0 production was greater for fermentative anaerobes (*H. modesticaldum* and *C. acetobutylicum*), regardless of growth ability. Based on previous studies and the conditions tested here, we could expect the availability of reduced ferredoxin to be limited for *G. sulfurreducens* or *E. coli* because of the slow reaction of PFOR in both strains or because alternate pathways to metabolize pyruvate are activated. It is possible that fermenters may have more reducing power available for Hg^{II} reduction compared to cells capable of respiration; this remains to be properly quantified.

5.4.7 Environmental relevance

In this work we provide the first evidence for Hg^{II} reduction in a previously unexplored family of anoxygenic phototrophs, the Heliobacteria, and propose a new mechanism for Hg^{II} reduction that is also supported during fermentation by another member of the Clostridiales (*C. acetobutylicum*). We have summarized our findings in **Fig B9**. Hg^{II} reduction was dependent on the ability of *H. modesticaldum* to generate reducing power (possibly ferredoxin) through the photosynthetic electron transport chain or organic carbon oxidation. Furthermore, Hg^{II} likely competes with other redox homeostasis pathways such as H_2 production for this pool of reductants.

H. modesticaldum exhibited some of the highest Hg^0 production yields relative to Hg^{II} substrate concentrations. This is interesting because in our study, Hg^{II} was supplied at pM levels; a compilation of other biotic and abiotic Hg^0 production data is provided in **Table 5.1**. Furthermore, *C. acetobutylicum* also exhibited Hg^0 production rates that agree with [Hg^0] published in previous studies [13-15, 18-21, 41-46] (**Table 5.1**). Taking into consideration Hg^0 concentrations reported from saturated soil, sediment and groundwater environments, our work suggests that photoheterotrophy (where light is available) and fermentation (in environments where the availability of light and/or external electron acceptors are limited) can contribute to observed environmental levels of Hg^0 (**Table 5.1**).

Although *H. modesticaldum* is a thermophile, it serves as a model representative for the family Heliobacteria. As a family, most Heliobacteria were isolated from terrestrial environments such as rice paddies and exhibit a mutualistic relationship with the rice plant (e.g., exchange of nutrients) [47]. With the rising safety issues concerning the

consumption of contaminated rice, future efforts should focus on characterizing the environmental conditions that stimulate the native photoheterotrophic and fermentative communities.

These metabolisms are well suited to limiting Hg methylation by reducing Hg^{II} to gaseous Hg^{0} that can readily evade to the atmosphere from shallow paddy soils. Such strategies could also limit Hg methylation through competition for resources because fermenters and Hg methylators (e.g., sulphate reducing bacteria, methanogens) occupy the same niches. However, the ability of some microbes to catalyze both Hg reduction and methylation deserves further investigation [45]. An understanding of the physiological controls of such processes and how they are coupled to carbon metabolism and redox homeostasis may offer novel insights into management of Hg pollution.

Our work suggests that microbial fermentative cells are poised to affect the redox cycling of (toxic) metals that can act as exogenous electron acceptors. In environments where fermenters thrive, cells at risk of Hg toxicity could benefit from Hg^{II} reduction as a detoxification strategy; this may have precluded the need to maintain strategies such as the *mer* operon for Hg detoxification. This idea is supported by the fact that very few studies report functional *mer* operons in obligate anaerobes [22] and no genetic determinants encoding for Hg detoxification strategies specific to anaerobes have been described so far. Our study highlights the importance of including microbial physiology in addition to genome-based tools when elucidating non-conventional Hg reduction pathways. Clearly, the redox conditions that can support microbial Hg^{II} reduction are more diverse than initially perceived and can occur across a wide range of metabolisms and environments.

5.5 FUNDING INFORMATION

Our work was funded by NSERC Discovery and Accelerator grants, CFI funding to AJP and NSERC graduate scholarship to DSG.

5.6 ACKNOWLEDGMENTS

We are thankful for *Geobacter sulfurreducens* PCA strain that was a gift from Jeffra Schaefer. We thank Ammar Saleem for assistance with HPLC analysis.

5.7 AUTHOR CONTRIBUTIONS

AJP and DSG designed the experiments, DSG and NCL carried them out, DG performed data analyses; AJP and DSG wrote the manuscript.

5.8 REFERENCES

1. Fitzgerald, W. F.; Lamborg, C. H.; Hammerschmidt, C. R., Marine biogeochemical cycling of mercury. *Chemical Reviews* **2007,** *107*, (2), 641-662.

2. Zhang, H.; Feng, X. B.; Larssen, T.; Qiu, G. L.; Vogt, R. D., In inland China, rice, rather than fish, is the major pathway for methylmercury exposure. *Environmental Health Perspectives* **2010,** *118*, (9), 1183-1188.

3. Rothenberg, S. E.; Windham-Myers, L.; Creswell, J. E., Rice methylmercury exposure and mitigation: A comprehensive review. *Environmental Research* **2014,** *133*, 407-423.

4. Parks, J. M.; Johs, A.; Podar, M.; Bridou, R.; Hurt Jr, R. A.; Smith, S. D.; Tomanicek, S. J.; Qian, Y.; Brown, S. D.; Brandt, C. C.; Palumbo, A. V.; Smith, J. C.; Wall, J. D.; Elias, D. A.; Liang, L., The genetic basis for bacterial mercury methylation. *Science* **2013,** *339*, (6125), 1332-1335.

5. Rothenberg, S. E.; Feng, X., Mercury cycling in a flooded rice paddy. *Journal of Geophysical Research: Biogeosciences* **2012,** *117*, 1-16.

6. Marvin-DiPasquale, M.; Windham-Myers, L.; Agee, J. L.; Kakouros, E.; Kieu, L. H.; Fleck, J. A.; Alpers, C. N.; Stricker, C. A., Methylmercury production in sediment from agricultural and non-agricultural wetlands in the Yolo Bypass, California, USA. *Science of the Total Environment* **2014,** *484*, 288-299.

7. Meng, B.; Feng, X. B.; Qiu, G. L.; Cai, Y.; Wang, D. Y.; Li, P.; Shang, L. H.; Sommar, J., Distribution patterns of inorganic mercury and methylmercury in yissues of rice (*Oryza sativa* L.) plants and possible bioaccumulation pathways. *Journal of Agricultural and Food Chemistry* **2010,** *58*, (8), 4951-4958.

8. Zhao, L.; Anderson, C. W. N.; Qiu, G. L.; Meng, B.; Wang, D. Y.; Feng, X. B., Mercury methylation in paddy soil: source and distribution of mercury species at a Hg mining area, Guizhou Province, China. *Biogeosciences* **2016,** *13*, (8), 2429-2440.

9. Zhao, L.; Qiu, G. L.; Anderson, C. W. N.; Meng, B.; Wang, D. Y.; Shang, L. H.; Yan, H. Y.; Feng, X. B., Mercury methylation in rice paddies and its possible controlling factors in the Hg mining area, Guizhou province, Southwest China. *Environmental Pollution* **2016,** *215*, 1-9.

10. Warner, K. A.; Roden, E. E.; Bonzongo, J. C., Microbial mercury transformation in anoxic freshwater sediments under iron-reducing and other electron-accepting conditions. *Environmental Science and Technology* **2003,** *37*, (10), 2159-2165.

11. Vidon, P. G.; Mitchell, C. P. J.; Jacinthe, P. A.; Baker, M. E.; Liu, X.; Fisher, K. R., Mercury dynamics in groundwater across three distinct riparian zone types of the US Midwest. *Environmental Sciences: Processes and Impacts* **2013,** *15*, (11), 2131-2141.

12. Colombo, M. J.; Ha, J.; Reinfelder, J. R.; Barkay, T.; Yee, N., Anaerobic oxidation of Hg(0) and methylmercury formation by *Desulfovibrio desulfuricans* ND132. *Geochimica et Cosmochimica Acta* **2013,** *112*, 166-177.

13. Hu, H. Y.; Lin, H.; Zheng, W.; Tomanicek, S. J.; Johs, A.; Feng, X. B.; Elias, D. A.; Liang, L. Y.; Gu, B. H., Oxidation and methylation of dissolved elemental mercury by anaerobic bacteria. *Nature Geoscience* **2013,** *6*, (9), 751-754.

14. Poulin, B. A.; Aiken, G. R.; Nagy, K. L.; Monceau, A.; Krabbenhoft, D. P.; Ryan, J. N., Mercury transformation and release differs with depth and time in a contaminated riparian soil during simulated flooding. *Geochimica Et Cosmochimica Acta* **2016,** *176*, 118-138.

15. Bouffard, A.; Amyot, M., Importance of elemental mercury in lake sediments. *Chemosphere* **2009,** *74*, (8), 1098-1103.

16. Wiatrowski, H. A.; Das, S.; Kukkadapu, R.; Ilton, E. S.; Barkay, T.; Yee, N., Reduction of Hg(II) to Hg(0) by magnetite. *Environmental Science and Technology* **2009,** *43*, (14), 5307-5313.

17. Bone, S. E.; Bargar, J. R.; Sposito, G., Mackinawite (FeS) reduces mercury(II) under sulfidic conditions. *Environmental Science & Technology* **2014,** *48*, (18), 10681-10689.

18. Gu, B.; Bian, Y.; Miller, C. L.; Dong, W.; Jiang, X.; Liang, L., Mercury reduction and complexation by natural organic matter in anoxic environments. *Proceedings of the National Academy of Sciences of the United States of America* **2011,** *108*, (4), 1479-1483.

19. Wiatrowski, H. A.; Ward, P. M.; Barkay, T., Novel reduction of mercury(II) by mercury-sensitive dissimilatory metal reducing bacteria. *Environmental Science and Technology* **2006,** *40*, (21), 6690-6696.

20. Lin, H.; Morrell-Falvey, J. L.; Rao, B.; Liang, L. Y.; Gu, B. H., Coupled mercury-cell sorption, reduction, and oxidation on methylmercury production by *Geobacter sulfurreducens* PCA. *Environmental Science & Technology* **2014,** *48*, (20), 11969-11976.

21. Grégoire, D. S.; Poulain, A. J., A physiological role for Hg(II) during phototrophic growth. *Nature Geoscience* **2016,** *9*, (2), 121-125.

22. Barkay, T.; Kritee, K.; Boyd, E.; Geesey, G., A thermophilic bacterial origin and subsequent constraints by redox, light and salinity on the evolution of the microbial mercuric reductase. *Environmental Microbiology* **2010,** *12*, (11), 2904-2917.

23. Marteyn, B.; Sakr, S.; Farci, S.; Bedhomme, M.; Chardonnet, S.; Decottignies, P.; Lemaire, S. D.; Cassier-Chauvat, C.; Chauvat, F., The *Synechocystis* PCC6803 MerA-like enzyme operates in the reduction of both mercury and uranium under the control of the glutaredoxin 1 enzyme. *Journal of Bacteriology* **2013,** *195*, (18), 4138-4145.

24. McKinlay, J. B.; Harwood, C. S., Carbon dioxide fixation as a central redox cofactor recycling mechanism in bacteria. *Proceedings of the National Academy of Sciences of the United States of America* **2010,** *107*, (26), 11669-11675.

25. Desrochers, K. A. N.; Paulson, K. M. A.; Ptacek, C. J.; Blowes, D. W.; Gould, W. D., Effect of electron donor to sulfate ratio on mercury methylation in floodplain sediments under saturated flow conditions. *Geomicrobiology Journal* **2015,** *32*, (10), 924-933.

26. Asao, M.; Madigan, M. T., Taxonomy, phylogeny, and ecology of the Heliobacteria. *Photosynthesis Research* **2010,** *104*, (2-3), 103-111.

27. Girija, K. R.; Vinay, B.; Sasikala, C.; Ramana, C. V., Novel heliobacteria of a few semi-arid tropical soils. *Indian Journal of Microbiology* **2010,** *50*, S17-S20.

28. Madigan, M. T., The Family Heliobacteriaceae. In *The Prokaryotes: Volume 4: Bacteria: Firmicutes, Cyanobacteria*, Dworkin, M.; Falkow, S.; Rosenberg, E.; Schleifer, K.-H.; Stackebrandt, E., Eds. Springer US: New York, NY, 2006; pp 951-964.

29. Tang, K. H.; Yue, H.; Blankenship, R. E., Energy metabolism of *Heliobacterium modesticaldum* during phototrophic and chemotrophic growth. *Bmc Microbiology* **2010,** *10*.

30. Lutke-Eversloh, T.; Bahl, H., Metabolic engineering of *Clostridium acetobutylicum*: Recent advances to improve butanol production. *Current Opinion in Biotechnology* **2011,** *22*, (5), 634-647.

31. Mahadevan, R.; Bond, D. R.; Butler, J. E.; Esteve-Núñez, A.; Coppi, M. V.; Palsson, B. O.; Schilling, C. H.; Lovley, D., Characterization of metabolism in the Fe

(III)-reducing organism *Geobacter sulfurreducens* by constraint-based modeling. *Applied and environmental microbiology* **2006,** *72*, (2), 1558-1568.

32. Kimble, L. K.; Mandelco, L.; Woese, C. R.; Madigan, M. T., *Heliobacterium modesticaldum*, sp. nov., a thermophilic heliobacterium of hot springs and volcanic soils. *Archives of Microbiology* **1995,** *163*, (4), 259-267.

33. Tang, K. H.; Feng, X. Y.; Zhuang, W. Q.; Alvarez-Cohen, L.; Blankenship, R. E.; Tang, Y. J., Carbon flow of Heliobacteria is related more to Clostridia than to the green sulfur bacteria. *Journal of Biological Chemistry* **2010,** *285*, (45), 35104-35112.

34. Hoffman, P. S.; Bruce, A. M.; Olekhnovich, I.; Warren, C. A.; Burgess, S. L.; Hontecillas, R.; Viladomiu, M.; Bassaganya-Riera, J.; Guerrant, R. L.; Macdonald, T. L., Preclinical studies of amixicile, a systemic therapeutic developed for treatment of *Clostridium difficile* infections that also shows efficacy against *Helicobacter pylori*. *Antimicrobial Agents and Chemotherapy* **2014,** *58*, (8), 4703-4712.

35. Sattley, W. M.; Asao, M.; Tang, J. K. H.; Collins, A. M., Energy conservation in Heliobacteria: Photosynthesis and central metabolism. In *The structural basis of biological energy generation, advances in photosynthesis and respiration*, Hohmann-Marriott, M. F., Ed. Springer Science: 2014; Vol. 39, pp 231-247.

36. Sattley, W. M.; Madigan, M. T.; Swingley, W. D.; Cheung, P. C.; Clocksin, K. M.; Conrad, A. L.; Dejesa, L. C.; Honchak, B. M.; Jung, D. O.; Karbach, L. E.; Kurdoglu, A.; Lahiri, S.; Mastrian, S. D.; Page, L. E.; Taylor, H. L.; Wang, Z. T.; Raymond, J.; Chen, M.; Blankenship, R. E.; Touchman, J. W., The genome of *Heliobacterium modesticaldum*, a phototrophic representative of the Firmicutes

containing the simplest photosynthetic apparatus. *Journal of Bacteriology* **2008,** *190*, (13), 4687-4696.

37. Hatchikian, E. C.; Forget, N.; Fernandez, V. M.; Williams, R.; Cammack, R., Further characterization of the [Fe]-hydrogenase from *Desulfovibrio desulfuricans* ATCC 7757. *European Journal of Biochemistry* **1992,** *209*, 357-365.

38. Schomburg, D.; Schomburg, I.; Chang, A., Class 1 - Oxidoreductases X EC 1.9 - 1.14. In *Springer Handbook of Enzymes*, Schomburg, D., Schomburg, I.,, Ed. Springer-Verlag: Berlin Heidelberg, 2006; Vol. 25, pp 373-381.

39. Speers, A. M.; Reguera, G., Electron donors supporting growth and electroactivity of *Geobacter sulfurreducens* anode biofilms. *Applied and Environmental Microbiology* **2012,** *78*, (2), 437-444.

40. Segura, D.; Mahadevan, R.; Juarez, K.; Lovley, D. R., Computational and experimental analysis of redundancy in the central metabolism of *Geobacter sulfurreducens*. *Plos Computational Biology* **2008,** *4*, (2), 12.

41. Schaefer, J. K.; Letowski, J.; Barkay, T., *mer*-mediated resistance and volatilization of Hg(II) under anaerobic conditions. *Geomicrobiology Journal* **2002,** *19*, (1), 87-102.

42. Poulain, A. J.; Amyot, M.; Findlay, D.; Telor, S.; Barkay, T.; Hintelmann, H., Biological and photochemical production of dissolved gaseous mercury in a boreal lake. *Limnology and Oceanography* **2004,** *49*, (6), 2265-2275.

43. Bagnato, E.; Aiuppa, A.; Parello, F.; D'Alessandro, W.; Allard, P.; Calabrese, S., Mercury concentration, speciation and budget in volcanic aquifers: Italy and Guadeloupe

(Lesser Antilles). *Journal of Volcanology and Geothermal Research* **2009,** *179*, (1-2), 96-106.

44. Liu, S.; Wiatrowski, H. A., Reduction of Hg(II) to Hg(0) by biogenic magnetite from two magnetotactic bacteria. *Geomicrobiology Journal* **2018,** *35*, (3), 198-208.

45. Lu, X.; Liu, Y.; Johs, A.; Zhao, L.; Wang, T.; Yang, Z.; Lin, H.; Elias, D. A.; Pierce, E. M.; Liang, L.; Barkay, T.; Gu, B., Anaerobic mercury methylation and demethylation by *Geobacter bemidjiensis* Bem. *Environmental Science and Technology* **2016,** *50*, (8), 4366-4373.

46. Zhao, L. D.; Chen, H. M.; Lu, X.; Lin, H.; Christensen, G. K.; Pierce, E. M.; Gu, B. H., Contrasting effects of dissolved organic matter on mercury methylation by *Geobacter sulfurreducens* PCA and *Desulfovibrio desulfuricans* ND132. *Environmental Science & Technology* **2017,** *51*, (18), 10468-10475.

47. Stevenson, A. K.; Kimble, L. K.; Woese, C. R.; Madigan, M. T., Characterization of new phototrophic Heliobacteria and their habitats. *Photosynthesis Research* **1997,** *53*, (1), 1-12.

5.9 FIGURES AND CAPTIONS

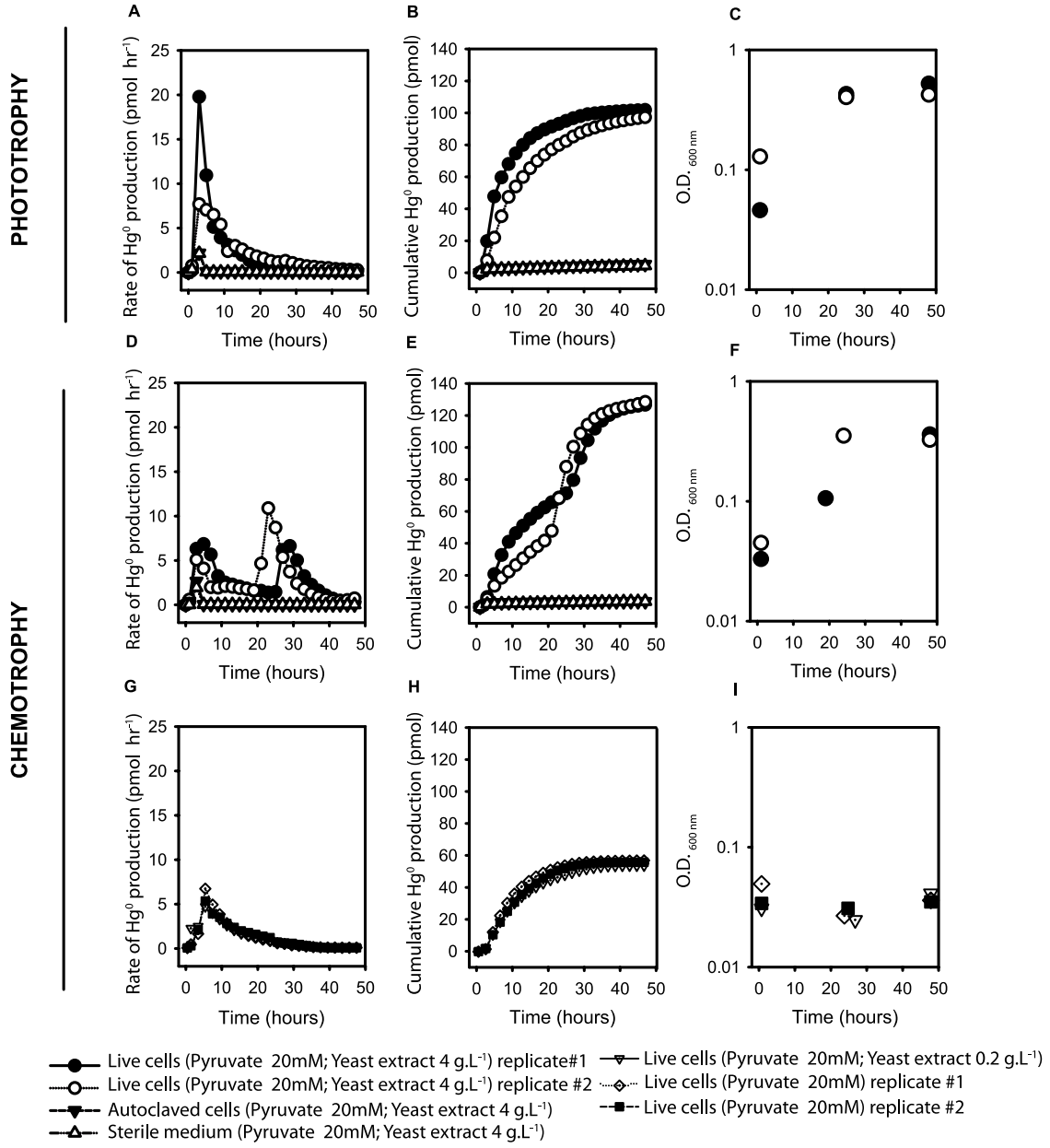

(Figure caption provided on the following page)

Figure 5.1: Hg^0 production by *Heliobacterium modesticaldum* Ice1 grown phototrophically and chemotrophically. A, D, G Rate of Hg^0 production for live cells, autoclaved cells and sterile medium under phototrophic (**A**) and chemotrophic (**D**) conditions and live cells supplied with pyruvate or pyruvate and trace amounts of yeast extract under chemotrophic conditions (**G**). **B, E, H** Cumulative Hg^0 production for live cells, autoclaved cells and sterile medium under phototrophic (**B**) and chemotrophic (**E**) conditions and live cells supplied with pyruvate or pyruvate and trace amounts of yeast extract under chemotrophic conditions (**H**). **C, F, I** Microbial growth as measured by O.D. 600 nm for phototrophic (**C**) and chemotrophic (**F**) conditions and live cells supplied with pyruvate or pyruvate and trace amounts of yeast extract under chemotrophic conditions (**I**). Hg was added to a final concentration of 250 pM.

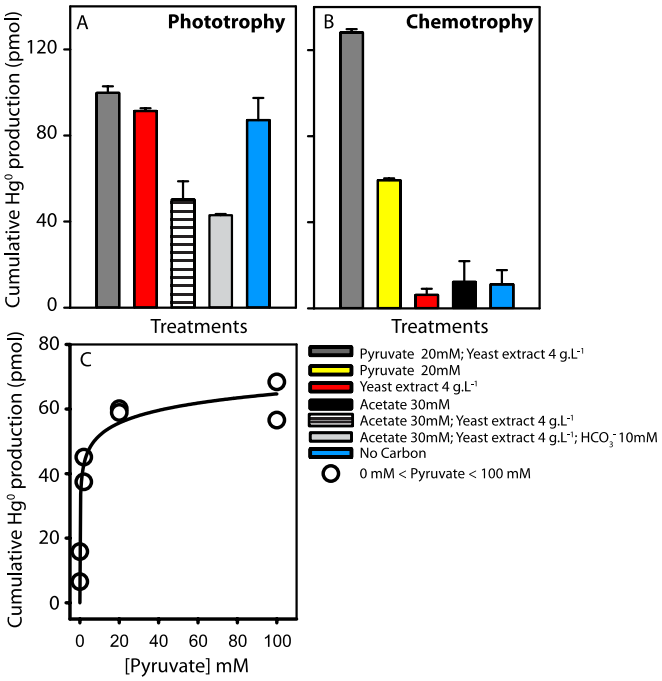

Figure 5.2 A and B: Cumulative Hg^0 production by *Heliobacterium modesticaldum* Ice1 grown phototrophically and chemotrophically with different carbon sources. Results shown here are the average of repeated experiments (n=2) and error bars represent the standard deviation. Note that the Acetate (30 mM) treatment was only performed for chemotrophically grown cells and the Acetate (30 mM) + YE (4 g L^{-1}) and Acetate (30 mM) + YE (4 g L^{-1}) + HCO_3^- (10 mM) were only performed for phototrophically grown cells. Hg was added to a final concentration of 250 pM. **C: Cumulative Hg^0 production for chemotrophically grown *Heliobacterium modesticaldum* Ice1 over a pyruvate gradient (0, 2, 20 and 100 mM)**. Cumulative Hg^0 production increased significantly ($p<0.05$) according to the non-linear function $y = 39.975 + 5.589 \ln(x)$ where $p = 0.0007$ and the adjusted $R^2 = 0.85$ for a data series of n = 8. Tests for constant variance and normal distribution were passed (significance threshold for rejection of null hypothesis $p = 0.05$) with $p = 0.50$ and $p = 0.53$, respectively. Hg was added to a final concentration of 250 pM.

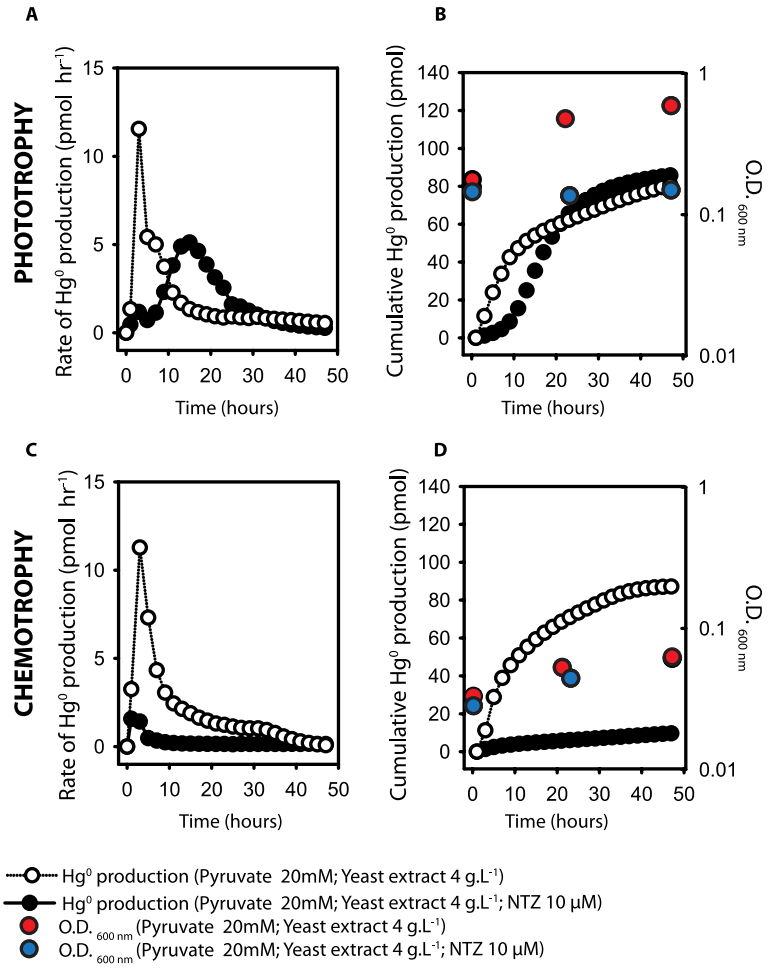

Figure 5.3: Hg^0 production by *Heliobacterium modesticaldum* Ice1 grown phototrophically and chemotrophically with or without nitazoxanide (NTZ). A, C Rate of Hg^0 production for live cells exposed to 10 µM NTZ and controls exposed 2.8 mM DMSO (NTZ solvent) under phototrophic (**A**) and chemotrophic (**C**) conditions. **B, D** Cumulative Hg^0 production and cell growth (as measured by O.D. 600 nm) for live cells, exposed to 10 µM NTZ and controls exposed to 2.8 mM DMSO (NTZ solvent) under phototrophic (**B**) and chemotrophic (**D**) conditions. Results are representative cases of replicated experiments (n=2). Each data point was recorded once per time step by the instrument as such no error bars were included. Hg was added to a final concentration of 250 pM.

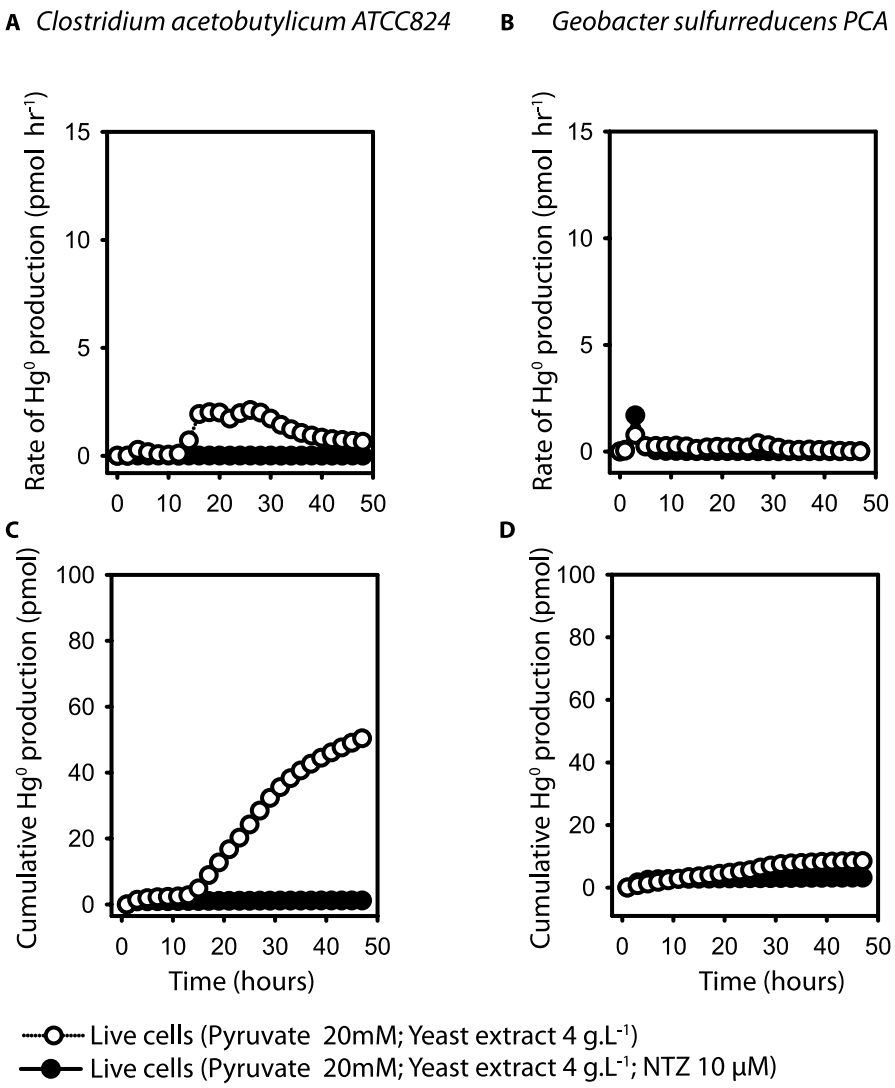

Figure 5.4: Hg^0 production by anaerobic bacteria grown chemotrophically in the presence of a pyruvate:ferredoxin oxidoreductase inhibitor (NTZ). A, B Rate of Hg^0 production for *Clostridium acetobutylicum* ATCC 824 (**A**), and *Geobacter sulfurreducens* PCA (**B**) cells exposed to 10 µM NTZ and controls exposed to 2.8 mM DMSO (NTZ solvent). **C, D** Cumulative Hg^0 production for *C. acetobutylicum* (**C**), and *G. sulfurreducens* (**D**) cells exposed to 10 µM NTZ and controls exposed to 2.8 mM DMSO (NTZ solvent). Hg was added to a final concentration of 250 pM.

5.10 TABLE

Table 5.1: Hg^0 production by anaerobic microbes and in anoxic environments

Model organism/system	[Hg] (pmol L^{-1})	Rate of Hg^0 production (pmol L^{-1} hr^{-1})	Relative Hg^0 production (%)	Ref.
Magnetotactic facultative anaerobic bacteria: *Magnetospirillum gryphiswaldense* MSR-1 and *Magnetospirillum magnetotacticum* MS-1	2.5×10^6	2.08×10^3 – 8.75×10^3	7.87 – 24.48[a]	44
Anaerobic *mer*-like reduction: *Geobacter bemidjiensis* Bem	2.5×10^4	1.19×10^3	38	45
Facultative anaerobe with *mer* operon: *Pseudomonas stutzeri* OX	2.00×10^6 – 2.50×10^7	1.83×10^4 – 9.50×10^5	30 - 80	41
Dissimilatory metal reducing bacteria: *Shewanella oneidensis* MR-1 and *Geobacter sulfurreducens* PCA	1.50×10^5 – 8.25×10^5	3.30×10^3 – 8.70×10^4	30 - 65	19
Dissimilatory metal reducing bacteria: *Geobacter sulfurreducens* PCA	2.50×10^4	3.75×10^3	60-64	20, 46
Dissimilatory metal reducing bacteria: *Geobacter sulfurreducens* PCA	250	1.92 – 4.06	7.11 – 11.65[b]	This study
Firmicute: *Clostridium acetobutylicum* ATCC 824	250	2.94 – 15.92	23.14 – 25.97[c]	This study
Heliobacteria: *Heliobacterium modesticaldum* Ice1	250	13.45 – 17.82	56.31 – 72.30	This study
Purple non-sulphur bacteria: *Rhodobacter capsulatus* SB1003, *Rhodobacter sphaeroides* 2.4.1, *Rhodopseudomonas palustris* TIE-1	250	0.30 – 3.30	4.97 – 20.28	21
In-situ metalimnetic incubation in a boreal lake	10	0.001	1	42
Photoreduction in surface lake waters	5.40 – 18.20	0.01 – 0.085	10 - 40	42
Hg^0 in Canadian Shield lake sediments	4.24×10^5 - 1.21×10^6	NA	7.40 - 28.4	15
Hg^0 in flooded soil core (A horizon)	2.00×10^5	120	54	14
Hg^0 in volcanic aquifer groundwater	190	NA	39.26	43
Abiotic reduction by DOM in anoxic conditions	1.00×10^4	1.75×10^3	70	18
Abiotic reduction by biogenic magnetite	2.50×10^5	1.07×10^4 – 8.09×10^4	8.55 – 64.7	44

[a] Experiments were carried out under microaerobic conditions; [b]11.65 pmol L^{-1} hr^{-1} is from experiments in *G. sulfurreducens*' optimal medium; [c]25.97 pmol L^{-1} hr^{-1} is from experiments in *C. acetobutylicum*'s optimal medium.

Chapter 6: Sulphur source controls mercury reduction in the anoxygenic phototroph *Heliobacillus mobilis*

Daniel S. Grégoire [a*], Noémie C. Lavoie [a*], Bejamin R. Stenzler [a] & Alexandre J. Poulain [a]

*contributed equally to this work

a- Biology Department, University of Ottawa, 30 Marie Curie, Ottawa, Ontario, K1N 6N5, Canada

Research highlights:

- Investigated whether sulphur source affects Hg reduction in *Heliobacillus mobilis*, an anoxygenic phototrophic Heliobacteria isolated from a rice padddy
- Tested whether oxidized sulphur sources, which require reducing power for assimilation, inhibited Hg reduction compared to more reduced sulphur sources
- Cells reduced 32% and 45% of Hg^{II} when provided with reduced thiosulphate and cysteine, respectively, and 11% when supplied with oxidized sulphate
- Cysteine concentration exerted dynamic control on Hg reduction in *H. mobilis*
- High levels of cysteine and organic matter catalyzed abiotic photoreduction
- Results suggest that competition for common pools of nutrients between anaerobic Hg reducers and Hg methylators may play an important role in determining Hg's fate in rice paddy systems

This chapter is being prepared for resubmission to Applied Environmental Microbiology

N.B. Supporting information for this chapter can be found in **Appendix C**

6.1 ABSTRACT

The consumption of rice has become a global food safety issue because rice paddies support the producton of high levels of the potent neurotoxin, methylmercury. The production of methylmercury is mediated by chemotrophic anaerobes that often rely on sulphate as a terminal electron acceptor. Sulphur can be a limiting nutrient in rice paddies and sulphate amendments are often used to stimulate crop production, potentially aggravating Hg accumulation issues. Hg redox cycling can affect Hg methylation by controlling the delivery of inorganic Hg substrates to methylators in anoxic habitats. Whereas sulphur is recognized as a key nutrient controlling methlmercury production, the control that sulphur has on other microbially-mediated mercury transformations remains poorly understood. In this study we use *Heliobacillus mobilis* Romero/Guest 6, a mesophilic anoxygenic phototrophic representative from the Heliobacteriacea family originally isolated from a rice paddy in Thailand, to explore the potential coupling points between sulphur assimilation and anaerobic Hg reduction. By comparing Hg^0 production over a sulphur redox gradient, we demonstrate that phototrophic Hg^{II} reduction is favoured in the presence of reduced sulphur sources such as thiosulphate and cysteine. We show that cysteine exerts dynamic controls on Hg bioavailability by affecting both Hg uptake and photoreduction. The findings from this study frame Heliobacteria as key players in Hg cycling in paddy soils and provide the basis for exploring management strategies to mitigate Hg accumulation in rice.

6.2 INTRODUCTION

Mercury (Hg) is a global contaminant that readily bioaccumulates in plant [1] and animal [2] tissue as neurotoxic monomethylmercury (MeHg). Recently, the consumption of contaminated rice has been identified as a route for Hg exposure in people [1, 3]. Rice paddies are frequently flooded and rich with nutrients that stimulate the metabolism of anaerobic microbes responsible for Hg methylation [4]. With rice being a staple food crop for over half of the world's population, MeHg accumulation in rice is becoming a global food safety issue [3].

In flooded anoxic rice paddies, Hg redox cycling can play a key role in determining the inorganic Hg substrate available to methylators. Hg^{II} reduction can lead to Hg^0 evasion from the paddy soils [5-7] or directly affect Hg's bioavailability to methylators [8, 9]. Hg^{II} reduction can occur through abiotic reactions with dissolved organic matter [10] and iron-bearing minerals [11, 12], but anaerobic microbes can also participate directly in Hg reduction [13-20]. Microbe mediated Hg reduction pathways that rely on dedicated detoxification strategies, such as those encoded by the *mer* operon, are largely absent in anaerobes [21]. Rather, anaerobic Hg^{II} reduction seems to occur as a cometabolic process during phototrophic [19, 20] and chemotrophic growth [13, 14, 17]. In line with this observation, core components of anaerobic respiration [14], fermentation [19] and anoxygenic photosynthesis [20] have shown to be essential to different anaerobic Hg^{II} reduction pathways. Despite metabolic machinery central to anaerobic metabolism driving Hg^{II} reduction, the contributions of anaerobes to Hg reduction in anoxic habitats remain overlooked.

Much of the evidence published to date suggests that Hg methylation is a cometabolic process linked to one-carbon compound metabolism [22, 23] in multiple clades of anaerobes [24-26]. In support of this, environmental variables such as carbon source composition [27, 28] and the availability of electron acceptors [29-31] have been shown to control anaerobic Hg methylation. Similar environmental variables likely control other Hg transformations that can potentially compete with Hg methylation such as anaerobic Hg reduction. Currently, the role that common pools of nutrients (e.g., C, N or S) play in controlling different cometabolic Hg transformations is rarely discussed. This is an important knowledge gap to address because anaerobic Hg^{II} reducers and Hg methylators occupy the same niche in the environment [30] and likely compete for Hg substrates and resources supporting anaerobic metabolisms.

We aim to address this knowledge gap by investigating the controls that sulphur exerts on anaerobic Hg^{II} reduction. In rice paddies, sulphur can become a limiting nutrient and sulphate amendments are employed to maintain agricultural productivity [32]. Such amendments would supply sulphate-reducing bacteria (SRB) that often dominate Hg methylation communities [33-35] with ample nutrients for anaerobic respiration, which can subsequently increase MeHg production [29, 36]. Reduced sulphur-bearing molecules such as sulphide [37, 38] and cysteine [39, 40], resulting from sulphur metabolism, can also act as ligands affecting Hg bioavailability to Hg methylators. While the role of sulphur in controlling Hg methylation has been well characterized, this is not the case for microbe mediated Hg reduction. To the best of our knowledge, there exists only one study investigating *mer*-mediated Hg^{II} reduction in aerobic sulphur oxidizing bacteria [41] and the influence of sulphur on anaerobic Hg reduction has yet to be explored.

In this study we use anoxygenic photosynthesis as the basis to explore coupling points between sulphur metabolism and anaerobic Hg^{II} reduction. Anoxygenic phototrophs such as purple and green sulphur bacteria play key roles in the sulphur cycle of anoxic habitats via dissimilatory processes coupled to autotrophic growth [42]. Similarly, a wide diversity of anoxygenic phototrophs including purple non-sulphur bacteria (PNSB) and Heliobacteria can influence sulphur cycling via assimilatory pathways [43]. When considered alongside the recent discovery that PNSB [20] and Heliobacteria can reduce Hg^{II} [19], anoxygenic phototrophs are poised to control nutrient and Hg cycling in photic anoxic habitats such as shallow paddy systems.

Our recent work with the model strain from the Heliobacteria family, *Heliobacterium modesticaldum* Ice1, showed that this strain was among the highest anaerobic Hg^{II} reducers on record [19]. Although *H. modesticaldum* is a thermophile [44], this observation is noteworthy in the context of rice paddies because many Heliobacteria isolates originate from such environments [45, 46]. In this study, we chose to work with the mesophile *Heliobacillus mobilis* Romero/Guest 6, a Heliobacteria isolate originally obtained from a rice paddy in Thailand [47], to evaluate the potential for Heliobacteria to alter Hg's fate in rice paddies. *H. mobilis* can grow on a variety of oxidized and reduced sulphur sources (from sulphate to cysteine) [47] making it an ideal system in which to explore the role of sulphur acquisition during anaerobic Hg redox cycling.

We hypothesize that sulphur assimilation and Hg reduction compete for reducing power in *H. mobilis* cells during phototrophic metabolism. Currently, there is no evidence of dissimilatory sulphur metabolism in *H. modesticaldum* (the only sequenced Heliobacteria genome available) or *H. mobilis* [47]. As such, we base our predictions on

assimilatory pathways. We predict that assimilating oxidized sulphur (e.g. sulphate) will require more reducing power that would otherwise be available for Hg^{II} reduction as compared to more reduced sulphur sources that are less costly to assimilate into biomass (e.g. thiosulphate, methionine and cysteine). We recognize that reduced sulphur compounds such as cysteine are strong ligands for Hg [39, 40] and have controlled for potential differences in Hg-sulphur complex bioavailability as part of our study.

In this work we demonstrate that phototrophic Hg^{II} reduction by *H. mobilis* is favoured in the presence of thiosulphate and low levels of cysteine, and minimal in the presence of sulphate. We show that cysteine exerts dynamic controls on anaerobic Hg^{II} reduction and explore new means by which cysteine can mediate abiotic Hg^{II} photoreduction. Finally, we discuss how the coupling of sulphur metabolism and Hg redox cycling can affect Hg's fate in anoxic habitats such as rice paddies.

6.3 MATERIALS AND METHODS

6.3.1 Anaerobic bioreporter assay and Hg speciation models

Anaerobic bioassays were performed according to the methods outlined in previous work which we will summarize here [48]. Two *Escherichia coli* biosensors were used (both from New England Biolabs); one, a Hg inducible biosensor (*E. coli* NEB5α harboring the pUC57merR-Pp plasmid) where the production of a flavin based fluorescent protein (FbFP) was under the control of *merR* (the transcription regulator of the *mer* operon [49]). The other was a constitutive biosensor (*E. coli* NEB5α harbouring the pUC19AH206-Pp plasmid), which expressed the FbFP irrespective of the presence of Hg. Experiments with both biosensors were performed in parallel to control for the effect of the conditions

tested on cell health. We observed that constitutive fluorescence production did not significantly decrease under any of the conditions tested compared to controls in minimal medium indicating that bioreporter cultures were healthy in all experiments (**Fig C1**).

Cell cultures were plated from -80˚C cryostock onto Lysogeny broth (LB) agar plates, selected for with ampicillin (210 µg mL^{-1}) and grown at 37˚C irrespective of changes in medium. A single colony was selected from the plate and grown overnight in liquid LB. Following this, cells were transferred as a 20% inoculum (v/v) to the anaerobic growth medium previously described [48] and grown for 6 to 7 hours. Cells were then transferred to fresh growth medium as 1% inoculum (v/v), grown overnight, inoculated into fresh medium as a 20% inoculum (v/v) and grown until they reached an O.D. 600 nm of 0.6. Cells were then resuspended twice in anaerobic exposure medium (BMAA) [48] to create the cell stock used in the biosensor assay.

For the biosensor assay, all manipulations were conducted in a Coy anaerobic chamber (97% $N_{2\,(g)}$ and 3% $H_{2\,(g)}$). All biosensor treatments and equilibrations with Hg were performed in 7 mL Teflon vials in either BMAA or DSMZ medium # 370 amended with 20 mM pyruvate (see ***Heliobacillus mobilis* culture conditions** section below). Hg was diluted from an 8 µM stock solution of $HgSO_4$ in 0.2 M H_2SO_4 to create a 100 nM working solution in BMAA in a 7 mL Teflon vial that was subsequently used to expose bioreporter cells to a final concentration of 5 nM Hg. Nitrate was added as $NaNO_3$ to final concentration of 200 µM in each final treatment. All treatments were equilibrated in the final solution for 1h, after which cells were added as a 1/20 dilution from the stock mentioned previously. Each treatment was then transferred to a 96 well non-binding surface black plate in analytical triplicates and placed in a Synergy HTX plate reader.

Fluorescence was measured using an excitation filter of 440/40 and emission filter of 500/27 at 37˚C for 20 hours. Each treatment of the Hg inducible biosensor was blanked to the same treatment without Hg and each treatment of the constitutive biosensor was blanked to the same treatment without NO_3^-. Fluorescence was quantified as the peak fluorescence emitted by the *E. coli* once 200 µM NO_3^- was consumed (2 to 3h). Fluorescence for each treatment was normalized to the fluorescence of the 5 nM Hg treatment to give % bioavailability and averaged over 3 biological replicates.

As part of the bioreporter assays, we modeled the speciation of Hg in BMAA across all sulphur treatments. We were unable to do so for the DSMZ medium #370 due to the undefined nature of the yeast extract included in the medium. All modeling for Hg chemical speciation was performed using PHREEQC v3.4.0. The distribution of predicted Hg species for each sulphur treatment and thermodynamic constants employed are provided in **Appendix C** in **Table C1** and **Table C2**.

6.3.2 *Heliobacillus mobilis* cell culture growth conditions

All growth conditions referred to in this section are summarized in **Table C3**. For bioreactor experiments we used the strain *Heliobacillus mobilis* Romero/Guest 6 from the DSMZ culture collection (strain number DSM-6151). Cell cultures were handled under anaerobic conditions in a Coy anaerobic glove box (atmosphere 97% $N_{2\,(g)}$ and 3% $H_{2\,(g)}$) or by using sterile anaerobic bench top techniques where all equipment was sparged with 100% $N_{2\,(g)}$ prior to use. For all growth assays and bioreactor experiments, new cell cultures were revived in the anaerobic glovebox from cryostocks kept at -80˚C by scraping frozen culture with a sterile pipette tip and discarding it into a Balch tube

containing growth medium #370 from DSMZ amended with 20 mM pyruvate to improve cell growth. Cells were revived in the presence of the sulphur source to be tested in growth assays and bioreactor experiments. Note that total sulphur content of the medium was normalized to 4 mM as per the culture collections recommendation except in experiments testing for the effect of cysteine concentration. Balch tubes were then crimped shut and the headspace was replaced with 100% $N_{2\ (g)}$. Cryostock revival cultures were incubated at 37°C with an incandescent light source providing photosynthetically active radiation (PAR) at an intensity of 80 µmol photon m^{-2} s^{-1} with a peak irradiance in the near-red red spectrum (600 to 700 nm) until cells reached mid-exponential stage. Additional growth assays were also performed at a visible light intensity of 20 µmol photon $m^{-2}s^{-1}$ using a light source with the same emission spectrum to characterize the impacts of light intensity and bubbling in the bioreactor on phototrophic growth. Cultures were then used to start new cultures with a 1% (v/v) inoculum into new Balch tubes containing 10 mL of the desired growth medium. For bioreactor experiments, cells were harvested again after reaching mid-exponential to start new cultures with a 1% inoculum in serum bottles containing 75 mL of the desired growth medium. Upon reaching mid to late exponential phase, these cultures were used as a 10% (v/v) inoculum in bioreactor experiments.

6.3.3 PCR for the *merA* gene in *Heliobacillus mobilis*

Although we suspected that *H. mobilis* could carry out Hg^{II} reduction via similar means as *H. modesticaldum,* we verified whether *H. mobilis* harboured the *merA* gene encoding for a dedicated mercuric reductase. There is currently no sequenced genome available for *H. mobilis* as such the presence of *merA* was evaluated with PCR. DNA was extracted from cultures of *H. mobilis* using the QIAGEN PowerSoil® DNA Isolation Kit according to the manufacturer's instructions (QIAGEN, Toronto, CA). The *merA* gene was amplified by PCR using the Nsf primer set: Forward – ATC CGC AAG TNG CVA CBG TNG G, Reverse – CGC YGC RAG CTT YAA YCY YTC RRC CAT [50]. The PCR reaction was performed using the EconoTaq® PLUS master mix according to the manufacturer's instructions (Lucigen, Middleton, WI). The Nsf PCR reactions consisted of an initial denaturing step at 95°C for 5 min; followed by 35 cycles with three steps: 95°C for 1 min, 61°C for 30s, and 72°C for 30s. Final extension was at 72°C for 10 min. Gel electrophoresis with TAE (1X) was performed to verify for the presence of *merA* (**Fig C2**). PCR reactions were performed using the Eppendorf MasterCycler ProS (Eppendorf Canada, Mississauga, ON, Canada). We acknowledge these primers may not capture the full diversity of *merA* but specific primers for anaerobes and phototrophs have yet to be designed due to the lack of *mer*-based determinants in anaerobes and phototrophs. Furthermore, we note that PCR is not a definitive means of demonstrating the absence of a gene, however this method was the best option available to us at the time of this study. Currently, we are working towards obtaining a sequenced and annotated genome for *H. mobilis*.

6.3.4 Bioreactor setup and sampling for cell density

All conditions tested in the bioreactor are summarized in **Table C3**. The bioreactor subsampling methodology is identical to that used in previous work [19, 20]. All bioreactor experiments were carried out at 37°C. Light was supplied using a 200 W incandescent light bulb with a visible light intensity maintained at 20 µmol photon $m^{-2}s^{-1}$ by means of multiple layers of dark screens. Peak irradiance for this light source occurred in the near-red to red spectrum (600 to 700 nm). Total sulphur content in the bioreactor was normalized to 4 mM except for experiments testing the effect of cysteine concentration. For experiments where 250 pM of cysteine was added to the bioreactor we could not rule out the effect of cysteine carry over from the initial inoculum as such we refer to this treatment as "trace cysteine" throughout the **Results and Discussion** section. All live cell bioreactor treatments were performed in triplicate and abiotic controls were performed in duplicate.

6.3.5 Statistical analyses

Two-way and one-way ANOVA analyses were used to test for the effect of sulphur source and cysteine concentration on Hg bioavailability and cumulative Hg^0 production. In the event that the assumptions of the normal distribution of residuals and constant variance were not fulfilled, non-parametric rank sum tests were employed. Treatments where a significant difference was observed were identified using a Tukey HSD *post hoc* test with the significance threshold set to $p<0.05$. All statistical analyses were performed in R v3.1.2 [51].

6.4 RESULTS & DISCUSSION

6.4.1 Cysteine exerts dynamic controls on Hg bioavailability

Our first objective was to control for the bioavailability of the Hg-sulphur complexes that were predicted to form in the presence of sulphate, thiosulphate, methionine and cysteine (**Table C1**). To achieve this, we measured and compared Hg bioavailability in the presence of these sulphur sources using an anaerobic Hg biosensor (constitutive and inducible strains) exposed to Hg in minimal BMAA exposure medium (**Materials and Methods** and **Table C1**). We were unable to model Hg speciation in complex DSMZ medium #370 due to the undefined nature of the yeast extract employed and this is why minimal medium data are solely presented (**Table C1**).

Both sulphur source and medium had a significant effect on Hg bioavailability ($p < 0.001$ for sulphur source and medium according to a two-way non-parametric rank sum test). Inducible biosensor cells exposed to Hg in the bioreactor medium showed higher overall Hg uptake compared to cells exposed to Hg in the minimal medium (average difference compared to minimal medium = 33.70 ± 19.73%) (**Fig 6.1A, C**). Similarly, constitutive bioreporter cells grown in the bioreactor medium emitted as much as three times higher fluorescence than cells in the minimal medium (**Fig C1**). These results suggest that the increased bioavailability of Hg in the bioreactor could be associated with the presence of higher nutrient concentrations supporting healthier cell populations. It is also possible that ligands facilitating Hg uptake present in the yeast extract component of the bioreactor medium were absent in the minimal medium [8, 52].

When isolating the effect of sulphur in the media tested, sulphur source maintained a significant effect on Hg bioavailability. Inducible bioreporter cells supplied with cysteine saw a strong decrease in Hg bioavailability ($p < 0.001$ for minimal medium and bioreactor medium according to separate one-way ANOVAs). Whereas total sulphur content was normalized to a final concentration of 4 mM in all experiments, as per the culture collection recommendations, and to ensure that all treatments were comparable, the results from these experiments suggested that we had to alter cysteine concentrations to maintain comparable Hg bioavailability across all treatments (**Fig 6.1**). To do so, we performed additional experiments where the Hg:cysteine ratio was increased from 1:1.25 x 10^6 to 1:2000 ([cysteine] = 10 μM) and 1:1000 ([cysteine] = 5 μM) (**Table C1**). Increasing the Hg:cysteine ratio significantly increased Hg bioavailability, which was comparable to the no sulphur control ($p < 0.001$ according to a one-way non-parametric rank sum test) (**Fig 6.1B**). At high Hg to cysteine ratios (e.g., [cysteine] = 5 and 10 μM), 62.6 to 74.6 % of Hg was predicted to exist as $Hg(Cys)_2H_2$ and 18.0 to 30.4 % was also predicted to form $Hg(Cys)H^+$ (**Table C1**). This is in contrast to the lower Hg to cysteine ratio treatment ([cysteine] = 4mM) where 90.7 % of Hg is predicted to exist as $Hg(Cys)_2H_2$ (**Table C1**). Thus, our results suggest that Hg uptake is favoured under conditions that support the formation of both charged $Hg(Cys)H^+$ and neutral $Hg(Cys)_2H_2$ species.

Ultimately, we were able to use the bioreporter to design conditions under which Hg bioavailability was comparable in the presence of sulphate, thiosulphate, methionine and low levels of cysteine despite the predicted differences in Hg speciation. By controlling for the bioavailability of different Hg-sulphur complexes we could reasonably

compare Hg^0 production over a range of redox states for sulphur [sulphate (S redox state +6), thiosulphate (S redox states +1, -5 [53]), methionine (S redox state -2) and cysteine (S redox state -2)] in subsequent bioreactor experiments.

6.4.2 Growth is not required for phototrophic Hg reduction by *H. mobilis*

During our preliminary tests to optimize bioreactor assay conditions, we discovered that the continuous sparging of the bioreactor required for volatile Hg^0 analysis affected cell growth. Although the bioreactor experiments showed that *H. mobilis* was capable of Hg^{II} reduction when supplied with conditions known to support photoheterotrophic growth [47] (**Fig 6.2**), cells were unable to grow in the bioreactor (**Table C3**). Growth inhibition was not linked to the sulphur sources provided because cells cultured in tubes demonstrated nearly identical growth regardless of the treatment in question (**Fig 6.3A**). Furthermore, we ruled out that low light intensity was inhibiting growth because cells were able to grow in closed tubes and a closed bioreactor (i.e., not connected to the continuous Hg analyzer) supplied with identical incubation conditions as other bioreactor experiments (**Fig 6.3B, C**). We suspect that the continuous bubbling required to measure Hg^0 was inhibiting growth due to the removal of gaseous CO_2. Inorganic carbon (e.g. CO_2 or HCO_3^-) is an essential substrate used in anaplerotic reactions required for biosynthesis in *H. modesticaldum* [54] and possibly other Heliobacteria (although this has yet to be confirmed). By removing endogenous CO_2 produced following organic carbon oxidation, *H. mobilis* would have been deprived of an essential nutrient required to replenish metabolic intermediates essential for generating biomass [47, 55].

We chose not to add HCO_3^- as an exogenous source of inorganic carbon. Indeed, photoheterotrophs can use inorganic carbon not only in anaplerotic reactions but also as an electron sink to maintain redox homeostasis [55, 56]. It is possible that the presence of HCO_3^- would have introduced a pathway that could compete for reducing power inside of the cell and confound our ability to test our hypothesis. While we recognize these conditions may have limited the ability of cells to assimilate the full amount of sulphur provided in the bioreactor, the fact that cells did not grow allowed us to tightly control the Hg to cell to sulphur ratios in all experiments. Although cells did not grow, as it is often the case in the environment, they were metabolically active as shown by the high levels of Hg^0 produced in the presence of live cells and the negligible amount of Hg^0 produced in the presence of heat-killed cells (**Fig C3**). We are in the midst of completing experiments to examine the influence of inorganic carbon assimilation on Hg^{II} reduction in *H. mobilis* however we still deem it valuable to discuss the effect of sulphur source on Hg^{II} reduction during anoxygenic phototrophic metabolism in light of our current results.

6.4.3 Reduced sulphur sources favour Hg^{II} reduction during anoxygenic photosynthesis

When comparing abiotic and biotic Hg^0 production, we observed that sulphur source had a significant effect on cumulative Hg^0 production ($p < 0.001$ according to a one-way ANOVA). Average Hg^0 production in the presence of live cells was highest when cells were provided with trace levels of cysteine (56.60 ± 3.77 pmol), followed by thiosulphate (40.62 ± 11.87 pmol), methionine (27.06 ± 13.72 pmol), sulphate (14.23 ± 11.30 pmol), and the 4 mM cysteine treatment (8.79 ± 5.00 pmol). Hg^0 production in the presence of

heat-killed cells and in the absence of cells was negligible except for the mM cysteine treatment (38.04 ± 14.50 pmol vs < 5 pmol for all other treatments) (**Fig 6.2** and **Fig C3**). The potential pathways contributing to the abiotic Hg^0 production observed in the presence of mM cysteine are discussed in the following section.

The trends observed for biotic Hg^0 production supported our hypothesis. The most oxidized sulphur source, sulphate, led to lower Hg^0 production compared to the thiosulphate and trace cysteine treatments, which provided cells with relatively more reduced sulphur [e.g. S redox states for individual S atoms in thiosulphate are -1 and +5 [53] and S redox state in cysteine is -2 vs. +6 in sulphate] (**Fig 6.2**). Our results also suggest that Hg^{II} reduction is inhibited when Hg bioavailability is limited (**Fig 6.1B** and **Fig 6.2**), supporting the presence of an intracellular Hg^{II} reduction pathway in *H. mobilis* as previously suggested for *H. modesticaldum* [19].

The only results that did not support our hypothesis were those of the methionine treatment where cells showed intermediate levels of Hg^0 production (**Fig 6.2**). Based on our previous bioreporter results, we can rule out that the lower Hg^0 production in the presence of methionine was associated with low Hg bioavailability (**Fig 6.1A**). Instead, we suspect that metabolic pathways that affect cell redox homeostasis and were uncontrolled for in our experimental design contributed to the results observed (summarized in **Fig C4**). Based on the genome annotation of *H. modesticaldum* and studies on the physiology of closely related Clostridiales [57], the reducing power requirements for the assimilation of inorganic sulphur sources into sulphide and cysteine is clear (**Fig C4**). The coupling between redox homeostasis and methionine metabolism is arguably more complex [57].

At this point, we are unable to better characterize the role of methionine metabolism during Hg^{II} reduction in *H. mobilis*. To the best of our knowledge, there is no sequenced genome for *H. mobilis* or genetic tools yet available to work with Heliobacteria. We are currently working on sequencing and annotating the genome for *H. mobilis*. Once we have this information in hand, we can develop genetic tools and potentially use quantitative molecular techniques such as real time PCR to address some of the questions mentioned above. Furthermore, we are also limited in our ability to directly measure the concentrations of reduced redox cofactors because we were unable to sample enough biomass from the bioreactor to extract reduced redox cofactors such as $NAD(P)H/NAD(P)^{+}$. Despite these limitations, our findings support that sulphur can affect Hg^{II} reduction during anoxygenic photosynthesis and highlight the interplay between sulphur assimilation and cometabolic Hg^{II} reduction.

The scenarios mentioned above underscore the challenges associated with identifying metabolic coupling points between cellular redox metabolism and Hg reduction. Despite these limitations, our study suggests that phototrophic Hg reduction is sensitive to the availability of reducing power inside the cell. Even when supplying cells with conditions where µM amounts of reduced redox cofactors are likely being generated thereby providing ample electron donors to reduce pM levels of Hg^{II}, we are still able to detect differences in Hg reduction that vary according to sulphur source redox state. These findings show that not all the Hg supplied is available for reduction and that perhaps not all the reducing power generated by the cell is either. Instead, it seems there exist discrete pools of reduced redox cofactors that fuel Hg reduction during anoxygenic photosynthesis. The localization of these pools of reducing power within the cell and the

nature of the reducing equivalents involved remain unknown and merit further investigation.

6.4.4 Cysteine and organic carbon catalyze Hg photoreduction at low light intensities

As previously shown, high levels of Hg^0 were produced under low visible light intensity in the presence of mM levels of cysteine and the absence of cells (**Fig 6.2**). Interestingly, under the same conditions, the mere addition of cells to the reactor inhibited Hg^0 production (**Fig 6.2**). While there is precedence for Hg photoreduction in the presence of cysteine and UV light [58], to the best of our knowledge there is no evidence of cysteine catalyzing Hg photoreduction at the low visible light intensities employed in our experiments (20 μmol photon m^{-2} s^{-1}). To further explore the potential mechanisms supporting abiotic Hg^0 production, we performed additional experiments to test for the role of light and organic carbon originating from yeast extracts (YE). To test for the role of light, we repeated experiments in the dark and with formaldehyde-killed cells to create cell-induced shading in the reactor (**Table C3**). To test for the role of organic carbon, we irradiated the bioreactor and removed all sources of organic carbon (i.e., YE) except for cysteine (**Table C3**).

All additional experimental treatments resulted in a strong inhibition of abiotic Hg^0 photoproduction that was comparable to the Hg^0 production observed in abiotic controls for sulphate, thiosulphate and methionine (**Fig 6.2** and **Fig C5**). These results suggest that abiotic Hg^{II} photoreduction relies on the presence of high levels of cysteine and components of YE. Here, we can effectively rule out that Hg^{II} was photoreduced

solely due to components of YE because all other abiotic sulphur treatments were supplied with the same amount of YE. By omitting all organic carbon except cysteine, we showed that the interaction between cysteine and organic compounds from YE is essential for Hg photoreduction. We suspect that mM levels of cysteine keep Hg from sorbing to cells, to the walls of the reactor or binding to less reactive sites on components of YE, thus facilitating Hg reduction. We recognize that the undefined nature of YE makes it difficult to provide a detailed description of the pathway supporting abiotic Hg^{II} photoreduction under the conditions tested and we are currently developing experiments to address this.

6.4.5 Sulphur cycling and cometabolic Hg transformations in the environment

In this work we show that *H. mobilis* can reduce Hg^{II} under conditions supporting phototrophic metabolism. We have demonstrated that after controlling for Hg bioavailability, phototrophic Hg^{II} reduction is favoured in the presence of reduced sulphur sources. Our study highlights the importance of sulphur as a nutrient driving anaerobic Hg^{II} reduction and provides the basis for exploring potential coupling points between sulphur assimilation, anaerobic Hg reduction and Hg methylation in anoxic habitats.

As previously mentioned, sulphur can be a limiting nutrient in rice paddies requiring rice growers to use sulphate amendments [32] that can potentially increase Hg methylation [59]. Our study has provided us with insights into how anaerobic Hg reducers could potentially affect Hg methylation under such conditions. Anaerobic Hg reducers (AMR) can potentially outcompete Hg methylators for nutrients and ligands that increase

Hg uptake [17, 60] or limit the availability of electron acceptors utilized by Hg methylating SRB. In the latter case, AMR could directly affect thiosulphate availability to SRB [61, 62] or decrease the delivery of sulphate to anoxic environments by removing the substrate for thiosulphate oxidation in oxic/anoxic transition zones [63, 64]. By limiting sulphatoreduction, AMRs may also control the bioavailability of Hg by limiting the formation of HgS species formed in the presence of sulphide [37, 65]. In all these scenarios, AMRs can limit Hg methylation by favouring Hg^0 evasion from paddy soil and overlaying water. At this point, we can only speculate as to how AMR affect Hg methylation in paddy systems. To test for this, we are in the process of developing mesocosm and field experiments.

Although our study was prompted by increased concerns surrounding MeHg accumulation in rice paddies, the scenarios mentioned above could also apply to other habitats that support steep redox gradients, competition for nutrients and cometabolic Hg transformations regardless of the presence of light. Indeed, whereas this study focused on phototrophic Hg reduction, Heliobacteria can grow fermentatively in the dark, along with other fermenters of the Clostridiales family. Our previous results with *H. modesticaldum* showed that Hg^0 production also occurs during fermentative growth in the dark [19]. Nutrient cycling and cometabolic Hg transformations stand to be closely linked in Hg methylation hotspots such as periphytic microbial mats [66], aquatic sediments [67, 68] and waterlogged soils [69]. While our study makes a case for sulphur cycling as a coupling point for competing cometabolic Hg transformations, other nutrients such as iron [13, 68, 70, 71] and organic carbon [19, 20, 27], which are known to control Hg methylation and Hg reduction, have the potential to fulfill a similar role. Curiously, the coupling between other macronutrients under strong microbial control such as nitrogen and Hg cycling

remain relatively unexplored despite the importance of nitrogen cycling in aquatic and terrestrial ecosystems. Given that the majority of cometabolic Hg transformation pathways outlined to date rely on the use of central metabolic machinery, it is possible that the cycling of a variety of nutrients essential to microbial life play a role in Hg cycling.

By characterizing the environmental variables that drive different cometabolic Hg transformations in future work, we hope to better predict how nutrient availability and microbial activity will affect Hg mobility and toxicity in the environment. This knowledge could be used to hone predictive models and develop tractable Hg pollution management strategies that rely on supplying environmental conditions that stimulate favourable cometabolic Hg transformations (e.g. reduction or sequestration) rather than unfavourable ones (e.g. methylation). Such strategies could take the form of targeted nutrient amendments that can be applied *in situ* to limit the availability of the inorganic Hg and nutritional substrates contributing to the accumulation of neurotoxic Hg in the environment.

6.5 FUNDING INFORMATION

Our work was funded by NSERC Discovery and Accelerator grants, CFI funding to AJP and NSERC graduate scholarship to DSG.

6.6 ACKNOWLEDGMENTS

We would like to thank Galen Guo for performing the PCR testing for the presence of the *merA* gene in *H. mobilis*.

6.7 AUTHOR CONTRIBUTIONS

DSG, NCL, BRS and AJP designed the experiments, DSG, NCL and BRS carried them out, DG, NCL and BRS performed data analyses; DSG, NCL and AJP wrote the manuscript.

6.8 REFERENCES

1. Zhang, H.; Feng, X.; Larssen, T.; Qiu, G.; Vogt, R. D., In inland China, rice, rather than fish, is the major pathway for methylmercury exposure. *Environmental Health Perspectives* **2010,** *118*, 1183-1188.

2. Sunderland, E. M., Mercury exposure from domestic and imported estuarine and marine fish in the U.S. seafood market. *Environmental Health Perspectives* **2007,** *115*, (2), 235-242.

3. Rothenberg, S. E.; Windham-Myers, L.; Creswell, J. E., Rice methylmercury exposure and mitigation: A comprehensive review. *Environmental Research* **2014,** *133*, 407-423.

4. Rothenberg, S. E.; Feng, X., Mercury cycling in a flooded rice paddy. *Journal of Geophysical Research: Biogeosciences* **2012,** *117*, 1-16.

5. Ao, M.; Meng, B.; Sapkota, A.; Wu, Y. G.; Qian, X. L.; Qiu, G. L.; Zhong, S. Q.; Shang, L. H., The influence of atmospheric Hg on Hg contaminations in rice and paddy soil in the Xunyang Hg mining district, China. *Acta Geochimica* **2017,** *36*, (2), 181-189.

6. Kim, K. H.; Kim, M. Y.; Kim, J.; Lee, G., Effects of changes in environmental conditions on atmospheric mercury exchange: Comparative analysis from a rice paddy field during the two spring periods of 2001 and 2002. *Journal of Geophysical Research-Atmospheres* **2003,** *108*, (D19).

7. Wang, X.; Lin, C. J.; Yuan, W.; Sommar, J.; Zhu, W.; Feng, X. B., Emission-dominated gas exchange of elemental mercury vapor over natural surfaces in China. *Atmospheric Chemistry and Physics* **2016,** *16*, (17), 11125-11143.

8. Chiasson-Gould, S. A.; Blais, J. M.; Poulain, A. J., Dissolved organic matter kinetically controls mercury bioavailability to bacteria. *Environmental Science & Technology* **2014,** *48*, (6), 3153-3161.

9. Colombo, M. J.; Ha, J.; Reinfelder, J. R.; Barkay, T.; Yee, N., Oxidation of Hg(0) to Hg(II) by diverse anaerobic bacteria. *Chemical Geology* **2014,** *363*, 334-340.

10. Gu, B.; Bian, Y.; Miller, C. L.; Dong, W.; Jiang, X.; Liang, L., Mercury reduction and complexation by natural organic matter in anoxic environments. *Proceedings of the National Academy of Sciences of the United States of America* **2011,** *108*, (4), 1479-1483.

11. Bone, S. E.; Bargar, J. R.; Sposito, G., Mackinawite (FeS) reduces mercury(II) under sulfidic conditions. *Environmental Science & Technology* **2014,** *48*, (18), 10681-10689.

12. Wiatrowski, H. A.; Das, S.; Kukkadapu, R.; Ilton, E. S.; Barkay, T.; Yee, N., Reduction of Hg(II) to Hg(0) by magnetite. *Environmental Science and Technology* **2009,** *43*, (14), 5307-5313.

13. Wiatrowski, H. A.; Ward, P. M.; Barkay, T., Novel reduction of mercury(II) by mercury-sensitive dissimilatory metal reducing bacteria. *Environmental Science and Technology* **2006,** *40*, (21), 6690-6696.

14. Lin, H.; Morrell-Falvey, J. L.; Rao, B.; Liang, L.; Gu, B., Coupled mercury-cell sorption, reduction, and oxidation on methylmercury production by *Geobacter sulfurreducens* PCA. *Environmental Science and Technology* **2014,** *48*, (20), 11969-11976.

15. Schaefer, J. K.; Letowski, J.; Barkay, T., *mer*-mediated resistance and volatilization of Hg(II) under anaerobic conditions. *Geomicrobiology Journal* **2002,** *19*, (1), 87-102.

16. Liu, S.; Wiatrowski, H. A., Reduction of Hg(II) to Hg(0) by biogenic magnetite from two magnetotactic bacteria. *Geomicrobiology Journal* **2018,** *35*, (3), 198-208.

17. Lu, X.; Liu, Y.; Johs, A.; Zhao, L.; Wang, T.; Yang, Z.; Lin, H.; Elias, D. A.; Pierce, E. M.; Liang, L.; Barkay, T.; Gu, B., Anaerobic mercury methylation and demethylation by *Geobacter bemidjiensis* Bem. *Environmental Science and Technology* **2016,** *50*, (8), 4366-4373.

18. Zhao, L. D.; Chen, H. M.; Lu, X.; Lin, H.; Christensen, G. K.; Pierce, E. M.; Gu, B. H., Contrasting effects of dissolved organic matter on mercury methylation by *Geobacter sulfurreducens* PCA and *Desulfovibrio desulfuricans* ND132. *Environmental Science & Technology* **2017,** *51*, (18), 10468-10475.

19. Grégoire, D. S.; Lavoie, N. C.; Poulain, A. J., Heliobacteria reveal fermentation as a key pathway for mercury reduction in anoxic environments. *Environmental Science and Technology* **2018,** *52*, 4145-4153.

20. Grégoire, D. S.; Poulain, A. J., A physiological role for Hg(II) during phototrophic growth. *Nature Geoscience* **2016,** *9*, (2), 121-125.

21. Barkay, T.; Kritee, K.; Boyd, E.; Geesey, G., A thermophilic bacterial origin and subsequent constraints by redox, light and salinity on the evolution of the microbial mercuric reductase. *Environmental Microbiology* **2010,** *12*, (11), 2904-2917.

22. Choi, S. C.; Chase Jr, T.; Bartha, R., Metabolic pathways leading to mercury methylation in *Desulfovibrio desulfuricans* LS. *Applied and Environmental Microbiology* **1994,** *60*, (11), 4072-4077.

23. Qian, C.; Johs, A.; Chen, H.; Mann, B. F.; Lu, X.; Abraham, P. E.; Hettich, R. L.; Gu, B., Global proteome response to deletion of genes related to mercury methylation and dissimilatory metal reduction reveals changes in respiratory metabolism in *Geobacter sulfurreducens* PCA. *Journal of Proteome Research* **2016,** *15*, (10), 3540-3549.

24. Parks, J. M.; Johs, A.; Podar, M.; Bridou, R.; Hurt, R. A.; Smith, S. D.; Tomanicek, S. J.; Qian, Y.; Brown, S. D.; Brandt, C. C.; Palumbo, A. V.; Smith, J. C.; Wall, J. D.; Elias, D. A.; Liang, L., The genetic basis for bacterial mercury methylation. *Science* **2013,** *339*, 1332-1335.

25. Podar, M.; Gilmour, C. C.; Brandt, C. C.; Soren, A.; Brown, S. D.; Crable, B. R.; Palumbo, A. V.; Somenahally, A. C.; Elias, D. A., Global prevalence and distribution of genes and microorganisms involved in mercury methylation. *Science Advances* **2015,** *1*, 1-13.

26. Gionfriddo, C. M.; Tate, M. T.; Wick, R. R.; Schultz, M. B.; Zemla, A.; Thelen, M. P.; Schofield, R.; Krabbenhoft, D. P.; Holt, K. E.; Moreau, J. W., Microbial mercury methylation in Antarctic sea ice. *Nature microbiology* **2016,** *1*, (10), 16127.

27. Christensen, G. A.; Somenahally, A. C.; Moberly, J. G.; Miller, C. M.; King, A. J.; Gilmour, C. C.; Brown, S. D.; Podar, M.; Brandt, C. C.; Brooks, S. C.; Palumbo, A. V.; Wall, J. D.; Elias, D. A., Carbon amendments alter microbial community structure and net mercury methylation potential in sediments. *Applied and Environmental Microbiology* **2018,** *84*, (3).

28. Bravo, A. G.; Loizeau, J. L.; Dranguet, P.; Makri, S.; Björn, E.; Ungureanu, V. G.; Slaveykova, V. I.; Cosio, C., Persistent Hg contamination and occurrence of Hg-methylating transcript (*hgcA*) downstream of a chlor-alkali plant in the Olt River (Romania). *Environmental Science and Pollution Research* **2016,** *23*, (11), 10529-10541.

29. Yu, R.-Q.; Reinfelder, J. R.; Hines, M. E.; Barkay, T., Syntrophic pathways for microbial mercury methylation. *The ISME Journal* **2018**.

30. Desrochers, K. A. N.; Paulson, K. M. A.; Ptacek, C. J.; Blowes, D. W.; Gould, W. D., Effect of electron donor to sulfate ratio on mercury methylation in floodplain sediments under saturated flow conditions. *Geomicrobiology Journal* **2015,** *32*, (10), 924-933.

31. Bravo, A. G.; Zopfi, J.; Buck, M.; Xu, J.; Bertilsson, S.; Schaefer, J. K.; Poté, J.; Cosio, C., Geobacteraceae are important members of mercury-methylating microbial communities of sediments impacted by waste water releases. *ISME Journal* **2018**, 1-11.

32. Blair, G.; Lefroy, R., Sulfur and carbon research in rice production systems. *Field Crops Research* **1998,** *56*, (1), 177-181.

33. Ma, M.; du, H.; Wang, D.; Sun, T., Mercury methylation in the soils and sediments of Three Gorges Reservoir Region. *Journal of Soils and Sediments* **2017**, 1-10.

34. Su, Y. B.; Chang, W. C.; Hsi, H. C.; Lin, C. C., Investigation of biogeochemical controls on the formation, uptake and accumulation of methylmercury in rice paddies in the vicinity of a coal-fired power plant and a municipal solid waste incinerator in Taiwan. *Chemosphere* **2016,** *154*, 375-384.

35. Vishnivetskaya, T. A.; Hu, H.; Van Nostrand, J. D.; Wymore, A.; Xu, X.; Qiu, G.; Feng, X.; Zhou, J.; Brown, S. D.; Brandt, C. C.; Podar, M.; Gu, B.; Elias, D. A., Microbial community structure with trends in methylation gene diversity and abundance in mercury-contaminated rice paddy soils in Guizhou, China. *Environmental Science: Processes & Impacts* **2018,** *20*, (4), 673-685.

36. Jeremiason, J. D.; Engstrom, D. R.; Swain, E. B.; Nater, E. A.; Johnson, B. M.; Almendinger, J. E.; Monson, B. A.; Kolka, R. K., Sulfate addition increases methylmercury production in an experimental wetland. *Environmental Science and Technology* **2006,** *40*, 3800-3806.

37. Pham, A. L. T.; Morris, A.; Zhang, T.; Ticknor, J.; Levard, C.; Hsu-Kim, H., Precipitation of nanoscale mercuric sulfides in the presence of natural organic matter:

Structural properties, aggregation, and biotransformation. *Geochimica et Cosmochimica Acta* **2014,** *133*, 204-215.

38. Ticknor, J. L.; Kucharzyk, K. H.; Porter, K. A.; Deshusses, M. A.; Hsu-Kim, H., Thiol-based selective extraction assay to comparatively assess bioavailable mercury in sediments. *Environmental Engineering Science* **2015,** *32*, (7), 564-573.

39. Schaefer, J. K.; Morel, F. M. M., High methylation rates of mercury bound to cysteine by *Geobacter sulfurreducens*. *Nature Geoscience* **2009,** *2*, 123-126.

40. Lin, H.; Lu, X.; Liang, L. Y.; Gu, B. H., Cysteine inhibits mercury methylation by *Geobacter sulfurreducens* PCA mutant Δ*omcBESTZ*. *Environmental Science & Technology Letters* **2015,** *2*, (5), 144-148.

41. Vazquez-Rodriguez, A. I.; Hansel, C. M.; Zhang, T.; Lamborg, C. H.; Santelli, C. M.; Webb, S. M.; Brooks, S. C., Microbial- and thiosulfate-mediated dissolution of mercury sulfide minerals and transformation to gaseous mercury. *Frontiers in Microbiology* **2015,** *6*.

42. Zerkle, A. L.; Kamyshny, A.; Kump, L. R.; Farquhar, J.; Oduro, H.; Arthur, M. A., Sulfur cycling in a stratified euxinic lake with moderately high sulfate: Constraints from quadruple S isotopes. *Geochimica et Cosmochimica Acta* **2010,** *74*, (17), 4953-4970.

43. Frigaard, N. U.; Dahl, C., Sulfur metabolism in phototrophic sulfur bacteria. In *Advances in Microbial Physiology, Vol 54*, Poole, R. K., Ed. 2009; Vol. 54, pp 103-200.

44. Kimble, L. K.; Mandelco, L.; Woese, C. R.; Madigan, M. T., *Heliobacterium modesticaldum*, sp. nov., a thermophilic heliobacterium of hot springs and volcanic soils. *Archives of Microbiology* **1995,** *163*, (4), 259-267.

45. Ormerod, J. G.; Kimble, L. K.; Nesbakken, T.; Torgersen, Y. A.; Woese, C. R.; Madigan, M. T., Endospore-forming Heliobacteria from rice field soils. *Archives of Microbiology* **1996,** *165*, 226-234.

46. Stevenson, A. K.; Kimble, L. K.; Woese, C. R.; Madigan, M. T., Characterization of new phototrophic Heliobacteria and their habitats. *Photosynthesis Research* **1997,** *53*, (1), 1-12.

47. Beer-Romero, P.; Gest, H., *Heliobacillus mobilis*, a peritrichously flagellated anoxyphototroph containing bacteriochlorophyll g. *FEMS Microbiology Letters* **1987,** *41*, 109-114.

48. Stenzler, B.; Hinz, A.; Ruuskanen, M.; Poulain, A. J., Ionic strength differentially affects the bioavailability of neutral and negatively charged inorganic Hg complexes. *Environmental Science & Technology* **2017,** *51*, (17), 9653-9662.

49. Barkay, T.; Miller, S. M.; Summers, A. O., Bacterial mercury resistance from atoms to ecosystems. *FEMS microbiology reviews* **2003,** *27*, (2-3), 355-384.

50. Wang, Y.; Boyd, E.; Crane, S.; Lu-Irving, P.; Krabbenhoft, D.; King, S.; Dighton, J.; Geesey, G.; Barkay, T., Environmental conditions constrain the distribution and diversity of archaeal *merA* in Yellowstone National Park, Wyoming, U.S.A. *Microbial Ecology* **2011,** *62*, (4), 739-752.

51. R Core Team *R: A Language and Environment for Statistical Computing*, R Foundation for Statistical Computing: 2014.

52. Schaefer, J. K.; Szczuka, A.; Morel, F. M. M., Effect of divalent metals on Hg(II) uptake and methylation by bacteria. *Environmental Science and Technology* **2014,** *48*, (5), 3007-3013.

53. Vairavamurthy, A.; Manowitz, B.; Luther, G. W.; Jeon, Y., Oxidation state of sulfur in thiosulfate and implications for anaerobic energy metabolism. *Geochimica et Cosmochimica Acta* **1993,** *57*, (7), 1619-1623.

54. Tang, K. H.; Feng, X. Y.; Zhuang, W. Q.; Alvarez-Cohen, L.; Blankenship, R. E.; Tang, Y. J., Carbon flow of Heliobacteria is related more to Clostridia than to the green sulfur bacteria. *Journal of Biological Chemistry* **2010,** *285*, (45), 35104-35112.

55. Richardson, D. J.; King, G. F.; Kelly, D. J.; McEwan, A. G.; Ferguson, S. J.; Jackson, J. B., The role of auxiliary oxidants in maintaining redox balance during phototrophic growth of *Rhodobacter capsulatus* on propionate or butyrate. *Archives of Microbiology* **1988,** *150*, (2), 131-137.

56. McKinlay, J. B.; Harwood, C. S., Carbon dioxide fixation as a central redox cofactor recycling mechanism in bacteria. *Proceedings of the National Academy of Sciences of the United States of America* **2010,** *107*, (26), 11669-11675.

57. Rodionov, D. A.; Vitreschak, A. G.; Mironov, A. A.; Gelfand, M. S., Comparative genomics of the methionine metabolism in Gram-positive bacteria: A variety of regulatory systems. *Nucleic Acids Research* **2004,** *32*, (11), 3340-3353.

58. Zheng, W.; Hintelmann, H., Isotope fractionation of mercury during Its photochemical reduction by low-molecular-weight organic compounds. *The Journal of Physical Chemistry A* **2010,** *114*, (12), 4246-4253.

59. Gilmour, C. C.; Henry, E. A.; Mitchell, R., Sulfate stimulation of mercury methylation in freshwater sediments. *Environmental Science and Technology* **1992,** *26*, (11), 2281-2287.

60. Liu, Y. R.; Lu, X.; Zhao, L. D.; An, J.; He, J. Z.; Pierce, E. M.; Johs, A.; Gu, B. H., Effects of cellular sorption on mercury bioavailability and methylmercury production by *Desulfovibrio desulfuricans* ND132. *Environmental Science & Technology* **2016,** *50*, (24), 13335-13341.

61. Dias, M.; Salvado, J. C.; Monperrus, M.; Caumette, P.; Amouroux, D.; Duran, R.; Guyoneaud, R., Characterization of *Desulfomicrobium salsuginis* sp nov and *Desulfomicrobium aestuarii* sp nov., two new sulfate-reducing bacteria isolated from the Adour estuary (French Atlantic coast) with specific mercury methylation potentials. *Systematic and Applied Microbiology* **2008,** *31*, (1), 30-37.

62. Ranchou-Peyruse, M.; Goni-Urriza, M.; Guignard, M.; Goas, M.; Ranchou-Peyruse, A.; Guyoneaud, R., *Pseudodesulfovibrio hydrargyri* sp nov., a mercury-methylating bacterium isolated from a brackish sediment. *International Journal of Systematic and Evolutionary Microbiology* **2018,** *68*, (5), 1461-1466.

63. Stubner, S.; Wind T Fau - Conrad, R.; Conrad, R., Sulfur oxidation in rice field soil: activity, enumeration, isolation and characterization of thiosulfate-oxidizing bacteria. (0723-2020 (Print)).

64. Wind, T.; Conrad, R., Sulfur compounds, potential turnover of sulfate and thiosulfate, and numbers of sulfate-reducing bacteria in planted and unplanted paddy soil. *FEMS Microbiology Ecology* **1995,** *18*, (4), 257-266.

65. Drott, A.; Lambertsson, L.; Björn, E.; Skyllberg, U., Importance of dissolved neutral mercury sulfides for methylmercury production in contaminated sediments. *Environmental Science and Technology* **2007,** *41*, (7), 2270-2276.

66. Olsen, T. A.; Brandt, C. C.; Brooks, S. C., Periphyton biofilms influence net methylmercury production in an industrially contaminated system. *Environmental Science & Technology* **2016,** *50*, (20), 10843-10850.

67. Correia, R. R. S.; Guimarães, J. R. D., Mercury methylation and sulfate reduction rates in mangrove sediments, Rio de Janeiro, Brazil: The role of different microorganism consortia. *Chemosphere* **2017,** *167*, 438-443.

68. Fleming, E. J.; Mack, E. E.; Green, P. G.; Nelson, D. C., Mercury methylation from unexpected sources: Molybdate-inhibited freshwater sediments and an iron-reducing bacterium. *Applied and Environmental Microbiology* **2006,** *72*, (1), 457-464.

69. Eklöf, K.; Bishop, K.; Bertilsson, S.; Björn, E.; Buck, M.; Skyllberg, U.; Osman, O. A.; Kronberg, R. M.; Bravo, A. G., Formation of mercury methylation hotspots as a consequence of forestry operations. *Science of the Total Environment* **2018,** *613-614*, 1069-1078.

70. Bravo, A. G.; Bouchet, S.; Guedron, S.; Amouroux, D.; Dominik, J.; Zopfi, J., High methylmercury production under ferruginous conditions in sediments impacted by sewage treatment plant discharges. *Water Research* **2015,** *80*, 245-255.

71. Sugio, T.; Fujii, M.; Takeuchi, F.; Negishi, A.; Maeda, T.; Kamimura, K., Volatilization of mercury by an iron oxidation enzyme system in a highly mercury-resistant *Acidithiobacillus ferrooxidans* strain MON-1. *Bioscience, Biotechnology and Biochemistry* **2003,** *67*, (7), 1537-1544.

6.9 FIGURES & CAPTIONS

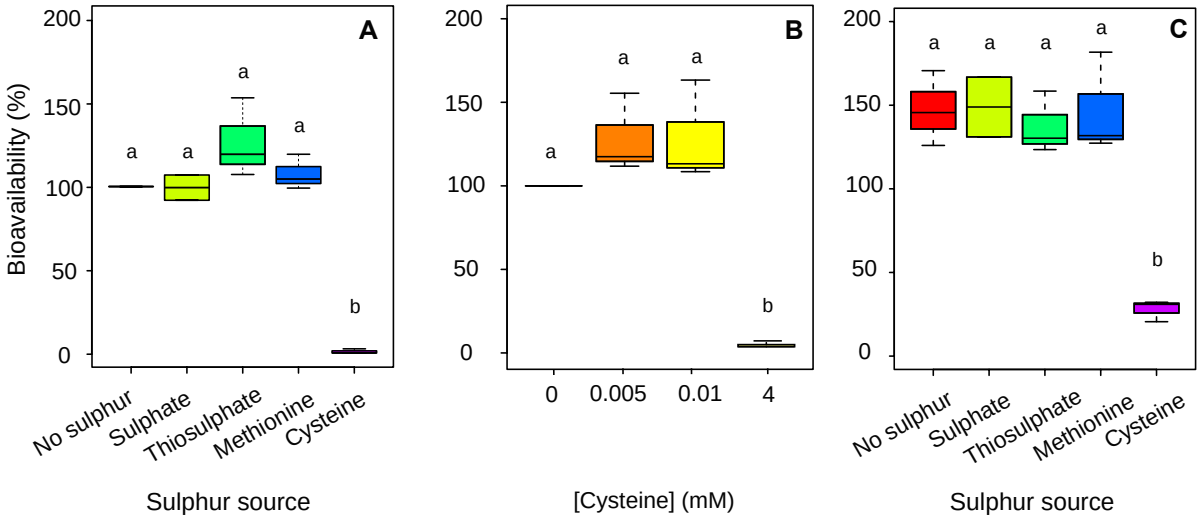

(Figure caption provided on the following page)

Figure 6.1: Bioavailability of 5 nM Hg in the presence of sulphate, thiosulphate, methionine and different concentrations of cysteine. Cells were exposed to Hg in BMAA minimal medium where [NO_3^-] was set to 0.2 mM (**A, B**) and DSMZ medium #370 amended with 20 mM pyruvate used in bioreactor experiments (**C**). All experiments were performed in triplicate except for sulphate, which was duplicated. For experiments comparing different sulphur sources total sulphur concentrations was normalized to 4 mM (**A, C**). The bottom and top of the boxes show the first and third quartiles respectively, the bar in the middle shows the median and the whiskers show the minimum and maximum for each treatment. One-way ANOVAs were run separately for experiments testing the effect of sulphur source and a one-way rank sum test was run for experiments testing the effect of cysteine concentration. Sulphur source had a significant ($p<0.05$) effect on Hg bioavailability in the minimal medium ($p = 6.39 \times 10^{-6}$) (**A**) and bioreactor medium ($p = 2.98 \times 10^{-4}$) (**C**) and cysteine concentration had a significant effect on Hg bioavailability ($p = 8.21 \times 10^{-4}$) (**B**). Tests for constant variance ($p = 0.11$ for sulphur source in minimal medium and $p = 0.07$ for sulphur source in bioreactor medium) and normal distribution ($p = 0.17$ for sulphur source in minimal medium and $p= 0.22$ for sulphur source in bioreactor medium) were passed ($p > 0.05$ for rejection of null hypothesis). The statistical conclusion for the effect of cysteine concentration was the same in the non-parametric and parametric tests ($p = 1.15 \times 10^{-4}$), as such multiple comparison results are included in the figure (**B**). Letters that are not shared between treatments indicate a significant difference according to the Tukey HSD test ($p < 0.05$).

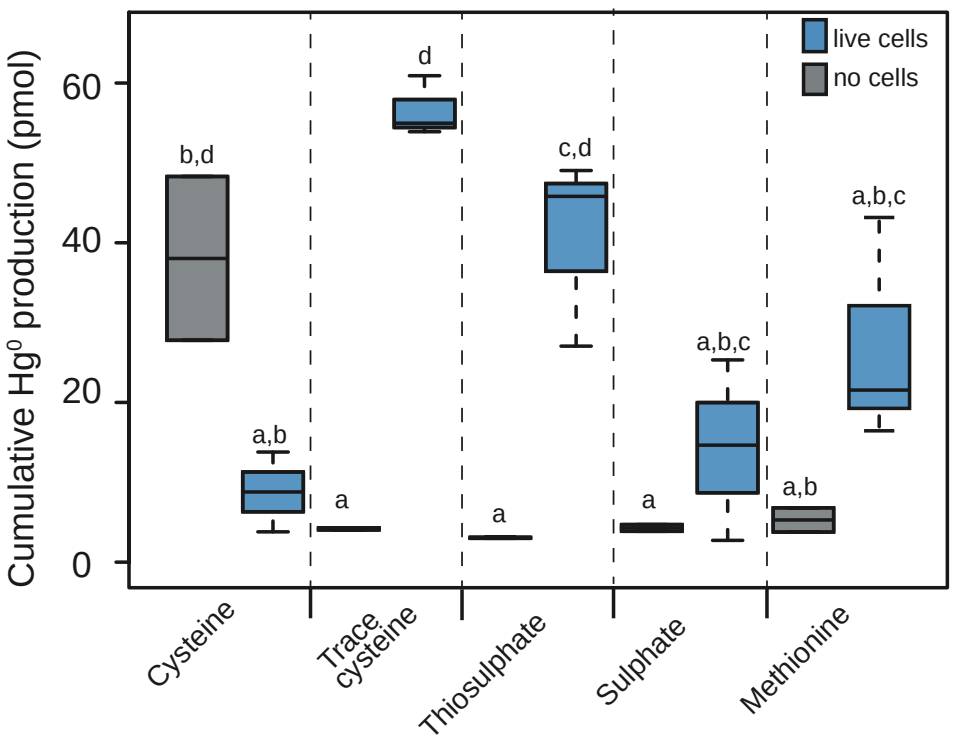

Figure 6.2: Cumulative Hg^0 production for phototrophically grown *H. mobilis* and no cell controls amended with cysteine, thiosulphate, sulphate and methionine. Total sulphur was normalized to 4 mM in all cases except the trace cysteine treatment, which was amended with 250 pM cysteine. All live cell experiments were performed in triplicate and no cell controls were performed in duplicate. $HgCl_2$ was added to a final concentration of 250 pM in all experiments. The bottom and top of the boxes respectively show the first and third quartiles, the bar in the middle shows the median and the whiskers show the minimum and maximum for each treatment. A one-way ANOVA showed that sulphur had a significant ($p<0.05$) effect on cumulative Hg^0 production ($p = 2.71 \times 10^{-5}$). Tests for constant variance ($p = 0.15$) and normal distribution ($p = 0.44$) were passed ($p > 0.05$ for rejection of null hypothesis). Letters that are not shared between treatments indicate a significant difference according to the Tukey HSD test ($p < 0.05$).

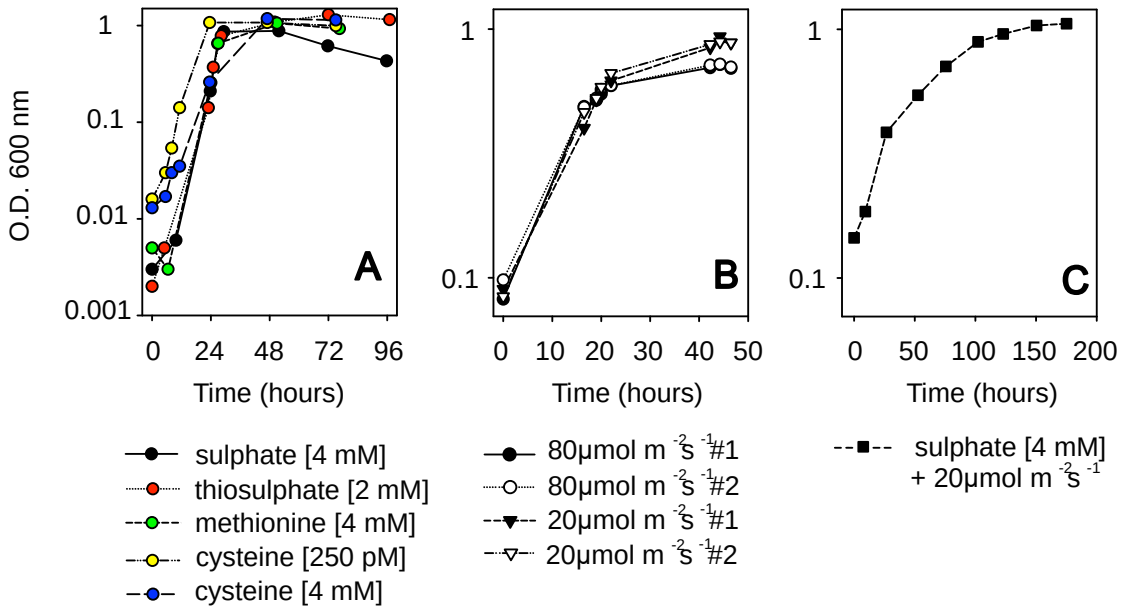

Figure 6.3: Phototrophic growth of *H. mobilis* in closed tubes in the presence of different sulphur sources and sulphur concentrations (**A**), 4 mM sulphate in the presence of different light intensities (**B**) and 4 mM sulphate in a closed bioreactor supplied with low light intensity (e.g. not connected to the Hg^0 analyzer) (**C**). All cultures were grown in DSMZ medium #370 amended with 20 mM pyruvate. Results shown in panel (**A**) are representative cases of replicated experiments.

Chapter 7: Hg stable isotope fractionation during anaerobic phototrophic Hg reduction

Daniel S. Grégoire [a]*, Sarah E. Janssen [b]*, Michael T. Tate [b]* & Alexandre J. Poulain [a]

* Contributed equally to this work

a - Biology Department, University of Ottawa, 30 Marie Curie, Ottawa, ON, K1N 6N5, Canada.

b - Wisconsin Water Science Center, USGS, Middleton, Wisconsin 53562, USA.

Research highlights:

- First study examining Hg stable isotope fractionation associated with Hg^{II} reduction during anoxygenic photosynthesis
- Developed methodology to capture volatile Hg^0 for stable isotope analyses at high temperature (50°C) under completely anoxic conditions
- Observed mass dependent but no mass independent fractionation in contrast to previous work on phototrophic Hg reduction and abiotic Hg photoreduction
- Isotope enrichment observed in the Hg^{II} pool (-0.8‰) was twice as high as values reported for microbial Hg reduction (-1.20 to -1.80‰) suggesting there is a distinct fractionation process associated with anoxygenic photosynthesis
- Study provides the basis to explore mechanisms supporting anaerobic Hg reduction in the environment and in other metabolisms such as fermentation

Manuscript in preparation for submission to Environmental Science & Technology

N.B. Supporting information for this chapter can be found in **Appendix D**

7.1 ABSTRACT

Mercury (Hg) is a global pollutant and potent neurotoxin that bioaccumulates in food webs as monomethylmercury (MeHg). The production of MeHg is controlled by the metabolic activity of anaerobic microbes that methylate Hg intracellularly. Anoxic Hg redox cycling pathways such as Hg reduction ultimately control the availability of Hg to methylators and there is a growing body of evidence that suggests anaerobes play an important role in Hg reduction in anoxic habitats. These pathways remain challenging to study because of the absence of dedicated genetic targets supporting them and the low levels of Hg^0 in anoxic environments. In this study we used emerging methods that rely Hg stable isotope fractionation to explore Hg reduction during anoxygenic photosynthesis in the model anaerobe *Heliobacterium modesticaldum* Ice1. We show that mass-dependent fractionation occurs during anoxygenic phototrophic growth, but mass-independent fractionation is absent, similar to previous work on microbial Hg reduction. We show that the isotopic enrichment associated with anoxygenic photosynthesis lies in between the values reported for microbial Hg reduction and abiotic photoreduction, suggesting the presence of an intermediary isotope fractionation process. Furthermore, the isotopic enrichment produced by phototrophic *H. modesticaldum* was twice as high compared to previous reports on microbial Hg reduction. These observations demonstrate that Hg isotope fractionation processes that occur during anoxygenic photosynthesis are distinct from other microbe mediated reduction and abiotic photoreduction pathways. The findings in this study can be used as the basis to further explore the mechanisms supporting cryptic anaerobic Hg reduction pathways in the environment.

7.2 INTRODUCTION

Mercury (Hg) is a global pollutant and potent neurotoxin that bioaccumulates in aquatic and terrestrial food webs as monomethylmercury (MeHg) [1]. Anaerobic microbes that carry the *hgcAB* gene cluster, which encodes for the metabolic machinery responsible for Hg methylation [2], are the major contributors to MeHg production in habitats such as aquatic sediments and flooded soils [3-5]. Hg methylation is thought to occur as an intracellular process and as such, it is ultimately controlled by the bioavailability of Hg to methylators in anoxic habitats.

Hg redox cycling plays a key role in determining the inorganic Hg substrates available to methylators. Atmospheric Hg^0 oxidation supplies the dissolved Hg^{II} required to generate MeHg whereas Hg^{II} reduction pathways can limit MeHg production by favouring Hg^0 evasion. Although it is well established that abiotic photochemical Hg reduction dominates Hg redox cycling in oxic surface systems where light is present [6-14], the contributions of Hg reduction pathways in anoxic surface and near subsurface environments where Hg methylation occurs remain challenging to assess.

Anoxic Hg reduction can occur via abiotic redox reactions with dissolved organic carbon [15] and the iron mineral magnetite [16, 17], but also through biotic pathways mediated by chemotrophic and phototrophic microbes [18-22]. Unlike many aerobes that use dedicated enzymatic machinery for Hg reduction encoded by the *mer* operon [23, 24], anaerobes appear to reduce Hg through cometabolic pathways tied to anaerobic respiration, fermentation and anoxygenic photosynthesis [18-22]. In contrast to *mer*-mediated Hg reduction and Hg methylation, dedicated genetic determinants have yet to be identified for anaerobic Hg reduction, making these pathways challenging to study from a mechanistic standpoint.

In addition to the challenges at the laboratory scale, the contributions of anaerobes to Hg reduction in the environment have largely been ignored. This is partially due to the cryptic nature of anoxic Hg redox cycling, which is challenging to assess because of the low environmental levels of the volatile reduced Hg species, Hg^0. Although some studies have shown that Hg^0 can dominate Hg speciation in anoxic habitats [25, 26], it is possible that Hg^0 levels are maintained at a steady state in which Hg is actively reduced and oxidized [27]. Despite the potential for anaerobic Hg reduction to affect delivery of Hg substrates to methylators, the environmental contributions of these pathways are difficult to track in the absence of net Hg^0 accumulation. As such, alternative approaches that do not rely on dedicated genetic targets or Hg^0 accumulation must be considered to characterize anaerobic Hg reduction pathways.

The use of stable Hg isotope fractionation has recently emerged as a powerful tool for providing biogeochemical proxies for different abiotic and biotic Hg transformations [28]. All abiotic and biotic Hg transformation pathways studied to date demonstrate mass dependent fractionation (MDF) in which the product pool becomes enriched with lighter Hg isotopes (e.g. ^{198}Hg) as the reaction proceeds [29]. Some pathways, such as abiotic photochemical reduction, also demonstrate mass independent fractionation (MIF), which is defined as the fractionation that occurs outside of the predicted MDF pattern [28]. MIF is most commonly observed due to the magnetic isotope effect for odd-Hg isotopes ^{199}Hg and ^{201}Hg in the presence of sunlight [30]. Generally speaking, the combination of MDF and MIF, and the degree of isotopic enrichment can be used to develop signatures for different Hg transformations. In this way, Hg stable isotopes can be used to determine

mechanistic details on Hg transformation pathways and track their contribution to Hg cycling in the environment.

Several laboratory studies have been published in the last 10 years examining Hg isotope fractionation during microbial transformations. Thus far, isotopic fractionation has been studied in microbes capable of *mer*-mediated reduction [31] and MeHg demethylation [32]; anaerobic non-*mer*-mediated Hg reduction [33]; Hg methylation [34-36]; and phototrophic MeHg degradation and Hg reduction [37]. These studies have yielded unique insights into how microbes interact with Hg at the atomic level during Hg transformations. In the case of the recent study on Hg methylation, it was shown that two Hg methylating strains displayed different MDF signatures, suggesting each strain accessed different pools of bioavailable Hg during methylation [36]. In another recent study on Hg reduction during oxygenic photosynthesis, it was shown that a model green alga displayed a MIF signal representative of Hg^{II} binding to thiols prior to being reduced by free radicals generated during photosynthesis [37]. The mechanistic details determined from these studies exemplify why Hg stable isotopes are a promising option for studying mechanisms for anaerobic Hg reduction, which remain poorly characterized.

Our objective in this study is to characterize Hg isotope fractionation patterns during anoxygenic phototrophic and fermentative Hg^{II} reduction for which there exists no data published to date. This study builds on previous work with *Heliobacterium modesticaldum* Ice1, which is a model anaerobe capable of high levels of Hg^{II} reduction during anoxygenic photoheterotrophic and fermentative growth [21]. This study focuses on photoheterotrophic growth and provides the first evidence of MDF during anoxygenic phototrophic Hg reduction. We demonstrate that MIF does not occur during anoxygenic

photosynthetic growth in the presence of photosynthetically active radiation (PAR) unlike what has previously been observed in oxygenic phototrophic Hg reduction [37] and abiotic Hg photoreduction [29]. Instead, we show that isotopic fractionation during anoxygenic phototrophic growth is more similar to what has been observed for chemotrophic microbial Hg reduction in the dark [31, 33]. Furthermore, we show that the isotopic enrichment that occurs in the reactant pool of Hg^{II} during MDF in *H. modesticaldum* is in between what has been reported for microbial Hg reduction [31, 33] and abiotic photochemical reactions [29, 37]. Finally, we discuss how these findings can be used to outline mechanisms for anaerobic Hg reduction and track cryptic anaerobic Hg redox cycling pathways in the environment.

7.3 METHODS

7.3.1 Cell growth conditions and bioreactor setup

All experiments with live cells employed the strain *Heliobacterium modesticaldum* Ice1 grown in PYE medium at a constant illumination and visible light intensity of 80 µmol photon m^{-2} s^{-1} with a peak irradiance in the near-red to red spectrum (600 nm to 700 nm) at 50°C in line with our previous work [21]. *H. modesticaldum* Ice1 was obtained from the DSMZ culture collection (catalogue number DSM-792). The bioreactor methodology employed in these experiments was similar to the one used in previous work [21] with the following modifications: the bioreactor was supplied with sterile nitrogen gas that passed through an activated carbon filter and a 0.2 µm pore size air filter at a flow rate of 0.25 L min^{-1}. The reactor outlet was connected to an empty container to capture condensation, followed by a soda lime trap to remove excess moisture prior to Hg^0 being captured on

two gold traps setup in series (schematic provided in **Appendix D**, **Fig D1**). Two gold traps connected in series were employed as a precaution to capture Hg^0 that passed through the first trap due to high levels of Hg^0 production and gold trap saturation.

The bioreactor was kept in an incubator set to 50°C. Light was supplied using a 60 W incandescent light bulb with a visible light intensity being maintained at 20 µmol photon $m^{-2}s^{-1}$ with a peak irradiance in the near-red to red spectrum (600 to 700 nm). The reactor was purged continuously for 2h prior to initiating all experiments to remove background Hg^0. Following this, a subsample was removed from the bioreactor to account for background Hg present in the growth medium. An additional subsample was spiked directly with the National Institute of Standards and Technology (NIST) 3133 standard (initial Hg concentration of 23.28 µM) to a final concentration of 2 nM or 10 nM Hg depending on the experiments in question. The isotopic compositions of these samples were compared to ultra filtered MiliQ water spiked with the same NIST 3133 standard to verify that no isotope fractionation occurred as a result of the medium composition and the incubation conditions employed (see **Table D1**). Following this step, phototrophically grown *H. modesticaldum* cells were added as a 10 % (v/v) inoculum to the reactor and an additional subsample was withdrawn to verify initial cell density via O.D. 600 nm. For sterile treatments, no cells were added to the bioreactor and the initial volume of growth medium was adjusted to ensure that all reactor experiments were carried out at a working volume of 500 mL. The bioreactor was purged for another hour to remove any background Hg linked to the initial subsampling steps after which the NIST 3133 standard was directly added to the bioreactor at a final concentration of 2 nM or 10 nM Hg. Two different concentrations were used because of adjustments made to

the methodology in between sets of experiments that are discussed in the following section.

7.3.2 Continuous bubbling for Hg^0 measurements

Experiments where the bioreactor was spiked with 2 nM Hg were supplied with constant bubbling. 2 nM of Hg was added to ensure we could effectively capture all of the Hg^0 produced and to minimize Hg^0 breakthrough on gold traps. 30 mL subsamples were periodically removed (0, 6, 12, 24, 48h) using a sterile stainless steel 18G needle and 60 mL BD syringe for total Hg analyses, cell growth measurements and stable isotope analyses. Following each subsample, the ¼ turn valves were rapidly closed to seal any Hg^0 in the reactor while quickly sealing and storing the gold traps for the corresponding time point (**Fig D1**). Following this step, new soda lime and gold traps were installed and the ¼ turn valves slowly opened to continue purging the reactor of Hg^0.

7.3.3 Periodic bubbling for Hg^0 measurements

For experiments where 10 nM Hg was supplied, the reactor was bubbled periodically rather than continuously. The decision to increase the Hg concentration from 2 nM to 10 nM Hg arose due to recovery issues in samples from later time points that prohibited the effective measurement of stable isotope fractionation. The decision to remove continuous bubbling was made because of the extremely high variability between isotope fractionation in samples from the earlier time points in the 2 nM Hg experiments that used continuous bubbling. In this case, we suspected that the continuous bubbling contributed to considerable evaporation that occurred over the course of the experiment

(~70 mL). This evaporation could have wet the soda lime and gold traps adding a confounding physical sorption process that could affect Hg isotope fractionation.

This sampling methodology differed from the continuous bubbling methodology in the sense that all ¼ turn valves remained closed and no gold traps were connected to the bioreactor until it was time for subsampling Hg^0 and Hg^{II} (0, 3, 6, 12, 24, 48h) (**Fig D1**). At that point, a gold trap was connected to the outlet of the bioreactor and gas flow was slowly re-initiated to purge Hg^0 from the reactor for 30 min. During the final 5 min, a 30 mL subsample was removed from the bioreactor for total Hg analyses, cell growth measurement and stable isotope analyses. At the end of the 30 min, the gold traps were sealed, all ¼ turn valves were closed and gas flow was stopped.

7.3.4 Sample storage and reactor disassembly

All gold traps were capped with sealed PTFE tubing and stored in clean plastic bags in the dark at room temperature until analyzed. All liquid samples were conserved with 1% (v/v) trace element grade HCl and the bottles were wrapped in foil and stored at 4°C. All liquid samples were weighed to account for the volume removed from the bioreactor. Once the reactor experiments were finished, the contents of the reactor were disposed of and the reactor was rinsed three times with 100 mL of 10 % (v/v) trace element grade HCl that was subsampled to account for Hg adsorbed to the glassware as part of the mass balance in line with previous methods [21].

7.3.5 Total Hg analyses and sample preparation for stable isotope measurements

In addition to having been conserved with HCl all samples for aqueous Hg analyses were conserved with 10 % (v/v) BrCl in line with previous work [36]. Prior to analysis, aqueous Hg samples were neutralized with hydroxylamine hydrochloride (HAH) and reduced with 10% (w/v) tin chloride [38]. Total Hg (THg) concentrations were determined using an automated Brooks Rand system following EPA method 1631 [38] which relies on capturing Hg^0 volatilized from aqueous samples with tin chloride onto gold traps and using CVAFS to measure peak fluorescence at 253.7 nm to asses Hg concentration. Total Hg mass balances were calculated in line with previous work [21, 22] although corrections were made to account for the mass of Hg removed for each subsample.

For Hg^0 collected onto gold traps a thermal desorption system was used to liberate Hg^0 over a 40 min desorption cycle which was then captured in 40% HNO_3:BrCl (3:1) oxidizing solution. An aliquot of the trapping solution was subsequently analyzed for THg concentration as stated above. Desorption efficiency during pre-concentration was tested by trapping a NIST 3133 standard with each batch of samples, and recoveries for standard trapping were all > 90%. THg recoveries obtained for both sets of experiments were 103.88 ± 11.23 % (n=3) and 92.90 ± 13.23 % (n=3) for the 2 nM and 10 nM Hg experiments, respectively (**Fig D2**).

7.3.6 Hg stable isotope analyses

Using the previously determined THg concentration, an aliquot of the trapping solution was diluted with water and any necessary matrix matching acids to make the appropriate analysis concentration of 1.0 ng mL^{-1} [39]. A Neptune Plus multicollector-inductively coupled plasma mass spectrophotometer (MC-ICP-MS) was used for Hg stable isotope ratio measurements. MC-ICP-MS conditions and analytical expectations are discussed in detail elsewhere [39]. As commonly found in literature, matrix-matched NIST 3133 Hg was used as the normalization solution [40]. Tl (NIST SRM 997, 40 ng mL^{-1} in 3% HCl) was introduced by Apex-Q nebulizer as an aerosol. To achieve detection at low Hg concentrations, Hg was reduced with stannous chloride in-line then pumped continuously into a custom designed gas liquid separator to efficiently extract gaseous Hg^0 with a counter stream of argon gas [39, 41]. The matrix ultimately reaching the plasma source consisted primarily of Tl aerosol, argon and Hg^0. The instrument was tuned (e.g. sample gases, stage positions, and lenses) to achieve optimal ^{202}Hg voltage, which was typically 1V/ppb Hg. A secondary standard (NIST RM 8610) was measured in 20% of samples to ensure instrument stability and accuracy. Average values obtained for NIST 8610 with 2SD were ($\delta^{202}Hg$= -0.53 ± 0.08; $\Delta^{199}Hg$ =-0.02 ± 0.06; $\Delta^{200}Hg$ =0.00 ± 0.04; $\Delta^{201}Hg$ =-0.04 ± 0.06; $\Delta^{204}Hg$ =0.00 ± 0.14, 2SD, n = 35) which agreed with certified values. Additionally, desorption check standards (NIST 3133) for Hg^0 traps were also measured to verify that no fractionation occurred during gold trap processing. Standards displayed average values in line with their initial isotopic composition ($\delta^{202}Hg$= -0.00 ± 0.06; $\Delta^{199}Hg$ =-0.02 ± 0.07; $\Delta^{200}Hg$ =0.02 ± 0.04; $\Delta^{201}Hg$ =-0.04 ± 0.06; $\Delta^{204}Hg$ =0.00 ± 0.14, 2SD, n = 6,) indicating no fractionation during processing.

7.3.7 Isotope calculations

Delta calculations followed the conventions set forth by others [40]. This convention calls for mass dependent fractionation (MDF) to be expressed in terms of $\delta^{xxx}Hg$ where graphically $\delta^{202}Hg$ is used to signify MDF. $\delta^{xxx}Hg$ is calculated as:

$$\delta^{xxx}Hg(‰) = [(^{xxx}Hg/^{198}Hg_{sample})/(^{xxx}Hg/^{198}Hg_{NIST\text{-}3133}) - 1] \times 1000. \quad (\textbf{Eq 1})$$

XXX is used to signify the isotope of interest. As mentioned in the **Introduction** section, Hg also undergoes MIF of both even and odd isotopes. Here, odd-MIF is described by $\Delta^{199}Hg$ and even-MIF by $\Delta^{200}Hg$. MIF is calculated as:

$$\Delta^{xxx}Hg \approx \delta^{xxx}Hg - (\delta^{202}Hg * \beta). \quad (\textbf{Eq 2})$$

β denotes the mass dependent scaling constant, which is determined by the laws of mass dependence [40].

Isotope enrichment effects (herein referred to as ε_{AP} for anoxygenic phototrophic reduction) were calculated using open system Rayleigh fractionation models to account for the Hg^0 product that was removed following the methods outlined in previous work on microbial Hg reduction [31]. This method involved fitting a linear regression (shown in **Fig D3**) based on the change in $\ln (R/R_0)$ as a function of $\ln(f_r)$.

Where:

$R = (\delta^{202}Hg/1000) + 1$ for Hg^{II} (reactant) or Hg^0 (product) at a given time point and $R_0 = (\delta^{202}Hg/1000) + 1$ at the beginning of the experiment (**Eq 3**)

f_r= Hg^{II} in the reactor at a given time point/ Hg^{II} in the reactor at the beginning of the experiment (**Eq 4**)

We chose to use the total Hg analyses from the bioreactor to establish f_r as this is a true representation of the instantaneous isotope fractionation rather than a time integrated sample following the methods outlined in previous work [31]. ε values for MDF were also compiled from previous studies on pure microbial cultures and photochemical Hg transformations for comparison purposes. Currently, there is no standard guideline for how to calculate ε and indicate whether the product or reactant was employed. We have attempted to convert all ε values from the literature to values that represent the conversion of reactants to products according to previous calculations used for microbial Hg^{II} reduction [31, 33]. If the isotope fractionation factor ($\alpha_{202/198}$) was presented instead of ε, α was converted to ε based on the following formula: ε = [(α-1)*1000]/-1 (**Eq 5**).
If the ratio of products to reactants was employed, the reciprocal value of α was used to calculate ε for reactant to product.

7.4 RESULTS AND DISCUSSION

7.4.1 Hg^0 production with continuous and periodic bubbling

Similar to previous work with *H. modesticaldum*, Hg^0 production relied on the presence of live cells although the bubbling method employed affected the amount of Hg^0 produced relative to the initial Hg^{II} supplied [21]. In both the 2 nM and 10 nM Hg experiments, cumulative Hg^0 production was an order of magnitude higher for the live cell treatments compared to abiotic controls with no cells (>0.4 nmol vs <0.05 nmol) (**Fig 7.1**). Despite achieving comparable cumulative Hg^0 production in both sets of experiments (**Fig 7.1B, E**), the amount of Hg^0 produced relative to the initial Hg^{II} supplied was 3 times higher in the 2 nM Hg experiments compared with the 10 nM Hg

experiments (45.07 ± 5.42 vs 13.67 ± 2.37 %). It is unlikely that the increased Hg concentration inhibited Hg^0 production due to toxicity because cells supplied with 10 nM Hg grew faster than those supplied with 2 nM Hg (0.069 ± 0.030 vs 0.098 ± 0.003 hr^{-1}) and achieved a comparable yield (final O.D. 600 nm 0.5 to 0.55 for all live cell experiments) (**Fig 7.1C, F**). Instead, these results could be attributed to CO_2 accumulation in the bioreactor. Although *H. modesticaldum* cannot grow autotrophically, inorganic carbon is a required nutrient that is reduced through anaplerotic reactions during phototrophic growth that are essential to replenishing metabolic intermediates generated via the tricarboxylic acid cycle to meet the biosynthetic needs of the cell [42]. By removing bubbling, cells would have had access to CO_2 generated following organic carbon oxidation, which may have provided cells with an electron sink that could compete with Hg^{II} reduction [22, 43]. Alternatively, these results could be due to Hg^0 oxidation in the absence of constant Hg^0 removal as has been observed in other anaerobes [44, 45]. We are currently developing experiments to test for the potential contributions of these processes to decreased relative Hg^0 production.

7.4.2 Mass dependent fractionation during anoxygenic phototrophic growth

As mentioned in the **Methods** section, we were unable to obtain reliable Hg isotope measurements for all time points in the 2 nM Hg experiments despite obtaining high recoveries in the total Hg mass balance (**Fig D2**). This meant we had insufficient data to fit the linear regressions required to calculate ε_{AP}. The changes made to the method in the 10 nM Hg experiments with periodic bubbling resolved this issue and are discussed in the remainder of this section.

Hg reduction in phototrophically grown *H. modesticaldum* resulted in positive MDF but no MIF (**Fig 7.2**) and no isotope fractionation was observed in the abiotic controls (**Table D1** and **Table D2**). As such, the remainder of the discussion will focus on biological Hg stable isotope fractionation. In the reactant pool, $\delta^{202}Hg^{II}$ increased steadily over time suggesting cells preferentially reduced lighter Hg^{II} (**Fig 7.2A**). A mirror trend was observed for $\delta^{202}Hg^{0}$, which was depleted in $^{202}Hg^{0}$ at the beginning of the experiment, became enriched with heavier isotopes as the reaction proceeded and eventually, approached the initial isotopic composition of the NIST 3133 standard (**Fig 7.2B**). Curiously, the $\delta^{202}Hg^{0}$ for the 3h time point in both live cell replicates showed that product pool was initially enriched with heavy Hg isotopes (**Fig 7.2B**). These results suggest that cells may have initially reduced a heavier pool of Hg that was bioaccessible following the addition of Hg to the bioreactor. Similar results have been observed in iron reducing bacteria that preferentially reduced heavier Fe^{III} [46] and anaerobic Hg methylators [36]. In the case of Hg methylation, the fractionation pattern was attributed to cells accessing different pools of bioavailable Hg [36]. Given that these results suggest there was an alternative process contributing to isotope fractionation earlier in the experiment, we omitted the 3h time points from isotopic enrichment calculations (**Fig D3**),

The linear trend observed from 6h on suggests that there were no competing Hg transformations, such as Hg^{0} re-oxidation, contributing to the Hg stable isotope fractionation observed (**Fig 7.2** and **Fig D3**). These results further support that the decrease in relative Hg^{0} production in the 10 nM Hg experiments is due to CO_2 accumulation in the reactor rather than Hg^{0} oxidation. Indeed, if oxidation of the newly produced Hg^{0} occurred (explaining lower net Hg^{0} production), we would have expected a

shift or inflection point in the isotope fractionation pattern for the later time points. Note that a direct test for Hg^0 oxidation is required because it is possible the isotope fractionation observed is the net result of several processes we are unable to tease apart at this time (e.g. Hg sorption, internalization, reduction and possibly oxidation) [47].

7.4.3 Isotope enrichment for photochemical and microbial Hg transformations

The ε_{AP} estimated for MDF in the reactant (e.g. Hg^{II}) and product pools (e.g. Hg^0) are -0.8 and -2.00 ‰, respectively (**Fig D3**). Although we present both values here, we will compare the ε values obtained in our study to that of others using the reactant Hg^{II} signature, as is the convention. We chose this approach so we could compare our results to previous studies that used Hg^{II} to avoid uncertainties associated with low Hg^0 recoveries from gold traps, which can contribute to an overestimation of ε [47]. We have also provided an estimation of variability based on 2 standard deviations, as is the convention, where data was available.

When compared with previous work, the isotopic enrichment observed for phototrophically grown *H. modesticaldum* falls between the values observed for abiotic photochemical and microbial Hg reduction pathways (**Fig 7.3**). The isotopic enrichment observed for *H. modesticaldum* is slightly lower compared with photoreduction in the presence of low concentrations of dissolved organic carbon (-0.60 ± 0.20 vs -0.80 ± 0.56 ‰) [29] but considerably lower compared with photoreduction in the presence of marine exudates and UVB light (1.47 vs -0.80 ± 0.56 ‰) [37] (**Fig 7.3**). When compared with Hg reduction during oxygenic phototrophic growth in the model green alga *Isochrysis galbana*, the isotopic enrichment observed for *H. modesticaldum* is also lower (0.14 to

0.60 vs -0.80 ± 0.56 ‰) [37] (**Fig 7.3**). Importantly, all of the pathways mentioned above also demonstrate MIF [29, 37], which was not observed during anoxygenic phototrophic growth (**Table D1** and **Table D2**). These results suggest that the processes affecting isotopic fractionation during anoxygenic photosynthesis in *H. modesticaldum* are distinct from those associated with oxygenic photosynthesis and abiotic photoreduction.

The occurrence of positive MDF and lack of MIF observed in *H. modesticaldum* are more in line with what has previously been reported for enzyme-mediated and cometabolic Hg reduction in chemotrophic bacteria. In this instance, we attribute the lack of MIF to the fact that we employed a visible light source at a low intensity to limit abiotic photochemical reduction while supporting phototrophic growth [21]. When compared with previous work on Hg reduction in pure cultures, the isotopic enrichment observed for *H. modesticaldum* (-0.80 ± 0.56 ‰) is up to two times higher than what has been reported for *mer*-mediated reduction (-1.60 ± 0.50 to -1.20 ± 0.10 ‰) [31] and cometabolic anaerobic Hg reduction in *Shewanella oneidensis* MR-1 (-1.80 ± 0.30 ‰) [33]. Despite displaying a similar trend in terms of MDF and lack of MIF, these results suggest that the mechanisms contributing to isotopic enrichment during anoxygenic photosynthesis are also distinct from other microbial Hg reduction pathways. When considered alongside the differences in isotope enrichment with respect to photochemical pathways, our study suggests that the mechanism contributing to Hg stable isotope fractionation in *H. modesticaldum* is as an intermediate fractionation process that lies between light-driven reactions and enzymatic Hg reduction. Importantly, Hg reduction during anoxygenic photosynthesis is still identifiable due to the lack of co-occurring photochemical effects.

Interestingly, when compared with Hg methylation in the anaerobic chemotroph *Geobacter sulfurreducens* PCA, the isotopic enrichment observed during anoxygenic phototrophic Hg reduction was only slightly higher (-0.90 vs -0.80 ± 0.56 ‰) [36]. Although the δ^{202}Hg observed for *G. sulfurreducens* eventually surpassed the initial δ^{202}Hg of the NIST 3133 standard, the δ^{202}Hg observed in *H. modesticaldum* did not (**Fig 7.2**). One can speculate that had the reaction supported by *H. modesticaldum* progressed further we may have obtained a similar fractionation pattern since the product pool of Hg^0 had already approached ~ 0 ‰ (e.g. the starting composition of the Hg standard provided), once ~15 % of the Hg^{II} was reduced. However, it is likely that *H. modesticaldum* utilized a heavier pool of Hg^{II} at the beginning of the reaction since the earliest time point of Hg^0 the experiment (3h) was isotopically enriched as well. These results suggest that uptake or partitioning processes similar to those occurring in *G. sulfurreducens* may take place in *H. modesticaldum* creating an enrichment of isotopes due to the separation of isotope pools prior to kinetic reactions. The similarity in isotopic signal is highlighted here to suggest that similar processes may affect Hg delivery to intracellular sites for Hg transformation regardless of the Hg transformation in question. Although it is outside of the scope of the current study, identifying the nature of these processes may provide insights into central controls that exist for Hg uptake and transformation in anaerobes.

7.5 FUTURE STEPS

In this study we have provided the first evidence that MDF occurs during Hg reduction associated with anoxygenic photosynthesis in the model anaerobe *H. modesticaldum*. We show that the isotopic enrichment observed during anoxygenic phototrophic growth is different from what has been previously reported for abiotic photochemical Hg reduction and other microbial Hg reduction pathways. Overall, our study suggests that the mechanisms contributing to Hg stable isotope fractionation during anoxygenic photosynthesis are distinct from those driving photochemical, enzymatic and chemotrophic cometabolic Hg reduction.

One outstanding knowledge gap that remains is how fermentative Hg^{II} reduction will affect isotope fractionation in *H. modesticaldum* and potentially other strains that support a multitude of cometabolic Hg transformation pathways. Perhaps by changing to a fermentative pathway, a fractionation pattern similar to what has previously been reported in chemotrophic anaerobes [33] will be observed. Alternatively, perhaps the signal will remain the same, suggesting a common mechanism driving Hg^{II} reduction regardless of the metabolic pathway employed. Given that all chemotrophic Hg reduction pathways examined to date show no MIF [47] it is assumed none will be observed under fermentative conditions. With a method now in hand that can reliably measure Hg isotope fractionation under strictly anoxic conditions and a wide range of growth temperatures, such research questions are ripe for exploration.

The distinction observed between our results and those of other microbial Hg transformation pathways underscore that Hg stable isotope fractionation is a powerful tool for studying microbial Hg transformations in the absence of identified genetic targets. Although it remains challenging to extend laboratory scale observations to the environment where several pathways likely contribute to isotope fractionation, additional work on Hg stable isotope fractionation during anaerobic Hg reduction may provide an isotopic signature that can be used to track these pathways in the environment. Such a discovery would offer a powerful tool for evaluating the processes that control the delivery of Hg to anoxic methylation sites, which has long eluded researchers.

7.6 FUNDING INFORMATION

Our work was funded by NSERC Discovery and Accelerator grants, CFI funding to AJP and NSERC graduate scholarship to DSG.

7.7 ACKNOWLEDGMENTS

We would like to thank Noémie Lavoie for help growing the microbial cultures and preparing material used in isotope experiments.

7.8 AUTHOR CONTRIBUTIONS

DSG, AJP, SEJ and MTT designed all experiments; DSG carried out bioreactor experiments; SEJ and MTT carried out total Hg and stable isotope analyses; DSG, AJP, SEJ and MTT wrote the manuscript.

7.9 REFERENCES

1. Selin, N. E., Global biogeochemical cycling of mercury: A review. In 2009; Vol. 34, pp 43-63.

2. Parks, J. M.; Johs, A.; Podar, M.; Bridou, R.; Hurt Jr, R. A.; Smith, S. D.; Tomanicek, S. J.; Qian, Y.; Brown, S. D.; Brandt, C. C.; Palumbo, A. V.; Smith, J. C.; Wall, J. D.; Elias, D. A.; Liang, L., The genetic basis for bacterial mercury methylation. *Science* **2013,** *339*, (6125), 1332-1335.

3. Fleming, E. J.; Mack, E. E.; Green, P. G.; Nelson, D. C., Mercury methylation from unexpected sources: Molybdate-inhibited freshwater sediments and an iron-reducing bacterium. *Applied and Environmental Microbiology* **2006,** *72*, (1), 457-464.

4. Han, S.; Narasingarao, P.; Obraztsova, A.; Gieskes, J.; Hartmann, A. C.; Tebo, B. M.; Allen, E. E.; Deheyn, D. D., Mercury speciation in marine sediments under sulfate-limited conditions. *Environmental Science and Technology* **2010,** *44*, (10), 3752-3757.

5. Podar, M.; Gilmour, C. C.; Brandt, C. C.; Soren, A.; Brown, S. D.; Crable, B. R.; Palumbo, A. V.; Somenahally, A. C.; Elias, D. A., Global prevalence and distribution of genes and microorganisms involved in mercury methylation. *Science Advances* **2015,** *1*, 1-13.

6. Gustin, M. S.; Biester, H.; Kim, C. S., Investigation of the light-enhanced emission of mercury from naturally enriched substrates. *Atmospheric Environment* **2002,** *36*, (20), 3241-3254.

7. Amyot, M.; Lean, D.; Mierle, G., Photochemical formation of volatile mercury in high Arctic lakes. *Environmental Toxicology and Chemistry* **1997,** *16*, (10), 2054-2063.

8. Whalin, L.; Kim, E. H.; Mason, R., Factors influencing the oxidation, reduction, methylation and demethylation of mercury species in coastal waters. *Marine Chemistry* **2007,** *107*, (3), 278-294.

9. Poulain, A. J.; Amyot, M.; Findlay, D.; Findlay, S.; Telor, S.; Barkay, T.; Hintelmann, H.; Amyot, M.; Findlay, D., Biological and photochemical production of dissolved gaseous mercury in a boreal lake. *Limnology* **2011,** *49*, 2265-2275.

10. Carpi, A.; Lindberg, S. E., Sunlight-mediated emission of elemental mercury from soil amended with municipal sewage sludge. *Environmental Science and Technology* **1997,** *31*, (7), 2085-2091.

11. Vandal, G. M.; Fitzgerald, W. F.; Rolfhus, K. R.; Lamborg, C. H., Modeling the elemental mercury cycle in Pallette Lake, Wisconsin, USA. *Water, air, and soil pollution* **1995,** *80*, (1-4), 529-538.

12. Zhang, H.; Lindberg, S. E., Sunlight and iron(III)-induced photochemical production of dissolved gaseous mercury in freshwater. *Environmental Science and Technology* **2001,** *35*, (5), 928-935.

13. Zhang, H., Photochemical redox reactions of mercury. In *Recent Developments in Mercury Science*, Atwood, D. A., Ed. 2006; Vol. 120, pp 37-79.

14. O'Driscoll, N. J.; Lean, D. R. S.; Loseto, L. L.; Carignan, R.; Siciliano, S. D., Effect of dissolved organic carbon on the photoproduction of dissolved gaseous mercury in lakes: Potential impacts of forestry. *Environmental science & technology* **2004,** *38*, (9), 2664-2672.

15. Gu, B.; Bian, Y.; Miller, C. L.; Dong, W.; Jiang, X.; Liang, L., Mercury reduction and complexation by natural organic matter in anoxic environments. *Proceedings of the National Academy of Sciences of the United States of America* **2011,** *108*, (4), 1479-1483.

16. Wiatrowski, H. A.; Das, S.; Kukkadapu, R.; Ilton, E. S.; Barkay, T.; Yee, N., Reduction of Hg(II) to Hg(0) by magnetite. *Environmental Science and Technology* **2009,** *43*, (14), 5307-5313.

17. Bone, S. E.; Bargar, J. R.; Sposito, G., Mackinawite (FeS) reduces mercury(II) under sulfidic conditions. *Environmental Science & Technology* **2014,** *48,* (18), 10681-10689.

18. Wiatrowski, H. A.; Ward, P. M.; Barkay, T., Novel reduction of mercury(II) by mercury-sensitive dissimilatory metal reducing bacteria. *Environmental Science and Technology* **2006,** *40,* (21), 6690-6696.

19. Lu, X.; Liu, Y.; Johs, A.; Zhao, L.; Wang, T.; Yang, Z.; Lin, H.; Elias, D. A.; Pierce, E. M.; Liang, L.; Barkay, T.; Gu, B., Anaerobic mercury methylation and demethylation by *Geobacter bemidjiensis* Bem. *Environmental Science and Technology* **2016,** *50,* (8), 4366-4373.

20. Lin, H.; Morrell-Falvey, J. L.; Rao, B.; Liang, L.; Gu, B., Coupled mercury-cell sorption, reduction, and oxidation on methylmercury production by *Geobacter sulfurreducens* PCA. *Environmental Science and Technology* **2014,** *48,* (20), 11969-11976.

21. Grégoire, D. S.; Lavoie, N. C.; Poulain, A. J., Heliobacteria reveal fermentation as a key pathway for mercury reduction in anoxic environments. *Environmental Science and Technology* **2018,** *52,* 4145-4153.

22. Grégoire, D. S.; Poulain, A. J., A physiological role for Hg(II) during phototrophic growth. *Nature Geoscience* **2016,** *9,* (2), 121-125.

23. Barkay, T.; Kritee, K.; Boyd, E.; Geesey, G., A thermophilic bacterial origin and subsequent constraints by redox, light and salinity on the evolution of the microbial mercuric reductase. *Environmental Microbiology* **2010,** *12,* (11), 2904-2917.

24. Grégoire, D. S.; Poulain, A. J., A little bit of light goes a long way: The role of phototrophs on mercury cycling. *Metallomics* **2014,** *6*, (3), 396-407.

25. Poulin, B. A.; Aiken, G. R.; Nagy, K. L.; Monceau, A.; Krabbenhoft, D. P.; Ryan, J. N., Mercury transformation and release differs with depth and time in a contaminated riparian soil during simulated flooding. *Geochimica Et Cosmochimica Acta* **2016,** *176*, 118-138.

26. Bouffard, A.; Amyot, M., Importance of elemental mercury in lake sediments. *Chemosphere* **2009,** *74*, (8), 1098-1103.

27. Grégoire, D. S.; Poulain, A. J., Shining light on recent advances in microbial mercury cycling. *FACETS* **2018,** *3*, (1), 858-879.

28. Blum, J. D.; Sherman, L. S.; Johnson, M. W., Mercury isotopes in Earth and environmental sciences. *Annual Review of Earth and Planetary Sciences* **2014,** *42*, (1), 249-269.

29. Bergquist, B. A.; Blum, J. D., Mass-dependent and -independent fractionation of Hg isotopes by photoreduction in aquatic systems. *Science* **2007,** *318*, (5849), 417-420.

30. Bergquist, B. A.; Blum, J. D., The odds and evens of mercury isotopes: Applications of mass-dependent and mass-independent isotope fractionation. *Elements* **2009,** *5*, (6), 353-357.

31. Kritee, K.; Blum, J. D.; Johnson, M. W.; Bergquist, B. A.; Barkay, T., Mercury stable isotope fractionation during reduction of Hg(II) to Hg(0) by mercury resistant microorganisms. *Environmental Science and Technology* **2007,** *41*, (6), 1889-1895.

32. Kritee, K.; Barkay, T.; Blum, J. D., Mass dependent stable isotope fractionation of mercury during mer mediated microbial degradation of monomethylmercury. *Geochimica et Cosmochimica Acta* **2009,** *73*, (5), 1285-1296.

33. Kritee, K.; Blum, J. D.; Barkay, T., Mercury stable isotope fractionation during reduction of Hg(II) by different microbial pathways. *Environmental Science & Technology* **2008,** *42*, (24), 9171-9177.

34. Rodríguez-González, P.; Epov, V. N.; Bridou, R.; Tessier, E.; Guyoneaud, R.; Monperrus, M.; Amouroux, D., Species-specific stable isotope fractionation of mercury during Hg(II) methylation by an anaerobic bacteria (*Desulfobulbus propionicus*) under dark conditions. *Environmental Science & Technology* **2009,** *43*, (24), 9183-9188.

35. Perrot, V.; Bridou, R.; Pedrero, Z.; Guyoneaud, R.; Monperrus, M.; Amouroux, D., Identical Hg isotope mass dependent fractionation signature during methylation by sulfate-reducing bacteria in sulfate and sulfate-free environment. *Environmental Science & Technology* **2015,** *49*, (3), 1365-1373.

36. Janssen, S. E.; Schaefer, J. K.; Barkay, T.; Reinfelder, J. R., Fractionation of mercury stable isotopes during microbial methylmercury production by iron- and sulfate-reducing bacteria. *Environmental Science & Technology* **2016,** *50*, (15), 8077-8083.

37. Kritee, K.; Motta, L. C.; Blum, J. D.; Tsui, M. T.-K.; Reinfelder, J. R., Photomicrobial visible light-induced magnetic mass independent fractionation of mercury in a marine microalga. *ACS Earth and Space Chemistry* **2017**.

38. EPA, U., Method 1631, Revision E: Mercury in water by oxidation, purge and trap, and cold vapor atomic fluorescence spectrometry. In US Environmental Protection Agency Washington, DC: 2002.

39. Yin, R.; Krabbenhoft, D. P.; Bergquist, B. A.; Zheng, W.; Lepak, R. F.; Hurley, J. P., Effects of mercury and thallium concentrations on high precision determination of mercury isotopic composition by Neptune Plus multiple collector inductively coupled plasma mass spectrometry. *Journal of Analytical Atomic Spectrometry* **2016,** *31*, (10), 2060-2068.

40. Blum, J. D.; Bergquist, B. A., Reporting of variations in the natural isotopic composition of mercury. *Analytical and Bioanalytical Chemistry* **2007,** *388*, (2), 353-359.

41. Lepak, R. F.; Yin, R.; Krabbenhoft, D. P.; Ogorek, J. M.; DeWild, J. F.; Holsen, T. M.; Hurley, J. P., Use of stable isotope signatures to determine mercury sources in the Great Lakes. *Environmental Science & Technology Letters* **2015,** *2*, (12), 335-341.

42. Tang, K. H.; Feng, X. Y.; Zhuang, W. Q.; Alvarez-Cohen, L.; Blankenship, R. E.; Tang, Y. J., Carbon flow of Heliobacteria is related more to Clostridia than to the green sulfur bacteria. *Journal of Biological Chemistry* **2010,** *285*, (45), 35104-35112.

43. Richardson, D. J.; King, G. F.; Kelly, D. J.; McEwan, A. G.; Ferguson, S. J.; Jackson, J. B., The role of auxiliary oxidants in maintaining redox balance during phototrophic growth of *Rhodobacter capsulatus* on propionate or butyrate. *Archives of Microbiology* **1988,** *150*, (2), 131-137.

44. Colombo, M. J.; Ha, J.; Reinfelder, J. R.; Barkay, T.; Yee, N., Anaerobic oxidation of Hg(0) and methylmercury formation by *Desulfovibrio desulfuricans* ND132. *Geochimica et Cosmochimica Acta* **2013,** *112*, 166-177.

45. Colombo, M. J.; Ha, J.; Reinfelder, J. R.; Barkay, T.; Yee, N., Oxidation of Hg(0) to Hg(II) by diverse anaerobic bacteria. *Chemical Geology* **2014,** *363*, 334-340.

46. Icopini, G. A.; Anbar, A. D.; Ruebush, S. S.; Tien, M.; Brantley, S. L., Iron isotope fractionation during microbial reduction of iron: The importance of adsorption. *Geology* **2004,** *32,* (3), 205-208.

47. Kritee, K.; Blum, J. D.; Reinfelder, J. R.; Barkay, T., Microbial stable isotope fractionation of mercury: A synthesis of present understanding and future directions. *Chemical Geology* **2013,** *336,* 13-25.

7.10 FIGURES AND CAPTIONS

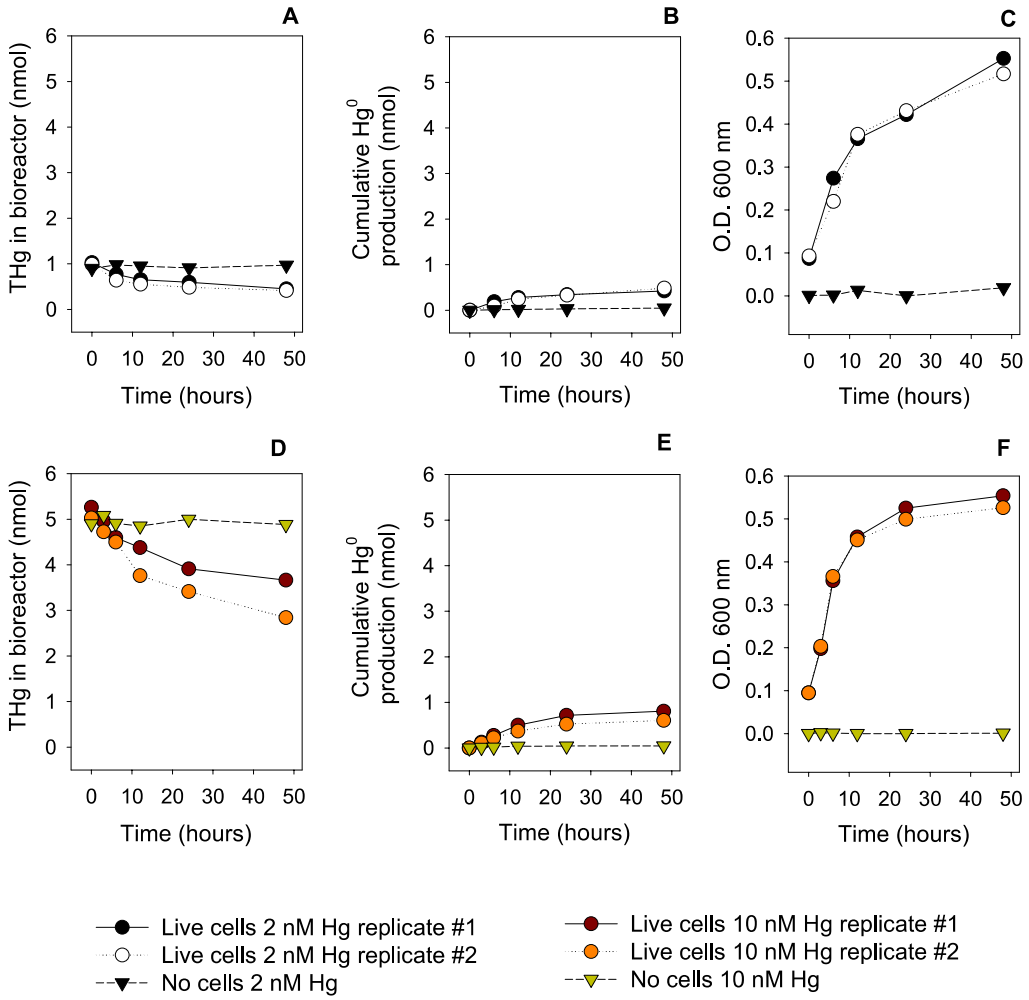

Figure 7.1: Total Hg and cumulative Hg^0 production by *H. modesticaldum* grown phototrophically. A, D THg for live cells and sterile controls without cells with 2 nM Hg and continuous bubbling (**A**) and 10 nM Hg with periodic bubbling (**D**). **B, E** Cumulative Hg^0 production for live cells and sterile controls without cells with 2 nM Hg and continuous bubbling (**B**) and 10 nM Hg with periodic bubbling (**E**). **C, F** Microbial growth as measured by O.D. 600 nm for live cells and sterile medium without cells with 2 nM Hg and continuous bubbling (**C**) and 10 nM Hg with periodic bubbling (**F**). All Hg was supplied from the same stock (NIST 3133).

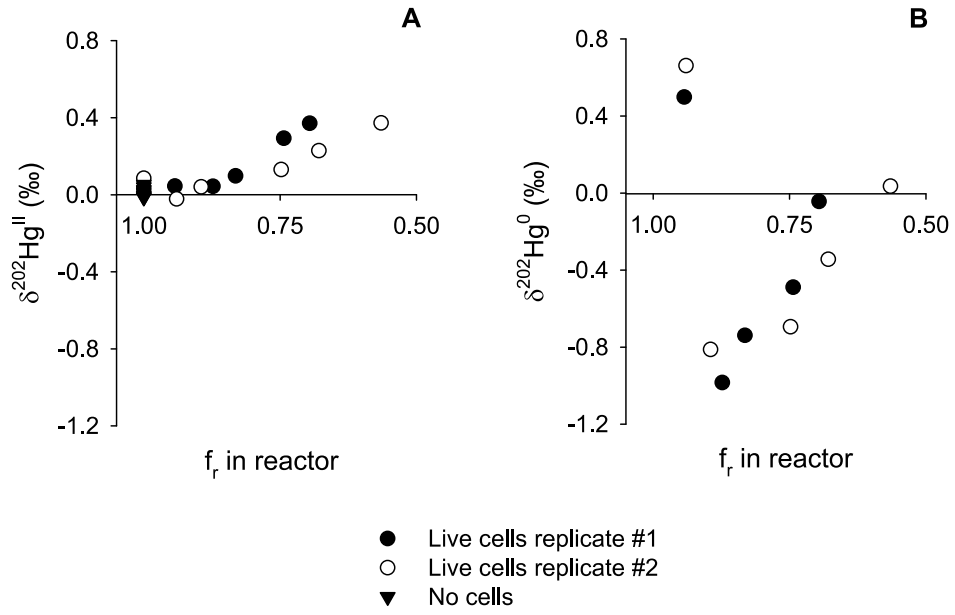

Figure 7.2: Mass dependent fractionation of ^{202}Hg in Hg^{II} (A) and Hg^0 (B) during phototrophic growth of *H. modesticaldum* and no cell control. δ^{202}Hg values for Hg^{II} and Hg^0 are plotted with respect to the fraction of remaining total inorganic Hg^{II} in the bioreactor. Insufficient Hg^0 was recovered from the no cell control and thus no results are displayed. Fitted lines are shown in **Figure D3** as are the fitting the parameters. 10 nM Hg was used in all experiments and Hg was supplied from the same stock (NIST 3133).

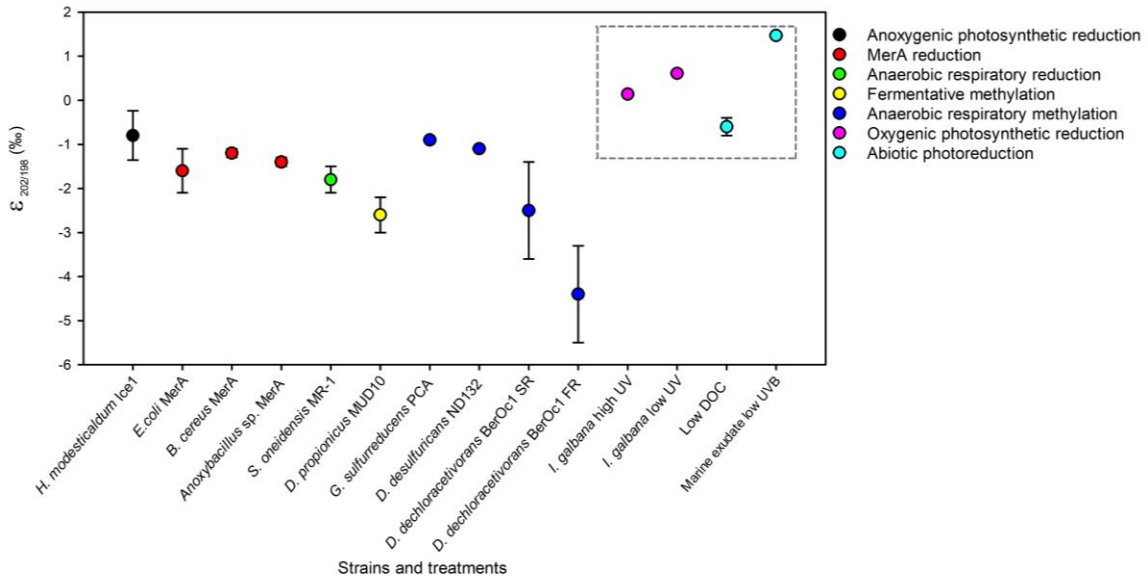

Figure 7.3: Compilation of isotopic enrichment factors from previous work on abiotic and biotic Hg^{II} reduction and biotic Hg^{II} methylation. Metabolisms are indicated based on colour coding and Hg transformations that are associated with mass-independent fractionation are outlined by grey dotted lines. The values in this figure were obtained form the following studies: anoxygenic photosynthetic reduction (this study), MerA reduction [33]; anaerobic respiration reduction [33]; fermentative methylation [34]; anaerobic respiration methylation [35, 36]; abiotic photodemethylation [29, 37]; oxygenic photosynthetic reduction [37]; abiotic photoreduction [29, 37]. Errors bars denote 2 standard deviations for studies where this data was available.

Chapter 8: Research synthesis

8.1 SUMMARY OF RESEARCH CONTRIBUTIONS

The overarching objective of my thesis research was to provide new mechanistic details for anaerobic and phototrophic Hg reduction pathways. By using a combination of physiological, biochemical and trace Hg analytical techniques, I have outlined novel Hg reduction pathways that rely on metabolic machinery central to anoxygenic photosynthesis and fermentation in a variety of anaerobic bacteria. At its core, my thesis frames anaerobic Hg reducers as key players in the global Hg cycle that can control the inorganic Hg substrates available for Hg methylation.

In **Chapter 4**, I tested the hypothesis that Hg reduction in PNSB was driven by a redox imbalance incurred during photoheterotrophic growth. In this study, I developed the first method for real-time measurements of anaerobic Hg^0 production at environmentally relevant concentrations of Hg (e.g. pM range). By carefully controlling growth conditions, I demonstrated that Hg^{II} was preferentially reduced by different PNSB when cells were supplied with light and reduced organic carbon. Furthermore, I showed that sublethal concentrations of Hg^{II} supported faster cell growth when cells were subject to a redox imbalance. These findings suggested that Hg could fulfill a physiological role as an electron sink during photoheterotrophic growth, similar to what has been observed for known redox homeostasis pathways such as inorganic carbon fixation [1, 2].

This was the first study to demonstrate that Hg^{II} reduction could be directly coupled to photosynthetic metabolism. In addition, this study was the first to show anoxygenic phototrophs could participate directly in Hg redox cycling. The rates of Hg^0 production observed in bioreactor experiments were in line with those from previous

work examining abiotic photoreduction [3] and Hg reduction in the metalimnion of thermally stratified aquatic ecosystems [4] (**Table A5**). When normalizing for the amount of light present in these experiments, I was able to show that PNSB were more efficient at reducing Hg^{II} per mol of photon compared to abiotic photoreduction (38 to 185 pmol L^{-1}. mol_{photon} m^2 in PNSB vs 0.01 to 1 pmol L^{-1}. mol_{photon} m^2 via abiotic photoreduction, **Table A6**). This finding suggests that PNSB can catalyze Hg redox cycling at low light intensities, providing a potential explanation for past trends where peaks in Hg^0 concentration have been observed in environments where photoreduction is limited [3-6]. Given that PNSB are ubiquitous in aquatic ecosystems [7], this study supports that anoxygenic phototrophs are important players in the Hg cycle of anoxic habitats where Hg methylation occurs.

In the follow up study presented in **Chapter 5**, I tested whether the Hg reduction pathways observed in PNSB were present in ecologically and phylogenetically distinct families of anoxygenic phototrophs. Furthermore, I wanted to assess whether anoxygenic phototrophs had the potential to control Hg's fate in rice paddies where flooded conditions support Hg methylation. To that gain, I explored mechanisms for Hg reduction in *Heliobacterium modesticaldum* Ice1, a representative from the family Heliobacteria capable of photoheterotrophic and fermentative growth.

In contrast with PNSB, *H. modesticaldum* preferentially reduced Hg^{II} during chemotrophic fermentative growth when all reducing power would normally go towards the energetic and biosynthetic needs of the cell. Although I was unable to demonstrate that redox imbalance drove Hg^{II} reduction, I found little evidence of a beneficial role for Hg during phototrophic and fermentative growth. By using physiological experiments

and metabolic inhibitors, I showed that Hg^{II} reduction relied on the ability of cells to generate reduced redox cofactors (most likely ferredoxin) through the photosynthetic electron transport chain and organic carbon oxidation in the absence of light. A similar mechanism was also observed in the fermenter *C. acetobutylicum*, which suggests that fermentative pathways for Hg reduction are potentially widespread in anoxic habitats.

The findings from **Chapter 5** further support that anoxygenic phototrophs play an important role in Hg redox cycling in both aquatic and terrestrial habitats. This study was the first study to propose a mechanism for fermentative Hg^{II} reduction in environments where light and external electron acceptors are limited. Furthermore, *H. modesticaldum* ended up being one of the best anaerobic Hg^{II} reducers recorded to date, suggesting that Heliobacteria play an important role in controlling Hg's fate in anoxic terrestrial environments. This finding is meaningful in the context of rice paddies where Hg accumulation is becoming a global food safety issue because the majority of Heliobacteria isolates originate from such environments [8]. The conclusions from this study and those from **Chapter 4** show that the redox conditions supporting cometabolic Hg^{II} reduction are more diverse than what has previously been reported. This study adds to the growing list of anaerobic metabolisms that support Hg^{II} reduction, which now includes anaerobic respiration, anoxygenic photosynthesis and fermentation (**Table 5.1**).

In **Chapter 6**, I shifted my focus away from pathways that generate reducing power to examine how assimilatory sulphur pathways that consume reducing power could control Hg^{II} reduction during anoxygenic photosynthesis. In this study I worked with *Heliobacillus mobilis* Romero/Guest 6, a Heliobacteria strain isolated from a rice paddy. I tested whether oxidized sulphur sources that required considerable reducing

power to assimilate into biomass would limit Hg^{II} reduction compared to more reduced sulphur sources that required less reducing power to incorporate into cell material. Although I faced a number of challenges linking complex assimilatory pathways to the reducing power available for Hg reduction, this study showed that more reduced sulphur sources did indeed support higher levels of Hg^0 production. The finding that *H. mobilis* could reduce Hg^{II} at comparable rates to *H. modesticaldum* further underscored the importance of Heliobacteria in rice paddy Hg cycling.

Given the importance of sulphur as a nutrient for Hg methylating SRB, the findings from this study suggest common pools of nutrients play an important role in controlling competing microbial Hg transformations in anoxic habitats. In the context of rice paddies, anaerobic Hg reducers may couple thiosulphate assimilation to Hg^{II} reduction, which could favour Hg^0 evasion from shallow paddy systems and limit the availability of terminal electron acceptors to Hg methylating SRB [9, 10]. Anaerobic Hg reducers may also outcompete methylators for Hg bound to cysteine, which can serve as a substrate for MeHg production [11, 12]. Importantly, this study also highlights the other extreme that can occur in the environment wherein anaerobic Hg reducers produce little Hg^0 in the presence of oxidized sulphate, which could instead stimulate MeHg production by SRB [13]. Ultimately, this study revealed the importance of considering how both assimilatory and dissimilatory pathways affect the overall redox state of the cell, which plays an important role in mediating cometabolic Hg^{II} reduction.

Unlike the other chapters in my thesis that were primarily hypothesis-driven, the work presented in **Chapter 7** outlined new analytical tools using Hg stable isotope fractionation to study anaerobic Hg reduction. This study was primarily motivated by the lack of dedicated genetic tools that exist for studying anaerobic Hg redox cycling in Heliobacteria strains and the challenges associated with detecting anaerobic Hg redox cycling in the environment. This study provided the first evidence of MDF for Hg reduction during anoxygenic photosynthesis in *H. modesticaldum* (e.g. cells preferentially reduced lighter Hg^{II}) and showed that no MIF occurred, similar to what has been observed for other microbial Hg reduction pathways [14, 15]. Interestingly, the isotopic enrichment calculated for phototrophically grown *H. modesticaldum* was in between the values reported for abiotic photoreduction [16, 17] and microbial Hg reduction [14, 15]. This finding suggests that although the isotope fractionation processes supported during anoxygenic phototrophic reduction bear some semblance to those that occur in light catalyzed and chemotrophic Hg reduction pathways, they ultimately remain distinct.

Although this method proved challenging to develop, particularly with respect to collecting enough Hg^0 for reliable isotope analyses, it revealed how Hg stable isotopes can be used to characterize different anaerobic Hg reduction pathways in the absence of a genetic system. It is difficult to extend the conclusions from **Chapter 7** to the environmental scale given the controlled nature of the experiments performed, however this study provides the basis for further exploration of the isotopic signatures associated with anaerobic Hg reduction pathways. Eventually, such studies may lead to the development of biogeochemical proxies that can be used to track cryptic anaerobic Hg redox cycling pathways in the environment.

8.2 ENVIRONMENTAL CONTEXT

The findings from my thesis suggest that anaerobic and phototrophic Hg redox cycling pathways are widespread in the environment. By focussing on the mechanistic details of anaerobic Hg reduction pathways, I was able to identify several variables including light intensity, organic carbon source composition and concentration, electron sink availability and sulphur source redox state, that can be used to further explore which habitats are hotspots for anaerobic Hg reduction. Validating whether similar controls exist at the environmental scale will be a key step in characterizing the ecological niches that can support anaerobic Hg reduction. By comparing where the niches of anaerobic Hg reducers overlap with those of Hg methylators, we can develop a better understanding of how microbial Hg redox cycling can limit MeHg accumulation in the environment.

Characterizing the contributions of anaerobes and phototrophs to Hg cycling at the environmental scale will become increasingly important with ongoing global environmental change. As mentioned in **Chapter 1**, predicted increases in phytoplankton blooms and eutrophication will potentially lead to a cascading series of events that will influence Hg's mobility and toxicity in the environment. The findings from my thesis suggest that increased eutrophication may lead to increased Hg redox cycling because of increased photosynthetic and mixotrophic metabolic activity. Although such pathways may favour Hg^0 evasion, the presence of physical barriers in thermally stratified water columns could prevent Hg volatilization. This scenario may result in the release of Hg^0 from poorly bioavailable ligands that can subsequently be used as a substrate for Hg methylation (**Fig 3.1**) [18, 19]. The oxygen depletion resulting from organic matter degradation following eutrophication may further stimulate anoxygenic phototrophic and

chemotrophic Hg reduction pathways alongside Hg methylation in anoxic habitats. Despite the impact that anaerobic Hg reduction pathways may have on Hg accumulation in aquatic food webs, how eutrophication will affect the relative contributions of competing microbial Hg transformations that control Hg's bioavailability remains unknown.

In addition to improving our understanding of Hg cycling in the environment, the work presented in my thesis could serve as the basis for developing strategies to better manage Hg pollution in line with the goals set forth in the Minamata Convention. Such strategies could draw on designs from other industrial applications involving anaerobes and phototrophs such as wastewater treatment [20], solvent production [21] and biofuel generation [22], to develop systems that remove Hg from contaminated water and soil. These treatment methods could take the form of a closed bioreactor, similar to the type employed in the Hg^0 experiments presented throughout my thesis, where conditions are optimized for the removal of Hg^{II} and Hg^0 is captured following volatilization. Alternatively, the findings in **Chapter 6** suggest *in situ* strategies that rely on supplying environmental conditions conducive to favourable Hg transformations vs unfavourable ones (e.g. reduction vs methylation) could also be employed at minimal cost.

During my graduate studies, I took concrete steps to apply my research to meet industry needs by participating in the incubator program Startup Garage. Together with Dr. Alexandre Poulain, I created the company Microbright with the goal of developing biotechnology to manage Hg pollution in the mining industry. I have provided a summary of Microbright's progress over the last two years in **Appendix E** to illustrate the challenges involved in scaling laboratory research to meet industry needs.

8.3 EVOLUTION OF ANAEROBIC MERCURY METABOLISM

One of the core findings from my research is that there exists an intimate link between cellular redox metabolism and cometabolic Hg^{II} reduction. Although such a link may seem intuitive given that reducing power is required to reduce oxidized molecules, linking the overall redox state of the cell to Hg^{II} reduction is rarely discussed. When we consider that anaerobes and anoxygenic phototrophs were present on Earth before the rise of oxygen [23], perhaps the ability to reduce Hg^{II} to Hg^{0} as a by-product of metabolism precluded the need for costly detoxification strategies such as the *mer* operon [24]. Given the diversity of anaerobes that are known to reduce Hg^{II}, the ability to reduce Hg may simply depend on cells being supplied with redox conditions optimized for specific anaerobic metabolic pathways that can support Hg reduction. If this is indeed the case, the work published to date on anaerobic and phototrophic Hg reduction has just scratched the surface of the diversity of microbes capable of Hg redox cycling.

Although there is little evidence of functioning *mer*-based strategies in anaerobes and phototrophs, there are a small number of reports that show *mer* homologues may be present in anaerobes and phototrophs [19]. With the increased availability of genomic information, it is entirely possible that novel *mer* operons may be uncovered in anaerobes and phototrophs. In the event that such pathways are discovered, it will be interesting to compare what selective forces drive the adoption *mer*-based vs. cometabolic Hg reduction strategies. Such a comparison would provide valuable insight into how microbes have adapted to tolerate Hg stress and potentially use otherwise toxic metals in their metabolism throughout Earth's history.

8.4 LIMITATIONS AND RECOMMENDATIONS

One of the more challenging aspects of using a physiological approach to elucidate mechanisms for microbial Hg reduction is linking Hg redox cycling to the redox state of the cell. Although I was able to do so in **Chapter 4**, this proved challenging in other experiments where cells did not yield enough biomass to effectively extract redox cofactors under the conditions tested. Future experiments would benefit from adopting more refined analytical techniques such as liquid chromatography mass spectrometry [25] or developing biosensors that can track the ratio of redox cofactors *in vivo* as has been done in past work [26]. In the context of obligate anaerobes, it will be important that such methods are optimized for completely anoxic conditions to provide an accurate picture of the relationship between anaerobic metabolism, cell redox state and Hg reduction.

In addition to improving the analysis of redox cofactors, future work should also consider using molecular approaches such as gene knockdowns or deletions to resolve mechanistic details for anaerobic Hg reduction pathways. These techniques could be coupled with proteomic or transcriptomic analyses in well-characterized model organisms to tease apart the metabolic coupling points that exist between Hg reduction and anaerobic metabolism. Such studies have recently been carried in the DMRB, *G. sulfurreducens* [27, 28], however this type of approach has yet to be applied to phototrophic or fermentative Hg reduction. These experiments will be important for identifying the physiological controls that exist for cometabolic Hg transformations and developing genetic targets that can be used to track anaerobic Hg reduction in the environment.

It is important to note that all of the experiments in my thesis were done using pure cultures under carefully controlled growth conditions. Although this was a necessary step for elucidating the mechanism supporting Hg reduction, it is not representative of microbial communities in the environment. Given the potential implications that anaerobic Hg reduction can have on Hg methylation, future work should consider using co-culture experiments with model anaerobic Hg reducers and Hg methylators to better understand how these pathways interact in the environment. Such experiments would provide a strong basis for environmental scale work that addresses how anaerobic Hg redox cycling affects MeHg production in natural microbial communities.

8.5 REFERENCES

1. Richardson, D. J.; King, G. F.; Kelly, D. J.; McEwan, A. G.; Ferguson, S. J.; Jackson, J. B., The role of auxiliary oxidants in maintaining redox balance during phototrophic growth of *Rhodobacter capsulatus* on propionate or butyrate. *Archives of Microbiology* **1988,** *150*, (2), 131-137.

2. McKinlay, J. B.; Harwood, C. S., Carbon dioxide fixation as a central redox cofactor recycling mechanism in bacteria. *Proceedings of the National Academy of Sciences of the United States of America* **2010,** *107*, (26), 11669-11675.

3. Amyot, M.; Mierle, G.; Lean, D.; McQueen, D. J., Effect of solar radiation on the formation of dissolved gaseous mercury in temperate lakes. *Geochimica et Cosmochimica Acta* **1997,** *61*, (5), 975-987.

4. Poulain, A. J.; Amyot, M.; Findlay, D.; Telor, S.; Barkay, T.; Hintelmann, H., Biological and photochemical production of dissolved gaseous mercury in a boreal lake. *Limnology and Oceanography* **2004,** *49*, (6), 2265-2275.

5. Peretyazhko, T.; Charlet, L.; Muresan, B.; Kazimirov, V.; Cossa, D., Formation of dissolved gaseous mercury in a tropical lake (Petit-Saut reservoir, French Guiana). *Science of the Total Environment* **2006,** *364*, (1-3), 260-271.

6. Vandal, G. M.; Fitzgerald, W. F.; Rolfhus, K. R.; Lamborg, C. H., Modeling the elemental mercury cycle in Pallette Lake, Wisconsin, USA. *Water, air, and soil pollution* **1995,** *80*, (1-4), 529-538.

7. Raven, J. A., Contributions of anoxygenic and oxygenic phototrophy and chemolithotrophy to carbon and oxygen fluxes in aquatic environments. *Aquatic Microbial Ecology* **2009,** *56*, (2-3), 177-192.

8. Asao, M.; Madigan, M. T., Taxonomy, phylogeny, and ecology of the Heliobacteria. *Photosynthesis Research* **2010,** *104*, (2-3), 103-111.

9. Dias, M.; Salvado, J. C.; Monperrus, M.; Caumette, P.; Amouroux, D.; Duran, R.; Guyoneaud, R., Characterization of *Desulfomicrobium salsuginis* sp nov and *Desulfomicrobium aestuarii* sp nov., two new sulfate-reducing bacteria isolated from the Adour estuary (French Atlantic coast) with specific mercury methylation potentials. *Systematic and Applied Microbiology* **2008,** *31*, (1), 30-37.

10. Ranchou-Peyruse, M.; Goni-Urriza, M.; Guignard, M.; Goas, M.; Ranchou-Peyruse, A.; Guyoneaud, R., *Pseudodesulfovibrio hydrargyri* sp nov., a mercury-methylating bacterium isolated from a brackish sediment. *International Journal of Systematic and Evolutionary Microbiology* **2018,** *68*, (5), 1461-1466.

11. Lu, X.; Liu, Y.; Johs, A.; Zhao, L.; Wang, T.; Yang, Z.; Lin, H.; Elias, D. A.; Pierce, E. M.; Liang, L.; Barkay, T.; Gu, B., Anaerobic mercury methylation and demethylation by *Geobacter bemidjiensis* Bem. *Environmental Science and Technology* **2016,** *50*, (8), 4366-4373.

12. Liu, Y. R.; Lu, X.; Zhao, L. D.; An, J.; He, J. Z.; Pierce, E. M.; Johs, A.; Gu, B. H., Effects of cellular sorption on mercury bioavailability and methylmercury production by *Desulfovibrio desulfuricans* ND132. *Environmental Science & Technology* **2016,** *50*, (24), 13335-13341.

13. Gilmour, C. C.; Henry, E. A.; Mitchell, R., Sulfate stimulation of mercury methylation in freshwater sediments. *Environmental Science and Technology* **1992,** *26*, (11), 2281-2287.

14. Kritee, K.; Blum, J. D.; Johnson, M. W.; Bergquist, B. A.; Barkay, T., Mercury stable isotope fractionation during reduction of Hg(II) to Hg(0) by mercury resistant microorganisms. *Environmental Science and Technology* **2007,** *41*, (6), 1889-1895.

15. Kritee, K.; Blum, J. D.; Barkay, T., Mercury stable isotope fractionation during reduction of Hg(II) by different microbial pathways. *Environmental Science & Technology* **2008,** *42*, (24), 9171-9177.

16. Kritee, K.; Blum, J. D.; Reinfelder, J. R.; Barkay, T., Microbial stable isotope fractionation of mercury: A synthesis of present understanding and future directions. *Chemical Geology* **2013,** *336*, 13-25.

17. Bergquist, B. A.; Blum, J. D., Mass-dependent and -independent fractionation of Hg isotopes by photoreduction in aquatic systems. *Science* **2007,** *318*, (5849), 417-420.

18. Colombo, M. J.; Ha, J.; Reinfelder, J. R.; Barkay, T.; Yee, N., Anaerobic oxidation of Hg(0) and methylmercury formation by *Desulfovibrio desulfuricans* ND132. *Geochimica et Cosmochimica Acta* **2013,** *112*, 166-177.

19. Grégoire, D. S.; Poulain, A. J., Shining light on recent advances in microbial mercury cycling. *FACETS* **2018,** *3*, (1), 858-879.

20. Hülsen, T.; Batstone, D. J.; Keller, J., Phototrophic bacteria for nutrient recovery from domestic wastewater. *Water Research* **2014,** *50*, 18-26.

21. Lutke-Eversloh, T.; Bahl, H., Metabolic engineering of *Clostridium acetobutylicum*: Recent advances to improve butanol production. *Current Opinion in Biotechnology* **2011,** *22*, (5), 634-647.

22. McKinlay, J. B.; Harwood, C. S., Photobiological production of hydrogen gas as a biofuel. *Current Opinion in Biotechnology* **2010,** *21*, (3), 244-251.

23. Anbar, A. D., Elements and Evolution. *Science* **2008,** *322*, (5907), 1481-1483.

24. Barkay, T.; Kritee, K.; Boyd, E.; Geesey, G., A thermophilic bacterial origin and subsequent constraints by redox, light and salinity on the evolution of the microbial mercuric reductase. *Environmental Microbiology* **2010,** *12*, (11), 2904-2917.

25. Sander, K.; Asano, K. G.; Bhandari, D.; Van Berkel, G. J.; Brown, S. D.; Davison, B.; Tschaplinski, T. J., Targeted redox and energy cofactor metabolomics in *Clostridium thermocellum* and *Thermoanaerobacterium saccharolyticum*. *Biotechnology for Biofuels* **2017,** *10*.

26. Knudsen, J. D.; Carlquist, M.; Gorwa-Grauslund, M., NADH-dependent biosensor in *Saccharomyces cerevisiae*: principle and validation at the single cell level. *Amb Express* **2014,** *4*.

27. Lin, H.; Hurt, R. A.; Johs, A.; Parks, J. M.; Morrell-Falvey, J. L.; Liang, L.; Elias, D. A.; Gu, B., Unexpected effects of gene deletion on interactions of mercury with the methylation-deficient mutant Δ*hgcAB*. *Environmental Science and Technology Letters* **2014,** *1*, (5), 271-276.

28. Qian, C.; Johs, A.; Chen, H.; Mann, B. F.; Lu, X.; Abraham, P. E.; Hettich, R. L.; Gu, B., Global proteome response to deletion of genes related to mercury methylation and dissimilatory metal reduction reveals changes in respiratory metabolism in *Geobacter sulfurreducens* PCA. *Journal of Proteome Research* **2016,** *15*, (10), 3540-3549.

Appendix A: Supporting information for Chapter 4

Daniel S. Grégoire [a] & Alexandre J. Poulain [a]

a - Biology Department, University of Ottawa, 30 Marie Curie, Ottawa, ON, K1N 6N5, Canada.

This appendix was originally published as supporting information accompanying:

Grégoire, D.S.; Poulain, A.J., A physiological role for Hg(II) during phototrophic growth. *Nature Geoscience* **2016,** *9***,** (2)**,** 121-125.

Direct link: https://www.nature.com/articles/ngeo2629

LIST OF SUPPORTING MATERIALS:
SUPPORTING METHODS

- **Section 1**: Summary of growth conditions employed in bioreactor experiments
- **Section 2**: Thermodynamic calculations
- **Section 3**: Bioreactor setup and elemental mercury measurements

SUPPORTING RESULTS AND DISCUSSION

- **Section 4**: Total mercury and water mass balance
- **Section 5**: Hg^0 production experiments for *Rhodobacter capsulatus* grown phototrophically on 15 mM butyrate supplied with 20 mM HCO_3^-, 1 µM Fe^{III}-citrate or 20 mM NO_3^- as KNO_3
- **Section 6**: Comparison of growth rate calculations for phototrophic cultures of *Rhodobacter capsulatus* supplied with sublethal concentrations of Hg
- **Section 7:** Hg^0 production for anaerobic metabolism and photochemical processes

SUPPORTING TABLES AND FIGURES

- **Table A1**: Summary of growth conditions for bioreactor cultures
- **Table A2**: Concentration ranges of products and reactants involved in the oxidation of butyrate to CO_2, polyhydroxybutyrate or biomass and coupled to the reduction of Hg^{2+}
- **Table A3**: Reactions and ΔG^0 for the oxidation of butyrate coupled to dimethylsulphoxide reduction.
- **Table A4**: Reactions, ΔG^0 and ΔG for the oxidation of butyrate coupled to Hg^{II} reduction.
- **Table A5:** Hg^0 production rates for anaerobic metabolism and photochemical processes.
- **Table A6**: Hg^0 production rates for phototrophic metabolism and abiotic photochemical processes normalized for incoming light energy
- **Figure A1**: Bioreactor schematic
- **Figure A2:** Total Hg and water recoveries for all bioreactor experiments with live *R. capsulatus*
- **Figure A3:** Repeat experiments of Hg^0 production normalized for cell density and cumulative Hg^0 production for phototrophically grown *R. capsulatus* supplied with 15 mM butyrate in the absence of HCO_3^- vs 20 mM HCO_3^- and sterile medium amended with 10 mM HCO_3^-
- **Figure A4**: Hg^0 production for *R. capsulatus* grown phototrophically on 15 mM butyrate in the presence of 20 mM NO_3^- and 1 µM Fe^{III}-citrate.

SUPPORTING METHODS

Section 1: Summary of growth conditions employed in bioreactor experiments

Table A1: Summary of growth conditions for bioreactor cultures.

Metabolism	Presence of light (Y/N)	Presence of oxygen (Y/N)	Strain	[Carbon source] and [exogenous electron acceptor]
Phototrophy	Yes	No	*Rp. palustris* *R. sphaeroides*	30 mM acetate 15 mM butyrate [a]
			R. capsulatus	30 mM acetate 15 mM butyrate 15 mM butyrate + 1 µM Fe^{III}-citrate 15 mM butyrate + 100 µM HCO_3^- 15 mM butyrate + 10 mM HCO_3^- 15 mM butyrate + 20 mM HCO_3^- 15 mM butyrate + 1 nM DMSO 15 mM butyrate + 20 mM DMSO 15 mM butyrate + 20 mM KNO_3 [b]
Chemotrophy	No	Yes	*Rp. palustris* *R. sphaeroides* *R. capsulatus*	30 mM acetate 15 mM butyrate [c]

a- *Rp. palustris* grown on 15 mM butyrate required 10 mM HCO_3^- to achieve suitable cell densities for the bioreactor.

b- *R. capsulatus* grown on 15 mM butyrate and 20 mM KNO_3 required 10 mM HCO_3^- to achieve suitable densities for the bioreactor.

c- *R. sphaeroides* grew poorly chemotrophically on 15 mM butyrate and did not achieve cell densities suitable for bioreactor experiments, as such, this treatment was omitted.

Section 2: Thermodynamic calculations

Table A2: Concentration ranges of products and reactants involved in the oxidation of butyrate to CO_2, polyhydroxybutyrate (PHB) or biomass and coupled to the reduction of Hg^{2+}.

		Concentration (M)	References
Reactants	$[Hg^{2+}]$	$1x10^{-12}$ - $1x10^{-10}$	1
	[Butyrate]	$1x10^{-7}$ - $1x10^{-5}$	2, 3
	$[NH_4^+]$	$1x10^{-9}$ - $1x10^{-3}$	
Products	$[Hg^0]$	$1x10^{-13}$ - $1x10^{-10}$	1
	$[H^+]$	10^{-6} - $1x10^{-8}$	4
	$[HCO_3^-]$	$1x10^{-5}$ - $1x10^{-3}$	5
	[PHB]	$1x10^{-17}$ - $1x10^{-14}$	6a
	[Biomass]	$1x10^{-8}$ - $1x10^{-6}$	7b

[a]Assuming 24 fg of protein per cell, a concentration of 0.5 µg of PHB per mg of protein and $2x10^3$ cells.mL^{-1}.

[b] Assuming the mass of a cell at 1 pg and the molecular weight of a purple bacterium to be 22.426 g.mol^{-1} and an abundance of $2x10^3$ cells.mL^{-1}

Table A3: Reactions and ΔG^0 for the oxidation of butyrate coupled to DMSO reduction.

	$\Delta G^0 = -nF(\Delta E^0)$ (kJ.mol^{-1})
$C_4H_8O_2 + 6H_2O + 10(CH_3)_2SO \rightarrow 4CO_2 + 18H_+ + 10(CH_3)_2S$	-984.1
$n(C_4H8O_2) + (CH_3)_2SO \rightarrow (C_4H_6O_2)n + nH_+ + (CH_3)_2S$	-98.4
$2C_4H_8O_2 + 1.44NH_{4+} + 2.72(CH_3)_2SO \rightarrow 2CH_{1.8}N_{0.18}O_{0.38} + 0.96H_2O + 3.44H_+ + 2.72(CH_3)_2S$	-133.8

Table A4: Reactions, ΔG^0 and ΔG for the oxidation of butyrate coupled to Hg^{2+} reduction. The range of data provided for ΔG was calculated using the minima and maxima of concentration ranges.

	$\Delta G^0 = -nF(\Delta E^0)$ (kJ.mol^{-1})	$\Delta G = \Delta G^0 + RTlnQ$ (kJ.mol^{-1})
$C_4H_8O_2 + 6H_2O + 10Hg^{2+} \rightarrow 4CO_2 + 20H^+ + 10Hg^0$	-2219.2	(-3300) – (-2840)
$n(C_4H_8O_2) + Hg^{2+} \rightarrow (C_4H_6O_2)n + 2nH^+ + Hg^0$	-221.9	(-395) – (-162)
$2C_4H_8O_2 + 1.44NH_4^+ + 2.72Hg^{2+} \rightarrow 2CH_{1.8}N_{0.18}O_{0.38} + 0.96H_2O + 5.44H^+ + 2.72Hg^0$	-301.8	(-591) – (-383)

Section 3: Bioreactor setup and elemental mercury measurements

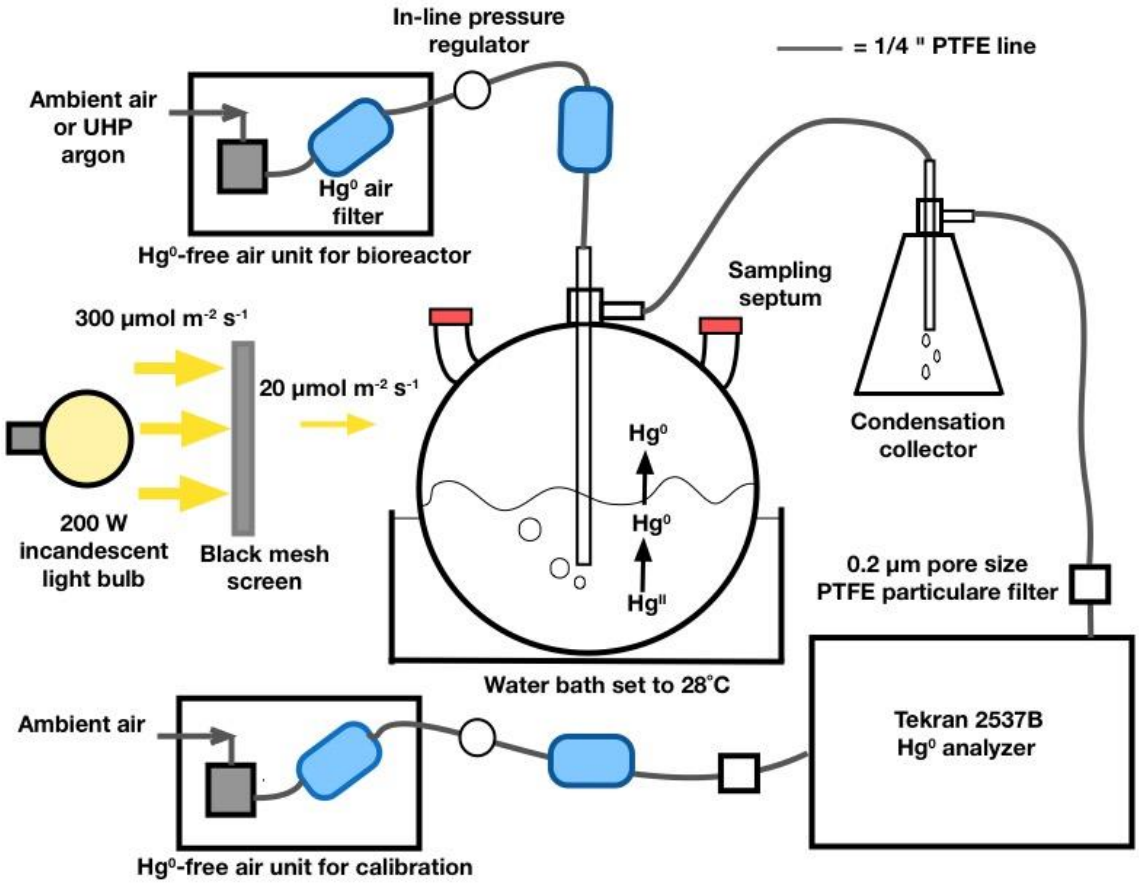

Figure A1: Schematic representation of bioreactor supplied with conditions for phototrophic growth.

SUPPORTING RESULTS

Section 4: Total Hg and water mass balance:

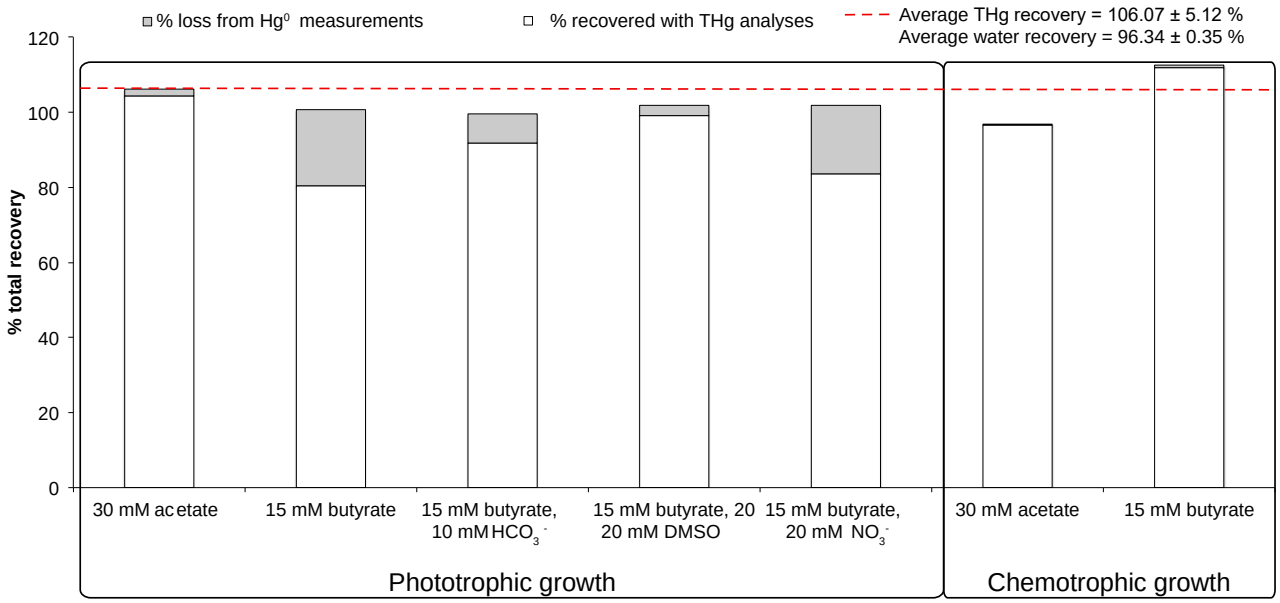

Figure A2: THg and water recoveries for bioreactor experiments with live *R. capsulatus*. The % total recovery is relative to the amount of THg measured at T_0 for each experiment.

Section 5: Hg^0 production experiments for *Rhodobacter capsulatus* grown phototrophically on 15 mM butyrate supplied with 20 mM HCO_3^-, 1 µM Fe^{III}-citrate or 20 mM NO_3^- as KNO_3

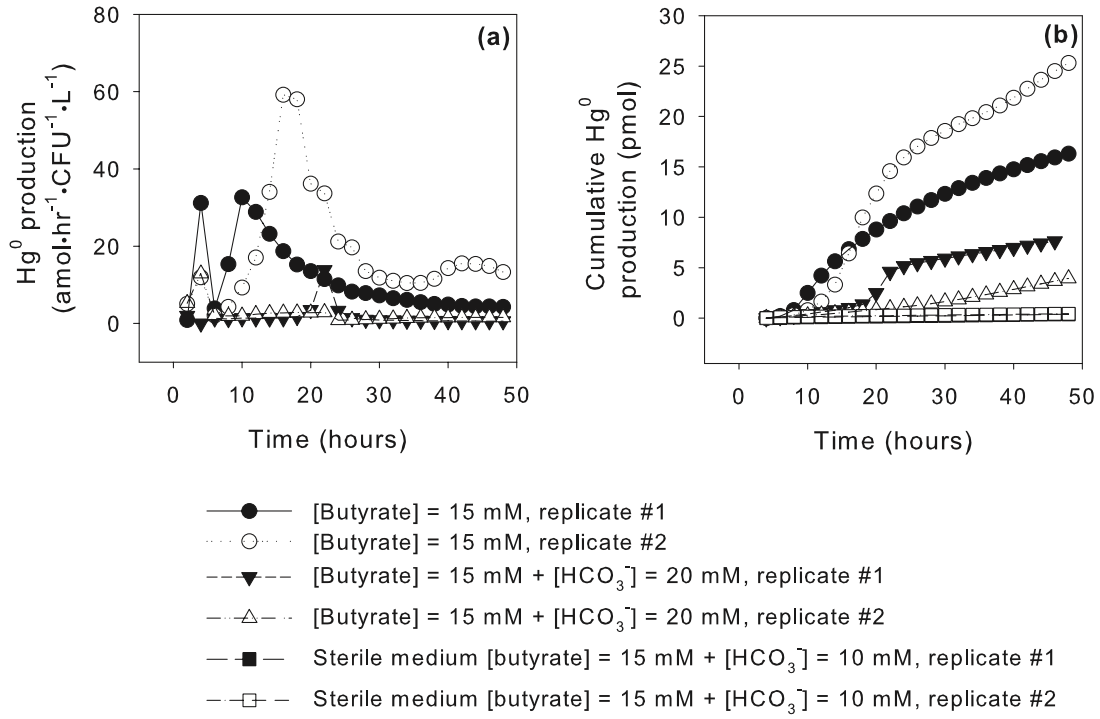

Figure A3: Repeat experiments of Hg^0 production normalized for cell density (**a**) and cumulative Hg^0 production (**b**) for phototrophically grown *R. capsulatus* supplied with 15 mM butyrate in the absence of HCO_3^- vs 20 mM HCO_3^- and sterile medium amended with 10 mM HCO_3^-.

Fig A3 has been provided to illustrate the variability associated with biotic and abiotic Hg^0 production for a representative subset of experiments with butyrate. When comparing Hg^0 production by live phototrophic cells supplied with 15 mM butyrate with and without 20 mM HCO_3^-, we repeatedly observed a decrease in Hg^0 production and sterile medium controls consistently showed negligible Hg^0 production.

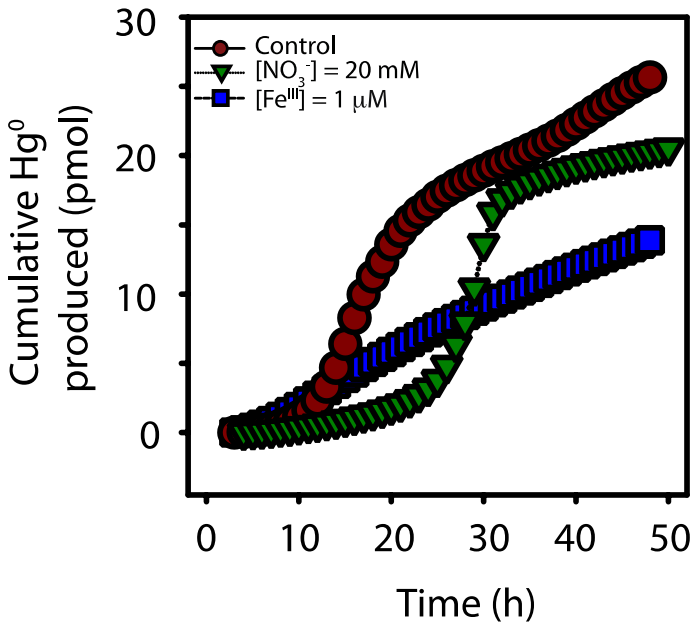

Figure A4: Hg^0 production for *R. capsulatus* grown phototrophically on 15 mM butyrate in the presence of 1 µM Fe^{III}-citrate or 20 mM NO_3^- as KNO_3.

While under standard conditions, the potential for Fe^{3+}/Fe^{2+} is similar to that of Hg^{2+}/Hg^0, free Fe^{III} is virtually absent from solution. Depending on whether Fe^{III} is present as insoluble oxides or dissolved and bound to an organic ligand, its redox potential will vary (for example, Fe^{3+}/Fe^{2+} E^0= 0.77V vs. Fe^{III}-citrate E^0=0.320V, Fe^{III}-oxide: $-0.2<E^0<+0.2$V). Similarly, depending on whether Hg^{II} [$0.7V < E^0(Hg^{2+}/ Hg^0) < 0.85V$] or Hg^I [present as Hg_2^{2+} $E^0(Hg_2^{2+}/Hg^0) = 0.4$ V] act as electron acceptors, the reduction potential of Hg will depend on the environmental conditions [8] and the ligands to which they are bound [9]. Iron oxides are poorly bioavailable and only outer-membrane bound enzymes could lead to their reduction. *R. capsulatus* does not possess such enzymes and has previously been shown to not catalyze Fe^{III} reduction [10]. Finally, while likely present at redox interfaces, iron oxides are not predicted to dominate the redox speciation of iron under anoxia that would be mostly present as soluble Fe^{II}.

That being said, to address the role of Fe^{III}, one of the most redox active metals in biological systems, we performed a competition experiment with Fe^{III}. We must stress that this experiment had one important caveat with respect to maintaining both Hg^{II} and Fe^{III} in solution: Fe^{III} was provided as soluble Fe^{III}-citrate (1μM) to prevent the formation of insoluble iron oxides and minimize the possibility of cells and Hg^{II} adsorption onto iron oxides. Providing citrate, a known metal chelator, will limit Hg^{II} bioavailability and therefore the expected Hg^{II} reduction rates.

With this possible caveat in mind, we report that phototrophic Hg^0 production proceeded in the presence of Fe^{III}-citrate, leading to the production of 15.00 pmol of Hg^0. These results suggest that it is unlikely Fe^{III} is a competing electron sink in the environment.

Section 6: Comparison of growth rate calculations for phototrophic cultures of *Rhodobacter capsulatus* supplied with sublethal concentrations of Hg

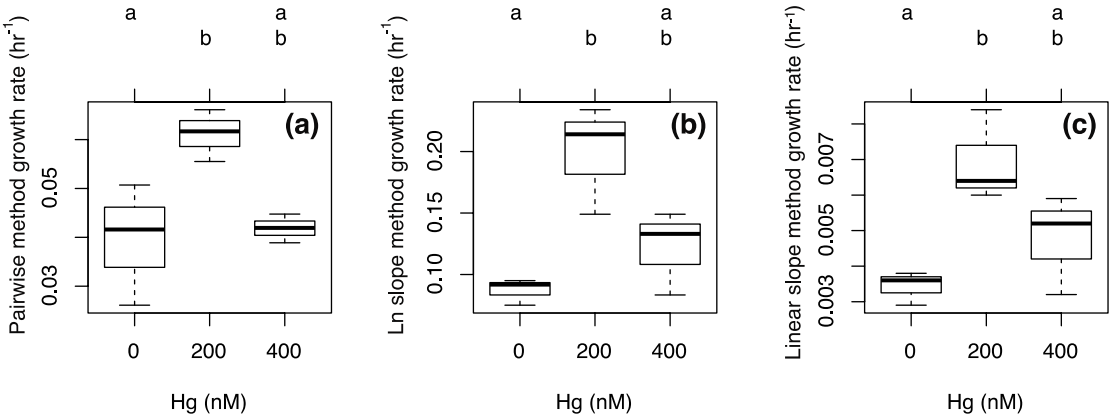

Figure A5: Comparison of growth rate calculations for phototrophic cultures of *R. capsulatus* supplied with sublethal concentrations of Hg. Growth rates obtained by calculating the slope chronologically between pairs of points (**a**), fitting a natural logarithmic curve (**b**) and a linear regression (**c**) are presented for cells grown on 1 mM butyrate (n = 3). The bottom and top of the boxes show the first and third quartiles, respectively, the bar in the middle shows the median and the whiskers show the minimum and maximum for each treatment. [Hg] had the same significant effect on growth rate ($p<0.05$) regardless of the calculation method employed and variability was comparable among growth rate calculation methods. Letters not shared between treatments indicate a significant ($p<0.05$) difference based on Tukey HSD test

Section 7: Hg^0 production for anaerobic metabolism and photochemical processes

Table A5: Hg^0 production rates for model anaerobic organisms and abiotic photochemical processes.

Organisms	Rate of Hg^0 production ($pmol.L^{-1}.h^{-1}$)	Hg^{II} ($pmol.L^{-1}$)	% Hg^0 produced per hour	Reference
Dissimilatory metal reducing bacteria: *Shewanella oneidensis* MR-1 and *Geobacter sulfurreducens* PCA	$3.3x10^3$ – $40x10^3$	$1.5x10^5$ – $8.25x10^5$	2.2-15.2	[11]
Dissimilatory metal reducing bacteria: *Geobacter sulfurreducens* PCA	$3.75x10^3$	$2.5x10^5$	15	[12, 13]
Anoxygenic phototrophs: *Rhodobacter capsulatus* SB1003, *Rhodobacter sphaeroides* 2.4.1, *Rhodopseudomonas palustris* TIE-1	0.3 - 3.3	250	0.1-1.3	This study
In-situ metalimnetic incubation Boreal lake	0.01	10	0.1	[1]
Photoreduction in surface lake waters	0.02 – 0.28	1-10	0.5-2.8	[1, 14]

Table A6: Hg^0 production rates for phototrophic metabolism and abiotic photochemical processes normalized for incoming light energy.

	Rate of Hg^0 production ($pmol.L^{-1}.mol_{photon}.m^2$)	Hg^{II} ($pmol.L^{-1}$)	% Hg^0 produced per $mol_{photon}.m^2$	Reference
Anoxygenic phototrophs: *Rhodobacter capsulatus* SB1003, *Rhodobacter sphaeroides* 2.4.1, *Rhodopseudomonas palustris* TIE-1	38.2-185.0	250	15-75	This study
Photoreduction in surface lake waters	0.01-1	1-10	0.1-10	[1, 15]

While rates of phototrophic Hg reduction are at the lower end of what is reported for dissimilatory metal reducing bacteria, they are comparable if not slightly higher than what is observed for photochemically-driven Hg^0 production in surface waters and can explain Hg^0 production observed during *in-situ* metalimnetic incubations.

Furthermore, our experimental design allowed us to calculate the maximum cell specific reduction rate of 75 amol.cell^{-1}.h^{-1}.L^{-1}. This rate was obtained at an optimal temperature of 28°C and can be corrected for the role of temperature on bacterial metabolism to obtain a rate more representative of lake conditions (i.e., at 10°C) [16]. This corrected value is 0.75 amol.cell^{-1}.h^{-1}.L^{-1}. Anoxygenic phototrophs can be found in wide diversity of environment and present at densities ranging from 10^3-10^6 cells.ml^{-1} in freshwaters [17]. Using a conservative value of 10^3 cells.ml^{-1}, we estimate that 0.75 pmol of Hg^{II} can be reduced per hour. This rate is enough to turn over almost all of the Hg present per liter of lake water over the course of a summer day (assuming ca. 10h of effective irradiance and $1 < [Hg^{II}] < 10$ pM). While this is an overestimation as other reactions such as oxidation, scavenging and methylation will also control Hg^{II} level in freshwater, this simple calculation provides contextual evidence, in addition to already existing field data, highlighting the importance of phototrophic Hg reduction in the lake Hg budget.

SUPPORTING REFERENCES

1. Poulain, A. J.; Amyot, M.; Findlay, D.; Telor, S.; Barkay, T.; Hintelmann, H., Biological and photochemical production of dissolved gaseous mercury in a boreal lake. *Limnology and Oceanography* **2004,** *49*, (6), 2265-2275.

2. Allen, H. L., Acetate in freshwater: Natural substrate concentrations determined by dilution bioassay. *Ecology* **1968,** *49*, (2), 346-349.

3. Nedwell, D. B., The input and mineralization of organic carbon in anaerobic aquatic sediments. In *Advances in Microbial Ecology*, Marshall, K. C., Ed. Springer US: Boston, MA, 1984; pp 93-131.

4. Stumm, W.; Morgan, J. J., *Aquatic chemistry: chemical equilibria and rates in natural waters*. John Wiley & Sons: 2012; Vol. 126.

5. Whitfield, C.; Aherne, J.; Watmough, S., Predicting the partial pressure of carbon dioxide in boreal lakes. *Canadian Water Resources Journal* **2009,** *34*, (4), 415-426.

6. Krasil'nikova, E. N.; Mil'ko, E. S.; Keppen, O. I.; Lebedeva, N. V.; Ivanovskii, R. N., Polyhydroxybutyrate accumulation by *Rhodobacter sphaeroides* phase variants. *Microbiology* **2015,** *84*, (3), 347-350.

7. McKinlay, J. B.; Harwood, C. S., Carbon dioxide fixation as a central redox cofactor recycling mechanism in bacteria. *Proceedings of the National Academy of Sciences of the United States of America* **2010,** *107*, (26), 11669-11675.

8. Scholz, F.; Lovrić, M., The standard potentials of the electrode “dissolved atomic mercury/dissolved mercury ions". *Electroanalysis* **1996,** *8*, (11), 1075-1076.

9. Gopinath, E.; Kaaret, T. W.; Bruice, T. C., Mechanism of mercury(II) reductase and influence of ligation on the reduction of mercury(II) by a water soluble 1,5-

dihydroflavin. *Proceedings of the National Academy of Sciences of the United States of America* **1989,** *86*, (9), 3041-3044.

10. Poulain, A. J.; Newman, D. K., *Rhodobacter capsulatus* catalyzes light-dependent Fe(II) oxidation under anaerobic conditions as a potential detoxification mechanism. *Applied and Environmental Microbiology* **2009,** *75*, (21), 6639-6646.

11. Wiatrowski, H. A.; Ward, P. M.; Barkay, T., Novel reduction of mercury(II) by mercury-sensitive dissimilatory metal reducing bacteria. *Environmental Science and Technology* **2006,** *40*, (21), 6690-6696.

12. Hu, H. Y.; Lin, H.; Zheng, W.; Tomanicek, S. J.; Johs, A.; Feng, X. B.; Elias, D. A.; Liang, L. Y.; Gu, B. H., Oxidation and methylation of dissolved elemental mercury by anaerobic bacteria. *Nature Geoscience* **2013,** *6*, (9), 751-754.

13. Lin, H.; Morrell-Falvey, J. L.; Rao, B.; Liang, L.; Gu, B., Coupled mercury-cell sorption, reduction, and oxidation on methylmercury production by *Geobacter sulfurreducens* PCA. *Environmental Science and Technology* **2014,** *48*, (20), 11969-11976.

14. Amyot, M.; Mierle, G.; Lean, D.; McQueen, D. J., Effect of solar radiation on the formation of dissolved gaseous mercury in temperate lakes. *Geochimica et Cosmochimica Acta* **1997,** *61*, (5), 975-987.

15. Garcia, E.; Poulain, A. J.; Amyot, M.; Ariya, P. A., Diel variations in photoinduced oxidation of Hg0 in freshwater. *Chemosphere* **2005,** *59*, (7), 977-981.

16. Price, P. B.; Sowers, T., Temperature dependence of metabolic rates for microbial growth, maintenance, and survival. *Proceedings of the National Academy of Sciences of the United States of America* **2004,** *101*, (13), 4631-4636.

17. Dworkin, M., *The Prokaryotes: Vol. 6: Proteobacteria: Gamma Subclass*. Springer Science & Business Media: 2006.

Appendix B: Supporting information for Chapter 5

Daniel S. Grégoire [a], Noémie C. Lavoie [a] & Alexandre J. Poulain [a]

a - Biology Department, University of Ottawa, 30 Marie Curie, Ottawa, ON, K1N 6N5, Canada.

Supporting information reprinted with permission from: **Grégoire, D. S**., Lavoie, N. C. & Poulain, A. J., Heliobacteria reveal fermentation as a key pathway for mercury reduction in anoxic environments. *Environmental Science and Technology* **2018,** *52***,** 4145-415.

LIST OF SUPPORTING MATERIALS

SUPPORTING METHODS

Strains, culture conditions and Hg growth assays
HPLC measurements of pyruvate and acetate
Statistical analyses

SUPPORTING DISCUSSION ON PYRUVATE METABOLISM IN MODEL ANAEROBES

SUPPORTING FIGURES

Figure B1: Total Hg mass balance for select experiments with live *Heliobacterium modesticaldum* Ice1 grown phototrophically and chemotrophically
Figure B2: Percent total Hg recovered for select experiments with live *Heliobacterium modesticaldum* Ice1 grown phototrophically and chemotrophically in PYE
Figure B3: Growth curves for *Heliobacterium modesticaldum* Ice1 grown phototrophically and chemotrophically with and without repeated spikes of Hg
Figure B4: Growth parameters for *Heliobacterium modesticaldum* Ice1 cells grown phototrophically (top panels) and chemotrophically (bottom panels) in the presence of 500 nM $HgCl_2$
Figure B5: Pyruvate and acetate concentrations for *Heliobacterium modesticaldum* Ice1 grown chemotrophically in PYE medium with 0.2 g L^{-1} yeast extract
Figure B6: Repeated experiments measuring Hg^0 production by *Heliobacterium modesticaldum* Ice1 grown phototrophically and chemotrophically in the absence of organic carbon
Figure B7: Repeated experiments measuring Hg^0 production by *Heliobacterium modesticaldum* Ice1 grown chemotrophically on pyruvate in the presence of a hydrogenase inhibitor, NO_2^-
Figure B8: Growth curves for *Heliobacterium modesticaldum* Ice1, *Clostridium acetobutylicum* ATCC 824 and *Geobacter sulfurreducens* PCA in PYE medium in the presence of NTZ and DMSO
Figure B9: Mechanistic summary of Hg^0 production during phototrophic growth of *Heliobacterium modesticaldum* Ice1 and chemotrophic pyruvate fermentation

SUPPORTING TABLES

Table B1: Summary of growth conditions in bioreactor experiments.
Table B2: Master dataset for all bioreactor experiments

SUPPORTING REFERENCES

SUPPORTING METHODS

Strains, culture conditions and Hg growth assays

Stock solutions used in cell cultures were all prepared following anaerobic techniques. Nitazoxanide (NTZ) stocks were prepared to a final concentration of 10 µM in pure DMSO sparged with N_2 and stored at 4°C in the dark. For DMSO controls, the DMSO solution was bubbled with N_2 prior to being added to the bioreactor; final concentration of DMSO in the reactor was 2.8 mM. Sodium nitrite stocks were prepared to a final concentration of 10 mM in ultra pure miliQ, filter-sterilized, sparged with N_2 and stored at 4°C in the dark; final concentration of NO_2^- in the reactor was 10 µM. For experiments where HCO_3^- was supplied, a stock solution of 1 M was prepared by dissolving $NaHCO_3$ in ultra pure MiliQ and autoclaving for 30 minutes at 121°C under 80% N_2/20% CO_2 atmosphere prior to use. Fumarate stock solutions were prepared at a final concentration of 40 mM in ultra pure miliQ, filter sterilized (0.2 µm pore size), bubbled with N_2, sealed and crimped shut in sterile serum bottles prior to use. All equipment used in the anaerobic glove box was conditioned for at least 48 hours prior to use.

For *Heliobacterium modesticaldum* Ice1, new cultures were started from a cryostock for every bioreactor experiment. Cells were revived in DSMZ medium 655 (herein referred to as PYE) previously used to isolate *H. modesticaldum* [1]. Cultures started from cryostock were grown phototrophically in PYE with an incandescent light source that emitted light primarily in the visible near-red to red spectrum (600 to 700 nm) at an intensity of 80 µmol photon $m^{-2}s^{-1}$ at 50°C in line with previous work [1] until reaching early stationary phase. Afterwards, a 10 % inoculum was used to re-inoculate 10 mL of fresh PYE and cells were grown phototrophically (with the same light intensity) or

chemotrophically (in the dark) at 50°C. These cultures were used to establish finely resolved growth curves and in Hg growth assays (see **Fig B1** and **B2**).

For experiments testing the effect of carbon source on Hg^0 production some modifications to the initial PYE medium growth protocol were made. Phototrophic *H. modesticaldum* cells were grown with pyruvate, acetate, acetate + HCO_3^- and/or yeast extract alone as a carbon source. Cells were grown until late exponential phase before being subsampled to supply a 10% inoculum for cultures with a final volume 75 mL destined for the bioreactor and grown under the same conditions (see **Table B1**). Chemotrophic cells were grown exclusively in PYE because no other carbon source supported chemotrophic growth. Upon reaching late exponential phase, cells were inoculated into the bioreactor as a 10 % inoculum in a final volume of 560 mL of media with the desired carbon source treatment.

For *Clostridium acetobutylicum* ATCC 824, new cultures were started for every bioreactor experiment. Cells were revived in DSMZ medium 104b (herein referred to as PYX). Cells were grown in the dark at 37°C until reaching early stationary phase after which point they were rotated as a 1 % inoculum in a final volume of 10 mL into fresh PYX. Cells were grown to late exponential phase and re-inoculated as a 1 % inoculum in a final volume of 75 mL of PYX in cultures destined for the bioreactor. Experiments were performed in PYE where all SO_4^{2-} salts were substituted with chloride salts (PYEΔSO_4^{2-}) to avoid competition between Hg^{II} reduction and SO_4^{2-} reduction. Cells were also supplied with Hg^{II} in DSMZ medium 104b to account for the effect of suboptimal growth medium (see **Table B1** and **Table B2**). Cells achieved extremely high densities as such a 1-2 % inoculum, rather than 10%, was chosen for the bioreactor

experiment to ensure initial cell densities were comparable amongst strains for the NTZ and/or DMSO experiments. The initial volume of medium in the bioreactor was corrected to ensure that identical volumes were maintained throughout all experiments.

Geobacter sulfurreducens PCA cells were revived from cryostock and grown in defined medium (herein referred to as GSMM) according to previous work [2] with the following modification: resazurin, the color indicator used to monitor anoxia, was removed to avoid issues with abiotic Hg reduction given that resazurin is a reducing agent. Cells were grown chemotrophically in the dark at 28°C. Cells took between 10 to 12 days to re-initiate growth, as such, cultures were maintained by re-inoculating fresh GSMM every 4 days with a 10 % inoculum in a final volume of 10 mL. Upon reaching late exponential phase, a 10 % inoculum was used to start cultures in GSMM with a final volume of 75 mL destined for the bioreactor. Upon reaching late exponential phase a 10 % inoculum was used to inoculate the bioreactor where cells were supplied with Hg^{II} in 560 mL of PYEΔSO_4^{2-} or GSMM medium (see **Table B1**).

Escherichia coli K-12 cultures were plated aerobically from cryostock onto LB medium and grown at 37°C overnight. A single colony was used to inoculate PYE medium and incubated at 37°C under 100% N_2 headspace for 24 hours before a 1 % inoculum was used to re-inoculate 75 mL of fresh PYE medium. These cultures were incubated at 37°C under 100 % N_2 headspace for 24 hours and a 10 % inoculum was used to inoculate a final volume of 560 mL of PYE medium in the bioreactor.

HPLC measurements of pyruvate and acetate

Separation of compounds was achieved on a Synergy Polar column (150 mm x 2.1 mm I.D., 1.7 µm particle size, Phenomenex, Torrance, CA, USA). The mobile phase consisted of 0.1% formic acid in water (Fisher optima LCMS). Quantification was performed based on the peak area in each sample analyzed compared to the peak areas of known concentrations of each compound in the calibration curve. The setup was comprised of an Agilent 1100 series system that had a quaternary pump, a 100 µL built in sampling loop, a column thermostat and a photo diode array detector. The optimized sample analysis conditions were as follows: the column thermostat was set 65°C, flow rate was 0.2 mL min^{-1}, mobile phase delivery was isocratic, the emission spectra used to detect each compound with the photodiode array detector was measured at 210 nm using the emission at 380 nm as reference, finally, 2 µL of each sample was injected. Chemstation B.03.02 software was used to acquire and analyze the data. Calibration curves for each compound were made using sodium pyruvate from Fisher scientific (BP356-100, purity 99%) and sodium acetate from Sigma-Aldrich (S5636-500g, purity 99%) dissolved in 0.1% formic acid.

Statistical analyses

One-way ANOVAs were performed for phototrophic and chemotrophic Hg exposure assays using R statistical software [3]. In the event of detecting a significant difference, assumptions of constant variance and normality were verified with the Brusch-Pagan test and the Shapiro-Wilks test, respectively, with the significance thresholds set to $p = 0.05$ for each test. Significant differences were then identified using the Tukey HSD test. The

sample size employed for growth assays was n = 3 per treatment. All assumptions were passed for significant differences and these values are reported in the figure legends (**Fig B4**). A non-linear regression model was fit to the cumulative Hg^0 production data as a function of pyruvate concentration using Sigmaplot software. In this instance, a natural logarithmic function was fit to a data set of n= 8. Given the significant fit, assumptions of constant variance and normality were verified with the Sigmaplot software with the significance threshold set to p = 0.05 for each test. All assumptions were passed, and these values are reported in the figure legends (**Fig 5.3**).

PYRUVATE METABOLISM IN MODEL ANAEROBES

Clostridium acetobutylicum ATCC 824 is a strict fermentative anaerobe known to have a central carbon metabolism similar to *H. modesticaldum* [4]. Both strains oxidize pyruvate to acetyl-CoA via PFOR and produce reduced ferredoxin, but the acetyl-CoA generated by *C. acetobutylicum* can be a precursor of several oxidized (e.g., acetate, acetone, CO_2) or reduced (e.g., butanol, butyrate) products, the ratios of which depend on environmental culture conditions [5].

Geobacter sulfurreducens PCA is a non-fermentative strain [6] known to reduce Hg^{II} [7, 8] that requires an exogenous terminal electron acceptor to generate energy [9]. *G. sulfurreducens* can also use pyruvate as a carbon source [10]. It has three enzyme systems capable of converting pyruvate to acetyl-CoA: pyruvate-ferredoxin oxidoreductase (PFOR with ferredoxin as a cofactor), pyruvate-formate lyase (PFL; no redox cofactor), and a putative pyruvate dehydrogenase complex (PDH, NADH/NAD+ and FADH/FAD+ as redox cofactors) [11]. PFOR appears essential for conversion of pyruvate into acetate,

CO_2 and reduced ferredoxin, but this reaction is slow [10]. Alternatively, pyruvate can be converted to acetyl-CoA via the PDH complex when fumarate is used as a terminal electron acceptor [10].

Finally, we also used *Escherichia coli* K-12, a facultative anaerobe. *E. coli* that can grow fermentatively and has several enzymes that can catalyze the conversion of pyruvate into acetyl-CoA including a PFL, a PDH complex and a PFOR. It has been shown for *E. coli* that PFOR is 100 to 1000 times less active than PFL or PDH and the latter two systems are the principal enzymes converting pyruvate into acetyl-CoA [12].

SUPPORTING FIGURES

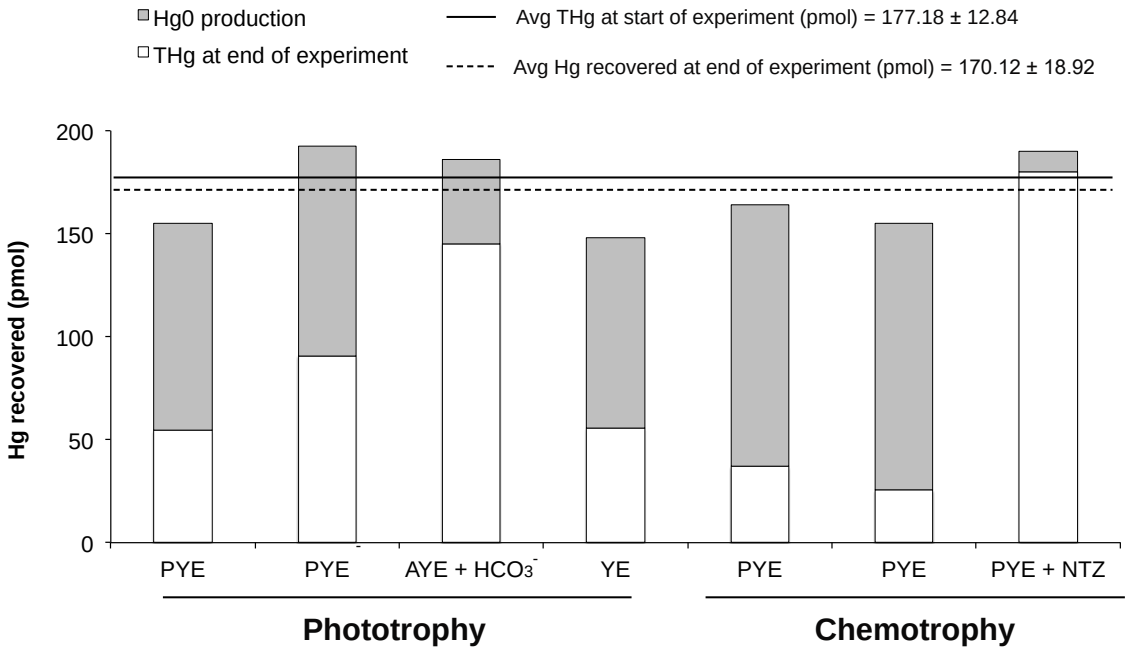

Figure B1: Total Hg mass balance for select experiments with live *Heliobacterium modesticaldum* Ice1 grown phototrophically and chemotrophically. The average (Avg) and standard deviation for quantities of Hg recovered at the beginning and end of the experiment are based on a sample size of n = 7.

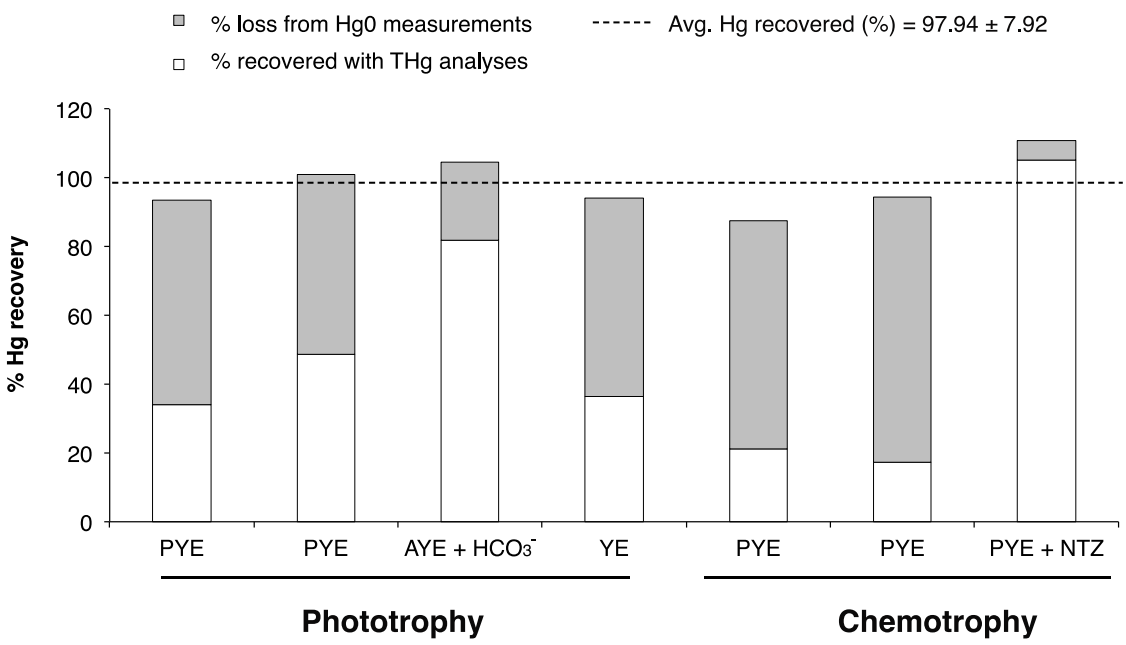

Figure B2: Percent total Hg recovered for select experiments with live *Heliobacterium modesticaldum* Ice1 grown phototrophically and chemotrophically in PYE. The average (Avg) and standard deviation for percentage of Hg recovered is based on a sample size of n = 7.

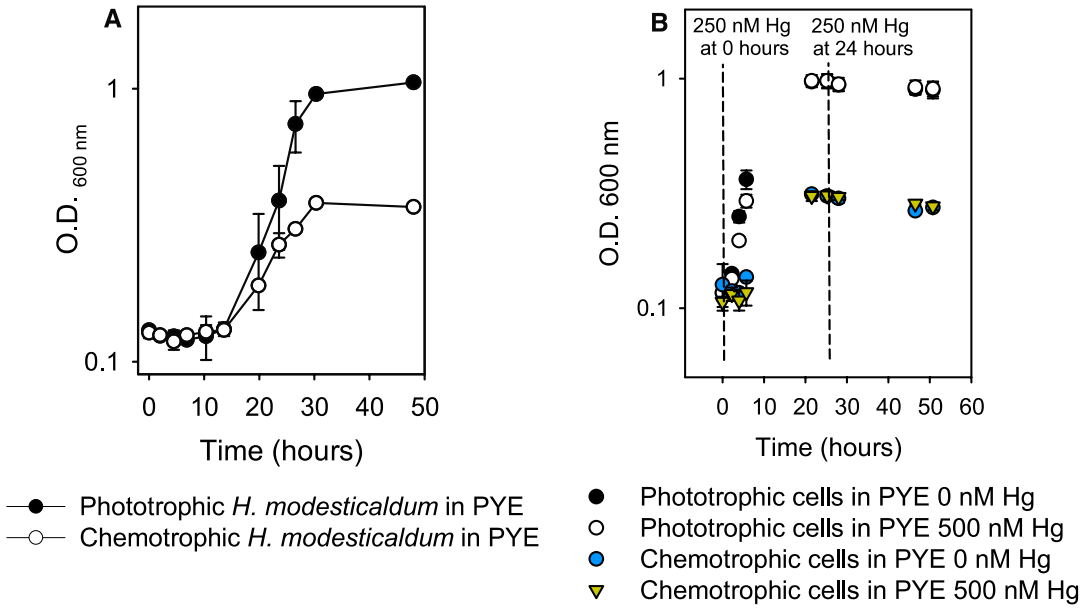

Figure B3: Growth curves for *Heliobacterium modesticaldum* Ice1 grown phototrophically and chemotrophically with and without repeated spikes of Hg. A, B growth curve for cells grown phototrophically and chemotrophically in the absence of Hg (**A**) and in the presence of 500 nM $HgCl_2$ supplied as two doses of 250 nM 24 hours apart (**B**). Data points are the average of n = 3 replicates and error bars represent standard deviations.

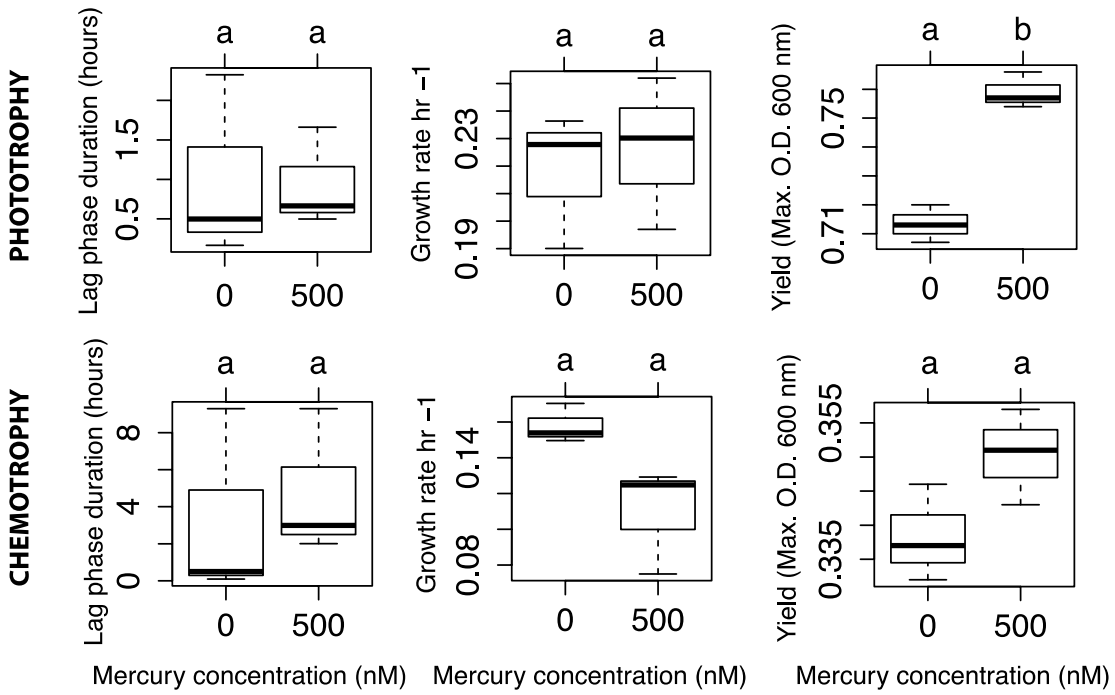

Figure B4: Growth parameters for *Heliobacterium modesticaldum* Ice1 cells grown phototrophically (top panels) and chemotrophically (bottom panels) in the presence of 500 nM $HgCl_2$. The bottom and top of the boxes show the first and third quartiles, respectively, the bar in the middle shows the median and the whiskers show the minimum and maximum for each treatment, all of which had a sample size of n = 3. [Hg] had a significant effect ($p < 0.05$) on yield for phototrophically grown cells (p = 0.0009). Tests for constant variance and normal distribution for phototrophic yield were passed (significance threshold for rejection of null hypothesis p = 0.05) with p = 0.88 and p = 0.29, respectively. Letters not shared between treatments indicate a significant ($p < 0.05$) difference according to the Tukey HSD test.

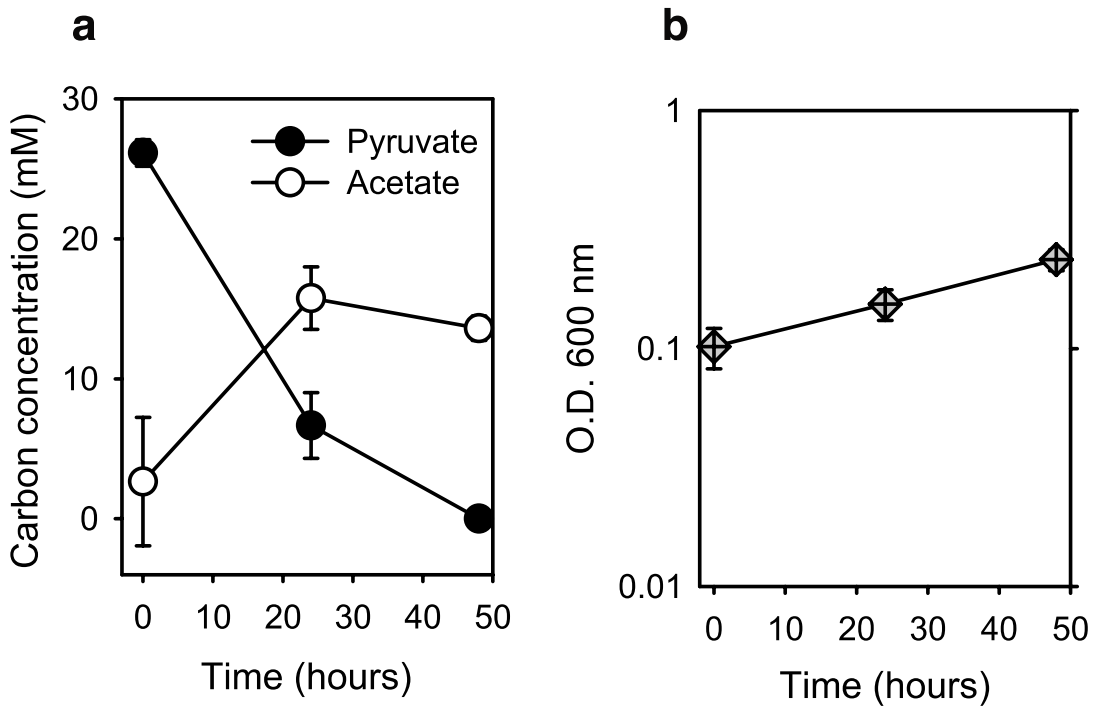

Figure B5: Pyruvate and acetate concentrations for *Heliobacterium modesticaldum* Ice1 grown chemotrophically in PYE medium with 0.2 g L^{-1} yeast extract. **A, B** Pyruvate and acetate concentrations as measured by HPLC (**A**) and microbial growth (**B**). Data points are the average of n = 3 and error bars represent standard deviations.

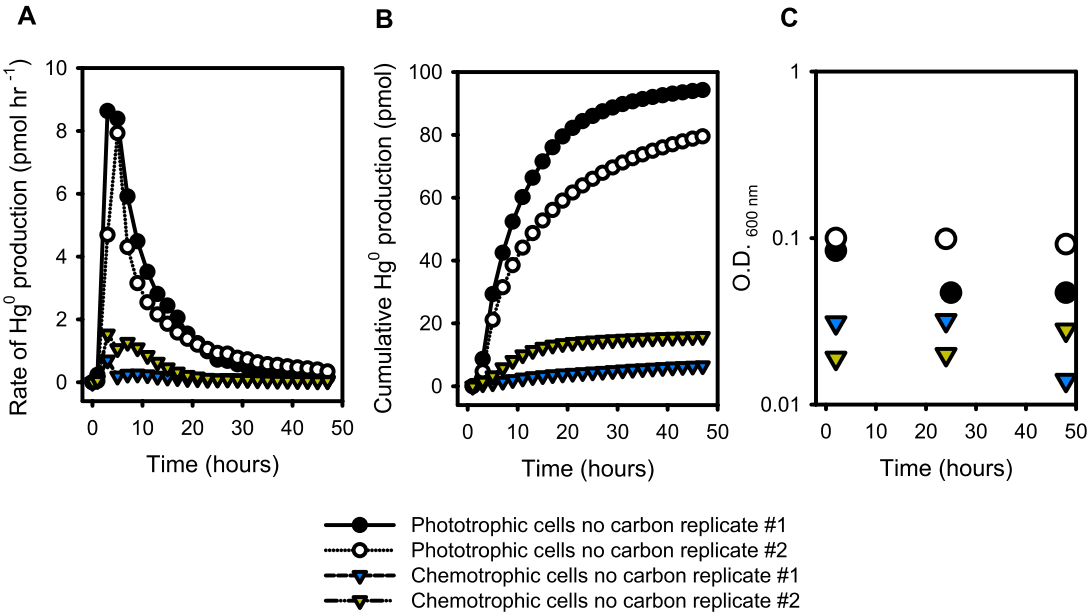

Figure B6: Repeated experiments measuring Hg^0 production by *Heliobacterium modesticaldum* Ice1 grown phototrophically and chemotrophically in the absence of organic carbon. A - C Rate of Hg^0 production (**A**), cumulative Hg^0 production (**B**) and microbial growth (**C**) for cells initially grown in PYE medium and supplied with Hg^{II} in the absence of organic carbon. The average quantity of $HgCl_2$ present at the beginning of each assay was 177.18 ± 12.84 pmol.

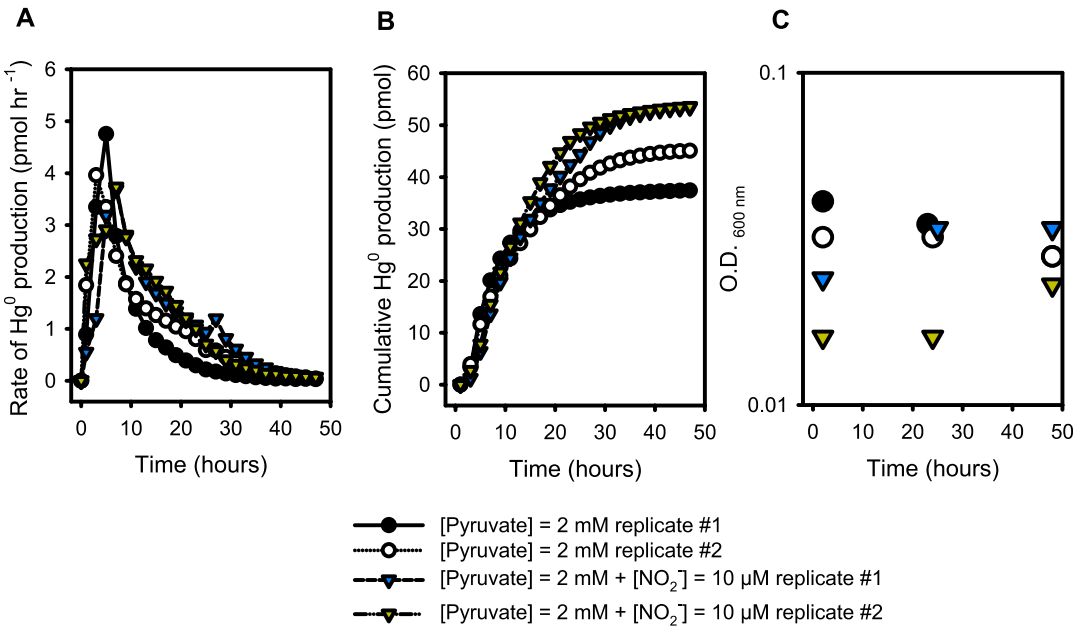

Figure B7: Repeated experiments measuring Hg^0 production by *Heliobacterium modesticaldum* Ice1 grown chemotrophically on pyruvate in the presence of a hydrogenase inhibitor, NO_2^-. A - C Rate of Hg^0 production (**A**), cumulative Hg^0 production (**B**) and microbial growth (**C**) for cells initially grown in PYE medium, supplied with 2 mM pyruvate as a sole carbon source and 10 µM $NaNO_2$ in the bioreactor. The average quantity of $HgCl_2$ present at the beginning of each assay was 177.18 ± 12.84 pmol

.

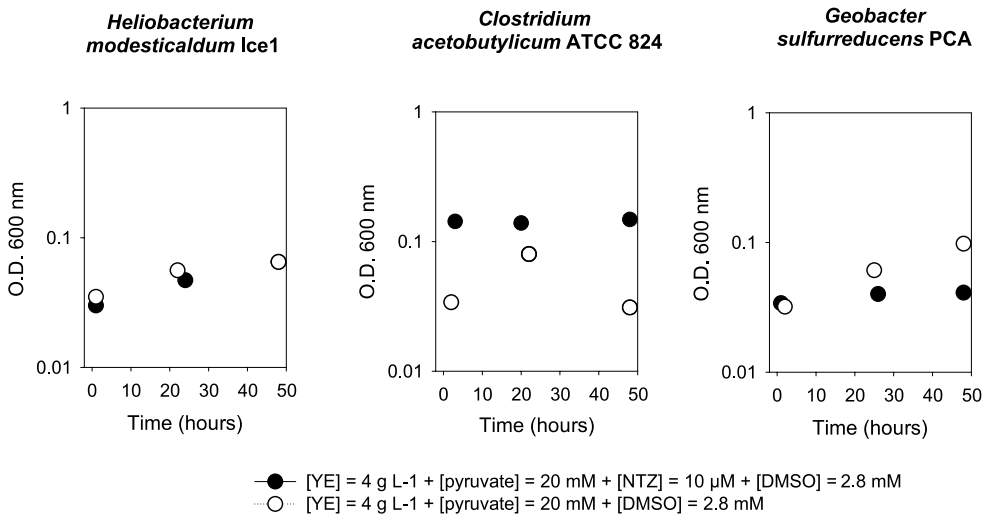

Figure B8: Growth curves for *Heliobacterium modesticaldum* Ice1, *Clostridium acetobutylicum* ATCC 824 and *Geobacter sulfurreducens* PCA in PYE medium in the presence of NTZ and DMSO.

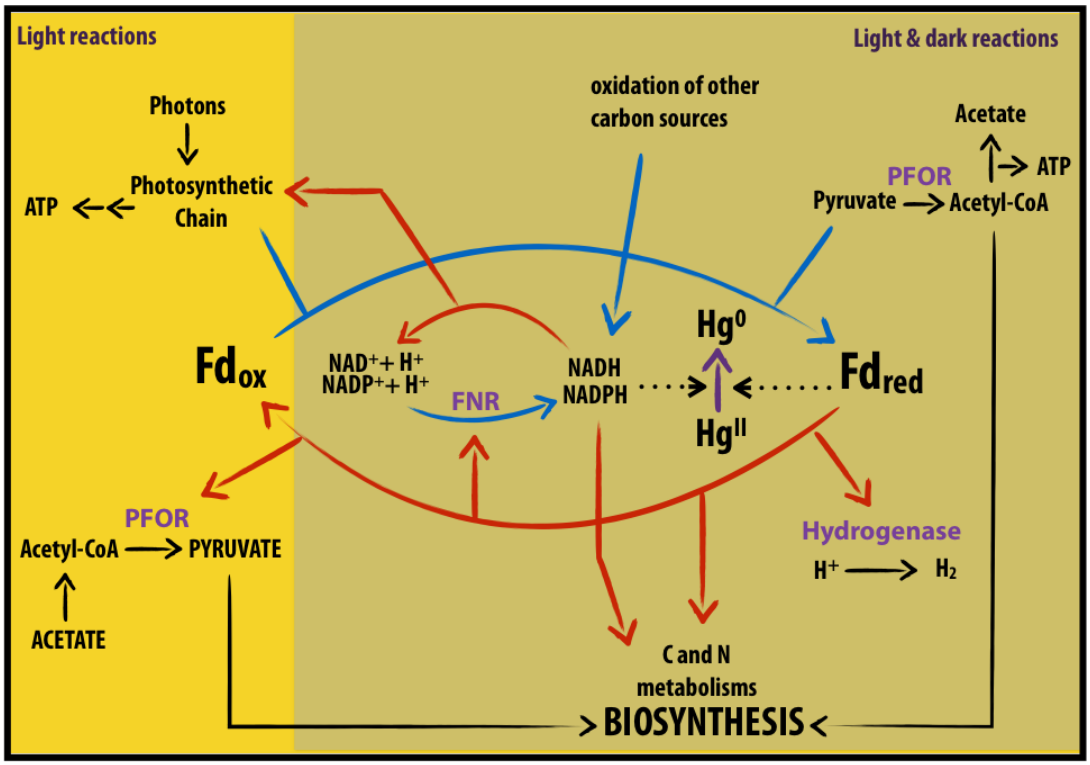

Figure B9: Mechanistic summary of Hg^0 production during phototrophic growth of *Heliobacterium modesticaldum* Ice1 and chemotrophic pyruvate fermentation.

Abbreviations: Oxidized and reduced ferredoxin = Fd ox. and Fd red., respectively; pyruvate:ferredoxin oxidoreductase = PFOR, ferredoxin- NAD(P)+ oxidoreductase = FNR. All red arrows correspond to reducing power consumption pathways and blue arrows correspond to reducing power production pathways. Adapted from Tang et al. 2010 [13].

Table B1: Summary of growth conditions in bioreactor experiments.

	Growth conditions				**Exposure conditions in bioreactor**		
Strain	Metabolism	T (°C)	Carbon source(s) (mM or g L^{-1})	e- sink (mM)	T (°C)	Carbon source(s) (mM or g L^{-1})	e- sink/inhib. treatment (µM or mM)
Heliobacterium modesticaldum Ice1	Phototrophy	50	Pyruvate (20 mM) + YE (4 g L^{-1})	NA	50	Pyruvate (20 mM) + YE (4 g L^{-1})	NA
							NTZ (10 µM) + DMSO (2.8 mM)
							DMSO (2.8 mM)
						No carbon	NA
			Acetate (30 mM) + YE (4 g L^{-1})			Acetate (30 mM) + YE (4 g L^{-1})	NA
						Acetate (30 mM) + YE (4 g L^{-1})	HCO_3^- (10 mM)
			YE (4 g L^{-1})			YE (4 g L^{-1})	NA
	Chemotrophy	50	Pyruvate (20 mM) + YE (4 g L^{-1})		50	Pyruvate (20 mM) + YE (4 g L^{-1})	NA
							NTZ (10 µM) + DMSO (2.8 mM)
							DMSO (2.8 mM)
						No Carbon	NA
						YE (4 g L^{-1})	NA
						YE (0.2 g L^{-1})	NA
						Acetate (30 mM)	NA
						Pyruvate (100 mM)	NA
						Pyruvate (20 mM)	NA
						Pyruvate (2 mM)	NA
							NO_2^- (10 µM)
Clostridium acetobutylicum ATCC 824	Chemotrophy	37	Glucose (28 mM) + Peptone (10 g L^{-1}) + YE (10 g L^{-1})	NA	37	Pyruvate (20 mM) + YE (4 g L^{-1})	NA
							NTZ (10 µM) + DMSO (2.8 mM)
							DMSO (2.8 mM)
						Glucose (28 mM) + Peptone (10 g L^{-1}) + YE (10 g L^{-1})[a]	NA
Geobacter sulfurreducens PCA	Chemotrophy	28	Acetate (10 mM)	Fumarate (20 mM)	28	Pyruvate (20 mM) + YE (4 g L^{-1})	NA
							NTZ (10 µM) + DMSO (2.8 mM)
							DMSO (2.8 mM)
							Fumarate (40 mM)
						Acetate (10 mM)[a]	Fumarate (40 mM)
Escherichia coli K-12	Chemotrophy	37	Pyruvate (20 mM) + YE (4 g L^{-1})	NA	37	Pyruvate (20 mM) + YE (4 g L^{-1})	NA

Abbreviations: yeast extract = YE, electron = e-. *C. acetobutylicum* and *G. sulfurreducens* were supplied with Hg in PYE where SO_4^{2-} salts were replaced with chloride salts (referred to in the manuscript as PYEΔSO_4^{2-})

[a] These medium recipes represent the optimal growth medium used to study additional model anaerobes referred to in the main body of text.

Table B2: Dataset for bioreactor experiments. Abbreviation = treatment (Treat); metabolism (Metabo); electron (e-), temperature (T), replicate (Rep), phototrophic (Photo), chemotrophic (Chemo), yeast extract (YE), no cells (NC) and autoclaved cells (Auto).

Treat	Strain	Metabo.	T (°C)	Carbon source (mM or g L-1)	e- sink/ Inhibitor/treatment (µM or mM)	Inoculum O.D. 600 nm	Metabo.	T (°C)	Carbon source (mM or g L-1)	Electron sink/Inhibitor/treatment (µM or mM)	Rep#	Initial O.D. 600 nm	Final O.D. 600 nm	Cumulative Hg^0 production (pmol)
Live	*Heliobacterium modesticaldum* Ice1	Photo	50	Pyruvate (20 mM) + YE (4 g L-1)	NA	0.574	Photo	50	Pyruvate (20 mM) + YE (4 g L-1)	NA	1	0.046	0.523	101.99
Live	*Heliobacterium modesticaldum* Ice1	Photo	50	Pyruvate (20 mM) + YE (4 g L-1)	NA	0.872	Photo	50	Pyruvate (20 mM) + YE (4 g L-1)	NA	2	0.129	0.424	97.59
Auto.	*Heliobacterium modesticaldum* Ice1	Photo	50	Pyruvate (20 mM) + YE (4 g L-1)	NA	0.582	Photo	50	Pyruvate (20 mM) + YE (4 g L-1)	NA	1	0.063	0.058	5.26
NC	*Heliobacterium modesticaldum* Ice1	Photo	50	Pyruvate (20 mM) + YE (4 g L-1)	NA	NA	Photo	50	Pyruvate (20 mM) + YE (4 g L-1)	NA	1	0.005	0.005	4.44
Live	*Heliobacterium modesticaldum* Ice1	Photo	50	Pyruvate (20 mM) + YE (4 g L-1)	NA	0.82	Photo	50	Pyruvate (20 mM) + YE (4 g L-1)	NTZ (10 µM) + DMSO (2.8 mM)	1	0.131	0.125	86.02
Live	*Heliobacterium modesticaldum* Ice1	Photo	50	Pyruvate (20 mM) + YE (4 g L-1)	NA	0.78	Photo	50	Pyruvate (20 mM) + YE (4 g L-1)	NTZ (10 µM) + DMSO (2.8 mM)	2	0.114	0.132	61.99
Live	*Heliobacterium modesticaldum* Ice1	Photo	50	Pyruvate (20 mM) + YE (4 g L-1)	NA	0.935	Photo	50	Pyruvate (20 mM) + YE (4 g L-1)	DMSO (2.8 mM)	1	0.148	0.495	81.23
Live	*Heliobacterium modesticaldum* Ice1	Photo	50	Pyruvate (20 mM) + YE (4 g L-1)	NA	0.446	Photo	50	Pyruvate (20 mM) + YE (4 g L-1)	DMSO (2.8 mM)	2	0.062	0.42	83.36
Live	*Heliobacterium modesticaldum* Ice1	Photo	50	Acetate (30 mM) + YE (4 g L-1)	NA	0.292	Photo	50	Acetate (30 mM) + YE (4 g L-1)	NA	1	0.042	0.061	58.06
Live	*Heliobacterium modesticaldum* Ice1	Photo	50	Acetate (30 mM) + YE (4 g L-1)	NA	0.205	Photo	50	Acetate (30 mM) + YE (4 g L-1)	NA	2	0.025	0.037	46.01
Live	*Heliobacterium modesticaldum* Ice1	Photo	50	Acetate (30 mM) + YE (4 g L-1)	NA	0.13	Photo	50	Acetate (30 mM) + YE (4 g L-1)	HCO3- (10 mM)	1	0.018	0.02	43.31
Live	*Heliobacterium modesticaldum* Ice1	Photo	50	Acetate (30 mM) + YE (4 g L-1)	NA	0.201	Photo	50	Acetate (30 mM) + YE (4 g L-1)	HCO3- (10 mM)	2	0.022	0.039	42.50
Live	*Heliobacterium modesticaldum* Ice1	Photo	50	YE (4 g L-1)	NA	0.383	Photo	50	YE (4 g L-1)	NA	1	0.041	0.035	92.27
Live	*Heliobacterium modesticaldum* Ice1	Photo	50	YE (4 g L-1)	NA	0.321	Photo	50	YE (4 g L-1)	NA	2	0.045	0.035	90.48
Live	*Heliobacterium modesticaldum* Ice1	Photo	50	Pyruvate (20 mM) + YE (4 g L-1)	NA	0.656	Photo	50	No Carbon	NA	1	0.084	0.047	94.46
Live	*Heliobacterium modesticaldum* Ice1	Photo	50	Pyruvate (20 mM) + YE (4 g L-1)	NA	0.792	Photo	50	No Carbon	NA	2	0.1	0.092	79.96
Live	*Heliobacterium modesticaldum* Ice1	Chemo	50	Pyruvate (20 mM) + YE (4 g L-1)	NA	0.236	Chemo	50	Pyruvate (20 mM) + YE (4 g L-1)	NA	1	0.033	0.361	126.94
Live	*Heliobacterium modesticaldum* Ice1	Chemo	50	Pyruvate (20 mM) + YE (4 g L-1)	NA	0.285	Chemo	50	Pyruvate (20 mM) + YE (4 g L-1)	NA	2	0.045	0.326	129.28

Continued on next page

Live	*Heliobacterium modesticaldum* Ice1	Chemo	50	Pyruvate (20 mM) + YE (4 g L-1)	NA	0.247	Chemo	50	Pyruvate (20 mM) + YE (4 g L-1)	NA	3	0.031	0.321	117.16
Auto.	*Heliobacterium modesticaldum* Ice1	Chemo	50	Pyruvate (20 mM) + YE (4 g L-1)	NA	0.265	Chemo	50	Pyruvate (20 mM) + YE (4 g L-1)	NA	1	0.045	0.034	3.51
NC	*Heliobacterium modesticaldum* Ice1	Chemo	50	Pyruvate (20 mM) + YE (4 g L-1)	NA	NA	Chemo	50	Pyruvate (20 mM) + YE (4 g L-1)	NA	1	0	0.016	3.69
Live	*Heliobacterium modesticaldum* Ice1	Chemo	50	Pyruvate (20 mM) + YE (4 g L-1)	NA	0.296	Chemo	50	Pyruvate (20 mM) + YE (4 g L-1)	NTZ (10 µM) + DMSO (2.8 mM)	1	0.03	0.065	9.85
Live	*Heliobacterium modesticaldum* Ice1	Chemo	50	Pyruvate (20 mM) + YE (4 g L-1)	NA	0.254	Chemo	50	Pyruvate (20 mM) + YE (4 g L-1)	NTZ (10 µM) + DMSO (2.8 mM)	2	0.028	0.057	4.43
Live	*Heliobacterium modesticaldum* Ice1	Chemo	50	Pyruvate (20 mM) + YE (4 g L-1)	NA	0.292	Chemo	50	Pyruvate (20 mM) + YE (4 g L-1)	DMSO (2.8 mM)	1	0.035	0.065	87.23
Live	*Heliobacterium modesticaldum* Ice1	Chemo	50	Pyruvate (20 mM) + YE (4 g L-1)	NA	0.276	Chemo	50	Pyruvate (20 mM) + YE (4 g L-1)	DMSO (2.8 mM)	2	0.026	0.036	46.72
Live	*Heliobacterium modesticaldum* Ice1	Chemo	50	Pyruvate (20 mM) + YE (4 g L-1)	NA	0.269	Chemo	50	Acetate (30 mM)	NA	1	0.036	0.038	5.50
Live	*Heliobacterium modesticaldum* Ice1	Chemo	50	Pyruvate (20 mM) + YE (4 g L-1)	NA	0.24	Chemo	50	Acetate (30 mM)	NA	2	0.034	0.055	19.11
Live	*Heliobacterium modesticaldum* Ice1	Chemo	50	Pyruvate (20 mM) + YE (4 g L-1)	NA	0.247	Chemo	50	YE (4 g L-1)	NA	1	0.032	0.037	8.24
Live	*Heliobacterium modesticaldum* Ice1	Chemo	50	Pyruvate (20 mM) + YE (4 g L-1)	NA	0.21	Chemo	50	YE (4 g L-1)	NA	2	0.026	0.034	4.18
Live	*Heliobacterium modesticaldum* Ice1	Chemo	50	Pyruvate (20 mM) + YE (4 g L-1)	NA	0.277	Chemo	50	Pyruvate (20 mM) + YE (0.2 g L-1)	NA	1	0.03	0.04	56.51
Live	*Heliobacterium modesticaldum* Ice1	Chemo	50	Pyruvate (20 mM) + YE (4 g L-1)	NA	0.27	Chemo	50	No Carbon	NA	1	0.031	0.014	6.53
Live	*Heliobacterium modesticaldum* Ice1	Chemo	50	Pyruvate (20 mM) + YE (4 g L-1)	NA	0.264	Chemo	50	No Carbon	NA	2	0.019	0.028	15.84
Live	*Heliobacterium modesticaldum* Ice1	Chemo	50	Pyruvate (20 mM) + YE (4 g L-1)	NA	0.311	Chemo	50	Pyruvate (2 mM)	NA	1	0.041	0.028	37.46
Live	*Heliobacterium modesticaldum* Ice1	Chemo	50	Pyruvate (20 mM) + YE (4 g L-1)	NA	0.261	Chemo	50	Pyruvate (2 mM)	NA	2	0.032	0.028	45.12
Live	*Heliobacterium modesticaldum* Ice1	Chemo	50	Pyruvate (20 mM) + YE (4 g L-1)	NA	0.265	Chemo	50	Pyruvate (2 mM)	10 µM NO2	1	0.024	0.034	53.47
Live	*Heliobacterium modesticaldum* Ice1	Chemo	50	Pyruvate (20 mM) + YE (4 g L-1)	NA	0.269	Chemo	50	Pyruvate (2 mM)	10 µM NO2	2	0.016	0.023	53.66
NC	*Heliobacterium modesticaldum* Ice1	Chemo	50	Pyruvate (20 mM) + YE (4 g L-1)	NA	NA	Chemo	50	Pyruvate (2 mM)	10 µM NO2	1	0	0	3.60
Live	*Heliobacterium modesticaldum* Ice1	Chemo	50	Pyruvate (20 mM) + YE (4 g L-1)	NA	0.27	Chemo	50	Pyruvate (20 mM)	NA	1	0.048	0.035	60.10

Continued on next page

Live	*Heliobacterium modesticaldum* Ice1	Chemo	50	Pyruvate (20 mM) + YE (4 g L-1)	NA	0.278	Chemo	50	Pyruvate (20 mM)	NA	2	0.033	0.034	58.92
Live	*Heliobacterium modesticaldum* Ice1	Chemo	50	Pyruvate (20 mM) + YE (4 g L-1)	NA	0.273	Chemo	50	Pyruvate (100 mM)	NA	1	0.037	0.01	68.41
Live	*Heliobacterium modesticaldum* Ice1	Chemo	50	Pyruvate (20 mM) + YE (4 g L-1)	NA	0.273	Chemo	50	Pyruvate (100 mM)	NA	2	0.035	0.025	56.56
Live	*Geobacter sulfurreducens* PCA	Chemo	28	Acetate (10 mM)	Fumarate (40 mM)	0.219	Chemo	28	Pyruvate (20 mM) + YE (4 g L-1)	NA	1	0.055	0.074	12.59
Live	*Geobacter sulfurreducens* PCA	Chemo	28	Acetate (10 mM)	Fumarate (40 mM)	0.243	Chemo	28	Pyruvate (20 mM) + YE (4 g L-1)	NTZ (10 µM) + DMSO (2.8 mM)	1	0.034	0.041	3.19
Live	*Geobacter sulfurreducens* PCA	Chemo	28	Acetate (10 mM)	Fumarate (40 mM)	0.232	Chemo	28	Pyruvate (20 mM) + YE (4 g L-1)	DMSO (2.8 mM)	1	0.032	0.098	8.46
Live	*Geobacter sulfurreducens* PCA	Chemo	28	Acetate (10 mM)	Fumarate (40 mM)	0.248	Chemo	28	Pyruvate (20 mM) + YE (4 g L-1)	Fumarate (40 mM)	1	0.023	0.185	6.65
Live	*Geobacter sulfurreducens* PCA	Chemo	28	Acetate (10 mM)	Fumarate (40 mM)	0.21	Chemo	28	Acetate (10 mM)	Fumarate (40 mM)	1	0.034	0.016	19.81
Live	*Geobacter sulfurreducens* PCA	Chemo	28	Acetate (10 mM)	Fumarate (40 mM)	0.275	Chemo	28	Acetate (10 mM)	Fumarate (40 mM)	2	0.036	0.038	21.48
Live	*Clostridium acetobutylicum* ATCC 824	Chemo	37	Glucose (28 mM) + Peptone (10 g L-1) + YE (10 g L-1)	NA	1.547	Chemo	37	Pyruvate (20 mM) + YE (4 g L-1)	NA	1	0.207	0.167	41.08
Live	*Clostridium acetobutylicum* ATCC 824	Chemo	37	Glucose (28 mM) + Peptone (10 g L-1) + YE (10 g L-1)	NA	1.546	Chemo	37	Pyruvate (20 mM) + YE (4 g L-1)	NTZ (10 µM) + DMSO (2.8 mM)	1	0.143	0.146	1.20
Live	*Clostridium acetobutylicum* ATCC 824	Chemo	37	Glucose (28 mM) + Peptone (10 g L-1) + YE (10 g L-1)	NA	1.254	Chemo	37	Pyruvate (20 mM) + YE (4 g L-1)	DMSO (2.8 mM)	1	0.215	0.139	41.00
Live	*Clostridium acetobutylicum* ATCC 824	Chemo	37	Glucose (28 mM) + Peptone (10 g L-1) + YE (10 g L-1)	NA	1.495	Chemo	37	Pyruvate (20 mM) + YE (4 g L-1)	DMSO (2.8 mM)	2	0.034	0.031	51.02
Live	*Clostridium acetobutylicum* ATCC 824	Chemo	37	Glucose (28 mM) + Peptone (10 g L-1) + YE (10 g L-1)	NA	1.5	Chemo	37	Glucose 27 mM + Peptone (10 g L-1) + yeast (10 g L-1)	NA	1	0.037	1.221	52.49
Live	*Escherichia coli* K-12	Chemo	37	Pyruvate (20 mM) + YE (4 g L-1)	NA	0.221	Chemo	37	Pyruvate (20 mM) + YE (4 g L-1)	NA	1	0.034	0.171	4.12

SUPPORTING REFERENCES

1. Kimble, L. K.; Mandelco, L.; Woese, C. R.; Madigan, M. T., *Heliobacterium modesticaldum*, sp. nov., a thermophilic heliobacterium of hot springs and volcanic soils. *Archives of Microbiology* **1995,** *163*, (4), 259-267.

2. Schaefer, J. K.; Morel, F. M. M., High methylation rates of mercury bound to cysteine by *Geobacter sulfurreducens*. *Nature Geoscience* **2009,** *2*, 123-126.

3. R Core Team *R: A Language and Environment for Statistical Computing*, R Foundation for Statistical Computing: 2014.

4. Tang, K. H.; Feng, X. Y.; Zhuang, W. Q.; Alvarez-Cohen, L.; Blankenship, R. E.; Tang, Y. J., Carbon flow of Heliobacteria is related more to Clostridia than to the green sulfur bacteria. *Journal of Biological Chemistry* **2010,** *285*, (45), 35104-35112.

5. Kim, B. H.; Bellows, P.; Datta, R.; Zeikus, J. G., Control of carbon and electron flow in *Clostridium acetobutylicum* fermentations: utilization of carbon-monoxide to inhibit hydrogen production and to enhance butanol yields. *Applied and Environmental Microbiology* **1984,** *48*, (4), 764-770.

6. Caccavo, F.; Lonergan, D. J.; Lovley, D. R.; Davis, M.; Stolz, J. F.; McInerney, M. J., *Geobacter sulfurreducens* sp-nov, a hydrogen-oxidizing and acetate-oxidizing dissimilatory metal-reducing microorganism. *Applied and Environmental Microbiology* **1994,** *60*, (10), 3752-3759.

7. Lin, H.; Morrell-Falvey, J. L.; Rao, B.; Liang, L. Y.; Gu, B. H., Coupled mercury-cell sorption, reduction, and oxidation on methylmercury production by *Geobacter sulfurreducens* PCA. *Environmental Science & Technology* **2014,** *48*, (20), 11969-11976.

8. Wiatrowski, H. A.; Ward, P. M.; Barkay, T., Novel reduction of mercury(II) by mercury-sensitive dissimilatory metal reducing bacteria. *Environmental Science and Technology* **2006,** *40*, (21), 6690-6696.

9. Lovley, D. R.; Holmes, D. E.; Nevin, K. P., Dissimilatory Fe(III) and Mn (IV) reduction. *Advances in microbial physiology* **2004,** *49*, 219-286.

10. Speers, A. M.; Reguera, G., Electron donors supporting growth and electroactivity of *Geobacter sulfurreducens* anode biofilms. *Applied and Environmental Microbiology* **2012,** *78*, (2), 437-444.

11. Methe, B. A.; Nelson, K. E.; Eisen, J. A.; Paulsen, I. T.; Nelson, W.; Heidelberg, J. F.; Wu, D.; Wu, M.; Ward, N.; Beanan, M. J.; Dodson, R. J.; Madupu, R.; Brinkac, L. M.; Daugherty, S. C.; DeBoy, R. T.; Durkin, A. S.; Gwinn, M.; Kolonay, J. F.; Sullivan, S. A.; Haft, D. H.; Selengut, J.; Davidsen, T. M.; Zafar, N.; White, O.; Tran, B.; Romero, C.; Forberger, H. A.; Weidman, J.; Khouri, H.; Feldblyum, T. V.; Utterback, T. R.; Van Aken, S. E.; Lovley, D. R.; Fraser, C. M., Genome of *Geobacter sulfurreducens*: Metal reduction in subsurface environments. *Science* **2003,** *302*, (5652), 1967-1969.

12. Blaschkowski, H. P.; Neuer, G.; Ludwig-Festl, M.; Knappe, J., Routes of flavodoxin and ferredoxin reduction in *Escherichia coli* CoA-acylating pyruvate:flavodoxin and NADPH:flavodoxin oxidoreductases participating in the activation of pyruvate formate-lyase. *European Journal of Biochemistry* **1982,** *123*, 563-569.

13. Tang, K. H.; Yue, H.; Blankenship, R. E., Energy metabolism of *Heliobacterium modesticaldum* during phototrophic and chemotrophic growth. *Bmc Microbiology* **2010,** *10*.

Appendix C: Supporting information for Chapter 6

Daniel S. Grégoire [a*], Noémie C. Lavoie [a*], Bejamin R. Stenzler [a] & Alexandre J. Poulain [a]

[*] contributed equally to this work.

a - Biology Department, University of Ottawa, 30 Marie Curie, Ottawa, Ontario, K1N 6N5, Canada

LIST OF SUPPORTING MATERIALS

SUPPORTING FIGURES :

SUPPORTING TABLES:

SUPPORTING REFERENCES

SUPPORTING FIGURES

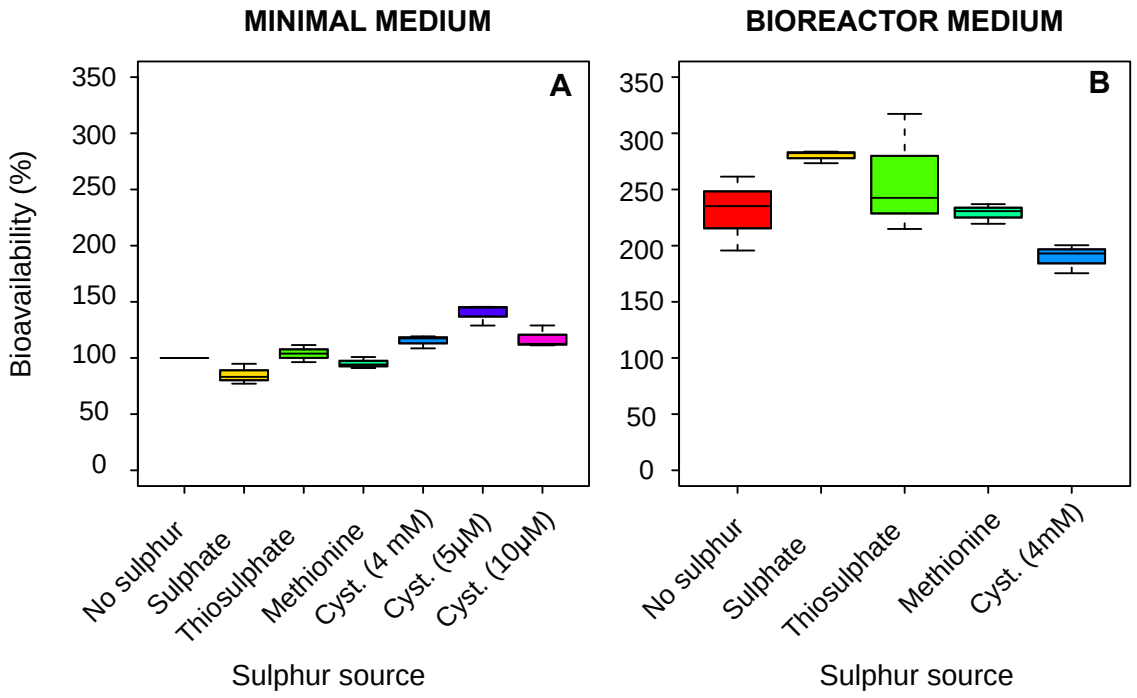

Figure C1: Fluorescence in the presence of 5 nM Hg, sulphate, thiosulphate, methionine and different concentrations of cysteine (denoted here as Cyst.) for constitutive bioreporter cells. Cells were exposed to Hg in BMAA exposure medium (**A**) and DSMZ medium #370 amended with 20 mM pyruvate (**B**) where [NO_3^-] was set to 0.2 mM. Data presented here are from technical triplicates. For experiments comparing different sulphur sources total sulphur concentrations was normalized to 4 mM. The bottom and top of the boxes show the first and third quartiles respectively, the bar in the middle shows the median and the whiskers show the minimum and maximum for each treatment.

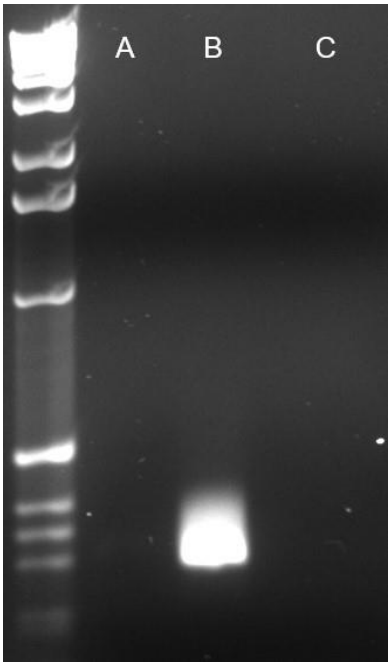

Figure C2: Gel electrophoresis (TAE 1X, 100V, 15 minutes) of the *merA* PCR product. Negative control – dH_2O (**A**), positive control – plasmid containing *merA* gene (**B**), *H. mobilis* DNA extract (**C**). No amplification of *merA* was detected in *H mobilis* DNA extract.

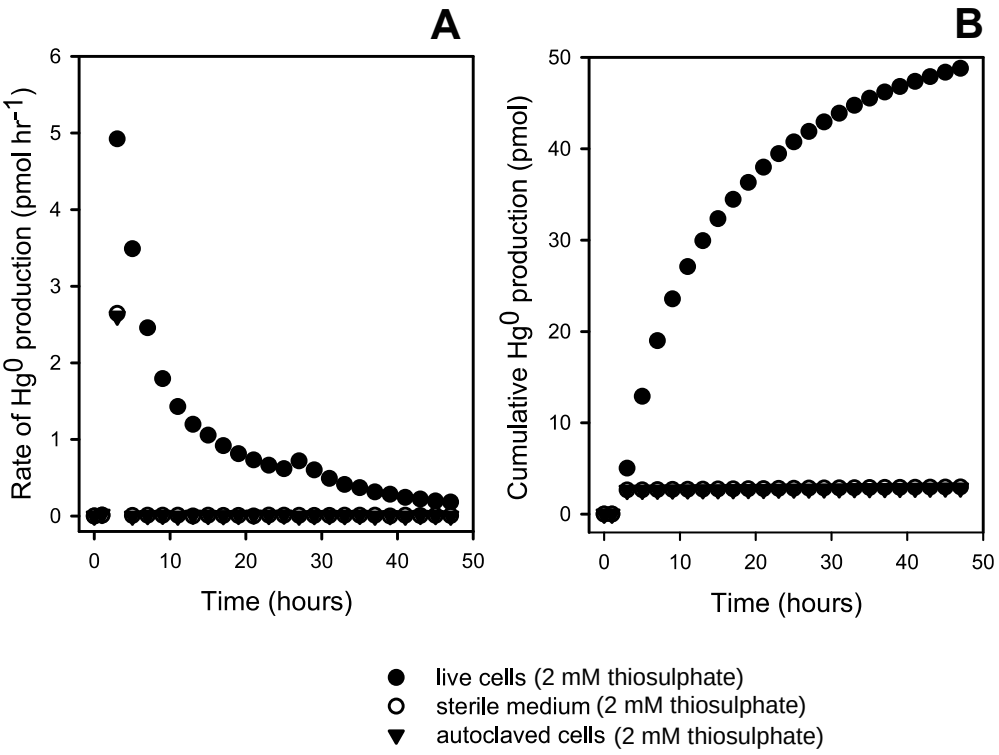

Figure C3: Hg^0 production by *H. mobilis* grown phototrophically with 2 mM thiosulphate as a sulphur source. Hg^0 production rate (**A**) and cumulative Hg^0 production (**B**) for live cells, sterile medium without cells and autoclaved cells. $HgCl_2$ was added to a final concentration of 250 pM in all experiments. Results are representative cases of replicated experiments, but each data point was recorded once by the instrument as such no error bars are included.

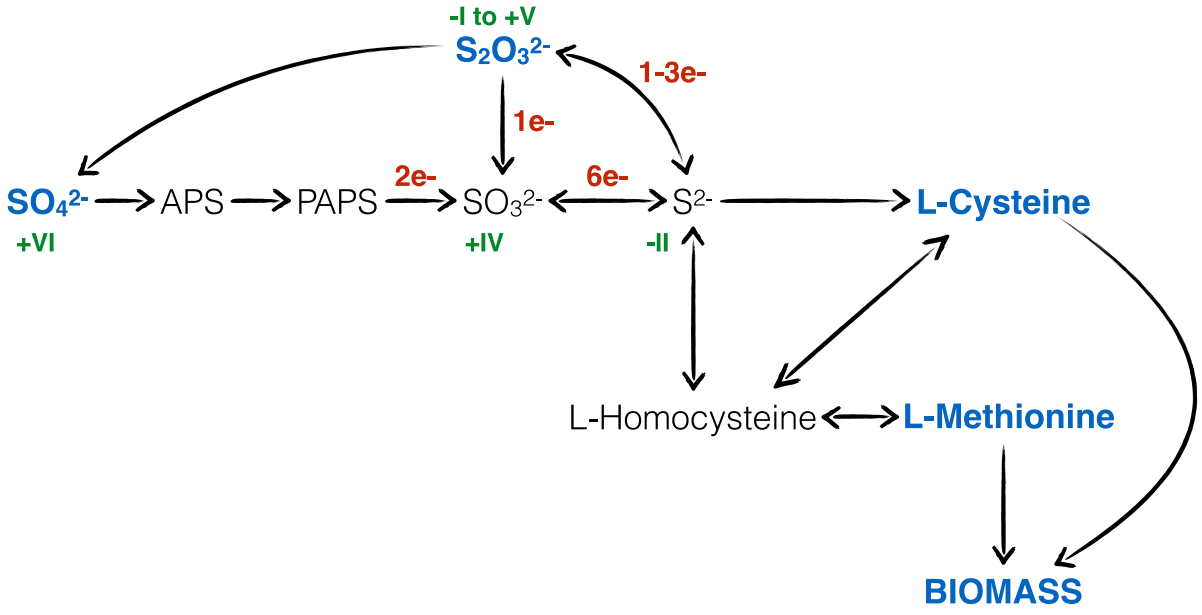

Figure C4: Summary of assimilatory sulphur metabolic pathways in bacteria modified from Rodionov et al. [1]. Abbreviations: APS (adenosine- 5'-phosphosulphate), PAPS (3'- phospho – adenosine 5' – phosphosulphate), e- (electron)

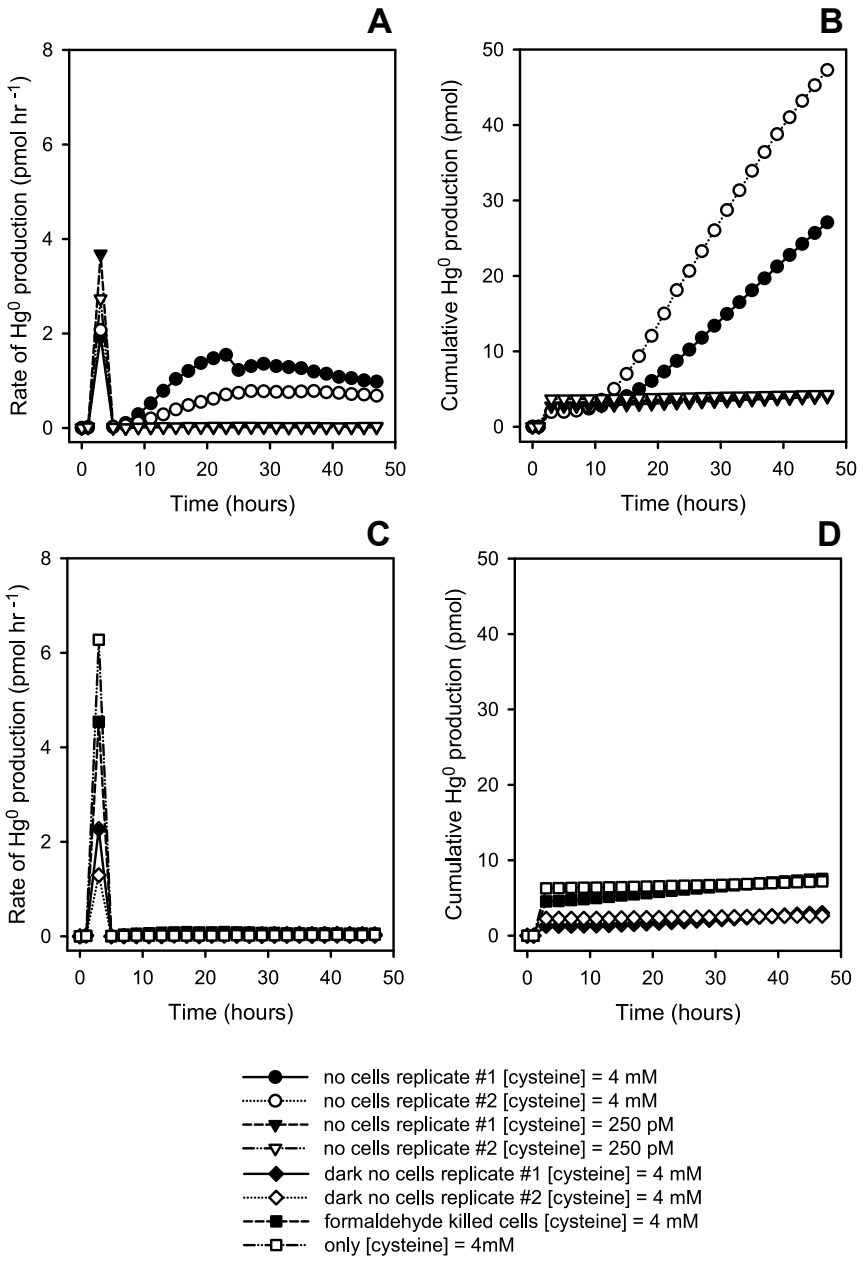

Figure C5: Abiotic Hg^0 production in the bioreactor amended with cysteine. All experiments were performed in the presence of light except for the dark treatment. Rate of Hg^0 production (**A**) and cumulative Hg^0 production (**B**) for sterile medium containing no cells and 4 mM cysteine, and sterile medium containing no cells and 250 pM cysteine. Rate of Hg^0 production (**C**) and cumulative Hg^0 production (**D**) for sterile medium with no cells and 4 mM cysteine in the dark, formaldehyde-killed *H. mobilis* with 4 mM cysteine, and sterile medium with no cells devoid of all organic carbon sources except 4 mM cysteine. $HgCl_2$ was added to a final concentration of 250 pM in all experiments

SUPPORTING TABLES

Table C1: Thermodynamic modeling data predicting dominant Hg species formed in the presence of sulphate (SO_4^{-2}), thiosulphate ($S_2O_3^{-2}$), methionine (met) and cysteine (cys) in BMAA media at 37°C. All sulphur sources were calculated at 4 mM unless otherwise stated.

Sulphur source	$Hg(OH)_2$	$Hg(S_2O_3)_2^{-2}$	$Hg(S_2O_3)_3^{-4}$	$Hg(NH_3)_2^{+2}$	$HgH_2(Cys)_2$	$HgH(Cys)_2^{-}$	$HgHCys^{+}$	$Hg(Met)_2$	$HgMet^{+}$
No sulphur	97.0	0	0	3.0	0	0	0	0	0
Sulphate	97.0	0	0	3.0	0	0	0	0	0
Thiosulphate	0	89.3	10.7	0	0	0	0	0	0
Methionine	1.2	0	0	0	0	0	0	97.4	1.4
Cysteine (4 mM)	0	0	0	0	90.7	9.2	0	0	0
Cysteine (5 µM)	0	0	0	0	62.6	5.4	30.4	0	0
Cysteine (10 µM)	0	0	0	0	74.6	6.4	18.0	0	0

Table C2: Equilibrium formation constants ($log_{10}K$, T = 25°C) for all aqueous Hg species considered in the speciation calculations. Activity corrections for ionic strength were made using the B-dot Equation if the ion-specific hard core diameter (å) was present, otherwise activity corrections were made according to the Davies equation. Temperature corrections to $log_{10}K$ were made using the Van't Hoff equation but if a temperature dependent analytical expression was present, $log_{10}K$ was calculated using the expression from Parkhurst et al., (2013) [2] with values A_1, A_2, A_3, A_4, A_5, A_6 and temperature in Kelvin:

Formula	**å**	**$log_{10}K$**	**ΔH(KJ/mol)**	**A_1, A_2, A_3, A_4, A_5, A_6**	**Reference**
$Hg^{2+} + 2H_2O = Hg(OH)_2 + 2H^+$	3.4			2.971E+2, 4.096E-2, -1.797E+4, -1.066E+2, 7.724E+5, 0	[3]
$NH_3 + H^+ = NH_4^+$	2.5			3.749E+1, -1.545E-3, -6.956E+2, -1.149E+1, 2.655E+5, 0	[4]
$Hg^{2+} + NH_3 = HgNH_3^{2+}$		8.8			[5]
$Hg^{2+} + 2NH_3 = Hg(NH_3)_2^{2+}$		17.8	-311		[5]
$Hg^{2+} + 3NH3 = Hg(NH_3)_3^{2+}$		18.156	-429		[5]
$Hg^{2+} + 4NH_3 = Hg(NH_3)_4^{2+}$		19.3	-548		[5]
$2Hg^{2+} + H_2O = Hg_2(OH)^{3+} + H^+$	8.2			6.069E+2, 9.088E-2, -3.232E+4, -2.212E+2, 1.650E+6, 0	[3]
$Hg^{2+} + H_2O = HgOH^+ + H^+$	4.1			2.785E+2, 4.231E-2, -1.780E+4, -9.968E+1, 1.056E+6, 0	[4]
$Hg^{2+} + SO_4^{2-} = HgSO_4$		2.535			[5]
$Hg^{2+} + NO_3^- = HgNO_3^+$		-0.3157			[5]
$Hg^{2+} + 2NO_3^- = Hg(NO_3)_2$		-0.697			[5]
$MOPS^- + H^+ = HMOPS$		7.184	-21.1		[6]
β-Gylcerophosphate^{2-} + H^+ = Hβ-Glycerophosphate$^-$		6.65	1.85		[6]
Hβ-Glycerophosphate$^-$ + H^+ = H_2β-Glycerophosphate		1.329	12.2		[6]

$H^+ + Cysteine^{2-} = HCysteine^-$	10.87		[7]
$2H^+ + Cysteine^{2-} = H_2Cysteine$	19.38		[7]
$3H^+ + Cysteine^{2-} = H_3Cysteine^+$	21.67		[7]
$Hg^{2+} + Cysteine^{2-} = HgCysteine$	35.73		[7]
$Hg^{2+} + H^+ + Cysteine^{2-} = HgHCysteine^+$	43.83		[7]
$Hg^{2+} + 2H^+ + Cysteine^{2-} = HgH_2Cysteine^{2+}$	46.12		[7]
$Hg^{2+} + 2Cysteine^{2-} = Hg(Cysteine)_2^{2-}$	44.55		[7]
$Hg^{2+} + H^+ + 2Cysteine^{2-} = HgH(Cysteine)_2^-$	53.97		[7]
$Hg^{2+} + 2H^+ + 2Cysteine^{2-} = HgH_2(Cysteine)_2$	62.04		[7]
$H^+ + Methionine^- = HMethionine$	9.26		[8]
$2H^+ + Methionine^- = H_2Methionine+$	11.56		[8]
$Hg^{2+} + Methionine^- = HgMethionine^+$	12.8		[9]
$Hg^{2+} + 2Methionine^- = Hg(Methionine)_2$	19.5		[9]
$Hg^{2+} + S_2O_3^{2-} = Hg(S_2O_3)_2^{2-}$	29.18		[10]
$Hg^{2+} + 3S_2O_3^{2-} = Hg(S_2O_3)_3^{4-}$	30.3		[10]
$S_2O_3^{2-} + 2H^+ = H_2S_2O_3$	3.4	1.497E+3, 2.381E-1, -8.404E+4, -5.420E+2, 5.037E+6, 0	[4]
$S_2O_3^{2-} + H^+ = HS_2O_3^-$	3.6	7.637E+2, 1.228E-1, -4.334E+4, -2.762E+2, 2.691E+6, 0	[4]
$Na^+ + S_2O_3^{2-} = NaS_2O_3^-$	3.6	1.604E+3, 2.468E-1, -8.865E+4, -5.815E+2, 5.218E+6, 0	[11]

Table C3 Bioreactor data table for all sulphur experiments. Abbreviation = Treatment (Treat), metabolism (Metabo), temperature (T), inoculum (Inoc), replicate (Rep), and phototrophy (Photo)

Treat.	Strain	Metabo.	T (°C)	Carbon source (mM or g L^{-1})	Sulphur source (pM or mM)	Light (µmol photon m^{-2} s^{-1})	Inoc. O.D. 600 nm	Metabo.	T (°C)	Carbon source (mM or g L^{-1})	Sulphur source (pM or mM)	Light (µmol photon m^{-2} s^{-1})	Rep #	Initial O.D. 600 nm	Final O.D. 600 nm	Cumulative Hg^0 production (pmol)
Live cells	*Heliobacillus mobilis*	Photo	37	Pyruvate (20 mM) + YE (10 g L-1)	4 mM Sulphate	80	1.212	Photo	37	Pyruvate (20 mM) + YE (10 g L-1)	4 mM Sulphate	20	1	0.21	0.305	2.73
Live cells	*Heliobacillus mobilis*	Photo	37	Pyruvate (20 mM) + YE (10 g L-1)	4 mM Sulphate	80	1.118	Photo	37	Pyruvate (20 mM) + YE (10 g L-1)	4 mM Sulphate	20	2	0.188	0.253	14.65
Live cells	*Heliobacillus mobilis*	Photo	37	Pyruvate (20 mM) + YE (10 g L-1)	4 mM Sulphate	80	0.841	Photo	37	Pyruvate (20 mM) + YE (10 g L-1)	4 mM Sulphate	20	3	0.122	0.175	25.32
Sterile medium	No cells	Photo	NA	NA	NA	NA	NA	Photo	37	Pyruvate (20 mM) + YE (10 g L-1)	4 mM Sulphate	20	1	0.001	0.011	4.71
Sterile medium	No cells	Photo	NA	NA	NA	NA	NA	Photo	37	Pyruvate (20 mM) + YE (10 g L-1)	4 mM Sulphate	20	2	0.01	0.016	3.85
Live cells	*Heliobacillus mobilis*	Photo	37	Pyruvate (20 mM) + YE (10 g L-1)	2 mM Sodium thiosulphate	80	0.803	Photo	37	Pyruvate (20 mM) + YE (10 g L-1)	2 mM Sodium thiosulphate	20	1	0.11	0.157	45.80
Live cells	*Heliobacillus mobilis*	Photo	37	Pyruvate (20 mM) + YE (10 g L-1)	2 mM Sodium thiosulphate	80	0.958	Photo	37	Pyruvate (20 mM) + YE (10 g L-1)	2 mM Sodium thiosulphate	20	2	0.148	0.191	27.04
Live cells	*Heliobacillus mobilis*	Photo	37	Pyruvate (20 mM) + YE (10 g L-1)	2 mM Sodium thiosulphate	80	1.21	Photo	37	Pyruvate (20 mM) + YE (10 g L-1)	2 mM Sodium thiosulphate	20	3	0.19	0.178	49.03
Sterile medium	No cells	Photo	NA	NA	NA	NA	NA	Photo	37	Pyruvate (20 mM) + YE (10 g L-1)	2 mM Sodium thiosulphate	20	1	0.004	0.009	2.98
Sterile medium	No cells	Photo	NA	NA	NA	NA	NA	Photo	37	Pyruvate (20 mM) + YE (10 g L-1)	2 mM Sodium thiosulphate	20	2	0.013	0.013	3.12
Autoclaved cells	*Heliobacillus mobilis*	Photo	37	Pyruvate (20 mM) + YE (10 g L-1)	2 mM thiosulphate	80	0.962	Photo	37	Pyruvate (20 mM) + YE (10 g L-1)	2 mM Sodium thiosulphate	20	1	0.143	0.161	2.87
Live cells	*Heliobacillus mobilis*	Photo	37	Pyruvate (20 mM) + YE (10 g L-1)	4 mM L-methionine	80	0.904	Photo	37	Pyruvate (20 mM) + YE (10 g L-1)	4 mM L-methionine	20	1	0.144	0.144	21.55
Live cells	*Heliobacillus mobilis*	Photo	37	Pyruvate (20 mM) + YE (10 g L-1)	4 mM L-methionine	80	0.895	Photo	37	Pyruvate (20 mM) + YE (10 g L-1)	4 mM L-methionine	20	2	0.133	0.205	16.95
Live cells	*Heliobacillus mobilis*	Photo	37	Pyruvate (20 mM) + YE (10 g L-1)	4 mM L-methionine	80	1.111	Photo	37	Pyruvate (20 mM) + YE (10 g L-1)	4 mM L-methionine	20	3	0.181	0.352	42.68
Sterile medium	No cells	Photo	NA	NA	NA	NA	NA	Photo	37	Pyruvate (20 mM) + YE (10 g L-1)	4 mM L-methionine	20	1	0.002	0.005	6.81
Sterile medium	No cells	Photo	NA	NA	NA	NA	NA	Photo	37	Pyruvate (20 mM) + YE (10 g L-1)	4 mM L-methionine	20	2	0.008	0.009	3.75
Live cells	*Heliobacillus mobilis*	Photo	37	Pyruvate (20 mM) + YE (10 g L-1)	4 mM L-cysteine	80	0.554	Photo	37	Pyruvate (20 mM) + YE (10 g L-1)	4 mM L-cysteine	20	1	0.114	0.092	3.79
Live cells	*Heliobacillus mobilis*	Photo	37	Pyruvate (20 mM) + YE (10 g L-1)	4 mM L-cysteine	80	0.76	Photo	37	Pyruvate (20 mM) + YE (10 g L-1)	4 mM L-cysteine	20	2	0.164	0.132	8.79
Live cells	*Heliobacillus mobilis*	Photo	37	Pyruvate (20 mM) + YE (10 g L-1)	4 mM L-cysteine	80	0.879	Photo	37	Pyruvate (20 mM) + YE (10 g L-1)	4 mM L-cysteine	20	3	0.173	0.14	13.79

Continued on next page

Sterile medium	No cells	Photo	NA	NA	NA	NA	NA	Photo	37	Pyruvate (20 mM) + YE (10 g L-1)	4 mM L-cysteine	20	1	0.001	0	48.29
Sterile medium	No cells	Photo	NA	NA	NA	NA	NA	Photo	37	Pyruvate (20 mM) + YE (10 g L-1)	4 mM L-cysteine	20	2	0	0	27.78
Sterile medium	No cells	Chemo	NA	NA	NA	NA	NA	Chemo	37	Pyruvate (20 mM) + YE (10 g L-1)	4 mM L-cysteine	20	1	0	0	2.66
Sterile medium	No cells	Chemo	NA	NA	NA	NA	NA	Chemo	37	Pyruvate (20 mM) + YE (10 g L-1)	4 mM L-cysteine	20	2	0.004	0	3.06
Formaldehyde killed cells	*Heliobacillus mobilis*	Photo	37	Pyruvate (20 mM) + YE (10 g L-1)	4 mM L-cysteine	80	NA (dead cells)	Photo	37	Pyruvate (20 mM) + YE (10 g L-1)	4 mM L-cysteine	20	1	0.17	0.197	7.54
Live cells	*Heliobacillus mobilis*	Photo	37	Pyruvate (20 mM) + YE (10 g L-1)	4 mM L-cysteine	80	0.642	Photo	37	Pyruvate (20 mM) + YE (10 g L-1)	250 pM L-cysteine	20	1	0.127	0.154	60.91
Live cells	*Heliobacillus mobilis*	Photo	37	Pyruvate (20 mM) + YE (10 g L-1)	4 mM L-cysteine	80	0.72	Photo	37	Pyruvate (20 mM) + YE (10 g L-1)	250 pM L-cysteine	20	2	0.166	0.219	54.97
Live cells	*Heliobacillus mobilis*	Photo	37	Pyruvate (20 mM) + YE (10 g L-1)	4 mM L-cysteine	80	0.586	Photo	37	Pyruvate (20 mM) + YE (10 g L-1)	250 pM L-cysteine	20	3	0.098	0.129	53.90
Sterile medium	No cells	Photo	NA	NA	NA	NA	NA	Photo	37	Pyruvate (20 mM) + YE (10 g L-1)	250 pM L-cysteine	20	1	0.002	0.006	4.02
Sterile medium	No cells	Photo	NA	NA	NA	NA	NA	Photo	37	Pyruvate (20 mM) + YE (10 g L-1)	250 pM L-cysteine	20	2	0.007	0.009	4.29
Sterile medium	No cells	Photo	NA	NA	NA	NA	NA	Photo	37	No carbon	250 pM L-cysteine	20	1	0.002	0	7.23

SUPPORTING REFERENCES

1. Rodionov, D. A.; Vitreschak, A. G.; Mironov, A. A.; Gelfand, M. S., Comparative genomics of the methionine metabolism in Gram-positive bacteria: A variety of regulatory systems. *Nucleic Acids Research* **2004,** *32*, (11), 3340-3353.

2. Parkhurst, D. L. a., *Description of input and examples for PHREEQC version 3--a computer program for speciation, batch-reaction, one-dimensional transport, and inverse geochemical calculations*. Reston, Virginia : U.S. Department of the Interior, U.S. Geological Survey, 2013.: 2013.

3. Blanc, P., Mercury associated physical and chemical constants: updating of the THERMODDEM database. *IMaHg project* **2012,** *rapport BRGM RP-61299-FR,* 32p.

4. Shock, E. L.; Sassani, D. C.; Willis, M.; Sverjensky, D. A., Inorganic species in geologic fluids: correlations among standard molal thermodynamic properties of aqueous ions and hydroxide complexes. *Geochimica et Cosmochimica Acta* **1997,** *61*, (5), 907-950.

5. Smith, R.; Martell, A.; Motekaitis, R., NIST standard reference database 46. *NIST Critically Selected Stability Constants of Metal Complexes Database Ver* **2004,** *2*.

6. Goldberg, R. N.; Kishore, N.; Lennen, R. M., Thermodynamic quantities for the ionization reactions of buffers. *Journal of physical and chemical reference data* **2002,** *31*, (2), 231-370.

7. Cardiano, P.; Falcone, G.; Foti, C.; Sammartano, S., Sequestration of Hg2+ by some biologically important thiols. *Journal of Chemical & Engineering Data* **2011,** *56*, (12), 4741-4750.

8. Pettit, L. D.; Powell, K., The IUPAC stability constants database. *Chemistry international* **2006**.

9. Van Der Linden, W.; Beers, C., Determination of the composition and the stability constants of complexes of mercury (II) with amino acids. *Analytica chimica acta* **1974,** *68*, (1), 143-154.

10. Nyman, C.; Salazar, T., Complex ion formation of mercury (II) and thiosulfate ion. *Analytical Chemistry* **1961,** *33*, (11), 1467-1469.

11. Wagman, D. D.; Evans, W. H.; Parker, V. B.; Schumm, R. H.; Halow, I. *The NBS tables of chemical thermodynamic properties. Selected values for inorganic and C1 and C2 organic substances in SI units*; National Standard Reference Data System: 1982.

Appendix D: Supporting information for Chapter 7

Daniel S. Grégoire [a]*, Sarah E. Janssen [b]*, Michael T. Tate [b]* & Alexandre J. Poulain [a]

* Contributed equally to this work

a - Biology Department, University of Ottawa, 30 Marie Curie, Ottawa, ON, K1N 6N5, Canada.

b - Wisconsin Water Science Center, US Geological Survey, Middleton, Wisconsin 53562, USA.

LIST OF SUPPORTING MATERIALS:

SUPPORTING FIGURES

SUPPORTING TABLES

SUPPORTING FIGURES

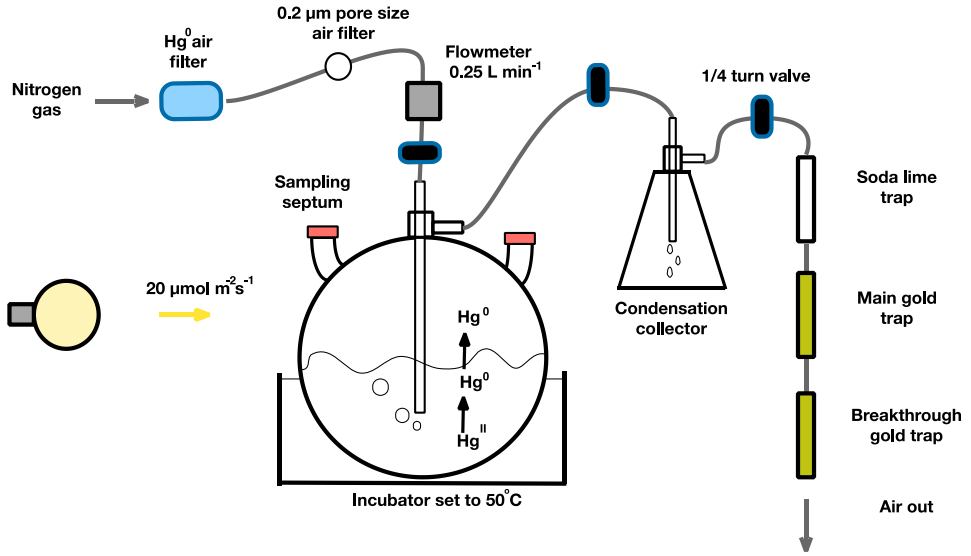

Figure D1: Schematic of the bioreactor setup used to measure Hg stable isotope fractionation for Hg^{II} and Hg^{0} during the anaerobic phototrophic reduction of Hg^{II}.

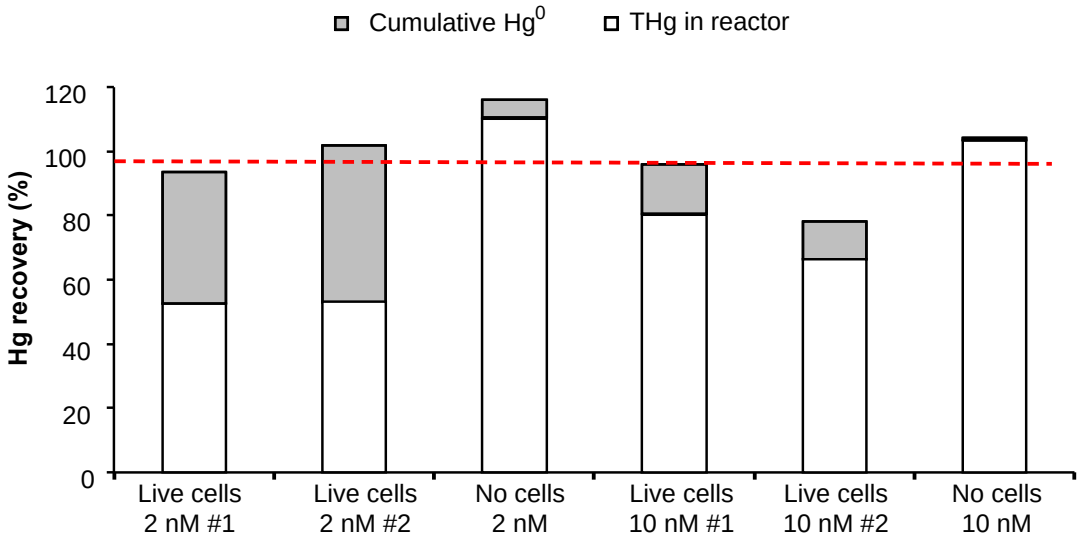

Figure D2: **Total Hg mass balance for isotope fractionation experiments with phototrophically grown *H. modesticaldum***. The average recovery across all experiments was 98.38 ± 12.52 % (n=6) and is shown by the dashed red line.

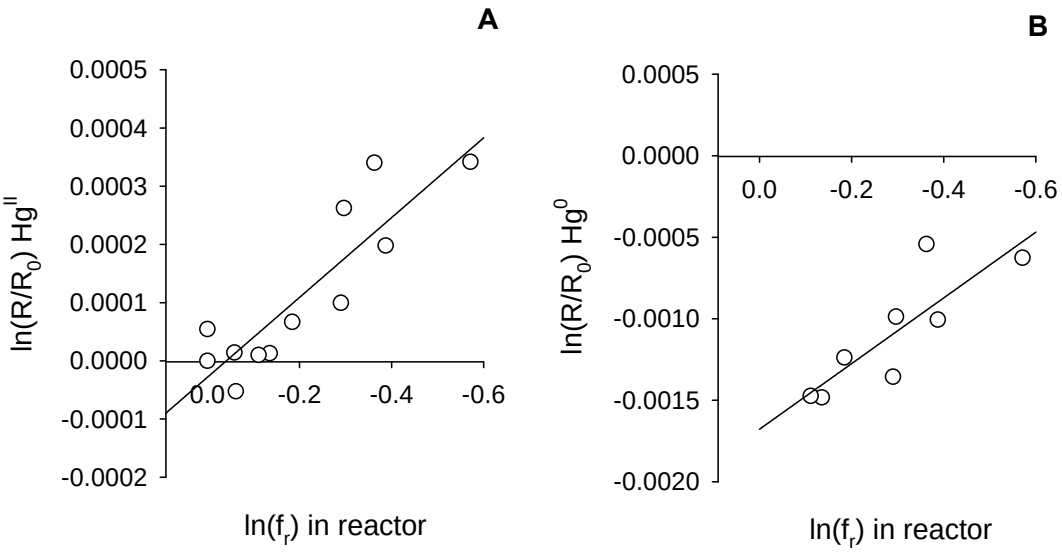

Figure D3: Mass dependent fractionation of $^{202}Hg^{II}$ and $^{202}Hg^{0}$ in phototrophically grown *H. modesticaldum*. δ^{202}Hg values for Hg^{II} (**A**) and Hg^{0} (**B**) are plotted as open system Rayleigh fractionation models with $\ln(R/R_0)$ vs $\ln(f_r)$. The amount of Hg^{II} remaining in the reactor was used to calculate f_r (see **Methods Chapter 7**). The 3h time point was omitted from the regression fitted to the data for Hg^{0} (**B**) as this suggested an alternative process was contributing to isotopic fractionation earlier on in the experiment. Significant regressions were obtained for both Hg^{II} where $y = -0.0007x - 2.82 \times 10^{-5}$ (Adjusted $R^2 = 0.76$, $p = 0.0001$) and Hg^{0} where $y = -0.002x - 0.0017$ (Adjusted $R^2 = 0.65$, $p = 0.0092$). Separate regressions were run for the Hg^{II} pool for replicated experiments that provided slope coefficients of -0.000999x and -0.000602x. These values were used to calculate an average and 2 x standard deviation for $\varepsilon_{AP} = -0.80 \pm 0.56$ ‰ and compare the variability associated with these experiment to previous work. 10 nM Hg was added from the same stock (NIST 3133) for all experiments.

SUPPORTING TABLES

Table D1: Total Hg concentrations and Hg isotope ratios for the reactant pool Hg^{II} in phototrophically grown cultures of *H. modesticaldum*. Each line corresponds to the average (Avg) of technical duplicates taken for each time point. Std represents the standard deviation from analytical replicates on the MC-ICP-MS. Abbreviations = treatment (Treat) and concentration ([Hg]).

Treat.	Sample	[Hg] (nM)	δ^{202}Hg Avg	δ^{202}Hg Std	Δ^{199}Hg Avg	Δ^{199}Hg Std	Δ^{200}Hg Avg	Δ^{200}Hg Std	Δ^{201}Hg Avg	Δ^{201}Hg Std
No cells	MED. BLANK	9.01	0.83	0.06	-0.05	0.03	-0.01	0.01	-0.03	0.03
	H2O BLANK	10.43	-0.04	0.05	-0.05	0.03	0.01	0.01	-0.04	0.03
	TIME 0HR	8.82	-0.03	0.04	0.00	0.03	0.00	0.03	0.00	0.02
	TIME 0HR	9.03	0.02	0.05	-0.06	0.03	-0.02	0.01	-0.02	0.02
	TIME 3HR	9.02	-0.03	0.03	-0.03	0.04	-0.03	0.02	0.00	0.02
	TIME 3HR	9.50	0.08	0.04	0.08	0.04	0.02	0.02	0.06	0.01
	TIME 6HR	9.11	0.05	0.04	0.02	0.04	0.02	0.04	0.06	0.03
	TIME 6HR	8.75	0.03	0.02	0.01	0.02	-0.02	0.04	-0.01	0.02
	TIME 12HR	8.97	0.00	0.05	-0.01	0.03	-0.02	0.04	-0.01	0.05
	TIME 12HR	8.67	-0.03	0.03	0.07	0.02	-0.01	0.04	0.03	0.05
	TIME 24HR	9.19	0.04	0.02	0.03	0.02	0.06	0.04	0.00	0.04
	TIME 24HR	9.15	-0.07	0.05	0.02	0.03	-0.03	0.02	-0.01	0.02
	TIME 48HR	9.00	0.05	0.03	0.13	0.03	0.02	0.03	-0.01	0.02
	TIME 48HR	8.89	0.06	0.03	0.04	0.04	0.04	0.01	0.02	0.02
Live cell 1	MED. BLANK	9.76	-0.02	0.03	-0.01	0.07	-0.01	0.03	0.02	0.02
	H2O BLANK	10.28	0.09	0.03	0.06	0.06	0.07	0.04	0.06	0.02
	TIME 0HR	9.48	0.04	0.04	-0.01	0.06	-0.04	0.02	-0.04	0.01
	TIME 0HR	9.50	0.02	0.03	-0.02	0.03	0.03	0.02	0.02	0.01
	TIME 3HR	8.71	0.08	0.06	0.02	0.02	0.03	0.01	-0.03	0.01
	TIME 3HR	9.20	0.01	0.05	0.01	0.03	-0.02	0.02	-0.04	0.05
	TIME 6HR	8.03	0.06	0.03	-0.01	0.03	0.00	0.04	0.01	0.04
	TIME 6HR	8.48	0.03	0.01	-0.04	0.02	-0.03	0.04	0.02	0.04
	TIME 12HR	7.96	0.02	0.05	-0.02	0.04	0.00	0.02	0.00	0.04
	TIME 12HR	7.67	0.17	0.02	0.02	0.03	0.00	0.02	0.00	0.05
	TIME 24HR	6.87	0.28	0.03	-0.02	0.04	0.02	0.04	-0.02	0.03
	TIME 24HR	6.77	0.31	0.02	-0.04	0.03	-0.01	0.02	-0.02	0.04
	TIME 48HR	6.18	0.45	0.05	-0.04	0.05	0.03	0.02	-0.03	0.04
	TIME 48HR	6.33	0.30	0.07	-0.10	0.05	-0.05	0.02	-0.04	0.04

Continued on next page

Table D1 ***(continued):*** Total Hg concentrations and Hg isotope ratios for the reactant pool Hg^{II} in phototrophically grown cultures of *H. modesticaldum*. Each line corresponds to the average (Avg) of technical duplicates taken for each time point. Std represents the standard deviation from analytical replicates on the MC-ICP-MS. Abbreviations = treatment (Treat) and concentration ([Hg]).

Treat.	Sample	[Hg] (nM)	δ^{202}Hg Avg	δ^{202}Hg Std	Δ^{199}Hg Avg	Δ^{199}Hg Std	Δ^{200}Hg Avg	Δ^{200}Hg Std	Δ^{201}Hg Avg	Δ^{201}Hg Std
Live cell 2	MED. BLANK	9.11	0.10	0.05	0.03	0.06	-0.03	0.01	0.00	0.03
	H2O BLANK	10.27	0.02	0.01	-0.05	0.02	-0.05	0.01	-0.04	0.05
	TIME 0HR	9.25	0.12	0.04	0.08	0.05	0.02	0.02	0.00	0.02
	TIME 0HR	8.89	0.05	0.04	-0.06	0.02	-0.05	0.02	-0.04	0.06
	TIME 3HR	8.48	0.00	0.06	0.00	0.05	0.01	0.03	-0.06	0.06
	TIME 3HR	8.58	-0.04	0.08	-0.03	0.05	0.02	0.03	0.03	0.06
	TIME 6HR	8.35	0.06	0.10	0.10	0.05	0.01	0.02	0.01	0.02
	TIME 6HR	7.85	0.02	0.09	0.00	0.05	0.00	0.02	0.00	0.03
	TIME 12HR	6.31	0.14	0.07	0.01	0.02	-0.01	0.02	-0.02	0.02
	TIME 12HR	6.88	0.12	0.06	-0.07	0.04	0.00	0.03	-0.06	0.03
	TIME 24HR	5.89	0.23	0.05	-0.04	0.03	0.00	0.03	-0.02	0.03
	TIME 24HR	5.81	0.23	0.03	-0.08	0.04	0.00	0.03	-0.01	0.03
	TIME 48HR	3.87	0.39	0.02	-0.01	0.03	-0.01	0.03	-0.03	0.03
	TIME 48HR	5.18	0.36	0.02	-0.04	0.02	-0.03	0.02	-0.07	0.02

Table D2: Total Hg and Hg isotope ratios recovered on gold traps for the product pool Hg^0 in phototrophically grown cultures of *H. modesticaldum*. Each line corresponds to the Hg present on two gold traps used to sample each time point in series. Std represents the standard deviation from analytical replicates on the MC-ICP-MS. Abbreviations = treatment (treat).

Treat.	Time (h)	Hg on trap (ng)	δ^{202}Hg Avg	δ^{202}Hg Std	Δ^{199}Hg Avg	Δ^{199}Hg Std	Δ^{200}Hg Avg	Δ^{200}Hg Std	Δ^{201}Hg Avg	Δ^{201}Hg Std
Live cell 1	3	25.18	0.50	0.06	0.16	0.05	-0.01	0.03	0.15	0.03
	6	29.76	-0.98	0.05	0.05	0.06	-0.01	0.03	0.02	0.03
	12	45.22	-0.74	0.05	0.12	0.06	0.02	0.03	0.12	0.04
	24	43.88	-0.49	0.03	0.15	0.05	0.04	0.02	0.10	0.02
	48	17.98	-0.04	0.02	0.15	0.01	-0.01	0.01	0.03	0.03
Live cell 2	3	21.34	0.66	0.04	0.17	0.05	-0.03	0.02	0.06	0.03
	6	23.17	-0.81	0.06	0.10	0.03	-0.02	0.01	0.04	0.03
	12	29.83	-0.69	0.07	0.21	0.05	0.00	0.03	0.11	0.02
	24	30.49	-0.34	0.07	0.17	0.02	0.08	0.02	0.11	0.01
	48	16.14	0.04	0.07	0.15	0.02	0.02	0.02	0.03	0.04

Appendix E: Making a business case for bioremediation

A personal essay by **Daniel S. Grégoire**

RATIONALE BEHIND MICROBRIGHT

One of the reasons I pursued research in biogeochemistry was my interest in bioremediation (e.g. environmental clean up strategies that use microbes). As I progressed through my PhD, I realized that despite numerous research articles demonstrating that microbes could be used to remove mercury (Hg) from water, very few methods moved beyond the laboratory scale. Although the research on Hg remediation suggested biological strategies have minimal environmental impact compared to current physical/chemical removal methods, there still seemed to be barriers preventing the wide adoption of bioremediation by industry.

As a student studying Hg cycling, I began to think about what role researchers play in removing barriers to adoption by industry and what steps are required to apply bioremediation methods in an industrial setting. I initially thought the role of researchers was to create innovative solutions that could be further developed and scaled up by likeminded industrial partners. I suspected that patenting research findings was crucial for attracting industrial collaborator and protecting the intellectual property moving forward. By attempting to patent some of my PhD research findings, I learned that it takes much more than innovative technology to secure an industrial partnership. In addition to possessing the expertise required to design an innovative bioremediation strategy, researchers must present a sound business case that outlines the resources required to scale technology to meet industry needs. Following this realization, Dr. Alexandre Poulain and myself started the company Microbright in 2016 to identify what steps were required to make a business case for bioremediation.

Microbright's goal was to develop bioremediation strategies for removing Hg from water using photosynthetic and fermentative microbes naturally found in the environment. In my attempt to build a business model that satisfied this objective, I learned how to communicate complex scientific topics to potential customers and how to acquire the resources necessary for scaling up water treatment methods. Most of the experience I acquired as an entrepreneur was through the incubator program Startup Garage in 2017 and in this essay, I provide a summary of my experience in this program. I will also offer comments on some of the parallels that exist between academic research and entrepreneurship. Finally, I will take the opportunity to highlight the milestones we've achieved with Microbright and discuss the future of the company.

VALIDATING THE PROBLEM

Microbright was accepted into Startup Garage when the company's business model was in the validation stage. Validation, in this instance, designates the process of testing what parts of the business model work with respect to the demands of the market. Validation activities include assessing which potential customers are interested in a given solution; the nature and severity of the challenges customers face; the major costs associated with running the company; and potential revenue streams. At its core, the business model is built to provide a solution for a specific problem in a given customer segment. In that regard, there exists a similarity between academic research and entrepreneurship; both aim to provide solutions to problems that have high value to stakeholders.

In the beginning, our logic for why industry would be interested in bioremediation strategies seemed intuitive because of the health concerns linked to Hg pollution. As mentioned in the introduction to my thesis (**Chapter 1**), the ratification of the Minamata Convention suggests there is a global desire to better manage Hg pollution linked to industrial activities such as mining and chlor-alkali production. As a starting point, we suspected these industries would be interested in developing more environmentally sustainable Hg removal strategies to improve their social image. Given that our team's expertise was in academic research, our initial plan to generate revenue was to license Microbright's intellectual property to industrial partners. Our aim was to build on this initial licensing agreement and leverage industry expertise to scale up Microbright's Hg removal technology for industrial use.

Prior to discussing Microbright's initial validation efforts, I feel it is important to identify a key difference that exists in the problem-solving approach used by entrepreneurs compared to that used by research scientists. In the context of a startup company, an entity must claim ownership of a problem that needs to be solved and this owner generally becomes a potential customer. The customer's definition of the problem and their personal/professional priorities determine the research needs of the company. These characteristics may not align with the initial version of the proposed solution in the business model, however an entrepreneur's priority it to develop a solution that provides maximum value to a customer based on their perceived problems. This approach differs from academic research where the objective analysis of scientific evidence defines the severity and scope of a problem regardless of ownership. Although the academic approach is crucial to developing science-based tools that advance human knowledge and

influence decision making processes, the entrepreneurial approach is also required to develop a scalable business model that can address industrial scale problems.

Once we began interviewing professionals in the mining and chlor-alkali industries, we realized that our initial business model was flawed because of the differences in problem-solving that exist in the entrepreneurial world compared with the realm of academic research. The act of "getting out of the building", as it is referred to in entrepreneurial circles, showed us that Microbright could not solely rely on scientific evidence to build a business model. This approach provided us with little insight into the practicalities of water treatment, the organizational structure of our potential customer bases and the decisions making processes our potential clients carried out daily.

In our attempts to understand the mindset of potential customers such as environmental engineering firms, Canadian mining companies and European chlor-alkali companies, it became clear we had to refine our business model. These interviews revealed that Hg pollution was not perceived as a major issue for many of the companies despite what the scientific literature suggested. When speaking to engineers for gold mining companies, an industry with a history of Hg pollution, we learned that companies are concerned about Hg, but that contamination tends to be site-specific and that Hg is but one of several metals mining companies must deal with daily. As such, many of the professionals we spoke to said they would prefer a solution that could remove several non-valuable metals from water used in mining.

In the case of the chlor-alkali industry, we learned that companies were unwilling to develop new Hg remediation technology because the old technology responsible for Hg pollution was being phased out at great cost. Ultimately, everyone we spoke with was much more interested in solutions that had already been proven at a larger scale, which was prohibitively expensive for us to demonstrate at the time.

As part of these interviews, we also tried to validate what aspects of Microbright's Hg removal methods had the most value. Given that we had just started validation, we proposed a simple framework for generating revenue that relied on licensing agreements and the eventual use of scaled up bioreactors for water treatment that could be installed on site. We suspected that companies would be most interested in the "green" image that accompanied our proposed Hg removal methods. This did not end up being the case as mining companies were much more concerned about the cost of water treatment and their operating expenses. Indeed, companies were much more interested in the potential use of solar power for energy because of concerns linked to energy consumption in remote areas. Similarly, the fact that our process did not require harmful chemicals (e.g. sulphide salts and strong acids) also appealed to mining companies that wanted to limit the fines associated with secondary pollution. These insights proved extremely valuable in terms of what aspects of the business we showcased moving forward.

PIVOTING AND PITCHING

The initial findings from our validation stage put Microbright in the unfortunate position of having invested considerable resources to address an issue that was not as severe as initially perceived. This added to the already existing challenge of having to demonstrate our water treatment techniques at a larger scale with limited funds. Whereas a software company could perform a "pivot" and redesign their business model to account for this new information, this was not practical for Microbright given the complexity of the issue we were trying to solve. Moreover, we were also limited by the time it would take to complete the research testing how our solution could remove other metals in water.

Although these interviews suggested that Hg pollution was not perceived as a serious issue by the mining industry, some of the professionals we spoke to expressed interest in Microbright's Hg removal technology for sites where Hg contamination had occurred. Due to the high costs associated with mining site water treatment (estimated at $5 to $20M per site per year based on our interviews), we still had a sizeable market even if we only treated water at a single site. As such, we decided to alter our business model and seek out mining companies with known Hg issues. We focussed on Canadian companies because they have a legal obligation to treat water used in mining, which we suspected could provide additional motivation for adopting new water treatment methods. Our long-term plan was to use our expertise with Hg to complete proof of principle experiments with a mining partner and build additional solutions to target other metals of concern such as arsenic and selenium in our future work.

With a new business model in hand, we set out once more to gauge industry interest in Microbright. During this time, I practiced pitching, which is one of the most important skills for entrepreneurs. Pitching involved summarizing the problem Microbright addressed and providing an overview of our business model in non-technical terms. Pitching differs from a typical scientific presentation in how the presenter draws attention to the issue being addressed. For example, where a scientific presentation on Hg pollution would start with an informative sentence such as: “Mercury is a global pollutant and potent neurotoxin that can accumulate in the tissue of fish in its organic form methylmercury”, a pitch would hook the audience by eliciting an emotional response by saying: “Imagine you lived in a village where your water was contaminated with mercury and every time you drank water you risked having neurological damage”. While the latter statement touches on Hg’s neurotoxicity, it gives little information on how Hg moves through the environment. This exemplifies one of the main differences between academic research and entrepreneurship: a scientific presentation’s purpose is to provide a factual overview of a topic and educate the audience whereas a pitch exists to entice a specific party.

The most common type of pitch I would deliver was a 3-minute pitch. We tailored Microbright’s pitch to a non-technical audience, as this comprised most people we presented to at pitching competitions through Startup Garage. When pitching to mining companies, we would add additional technical details concerning water treatment and highlight our expertise in metal biogeochemistry to build our team’s credibility. The general outline of Microbright’s 3-minute pitch was:

1. One sentence elevator pitch containing essential information about the company
2. Identify the problem and who suffers from it
3. Describe the advantages of Microbright's solution compared to competitors
4. Outline customer segments and estimate market value
5. Summary of progress to date
6. Future goals and the "Ask"

The "Ask" is a notable feature of the pitch that does not typically occur in scientific communications. Whereas a scientific presentation usually ends with a comment on the broader applications of research findings, a pitch ends by asking for something specific that will help a company reach their next milestone. Although at first glance this "Ask" seems quite blunt, it is essential to building scalable business models, securing funding, and developing partnerships. We relied on this approach for networking within large international mining companies and finding people who could champion our solution from within a given organization. We relied on the "Ask" to secure funding and negotiate industrial partnerships, which helped pave the way for Microbright's future.

MICROBRIGHT'S PROGRESS AND FUTURE

My experience with Microbright began as an effort to patent my research findings and became an intense two-year journey through the world of entrepreneurship. Being a part of Startup Garage provided Microbright with several networking and funding opportunities that helped the company grow. Microbright's progress was recognized by one of the sponsors of Startup Garage, the Ontario Centre of Excellence, who awarded the company a $1500 prize at the final pitch day in August 2017. Microbright's team also

secured a first-place victory with a prize of $2500 at #Hackmining, a national pitching competition held by various Canadian mining companies. This victory also gave us the chance to pitch to the CEO of MacEwen Mining. Furthermore, the resources obtained from Startup Garage allowed us to hire employees and build scaled up prototypes for bioreactors that we used in demonstrations at industry events.

Ultimately, Microbright's efforts culminated in securing an industrial partnership with an international mining company that agreed to collaborate with us on a pilot project at one of their field sites. The successful negotiation of this partnership helped us present a more substantial business case for Microbright to Innovation Support Services at the University of Ottawa who graciously financed the filing of patents in the United States and Canada for Microbright's Hg removal process. Microbright's next steps are to strengthen the intellectual property in these patents by planning and executing a 2-year pilot scale project with our industrial partner, which we hope to begin in late 2019.